11-15-2013 12:00 AM

Development of Biodegradable and Stimuli-Responsive Macromolescules and Their Assemblies

Ali Nazemi
The University of Western Ontario

Supervisor
Dr. Elizabeth R. Gillies
The University of Western Ontario

Graduate Program in Chemistry
A thesis submitted in partial fulfillment of the requirements for the degree in Doctor of Philosophy
© Ali Nazemi 2013

DEVELOPMENT OF BIODEGRADABLE AND STIMULI-RESPONSIVE
MACROMOLECULES AND THEIR ASSEMBLIES

(Thesis format: Integrated Article)

by

Ali Nazemi

Graduate Program in Chemistry

A thesis submitted in partial fulfillment
of the requirements for the degree of
Doctor of Philosophy

The School of Graduate and Postdoctoral Studies
The University of Western Ontario
London, Ontario, Canada

Abstract

Polymersomes are potentially multifunctional soft materials constructed by the self-assembly of amphiphilic block copolymers in aqueous medium. While much research has focused on controlling the assembly and encapsulation properties of polymersomes, their surface functionalization has been relatively unexplored. This is important because it plays a critical role in determining their properties such as toxicity and biodistribution behavior. The work described in this thesis involves the development of a biocompatible and biodegradable polymersome systems based on poly(ethylene oxide)-*b*-polycaprolactone (PEO-PCL) block copolymers with azide surface groups as a novel scaffold for various biomedical applications. The surface functionalization of these polymersomes with polyester dendrons bearing alkyne focal points with different peripheral groups, such as amines and guanidines, as well as a small molecule rhodamine dye is accomplished and their conjugation yields are compared to each other. Moreover, dendritic and non-dendritic polymersome-based MRI contrast agents, with the highest currently reported longitudinal relaxivity for a polymersome system, are developed by decorating PEO-PCL polymerosomes' surfaces with both non-dendritic and dendritic Gd(III)-based contrast agents. In addition, PEO-PCL polymersomes were employed to develop a multifunctional system with the potential to interfere with the viral infection process at two levels. In addition to their use as materials for functionalizing the surfaces of nanomaterials, dendrimers and their assemblies have been widely used as drug delivery vehicles. In order to enable a new level of control over drug release, backbone photodegradable dendrimers and dendrons are synthesized by incorporation of a monomer unit based on *o*-nitrobenzyl esters and 2,2-bis(hydroxymethyl)propionic acid. It is shown that these dendrimers undergo effective photolysis to release only small molecules upon irradiation with UV light. Finally, these dendrons are incorporated into amphiphilic Janus dendrimer structures and their self-assembly to dendrimersomes followed by their photodegradation are discussed.

Keywords

Polymersome, biodegradable, dendrimer, dendron, MRI contrast agent, influenza virus, photodegradable, dendrimersome

Co-Authorship Statement

The research discussed in this thesis is a result of contributions from the author as well as coworkers from Western University and supervisor Dr. Elizabeth Gillies whose exact contributions are described here.

Chapter 1 contains materials that are submitted for publication in a journal article and a book chapter. Subsection "Dendrimer Conjugates with Imaging Agents", is a part of the submitted book chapter, and "Surface Functionalization of Polymersomes", is a part of the submitted journal article. These sections were written collaboratively by the author and supervisor Dr. Elizabeth Gillies.

Chapter 2 describes a project proposed by Dr. Elizabeth Gillies and Dr. Colin Bonduelle. Dendrons used for this work were supplied by Ryan Amos, a graduate student in the Gillies group at the time. All other experimental work was carried out by the author under the supervision of Dr. Gillies. The manuscript was initially drafted by the author and Dr. Gillies provided assistance with editing and final preparation.

Chapter 3 comprises work proposed by Dr. Gillies and the author. Relaxivity measurements of the developed contrast agents were performed by Dr. Francisco Martinez and Dr. Timothy Scholl at the Robarts Research Institute at Western. All the other experimental work were accomplished by the author under the supervision of Dr. Gillies. The manuscript was initially drafted by the author and Dr. Gillies provided assistance with editing and final preparation.

Chapter 4 describes a project proposed by Dr. Gillies. Dr. S. M. Mansour Haeryfar's research laboratory in the Department of Microbiology and Immunology at Western University provided input on the antiviral potential of these molecules and reviewed the manuscript. All the experimental work as well as the biological assay were carried out by the author. The manuscript was initially drafted by the author and Dr. Gillies provided assistance with editing and final preparation.

The project described in Chapter 5 was proposed by the author. Preliminary synthetic effort was carried out by the author, but thereafter a large portion of intermediates and dendrons were synthesized by Tylor Schon, a fourth year undergraduate student supervised by the author. All the other dendrimer synthesis experiments and photodegradation studies were carried by the author under the supervision of Dr. Gillies. The manuscript was initially drafted by the author and Dr. Gillies provided assistance with editing and final preparation.

Chapter 6 describes a project proposed by the author. All the experimental work was accomplished by the author under the supervision Dr. Gillies. This chapter was initially drafted by the author and Dr. Gillies provided assistance with editing and final preparation.

Acknowledgments

I would like to give my sincere thanks to my supervisor, Dr. Beth Gillies, for giving me the opportunity to join her research team and for supporting me throughout my time in her group. Beth, you are a great supervisor. Under your supervision, I not only trained in many experimental skills, but I also learned how to think critically and develop scientific ideas.

I would also like to thank all the past and present members of the Gillies group for all their help and for creating such an excellent environment in the lab, that leaves me with many unforgettable memories. Many thanks to all the staff at UWO without whom this thesis would not have been possible: Mat Willans, Doug Hairsine, Darlene McDonald, the main office crew, all the ChemBio Store and Electronics Shop staff, and the undergraduate lab technicians for all their support during TAing. Furthermore, I am thankful to my thesis examiners Dr. Guthrie, Dr. Hudson, Dr. Min, and Dr. Yousaf for reading through my thesis.

Special thanks to my wife, Mahboubeh, who has been by my side since the undergraduate level. Mahboubeh, I have no doubt that I could not have come this far if it was without you, and I cannot tell you how grateful I am for all the unconditional support you have had for me. We all know that research does not go well most of the time and this leaves us with frustration. You have always cheered me up during such times and celebrated with me for my successes. I cannot wait to celebrate your successful defense in the near future.

Last but definitely not least, I am deeply grateful to my father, mother, and brothers for all their encouragement, support, and unconditional love throughout my life. You guys have always been there for me. Mom and Dad, I know how difficult it was for you to live in a foreign country while you had your whole life back in Iran. You forfeited all you had back there and came this far just to provide a better life for us. I know it is impossible to make up for all you have done; however, to show my sincere appreciation, I would like to dedicate this thesis to you, my dear Mom and Dad.

Table of Contents

List of Tables

List of Figures

List of Schemes

List of Abbreviations

A	absorption
Ac	acetyl
AJD	amphiphilic Janus dendrimer
aq	aqueous
ATRP	atom-transfer radical polymerization
BCP	block copolymer
bis-MPA	2,2-bis(hydroxymethyl) propionic acid
Boc	*tert*-butoxycarbonyl
BOP	(benzotriazol-1-yloxy)tris(dimethylamino)phosphonium hexafluorophosphate
br	broad
BSA	bovine serum albumin
CL	ε-caprolactone
Con A	Concanavalin A
CT	computed tomography
d	doublet
DAB	3,3'-diaminobenzidine
DCC	*N,N'*-dicyclohexylcarbodiimide
DIPEA	*N,N*-diisopropylethylamine
DLS	dynamic light scattering
DMAP	4-dimethylaminopyridine
DMEM	dulbecco's modified eagle medium
DMF	*N,N*-dimethylformamide
DNA	deoxyribonucleic acid
DOTA	1,4,7,10-tetraazacyclododecane-1,4,7,10-tetraacetic acid
DOX	doxorubicin
DTPA	diethylenetriaminepentaacetic acid
EDC	*N*-(3-dimethylaminopropyl)-*N'*-ethylcarbodiimide
EI	electron impact
ELLA	enzyme-linked lectin inhibition assay
EPR	enhanced permeability and retention
equiv	equivalent
ESI	electrospray mass spectrometry
Et_3N	*N,N,N*-triethylamine
EtOAc	ethyl acetate
$f_{hydrophilic}$	hydrophilic volume fraction
FBS	fetal bovine serum
G	generation
h	hour(s)
HA	hemagglutinin
HABA	2-(4'-Hydroxybenzeneazo)benzoic acid
HBP	hyperbranched polymer
HBTU	*o*-(benzotriazol-1-yl)-*N,N,N',N'*-tetramethyluronium hexafluorophosphate
HCl	hydrochloric acid

HIV	human immunodeficiency virus
HOBt	1-hydroxybenzotriazole
HOPO	hydroxypyridinone
HPLC	high-performance liquid chromatography
HRMS	high-resolution mass spectrometry
HRP-LFA	horseradish peroxidase-labeled LFA
Hz	hertz
IC_{50}	inhibitory concentration-50
ICP-MS	inductively coupled plasma mass spectrometry
IR	infrared
IUPAC	International Union of Pure and Applied Chemistry
J	coupling constant
LCST	lower critical solution temperature
LFA	*Limax flavus* agglutinin
LSM	laser scanning microscope
m	multiplet
MALDI-MS	matrix-assisted laser desorption/ionization mass spectroscopy
MALS	multi-angle light scattering
MeOH	methanol
min	minute(s)
M_n	number average molecular weight
mp	melting point
MRI	magnetic resonance imaging
MSA	methanesulfonic acid
M_w	weight average molecular weight
MW	molecular weight
MWCO	molecular weight cutoff
NA	neuraminidase
NaAsc	sodium ascorbate
NaOMe	sodium methoxide
Neu5Ac	*N*-acetylneuraminic acid
NIPAAm	*N*-isopropylacrylamide
NIR	near infrared
NMR	nuclear magnetic resonance
PAMAM	poly(amido amine)
PBD	polybutadiene
PBD-PEO	poly(butadiene-*b*-ethylene oxide)
PBS	phosphate buffered saline
PBST	phosphate buffer solution containing 0.05% (v/v) Tween 20
PCL	polycaprolactone
PDI	polydispersity index
PDLLA	poly(D/L-lactic acid)
PE	polyester
PEG	poly(ethylene glycol)
PEO	poly(ethylene oxide)
PEO-PCL	poly(ethylene oxide)-*b*-polycaprolactone

PET	positron emission tomography
PGA	poly(glycolic acid)
PLLA	poly(L-lactic acid)
PMOXA	poly(2-methyl-2-oxazoline)
PPh_3	triphenylphosphine
PPI	poly(propylene imine)
quant	quantitative
r_1	longitudinal relaxivity
RAFT	reversible addition-fragmentation chain-transfer polymerization
RES	reticuloendothelial system
RI	refractive index
ROMP	ring-opening metathesis polymerization
ROP	ring-opening polymerization
rpm	revolutions per minute
rt	room temperature
SEC	size exclusion chromatography
SPECT	single photon emission computed tomography
t	triplet
TAX	paclitaxel
TEM	transmision electron microscopy
TEG	triethylene glycol
TFA	trifluoroacetic acid
THF	tetrahydrofuran
TLC	thin layer chromatography
TLQ	trimethyl-locked quinone
UV	ultraviolet
ε	molar extinction coefficient
μwave	microwave
τ_R	rotational correlation time

Chapter 1

1 Biodegradable Polymersomes and Dendrimers in Biomedical Applications[*]

1.1 Introduction to Macromolecules

The word macromolecule is a Greek-Latin hybrid word that contains two contradictory terms. It refers to a small mass (Greek: *molecula*, diminutive of moles = mass) that is large (Large: *makros*).[1] Thus, they are simply large molecules. According to the International Union of Pure and Applied Chemistry (IUPAC), a macromolecule is defined as

> "a molecule of high relative molecular mass, the structure of which essentially comprises the multiple repetition of units derived, actually or conceptually, from molecules of low relative molecular mass."

Macromolecules are either natural, such as proteins, DNA, and polysaccharides, or synthetic, such as synthetic rubbers, fibers and dendrimers, with molecular weights (MWs) of several thousands to millions. Humankind has used naturally occurring macromolecules since the early days of civilization. For instance, proteins in meat and polysaccharides in grain are essential constituents of food, and a high MW resin called Amber was used in old Greece as jewelry. On the other hand, the first synthetic and semisynthetic macromolecules, such as nitrocellulose in 1869, were prepared without any insight to their chemical structure. It was not until 1920s when scientists began to obtain knowledge about the structures of macromolecules, and soon after, fully synthetic macromolecules such as polychloroprene, polystyrene, and nylon 6.6 were discovered and commercialized.[1]

Compared to traditional small molecules with single molar masses, synthetic macromolecules display molar mass distributions. Among the different techniques developed to measure these molar mass distributions,[1] mass spectroscopy techniques such as matrix-assisted laser desorption/ionization mass spectroscopy (MALDI-MS) and size exclusion chromatography (SEC) have found widespread applications in chemistry and materials science laboratories. Compared to mass spectroscopy, which is an absolute method for molar mass determination, most SEC requires a correlation of the measured properties of standards with molar masses that have been independently determined with those of the sample. Because of the presence of the above-mentioned molar mass distribution in most synthetic macromolecules, their molar mass is often calculated around an *average* value. Depending on the statistical method that is applied to calculate the average molar mass, different average values can be defined, among which *number average molar mass*, M_n, and *weight average molar mass*, M_w, are most commonly used. Mathematical expressions for M_n and M_w are shown in Figure 1.1. In these equations, N_i is defined as the number of moles of each macromolecule species and M_i as the molar mass of that species. Another term widely used in macromolecular science is *polydispersity index* (PDI), which is calculated as M_w/M_n. PDI indicates the distribution of individual molar masses in a batch of polymer sample. It has a value of greater than 1. However, as the polymer chain lengths become more uniform, the PDI approaches 1.

$$M_n = \frac{\sum M_i N_i}{\sum N_i} \qquad\qquad M_w = \frac{\sum M_i^2 N_i}{\sum M_i N_i}$$

Figure 1.1. Mathematical equations for M_w and M_n.

Among various natural and synthetic macromolecules, of particular interest to this thesis are biodegradable polymers, block copolymers (BCPs), and dendritic architectures. In the following sections, these families of macromolecules will be briefly introduced and recent advancements in their self-assembly behaviors and their use in biomedical applications will be highlighted.

1.1.1 Biodegradable Polymers

During the past few decades, the field of synthetic polymers has progressed to such an extent that synthetic polymers are essential in daily life. This mainly stems from their low cost, reproducibility in production, and their resistance to physical aging.[2] However, when they are intended to be used for a limited period of time, such as in surgery, pharmacology, or agriculture, such resistance becomes problematic. In all these time-limited applications, elimination of the artificial materials after use is desirable. For such applications, biodegradable polymers have been emerged as an important class of materials. These are defined as materials that can degrade by the action of living organisms. Biodegradable polymers have found use in applications ranging from bulk commercial materials such as biodegradable plastics to highly specialized drug delivery vehicles. Mainly, they include polyesters such as polycaprolactone (PCL), poly(D/L-lactic acid) (PDLLA), poly(L-lactic acid) (PLLA), and poly(glycolic acid) (PGA) (Figure 1.2). In addition to these commonly used biodegradable polymers, other backbones such as polyamides, polyanhydrides, polyphosphazenes, polydisulfides, polyacetals, poly(ortho ester)s, and other polyesters derived from diacids and diols have been used as biodegradable polymers. These biodegradable polymers have found widespread biomedical applications in materials such as stents and sutures,[3] tissue engineering,[4-9] and drug delivery vehicles.[10,11]

| 1.1 | 1.2 | 1.3 | 1.4 |
| Polycaprolactone | Poly(glycolic acid) | Poly(D/L-lactic acid) | Poly(L-lactic acid) |
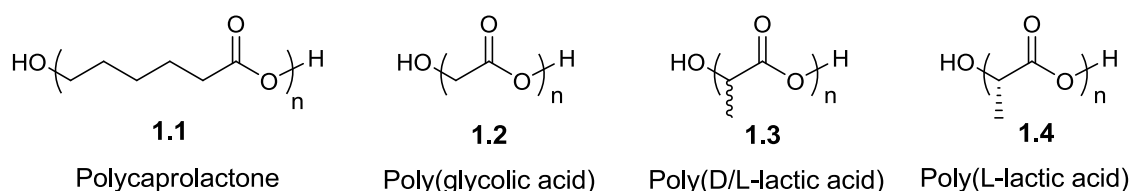
Figure 1.2. Chemical structures of the most common polyesters.

1.1.2 Block Copolymers

BCPs are macromolecules containing two or more chemically distinct homopolymer blocks that are linked together. As shown in Figure 1.3, BCPs can be classified into a number of architecturally different categories. Linear BCPs contain two or more polymer chains in sequence. On the other hand, a star BCP is composed of more than two linear

BCPs attached at a common branch point. Architecturally similar to star BCPs, when polymers containing at least three homopolymers are attached at a common branching point, are called mixed-arm star BCPs.
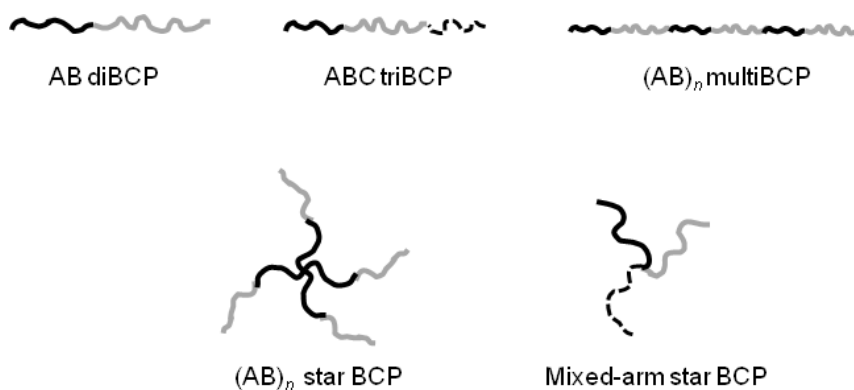
Figure 1.3. Representation of various BCP architectures.

BCPs exhibit many interesting properties, one of which is their ability to phase separate both in thin films and in solution. This property stems from the inherent immiscibility of the chemically different polymer blocks. As a consequence of phase separation, BCPs form nanoscopic patterns in thin films,[12] while self-assembling into a wide range of morphologies in solution.[13] To better control these processes, BCPs with well-defined structures, specific chain lengths, and low PDIs are required. A great deal of control over these parameters has been achieved by the development of various living polymerization techniques including certain classes of ionic polymerization,[14-16] atom-transfer radical polymerization (ATRP),[17,18] reversible addition-fragmentation chain-transfer polymerization (RAFT),[19] nitroxide-mediated polymerization,[20] and ring-opening metathesis polymerization (ROMP). [21,22] These advanced techniques allow for the precise tailoring of BCPs architecture and composition.

1.1.3 Block Copolymer Self-Assembly in Solution

As described above, one of interesting properties of BCPs is their ability to undergo self-assembly in solution as a result of the inherent immiscibility of the polymer blocks. Amphiphilic BCPs are composed of both hydrophilic and hydrophobic polymer blocks. In aqueous solution, well-defined amphiphilic BCPs undergo self-assembly in order to minimize energetically unfavorable hydrophobe–water interactions.[13] The resulting

morphologies obtained from self-assembly include spherical micelles,[23] helical rods,[24] toroids,[25] vesicles,[26,27] macroscopic tubes,[28] and multicompartment cylinders.[29] These morphologies are a result of the inherent molecular curvature of the BCPs.[30] More specifically, for an amphiphilic diBCP suspended in aqueous solution it's been shown that the resulting self-assembled morphology is dictated by the hydrophilic volume fraction of the BCP ($f_{hydrophilic}$).[31] In aqueous medium, polymers with $f_{hydrophilic}$ between 20 % and 42 % are expected to form vesicles. BCPs with $f_{hydrophilic}$ between 42 % and 50 % are expected to form worm-like assemblies while ones with $f_{hydrophilic} > 50$ % are expected to form spherical micelles.

Two morphologies that have been extensively studied are polymeric micelles and vesicles. In micelles (Figure 1.4a), the hydrophobic portions of the BCP aggregate with each other to avoid contact with water, while the hydrophilic portions are directed towards water. When compared to micelles formed by surfactants, micelles formed by BCPs show significant improvements in their thermodynamic stability with a lower critical micelle concentration.[32] The diameters of polymeric micelles typically fall in the range of 10-100 nm.[33] In addition to polymeric micelles, another morphology that has received great interest in recent years is BCP vesicles, often called "polymersomes" (Figure 1.4b).

a)

b)

Polymer micelle
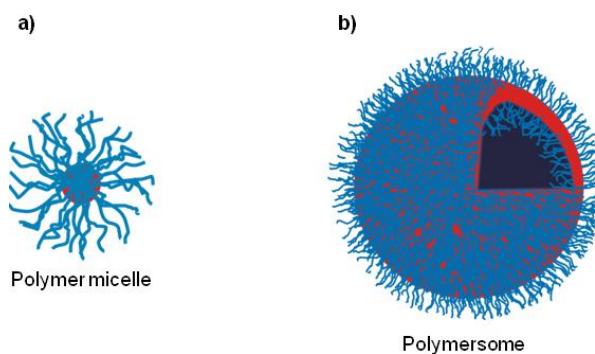
Polymersome

Figure 1.4. Cartoon representation of a) polymer micelles, b) polymersomes.

Polymersomes are morphologies with membranes that resemble those of liposomes, vesicles obtained from phospholipids. This self-assembled structure consists of hydrophilic blocks directed towards the external and internal aqueous solution, and hydrophobic blocks that repel water and thus form the interior of the membrane. In

comparison with phospholipid vesicles, polymersomes have been shown to have several improved properties. Based on the fact that the MWs of the polymers are usually several times greater than those of phospholipids, polymersome membranes are thicker, which results in higher stability and lower permeability than common phospholipid bilayers.[34] In addition, chemical versatility of the BCP syntheses creates endless opportunities to tune the polymersome properties. While micelles can only encapsulate hydrophobic drugs in the core, polymersomes are capable of entrapping hydrophobic drugs within their membrane as well as encapsulating hydrophilic species in their aqueous core.

Polymeric micelles and vesicles have been prepared by a variety of different methods. The method of preparation often depends on solubility and other properties of the constituent BCPs. The easiest method for the preparation BCP micelles and vesicles is the direct dissolution of BCPs in water.[34,35] In addition, film rehydration methods have also been widely used for assembly formation.[36,37] In this method, the BCP is first dissolved in a volatile organic solvent. The solvent is then removed under a stream of air or nitrogen. After subjecting to vacuum to remove most of the organic solvent, the resulting film is hydrated by pure water or buffer solution. The assemblies are normally formed upon stirring/sonication. In a method known as "solvent switch", "phase inversion", or "nanoprecipitation", a solution of polymer in an organic solvent which is miscible with water (such as ethanol or tetrahydrofuran) and is a good solvent for both blocks, is diluted or injected into water or buffer solution. The organic solvent is then normally removed by dialysis.[38,39] Alternatively, these assemblies can be formed by oil in water emulsion procedures.[40,41] In this approach, the BCP is dissolved in a volatile organic solvent that is immiscible with water, and this solution is then injected into a rapidly stirring aqueous media. The organic solvent is then left to evaporate. Solvent-free techniques such as electroformation have also been employed for the preparation of assemblies.[42]

1.1.4 Other Macromolecular Architectures: Dendrimers

In addition to the above-mentioned polymers and BCPs, dendritic architectures including hyperbranched polymers (HBPs) and dendrimers are another major class of macromolecules. This class of macromolecules is characterized by their three-

dimensional globular architecture. Structurally, HBPs are comprised of dendritic units, linear units, and terminal groups (Figure 1.5a). An important characteristic of HBPs is that these structural units are randomly distributed along their backbone.[43] In other words, they possess an irregular dendritic structure. Compared to HBPs with irregular structures, and linear polymers and BCPs with molar weight distributions, dendrimers are structurally perfect dendritic structures with a single or very narrow molar weight distribution (Figure 1.5b). Dendrimers comprise three structural regions: a) a core, b) layers of branching repeat units comprising the backbone, where each layer typically results from one stage of growth and is termed a "generation", and c) end groups on the peripheral layer. Alternatively, when dendrimers are prepared from a monovalent core moiety (focal point), a wedge-like structure typically called a "dendron" results (Figure 1.5c).
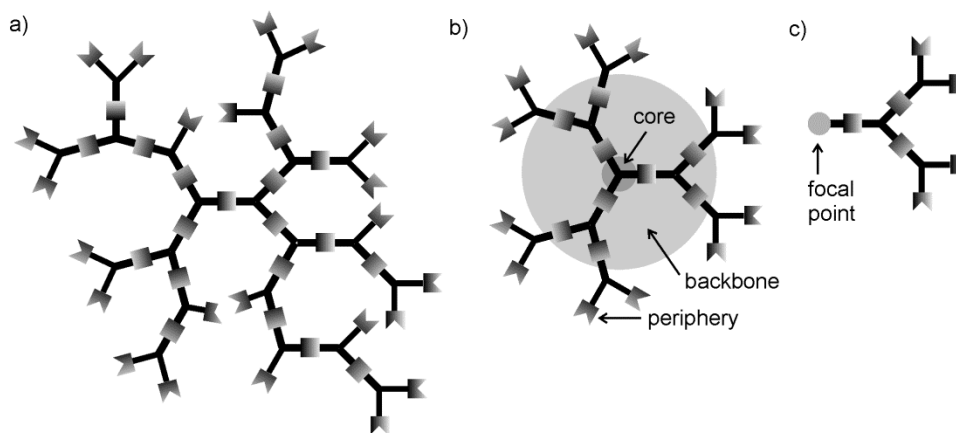
Figure 1.5. Schematics of a) a hyperbranched polymer; b) a dendrimer; c) a dendron.

The iterative synthesis of dendrimers can generally be categorized into two strategies, the divergent approach and the convergent approach. In the divergent approach,[44-48] the dendrimer is grown outwards from the core by the repetition of coupling and activation steps. This approach is the preferred one for the large scale preparation of dendrimers because the quantity of dendrimer sample increases with each generation and the removal of excess reagents by techniques such as precipitation, distillation, or ultrafiltration is facilitated by their differences in mass. However, the exponentially increasing number of coupling reactions required for each subsequent generation means that the number of side

reactions or incomplete couplings also increases, ultimately leading to incomplete branching and flawed structures that are nearly impossible to separate from the target molecule.

In the convergent approach,[49] growth initiates from what will become the dendrimer periphery and progresses towards the core. When the desired generation is reached, the resulting "dendrons" are coupled to a core molecule. As this approach only involves a small number of coupling reactions at each generation, the molecules that result from incomplete couplings can often be separated from the desired molecules as they are sufficiently different in structure. This affords dendrimers with higher structural homogeneity and monodispersity than the divergent approach. Nevertheless, the couplings become increasingly challenging due to steric hindrance as the dendrons approach higher generations. Furthermore, although the molar mass increases with each generation, the excesses of dendrons used in the couplings, incomplete couplings and losses associated with the purification generally result in a decrease in the overall mass of material at each step, making this approach less attractive on a large or industrial scale.

Due to their iterative syntheses and highly branched structures, dendrimers and dendrons possess several properties that are unique relative to traditional polymers. As mentioned above, while most syntheses of linear and HBPs lead to a range of molecules differing in MWs, the iterative syntheses of dendrimers leads to molecules with a single or very narrow range of MWs. Furthermore, while linear or HBPs can theoretically be grown infinitely, the growth of dendrimers is mathematically limited. This is due to the exponential increase in the number of monomer units with each generation, while the volume available for these units increases with the cube of the dendrimer radius. Finally, one of the most important differences in the context of bioconjugate chemistry is that while linear polymers have only two end groups, dendrimers have an exponentially increasing number of end groups. This results in the properties of dendrimers being dominated by these end groups at high generations, and also provides many sites for the conjugation of functional moieties. Based on these unique properties, dendrimers and dendrons have found widespread applications in biomedical research.[50-53]

Over the past few decades, tremendous progress has been made in the optimization of dendrimer syntheses and a diverse array of backbones are now readily accessible. Some of the more commonly used backbones include the poly(amido amine) (PAMAM) "Starburst" (Figure 1.6a), polyester (PE) dendrimers based on 2,2-bis(methylol)propionic acid (Figure 1.6b), poly(propylene imine) (PPI) (Figure 1.6c), and poly(L-lysine) (PLL) (Figure 1.6d).
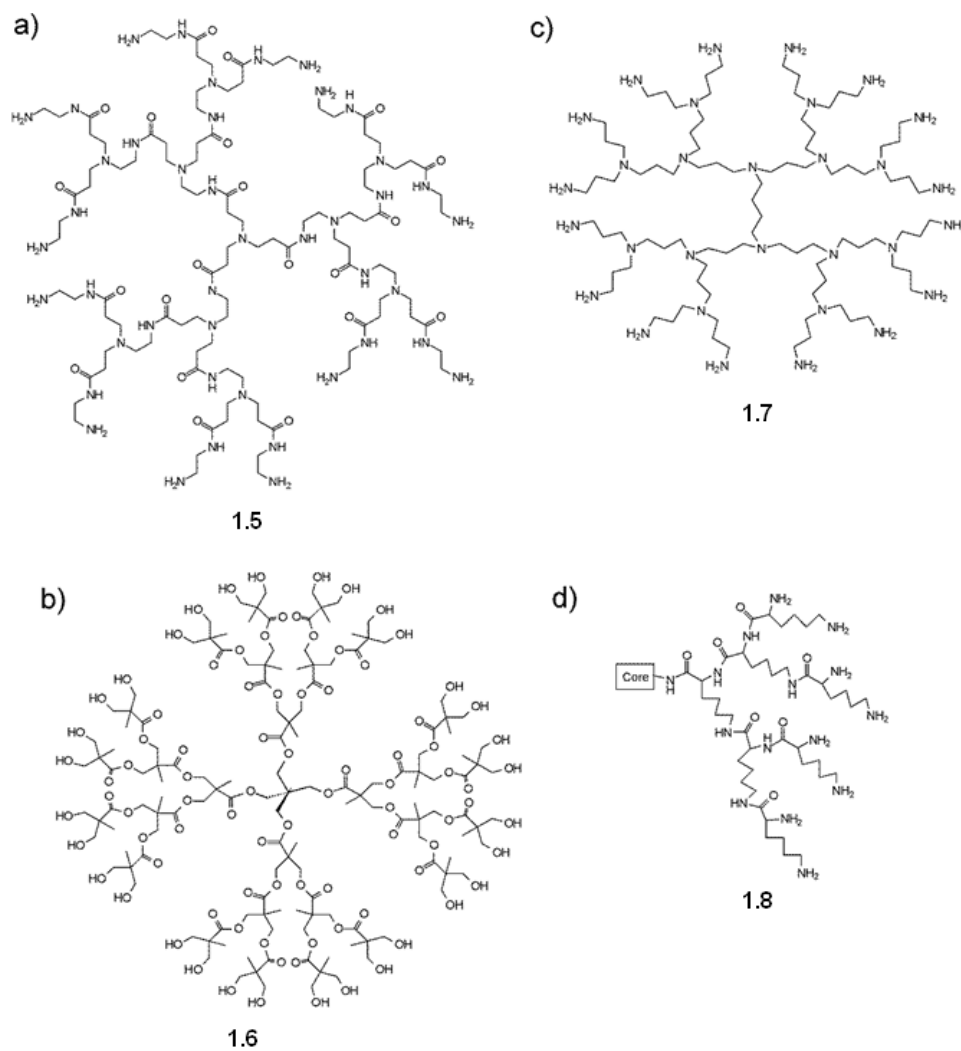
Figure 1.6. Readily accessible dendrimer backbones: a) PAMAM; b) PE; c) PPI; d) PLL.

Many of these dendrimers are now available from commercial supplies.

1.1.5 Amphiphilic Janus Dendrimers and Their Assemblies

In addition to conventional dendrimers with uniform compositions as shown above, there also exists a unique class of dendrimers known as "Janus dendrimers". These are dendrimers with well-defined but asymmetric architectures of two chemically distinct dendrons on opposite sides with different chemical compositions, peripheral groups, or polarities. They are also known as surface-block dendrimers, diblock dendrimers, codendrimers, diblock co-dendrimers, or bow-tie dendrimers.[54]

As shown in Figure 1.7, three main approaches have been proposed for the synthesis of Janus dendrimers.[54]
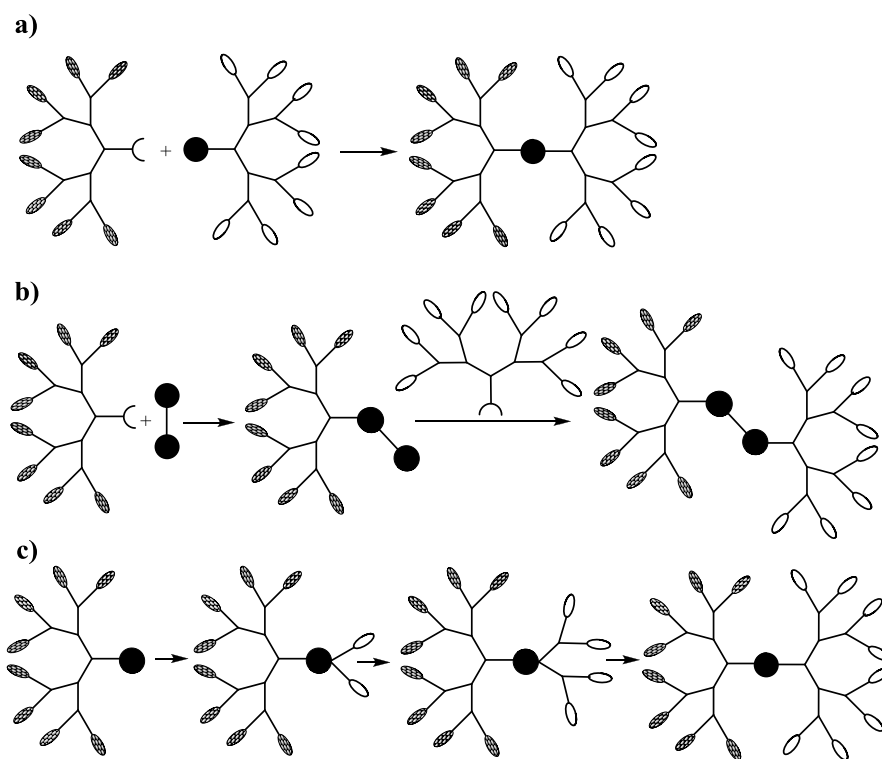
Figure 1.7. Schematic representation of main methods for the synthesis of Janus dendrimers.

In the simplest approach, two dendrons with complementary functional groups at their focal points are reacted with each other to obtain the desired Janus dendrimer (Figure 1.7a). In the second method, one of the dendrons is first reacted with a multifunctional core molecule and then the second dendron is grafted to the remaining functionality

(Figure 1.7b). In the final approach, the focal point of one of the dendrons is used for the divergent growth of the second dendron (Figure 1.7c). This method has not been found as popular as the previous two approaches. It should be noted that as the purification of macromolecules is often a difficult and tedious task to perform, highly efficient reactions need to be employed for the synthesis of Janus dendrimers. Despite the difficulty in the synthesis of Janus dendrimers compared to symmetrical dendrimers, Janus dendrimers with various backbones such as benzyl ether, phenylene, phosphorous, PAMAM, 3,3'-diaminobenzidine (DAB), lysine, ester, *etc.*, have been synthesized via the above-mentioned methods (Figure 1.8).[54] The difficulties in their syntheses can certainly account for the relatively limited number of examples of Janus dendrimers in comparison to conventional symmetrical dendrimers.
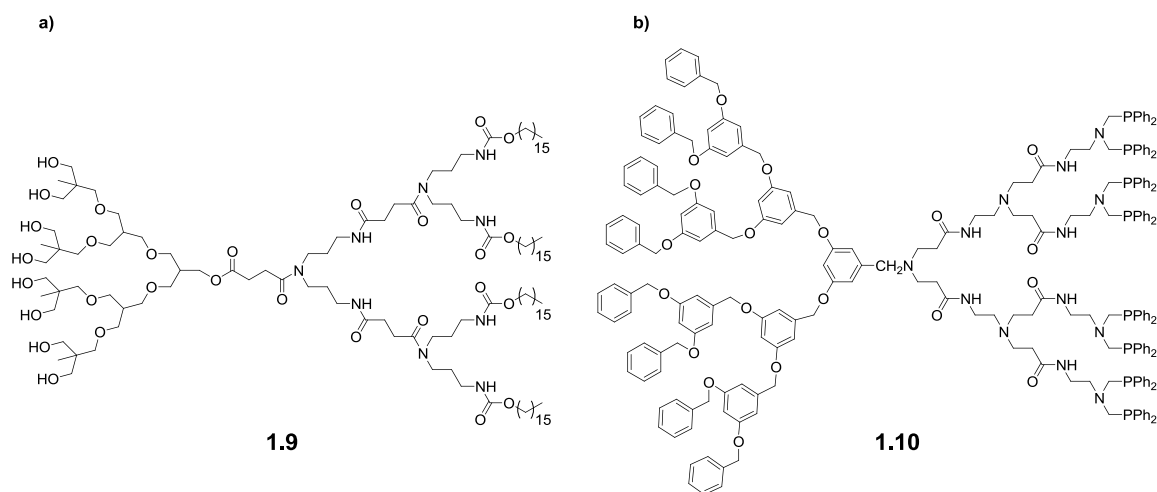
Figure 1.8. Examples of Janus dendrimers based on a) ether/amide linkages; b) benzyl ether and PAMAM dendrons.

Similar to amphiphilic BCPs, when constituents of Janus dendrimers are hydrophilic and hydrophobic dendrons, they are called "amphiphilic Janus dendrimers (AJDs)". To date, AJDs with a variety of dendritic backbones have been synthesized[54] and their self-assembly behaviours have been studied, resulting in the formation of different morphologies ranging from nano-aggregates[55] to vesicles,[56,57] multilamellar aggregates,[57] button structures,[58] and ribbons.[59,60] More recently, Percec and coworkers have synthesized a total number of 107 AJDs, with different backbones and generation numbers, and screened their self-assembly behaviour in water.[61,62] It was shown that such

macromolecules were able to form structures including vesicles (named as dendrimersomes), cubosomes, disks, tubular vesicles, and helical ribbons. The authors concluded that dendrimersomes not only exhibit stability and mechanical strength of polymersomes, but also have the advantages of superior size uniformity, ease of formation, and chemical modification.[61] A cartoon representation of a dendrimersome is shown in Figure 1.9.
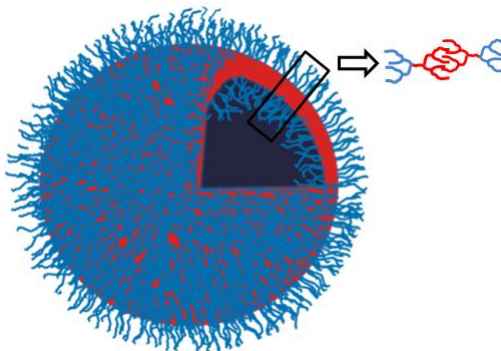
Figure 1.9. Schematic representation of a dendrimersome.

In a follow up study by the same group, it was observed that dendrimersome size and stability were inversely proportional to the membrane thickness, meaning that dendrimersomes with thinner membrane were larger and more stable. They attributed this observation to the increased degree of interdigitation of the membrane-forming hydrophobic dendron, which resulted in the shrinkage of the membrane thickness and its higher stability.

1.2 Macromolecules for Biomedical Applications

For living cells to function, nature employs macromolecules and finds intelligent ways of regulating their self-assembly behaviour to impart specific chemical and structural functions. To mimic such systems, improve the biological functions of organs and tissues, and cure diseases, researchers have prepared a wide range of synthetic macromolecules with similar/improved features and established the field of nanobiotechnology. Synthetic macromolecules, both in their molecular and self-assembled structures, have been the focus of intense research for a wide range of biomedical applications during the past few decades.[10,11,63-65] These include applications

in tissue engineering,[4-9] sutures,[3] bone fixation devices and vascular grafts,[66] drug delivery systems,[10,11,67,68] and diagnostics.[69-71] In the following sections, recent advances made in the biomedical applications of BCPs and their assemblies, and dendrimers will be highlighted.

1.2.1 Block Copolymer Assemblies for Drug Delivery

Over the past several decades, many advances have been made in the development of therapeutics to treat human diseases. However, many current drugs and new drug candidates still suffer from significant limitations. For example, the low aqueous solubilities of hydrophobic drugs are major obstacles for their administration. One of the ways to overcome solubility problems is the use of excipients. However this can result in undesirable side effects, such as when Cremophor EL or ethanol are used for the solubilization of paclitaxel (TAX).[72] An additional challenge encountered is the rapid elimination of drug molecules from the blood stream, which limits their therapeutic efficacy and increases the required dose. Moreover, many drugs exhibit a lack of specificity for their therapeutic target. For example, many anti-cancer drugs not only affect cancer cells but also kill non-cancerous and healthy cells causing severe side effects. These challenges have motivated significant interest in the development of drug delivery systems, where the incorporation of a drug into a polymeric system can enhance its solubility, prolong its circulation time, and enhance its specificity for its target. Among the various structures obtained by engineering BCP self assembly, which were described earlier, polymeric micelles and vesicles are among the extensively investigated systems. Therefore, the recent advances made in their applications as drug careers will be discussed in this section.

There are several considerations that need to be taken to an account in the application of self-assembled materials for *in vivo* drug delivery. Generally, delivery materials need to avoid uptake by reticuloendothelial system (RES) and have prolonged circulation time in the blood.[73] One of the factors to control this property is the corona-forming hydrophilic polymer block composition. A few examples of synthetic hydrophilic blocks that have been used to achieve this property include poly(ethylene oxide) (PEO),[74] poly (acrylic acid),[26] poly(acryloylmorpholine),[75] poly(2-methyl-2-oxazoline) (PMOXA),[76]

and polyvinylpyrrolidone.[75] Although these hydrophilic blocks give so called "stealth" properties to the assemblies, PEO has been found to be the most effective candidate due to its excellent biocompatibility and minimal protein adsorption.[75,77-79] In addition, the size of the delivery vehicle also plays an important role in determining its circulation time. It's been found that particles with diameters less than 200 nm can overcome the clearance by RES.[80] Furthermore, the lower size limit for the particles in order to avoid renal clearance and thus rapid urinary excretion has been shown to be 5.5 nm.[81] Particles with diameters larger than 100 nm are found to accumulate mostly in liver and spleen.[82]

To minimize the side effects of drugs, it is preferable that drug delivery vehicles selectively accumulate in the therapeutic sites. This is often achieved through selective targeting. For cancerous tumors, there are two main targeting mechanisms, namely *passive* and *active* targeting. Due to the tendency of tumor cells for rapid growth, it has been shown that solid tumor tissues generally possess unusual characteristics such as hypervasculature and incomplete vascular architecture which result in their leaky behaviour.[83] Because of these properties, tumor blood vessels show high permeability to macromolecules and nano-sized particles.[83] Additionally, because of the immature lymphatic capillaries in cancer tissues, their lymphatic drainage system fails to operate as in normal tissue.[83] As a result, the uptaken nanoparticles are retained for prolonged periods of time in tumor cells. This effect, known as the enhanced permeability and retention (EPR) effect, is the basis for the passive tumor targeting by polymeric systems. On the other hand, in active targeting, biologically specific interactions between the diseased cells and the delivery vehicles are sought. This includes interactions such as antigen-antibody binding. In this case, because of the overexpression of tumor-associated antigens on tumor cells, specific antibodies that interact with those antigens can be chosen and engineered onto the surface of the assembled materials.[84] Other active targeting mechanisms involving the binding of small molecules such as folate[85] or peptides such as RGD[86] to receptors overexpressed in cancerous tissue have also been explored.

1.2.1.1   Polymeric Micelles for Drug Delivery

Polymeric micelles have been prepared using a wide range of BCP compositions. Readers are referred to several comprehensive review articles published in this context.[11,83,87-89] With the advances made in this field, several BCP micellar drug delivery systems have reached clinical trials. For instance, doxorubicin (DOX)-BCP micelles, TAX-BCP micelles, and cisplatin BCP micelles are all in the Phase II of clinical trials.[88] It should be noted that hydrophobic drugs can either be physically entrapped within the hydrophobic core of BCP micelles or chemically conjugated to the hydrophobic polymer block and the drug release mechanism is mainly dependent on the type of encapsulation. It has been proposed that in the case of covalently bound drug, bulk degradation of polymer matrix or surface degradation is the main pathway of release, while for the physically entrapped drug, diffusion plays the main role for drug release.[83] Kataoka and coworkers[90] incorporated DOX at the core of BCP micelles composed of poly(ethylene oxide-*b*-benzyl L-aspartate) by physical entrapment and showed that drug release occurs very slowly from the micelles. In fact, it was found that even after 100 hours (h) only a small percentage of the encapsulated DOX was released from the micelles. This was suggestive of the stability of such micelle-drug complex. In an example of covalently linked micelle-drug conjugate, Hruby and coworkers[91] prepared micelle-DOX bioconjugates via a pH-sensitive hydrazone linkage. In this study, poly(ethylene oxide-*b*-allyl glycidyl ether) BCP was first functionalized with hydrazide groups by first reacting the allyl side chains of the polymer with methyl sulfanylacetate and then treating the resulting product with hydrazine hydrate. The resulting hydrazide groups of the polymer were then reacted with the ketone moiety of DOX, to provide a hydrazone linkage and yield a drug-containing BCP with approximately 3 wt.% drug loading. It was shown that micelles formed from this BCP were able to release 43% of their drug upon incubation at pH 5.0 for 24 h, while incubation at pH 7.4 resulted in 16% drug release. This illustrates the importance of a labile linkage between drugs and micelles for the release of covalently-constructed micelle-drug bioconjugates.

1.2.1.2   Polymersomes for Drug Delivery

Unlike BCP micelles, owing to their aqueous core and hydrophobic membrane, polymersomes can potentially be multifunctional. They are capable of encapsulating hydrophilic drugs in their cores and entrapping hydrophobic species within their membranes. Given the multifunctional capabilities of polymersomes and advances made in the area of polymer synthesis, polymersomes composed of a wide range of BCPs have been prepared and studied. These include polymer-polymer, polymer-polypeptide, polymer-polysaccharide, and polypeptide-polysaccharide BCPs. Readers are referred to several review articles published in this context for more details.[30,79,92-95] Owing to their aqueous core, they have not only been investigated as drug careers, but have also been used as vehicles for proteins, DNA, and imaging agents. For the sake of space, only a few examples of these systems will be discussed in this section.

Discher and coworkers have elegantly used polymersomes composed of a blend of PEO-*b*-poly(lactic acid) and PEO-polybutadiene (PBD) to encapsulate both DOX and TAX. In this system, DOX was loaded into the aqueous cores of the polymersomes while TAX was entrapped within their hydrophobic membranes. The authors showed that when used *in vivo*, this system demonstrated a higher maximum tolerated dose and increased tumor shrinkage and maintenance compared to the case when both drugs were administered as free drugs.[96] In another example, Zhong and coworkers used a dually responsive polymersome for protein delivery.[97] Polymersomes were comprised of poly(ethylene glycol)-S-S-poly(2-(diethyl amino)ethyl methacrylate) diBCP. In this BCP, the poly(2-(diethyl amino)ethyl methacrylate block is the hydrophobic block that can be protonated under mildly acidic conditions, resulting in disintegration of polymersomes. Moreover, the disulfide bond ensures the responsiveness of polymersomes under intracellular-mimicking reductive environments. This BCP self-assembled into polymersomes of 55-67 nm, which were able to efficiently encapsulate proteins such as bovine serum albumin (BSA) and cytochrome C. The authors showed that while protein release was minimal at neutral pH and 37 °C, the release rate was significantly enhanced at pH 6.0 due to disintegration of the polymersomes. Interestingly, it was found that the fastest protein release occurred under intracellular-mimicking reductive environments (10

mM dithiothreitol, pH 7.4). These polymersomes were able to efficiently deliver cytochrome C protein to MCF-7 cells upon hours of incubation with the cells and induced increased apoptosis of the cells. Thus, polymersomes are promising delivery vehicles for future protein therapies, which currently suffer from delivery difficulties.

To demonstrate the potential of polymersomes for gene delivery, Li and coworkers[98] synthesized poly[(*n*-butyl methacrylate)-*b*-(*N*-acryloylmorpholine)] amphiphilic BCPs, self-assembled them into polymersomes, and used them for DNA delivery in gene therapy. Compared to the traditional polyethylenimine as a DNA complexing agent, these polymersomes exhibited improved plasmid DNA condensing efficiency, DNase I degradation protection, and cellular uptake by renal tubular epithelial and human hepatocellular carcinoma cell lines. Moreover, compared to polyethylenimine, these polymersomes were not cytotoxic and showed high serum stability, making them promising candidates for DNA delivery. In addition to their use for drug delivery purposes, polymersomes have also been employed for the encapsulation of various types of imaging agents. Some examples include the encapsulation of near infrared (NIR)-emissive porphyrin-based fluorophores,[99] hydrophilic lanthanide complexes,[100] and membrane-entrapped superparamagnetic iron oxide nanoparticles.[101]

1.2.2 Dendrimers for Biomedical Applications

Whether prepared by a convergent or divergent approach, dendrimers are still much more costly than conventional polymers. This means that over the longer term, the applications of dendrimers will almost certainly be limited to high value added products. One area that meets this criterion is biomedical materials, where the cost of a material is less important than its performance. In addition, very well-defined materials are typically required by regulatory agencies to approve their use in the human body. For this, the structural homogeneity of dendrimers that results from their iterative syntheses is a distinct advantage over other classes of synthetic macromolecules. As a result, the biomedical applications of dendrimers are starting to be widely investigated. The following subsections will discuss recent advances made in applications of dendrimers as drug careers, imaging agents, and multivalent carbohydrate scaffolds (glycodendrimers). A focus will be to explore how bioconjugation chemistry can be used to covalently attach

biologically relevant molecules to dendrimers. It will explore how the specific conjugation chemistries are determined based on the application, the chemical functionalities available on the molecules of interest and those on the dendrimer's focal point or periphery.

1.2.2.1   Dendrimer-Drug Conjugates

Among the currently studied drug delivery systems, dendrimers have emerged as an attractive class of materials, mainly because of their well-defined structures. In addition, they possess many peripheral groups for drug conjugation and their nanoscale sizes can lead to enhanced blood circulation times and selective accumulation in tumors via the EPR effect.

As reviewed recently in the context of chemotherapeutics,[51,52] drugs can be incorporated into dendrimers either by covalent conjugation to the periphery or by noncovalent encapsulation within the backbone of the dendrimer. Both classes of delivery systems have been demonstrated to be more effective than the free drug in certain laboratory studies and each approach is associated with its own advantages and disadvantages. However, control over the drug:dendrimer ratio in a noncovalent system can present challenges and noncovalently incorporated drugs are often released too rapidly under physiological conditions. This has limited their *in vivo* efficacy thus far. With the use of optimized chemical reactions, the covalent attachment of drugs to dendrimers benefits from superior control over the ratio of drug:dendrimer in the resulting conjugate. Moreover, the problem of the burst release observed for physically entrapped drugs upon injection can be mitigated to a great extent by covalently attaching drugs to dendrimers. In selecting the appropriate bioconjugation chemistry for dendrimer-drug conjugates, there are some important considerations. In order to achieve a controlled release of the drug from a dendrimer-drug bioconjugate, the linker stability under various physiological conditions is crucial. The lability of a given linker in a specific microenvironment plays an important role in the specificity and the rate of drug release. For example, to obtain selective and controlled release of drug in cancerous tissues or within the endosomes and lysosomes of cells, which are known to be more acidic than healthy tissues, an acid-labile linkage such as an ester or hydrazone can prove

effective.[102] In addition, the released drug derivative needs to be identical to, or as active as the original drug in order to be effective.[103]

The review of various dendrimer-drug conjugates is out of the scope of this thesis. For this purpose, readers are directed to several comprehensive reviews published in the literature.[52,104] Here, to illustrate the importance of the linkage type in pharmacological behavior of drugs, one example will be discussed. In this example, Kono and coworkers prepared PAMAM-DOX-PEO conjugates via both amide (Figure 1.10a) and hydrazone (Figure 1.10b) linkages and observed that the conjugates containing hydrazone linkages exhibited seven times higher cytotoxicity to HeLa cancer cells than the conjugates containing amides. This result highlights the importance of the more labile hydrazone linkage for the treatment of the cancerous cells. However, both conjugates showed lower cytotoxicity to the same cell line when compared to free DOX.[105]
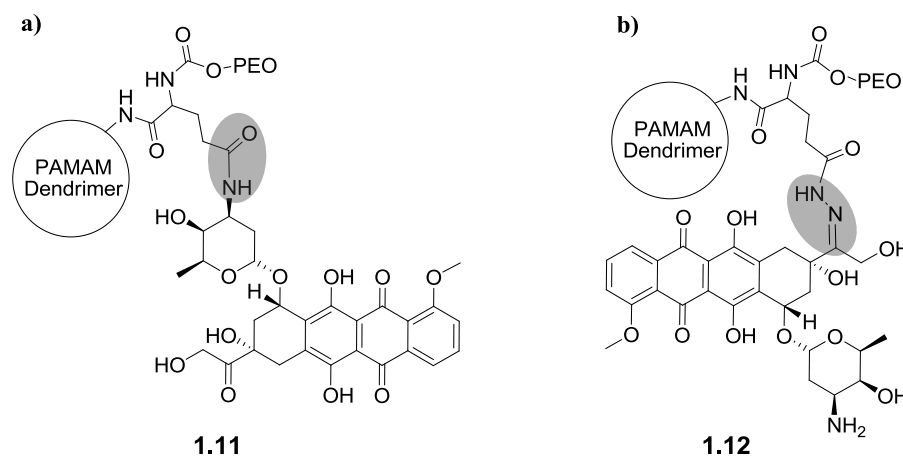
Figure 1.10. PAMAM-DOX conjugates with a) amide and b) hydrazone linkages

1.2.2.2 Dendrimer-Carbohydrate Conjugates

Carbohydrates are the most abundant group of natural products found on the earth. Aside from their important roles in supplying energy to cells and structural support to plants, carbohydrates are implicated in a vast array of biological processes. These include hormonal activities, fertilization, embryogenesis, neural development, and many other cellular processes such as cell-cell recognition, cell proliferation, cellular transport, viral infection, bacterial adhesion, and tumour cell metastasis.[106] Thus, it is not surprising that

the efficient synthesis of saccharides and their incorporation into various systems to obtain specific biological effects has attracted much attention in the past few decades. One such example is the tremendous effort that has been devoted to enhancing the multivalency of carbohydrates by incorporating them onto multivalent architectures such as dendrimers. It is known that multivalent interactions are prevalent in biology, such as in the adhesion of viruses and bacteria to cell surfaces and in the binding of cells to other cells.[107] Many of these processes involve the interactions of carbohydrates with protein receptors called lectins. While the interactions of individual carbohydrate ligands with lectins is often weak, multivalency provides a means of significantly increasing the strength of the interaction.[107]

A wide variety of nanoscale materials such as linear and HBPs, nanoparticles, and polymer assemblies can be used as backbones to present carbohydrates in a multivalent manner,[108-111] but the well-defined nature of the dendrimer backbone provides advantages. For example, the number of carbohydrate ligands present on a given molecule can be precisely determined, allowing advancements in the fundamental understanding of carbohydrate-lectin interactions. In addition, the product monodispersity and reproducibility in its synthesis is advantageous for the development of a clinical therapeutic. A wide range of saccharides including mannose, galactose, glucose, lactose, maltose, xylose, *N*-acetylneuraminic acid (Neu5Ac) (sialic acid), and other oligosaccharides have been conjugated to various dendrimer peripheries via different linkages such as amide, hydrazide, amine, thioether, thriourea, and triazole linkages.[112] Unlike dendrimer-drug conjugates, in which fine-tuned lability of the linkage is essential for controlled release of the drug, carbohydrates typically do not need to be released from the dendrimer periphery in order to exhibit activity. Thus, although the linkages can have modest effects on the binding affinities of multivalent carbohydrates, the choice of linkage is determined primarily by synthetic requirements. In this section, the conjugation of Neu5Ac, which is relevant to this thesis, to the peripheries of various dendrimer backbones will be discussed and the biological properties of the resulting bioconjugates will be briefly introduced. This discussion provides representative examples of the different conjugation chemistries that can be for coupling of dendrimers with carbohydrates.

1.2.2.2.1 Dendrimer-*N*-Acetylneuraminic Acid Conjugates

Neu5Ac is the most abundant sialic acid found in mammalian cells. This negatively charged molecule is found in complicated glycans on mucin and in glycoproteins that are embedded in cell membrane. It is known that all types of influenza viruses interact with Neu5Ac residues on the host cell surface through their trimeric lectin hemagglutinin (HA), and this is followed by endocytosis of the virus into the cell.[107] Monovalent Neu5Ac can inhibit this interaction at millimolar concentrations, but there is significant interest in the development of multivalent Neu5Ac derivatives in order to obtain higher binding affinity. For this purpose, various dendrimer-Neu5Ac conjugates have been developed. Different strategies to construct such bioconjugates is shown in Figure 1.11.
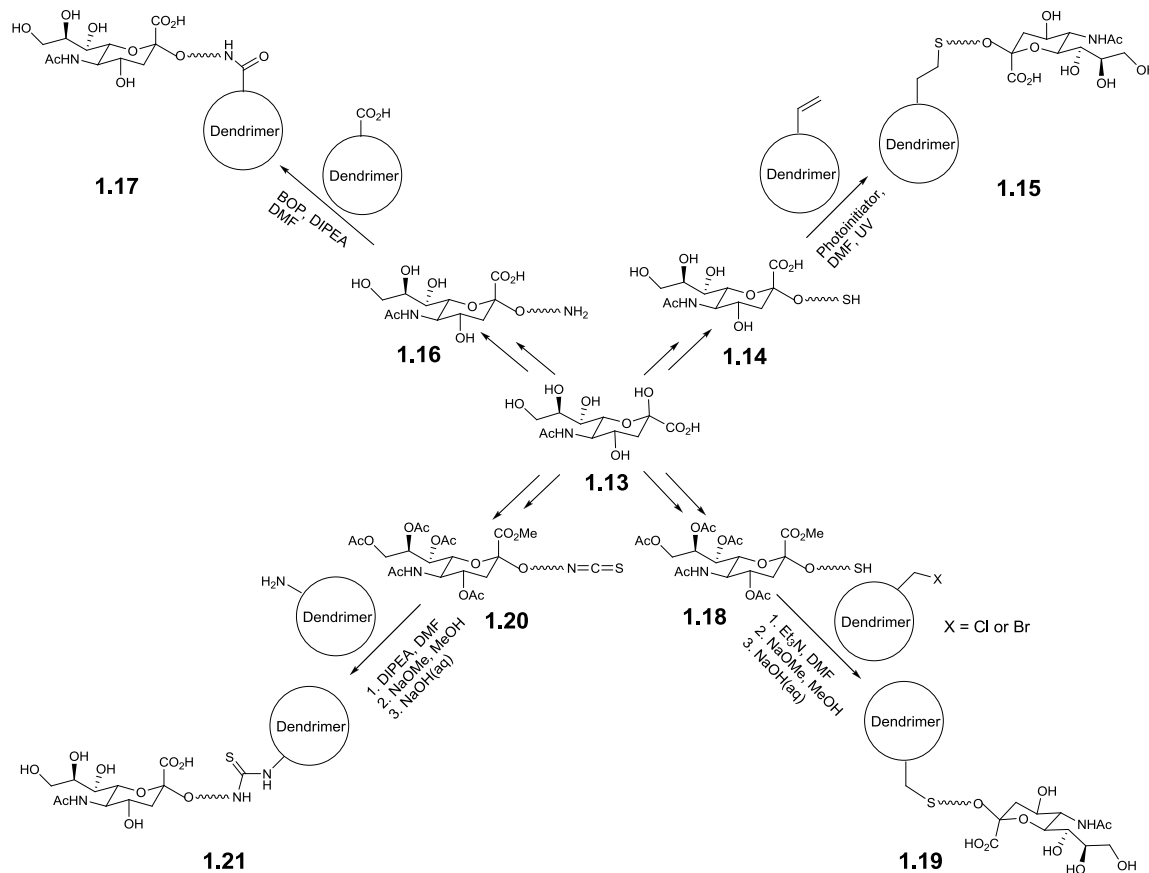
Figure 1.11. Conjugation strategies for Neu5Ac.

Thus far, the formation of a thioether linkage is the most commonly reported approach for the conjugation of Neu5Ac to the peripheries of dendrimers.[113-120] To construct these conjugates, a thiol must be installed on either sialic acid or on the dendrimer periphery. Because unprotected thiols tend to dimerize readily, a process that is facilitated on the dense peripheries of dendrimers, the introduction of the thiol to Neu5Ac has been a more viable approach. For example, Roy and coworkers have prepared a protected 2-α-thioacetyl-Neu5Ac and reacted it with three types of *N*-chloroacetylated dendrimers including polypeptide,[113] PAMAM,[114,115] and gallic acid-oligoethylene glycol dendrimers.[116] The acetyl groups on the sugars were then removed under basic conditions to yield the unprotected dendrimers. An enzyme-linked lectin inhibition assay using human α_1-acid glycoprotein as the coating antigen and horseradish peroxidase-labeled *Limax flavus* agglutinin (LFA) for detection purposes was performed. Their results showed that the globular dendrimer with a valency of 12 exhibited a 182-fold increase in inhibitory potency compared to the reference monomeric Neu5Ac.[115]

To investigate different spacers between Neu5Ac and dendrimers, Matsuoka and coworkers prepared a library of brominated carbosilane dendrimers with different types of spacers on their peripheries.[118,119] The thiol-functionalized Neu5Ac derivative was similar to that employed by Roy and coworkers but with an additional 5-carbon aliphatic spacer between the sugar and the thiol. Introduction of this molecule onto different brominated carbosilane dendrimers with either normal, ether elongated, or amide elongated peripheral groups was accomplished by initially treating the thioacetic acid-functionalized sugar and bromide terminated dendrimer mixture with sodium methoxide (NaOMe)/methanol (MeOH) in *N,N*-dimethylformamide (DMF) followed by addition of acetic anhydride/pyridine. Fully deprotected dendrimers were obtained by treatment of these dendrimers with NaOMe/MeOH and 0.1 M sodium hydroxide solution. Biological evaluations of these glycodendrimers showed that all of the ether- and amide-elongated compounds had inhibitory activities for the influenza sialidases in the millimolar range. Surprisingly, the glycodendrimers having normal aliphatic linkages did not exhibit any activities except for a dendrimer with a valency of 12.[119]

Hawker and coworkers recently reported the glycosylation of a 4th generation dendrimer via a free-radical thiol-ene coupling reaction between thiol-functionalized carbohydrates including Neu5Ac, mannose, glucose, and lactose and a dendrimer having peripheral alkene moieties.[120] This reaction results in the formation of a thioether linkage in high yield.

McReynolds and coworkers have investigated amide linkages between Neu5Ac and PAMAM dendrimers.[120] They have constructed their bioconjugates with or without spacers between the dendrimer and Neu5Ac. In the case without any spacers, commercially available Neu5Ac was directly conjugated to the amine peripheral groups of the dendrimers using (Benzotriazol-1-yloxy)tris(dimethylamino)phosphonium hexafluorophosphate (BOP). Alternatively, to minimize steric congestion between Neu5Ac and the dendrimer, a bifunctional spacer molecule was first conjugated to the carboxylic acid functionality of Neu5Ac. After deprotection of the other terminus of the spacer, which resulted in the formation of a free amine, it was coupled to the periphery of acid-functionalized PAMAM dendrimers. Subsequent sulfation of the conjugates was accomplished by reacting the obtained dendrimers with an SO_3-pyridine complex. When evaluated for inhibition of Human immunodeficiency virus (HIV)-1 infection, the sulfated Neu5Ac-PAMAM glycodendrimer bearing 16 Neu5Ac moieties with 11 sulfate groups was found to inhibit all four HIV-1 strains tested in the low micromolar range.

Finally, thiourea conjugates of Neu5Ac and dendrimers have also been prepared. An acetate protected *p*-isothiocyanatophenyl derivative of Neu5Ac was prepared and was coupled to the peripheral amines of PAMAM dendrimers to give the protected Neu5Ac dendrimers in high yields (71-100%).[121,122] Complete deprotection was accomplished by sequential ester hydrolysis in first NaOMe/MeOH followed by 50 mM NaOH solution to hydrolyze the acetyl followed by methyl ester groups. By performing a competitive enzyme-linked lectin assay, it was demonstrated that these dendrimers exhibited a substantial 210-fold increase in the inhibitory activity compared to monomeric Neu5Ac.[121]

1.2.2.3   Dendrimer Conjugates with Imaging Agents

With rapid developments in imaging technology, along with an increased focus on the early detection of diseases and the monitoring of treatment effects, there has been great interest in the development of new contrast agents for various imaging modalities including magnetic resonance imaging (MRI), x-ray computed tomography (CT), single photon emission computed tomography (SPECT), positron emission tomography (PET) and optical imaging. These contrast agents aid in distinguishing between normal and diseased tissues through their localization at specific sites *in vivo*. Among the new contrast agents under development, nanosized agents based on materials such as linear polymers, organic and inorganic nanoparticles, proteins, and dendrimers have received particular attention in recent years. When the size and chemical functionalities of these agents are optimized, they can exhibit significantly longer *in vivo* circulation times than small molecule analogues. This enables new applications such as vascular imaging and the targeting of specific disease sites such as tumors to be explored. In addition, nanosized agents enable the conjugation of multiple contrast agent molecules to a nanomaterial, enhancing the contrast on a per molecule or per particle basis. Furthermore, this same attribute can allow the conjugation of both contrast agents and targeting moieties or multiple contrast agents for different imaging modalities to the same system providing enhanced, multifunctional properties.

Among the various nanomaterials available, as previously discussed, the well-defined chemical structures of dendrimers provide a significant advantage in terms of reproducibility in the synthesis and resulting properties of the agents, allowing well-characterized materials to be prepared to the satisfaction of regulatory agents. Relevant to this thesis are dendrimer conjugates as MRI contrast agents. As a result, various examples involving the conjugation of MRI contrast agents will be described.

1.2.2.3.1   Dendrimer Conjugates for MRI

MRI is a prominent noninvasive imaging modality due to its excellent spatial resolution, soft tissue contrast, and the absence of harmful ionizing radiation in its application. Despite its high levels of soft tissue contrast, contrast agents based on small molecule

chelates of Gd(III) are frequently employed in clinical MRI scans to aid in the differentiation between healthy and diseased tissues.[123-125] These agents, which act by altering the relaxation times of the protons in nearby water molecules, have enabled significant advancements in MRI over the last couple of decades. However, the low contrast efficiency (ie. low relaxivity), fast renal excretion, and low specificity of these agents results in a requirement for high doses. This can be problematic for patients with chronic renal disease.[126] It can also limit their applicability in molecular imaging applications, where target receptors are present only at low concentrations.[127] Dendrimer-based MRI contrast agents have been intensively investigated over the past couple of decades for several reasons.[128,129] First they allow for the attachment of multiple MRI labels to a single scaffold, greatly increasing the molecular relaxivity and allowing a single targeting moiety to carry multiple labels. In addition, their size can be well-controlled by tuning both their core and generation, allowing their biodistribution properties to be tuned. Finally, because of the nanoscale dimensions of the dendrimer and steric hindrance at the periphery, the molecular tumbling rate of the conjugated Gd(III) chelates is significantly slowed, resulting in an increase in τ_R, the rotational correlation time. This can result in substantial enhancements in the longitudinal relaxivity (r_1) of the contrast agents, as predicted by Solomon-Bloombergen-Morgan theory, which is described in detail elsewhere.[123,130]

An important class of clinically used small molecule Gd(III) chelates is based on the ligand diethylenetriaminepentaacetic acid (DTPA) (Figure 1.12a). Seminal work by Lauterbur and coworkers in the area of dendrimer MRI contrast agents involved the conjugation of a DTPA derivative containing an aromatic isothiocyanate to various generations of PAMAM dendrimers having peripheral amine groups (Figure 1.12b).[131] Gd(III) was introduced in the final synthetic step. On a per ion basis, r_1 of this agent was found to be 34 mM^{-1}s^{-1}, about 6-fold greater than that of the clinical agent Gd(III)-DTPA (Magnevist®). This result was attributed to the slower tumbling rate of the chelates at the dendrimer periphery. Subsequently, a series of PPI dendrimer-DTPA conjugates up to the 5th generation were synthesized by Kobayashi and coworkers using the same linker chemistry and increasing relaxivity was observed with increasing generation, up to 29

mM^{-1}s^{-1}.[132] In other work, Meijer and coworkers used a different linker to conjugate the DTPA derivative (Figure 1.12c).[133] This resulted in a less significant increase in r_1, up to a maximum of 20 mM^{-1}s^{-1} for the 5th generation dendrimer. In this case, the flexibility of the linker likely allowed for relatively high local mobility of the chelates at the dendrimer periphery, illustrating the importance of the conjugation chemistry.
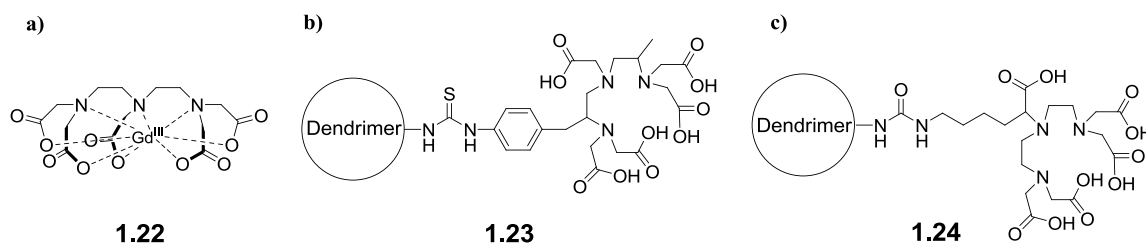
Figure 1.12. Chemical structures of: a) the clinical agent Gd(III)-DTPA (Magnevist®) and dendrimer conjugates of DTPA derivatives containing b) an aromatic isothiocyanate and c) a more flexible aliphatic isocyanate.

Another major class of clinical Gd(III) chelates is based on the ligand 1,4,7,10-tetraazacyclododecane-1,4,7,10-tetraacetic acid (DOTA) (Figure 1.13a). This chelate forms Gd(III) complexes that are kinetically and thermodynamically more stable than those formed with DTPA. Like DTPA, DOTA derivatives have also been conjugated to PAMAM dendrimers from the 2nd to 10th generations. Isothiocyanate linkages have commonly been used to conjugate these ligands to the peripheral amine groups of the dendrimer (Figure 1.13b). It was found that the ionic (per Gd(III)) r_1 values for these dendrimers plateaued at 36 mM^{-1}s^{-1} due to slow water exchange with the chelates, an important consideration for systems with long τ_R.[134,135] A derivative containing a phosphinic acid moiety in the linkage was also investigated with PAMAM dendrimers, resulting in good relaxivity values due to steric crowding and the formation of a secondary hydration sphere by the bulky phosphinate group (Figure 1.13c).[136,137] Researchers at Schering AG (Berlin, Germany) have developed Gadomer-17, bearing 24 DOTA derivatives attached to a lysine based dendrimer backbone via amide linkages (Figure 1.13d).[138] In a different approach, DOTA has also been incorporated at the core of polyglycerol dendrimers, where the motion of the Gd(III) should be coupled to the motion of the whole dendrimer.[139] The dendritic arms were conjugated to the chelates via

amide linkages. This indeed resulted in a remarkably high relaxivity of 39 mM^{-1}s^{-1}, though the rate of water exchange was slowest for the largest dendrimer limiting further gains in r_1.
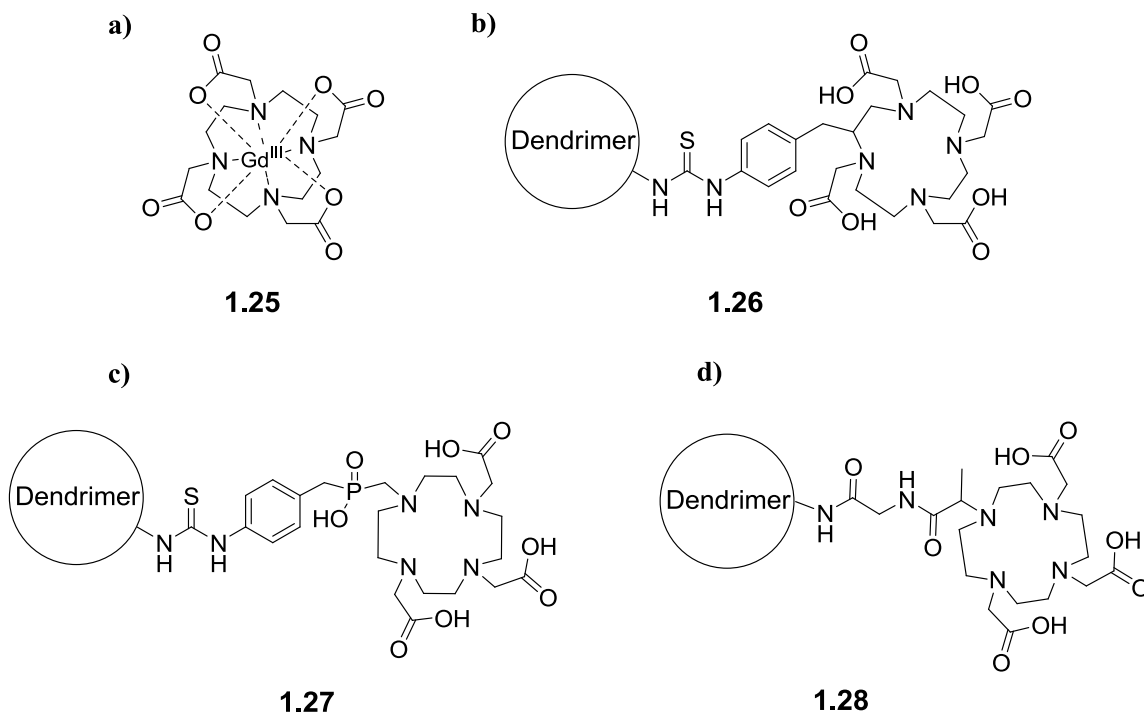
Figure 1.13. Chemical structures of: a) the clinical agent Gd(III)-DOTA (Dotarem®) and dendrimer conjugates of DOTA derivatives containing b) an aromatic isothiocyanate linker; c) a a phosphinic acid linker; d) an amino acid-based linker.

As described above, for the highest generation dendrimers, when τ_R is increased by substantially slowing the tumbling rates of the Gd(III) chelates, the rate of water exchange can be a limiting factor in achieving higher relaxivity values. Chelates with faster water exchange rates are desired. In addition, the coordination of multiple water molecules can also increase r_1. However, due to the toxicity of unchelated Gd(III), it is also critical to maintain the stability of the complexes. These aspects have been addressed by Raymond and coworkers through the development of a new class of ligands based on hydroxypyridinone (HOPO).[140] The Gd(III) chelates of these ligands bind two water molecules yet exhibit high stability due to their oxygen donor atoms and the high oxophilicity of the Gd(III) center. In addition, they possess rapid, near optimal water

exchange rates. This results in enhanced relaxivities about 2-fold higher than the DTPA or DOTA chelates.

   HOPO derivatives have also been incorporated into dendrimer systems. Initially, HOPO was conjugated to the focal point of a dendron based on aspartic acid and tris(hydroxymethyl)aminomethane via the formation of a rigid amide linkage between an aromatic carboxylate of the ligand and the amine of the focal point aspartic acid (Figure 1.14a).[141] HOPO derivatives have also been conjugated to the peripheries of PLL and esteramide dendrimers that also bear solubilizing poly(ethylene glycol) (PEG) chains.[142] In this case, N-(3-dimethylaminopropyl)-N'-ethylcarbodiimide (EDC)-mediated amide bond formation was performed using the peripheral carboxylic acids of the dendrimers and the amines of the HOPO chelates containing precomplexed Gd(III). This precomplexation was argued to prevent the nonspecific binding of Gd(III) to the dendrimer backbone, which might occur if a subsequent Gd(III) chelation step were performed. The effect of the linker was investigated and it was found that the shorter ethylene diamine spacer (Figure 1.14b) provided an r_1 of 38 mM^{-1}s^{-1} with the esteramide dendrimer, whereas a more flexible diethylene triamine spacer resulted in a lower r_1 of 32 mM^{-1}s^{-1} with the same dendrimer. In addition, the PLL dendrimer backbones resulted in lower relaxivity, perhaps due to increased hydrogen bonding between the dendrimer backbone and the water coordination sites or due to a shorter τ_R of the conjugated chelates. Overall, these results again demonstrate the importance of the bioconjugation chemistry, with shorter, more rigid spacers leading to the highest relaxivity values for Gd(III) contrast agents.
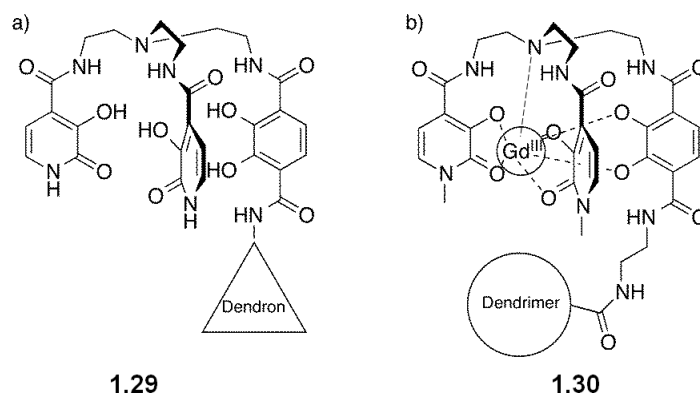
Figure 1.14. Dendrimer conjugates of HOPO derivatives using a) a rigid amide linkage between the carboxylic acid on the ligand and the dendron's focal point amine; b) an ethylene diamine spacer between the ligand and the dendrimer's peripheral carboxylic acids.

Several of the above dendrimer MRI contrast agents have been investigated *in vivo*.[128,129] In general, it has been found that low generation dendrimers such as the 3rd and 4th generations exhibit rapid renal clearance, while higher generations remain in the bloodstream for longer periods making them useful for the visualization of vasculature. The highest generation dendrimers such as the 8th and 9th generations tend to accumulate in the liver but they have also been useful for MR lymphangiography. Exploiting the multivalent peripheries of dendrimers, moieties for targeting specific tissues *in vivo* have been conjugated along side the Gd(III) chelates. However, a noteworthy example is a 4th generation dendrimer with DTPA and folic acid conjugated to the periphery, which enabled the selective labeling of ovarian cancer tumors overexpressing the folate receptor.[143,144]

1.3 Surface Functionalization of Polymersomes

As discussed in the earlier sections, a wide range of materials with various compositions and architectures have been developed for biomedical applications. While the bulk composition of a material is important for its function and long-term biocompatibility, the functionalities present at its surface are also critical. It is the surface of a material that will first come into contact with the biological system and as such will play a major role in its toxicity and biodistribution behavior.[145] The surface can also provide sites for the

introduction of drugs and moieties to target the material to specific sites *in vivo*.[146,147] Furthermore, the high levels of multivalency available at the surface of a material can provide therapeutic properties by inhibiting undesirable multivalent interactions between host cells and pathogens including bacteria and viruses using ligands such as carbohydrates.[107,148] Of particular interest to this thesis are polymersomes. In this section, approaches to the surface functionalization of polymersomes with a focus on dendritic groups will be discussed.

Two main approaches for the surface functionalization of polymersomes with functional ligands can be envisioned. In the first approach, polymersomes with functional handles on their surfaces are first formed. In a second step, ligands of interest with complementary functional groups are installed onto their surfaces. The attachment of the ligands onto the surfaces of polymersomes via this approach can be accomplished through either covalent or non-covalent attachment of the ligand. Covalent attachment of the ligand takes advantage of high-yielding chemical reactions such as Cu(I)-catalyzed alkyne-azide cycloaddition click reactions, thiol-*N*-hydroxysuccinimidyl ester and thiol-vinyl sulfone reactions to form S-C bonds, amine- succinimidyl ester reactions to form amide bonds, aldehyde-amine reactions to form imines, and conjugation reaction via bis-arylhydrazone bond formation.[149,150] On the other hand, in functionalization of polymersomes via the non-covalent attachment approach, strong non-covalent attractions such as biotin–streptavidin binding, nitrilotriacetic acid–metal complexation binding, and cyclodextrin–adamantane interactions have been employed.[149,150] One advantage of covalent over non-covalent attachment of ligands is the increased ligand binding stability, which is accompanied with its higher site specificity and reproducibility. Using these two methods various surface ligands have been conjugated to the surface of polymersomes including proteins, peptides, dendrons, carbohydrates, imaging agents, and antibodies [93,94,149,150].

In the second approach, the hydrophilic terminus of the BCPs is first pre-functionalized with the ligand of interest. In the second step, the functionalized BCP is used for polymersome formation. As a result, this approach makes it possible to isolate, purify, and characterize the newly functionlized polymer. In addition, by blending

appropriate ratios of the functionalized and non-functionalized polymers it is possible to have precise control over the surface density of desired ligand. However, a disadvantage of this approach is that potentially 50% of the ligands will be inaccessible in the interior of the polymersome for the given application. Applying this approach, different carbohydrates and organic dyes have been incorporated onto the surfaces of polymersomes.[93,94,149,150]

1.3.1 Dendritic Surface Functionalization of Polymersomes

Based on the unique properties of dendrons and dendrimers discussed in the earlier sections, the introduction of dendritic groups to polymersome surfaces provides the opportunity to alter the surface chemistry in a single step without changing the BCPs comprising the polymersome membranes. This provides a unique opportunity to impart new biological properties and functions.

In previous work by the Gillies group,[151] as shown in Figure 1.15, polymersomes composed of the amphiphilic linear diBCP poly(butadiene-*b*-ethylene oxide) (PBD-PEO) were used. An azide was introduced to the polymer terminus and polymersomes were prepared containing varying ratios of the azide and hydroxyl terminated polymers. A polyester dendron, having an alkyne focal point and peripheral amine groups with ~1 rhodamine dye per dendron, was reacted with the polymersomes under standard click conditions involving $CuSO_4$, sodium ascorbate, and the ligand bathophenanthrolinedisulfonic acid. It was found that the use of this ligand prevented the adsorption of copper ions to the dendritic amines. The conjugation yields for the various polymersomes were quantified based on the ultraviolet (UV)-visible absorbance of the rhodamine dye on the dendrons.
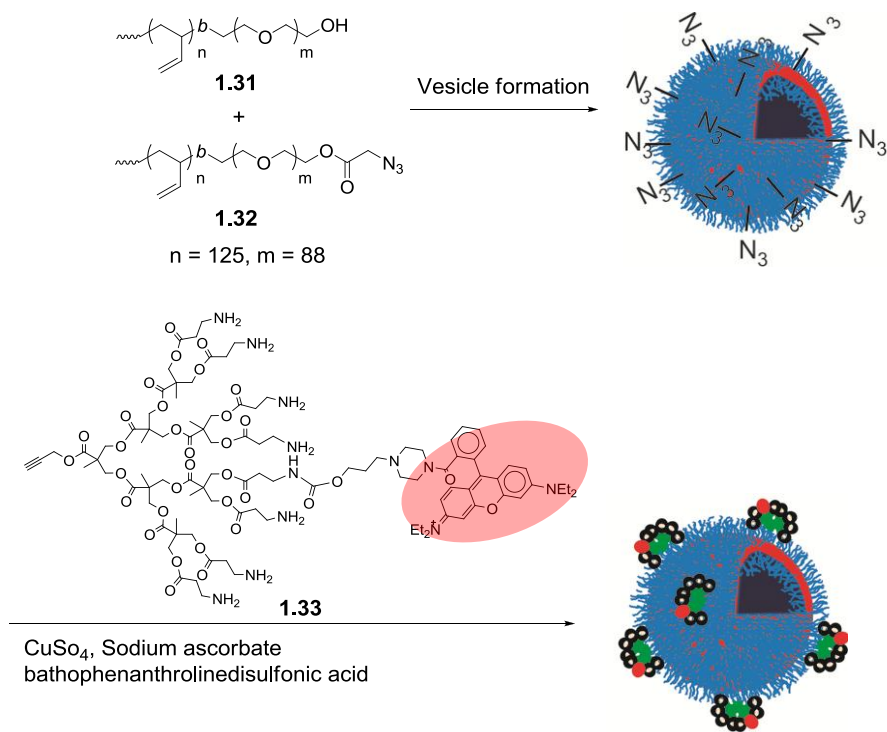
Figure 1.15. Schematic showing the functionalization of polymersomes bearing peripheral azide groups with dendrons having focal point alkynes.

It was found that the conjugation yields were typically greater than 60% at low surface azide content (≤ 20%). This was greater than expected as ~50% of the azides would be on the interior of the polymersome and it was not expected that the dendrons could pass through the membrane into the polymersome's aqueous core. However, it is likely that through various processes, some interior azides can move to the surface during the 24 h reaction time. At higher azide content, the conjugation yields dropped off dramatically. This was attributed to steric hindrance at the polymersome surface due to the bulky nature of the dendrons. In addition, well-dispersed polymersomes were observed at low azide content. On the other hand, at higher azide content, significant aggregation was observed which may be attributed to either a disruption of the hydrophilic/hydrophobic balance within the polymersome membrane upon dendron conjugation, or to interactions between the dendrons on different polymersomes. However, at azide content ≤ 20% this method was highly promising for the surface functionalization of polymersomes. Overall, this proof of concept study indicated that this approach could be used as an effective method to impart new properties to polymersomes.

In a subsequent study, the surface functionalization of PBD-PEO polymersomes with dendritic versus non-dendritic ligands was studied.[152] Mannose was selected as the ligand as its multivalent binding to targets such as Concanavalin A (Con A) has been extensively investigated and a number of assays have been developed to evaluate this binding. In this study, a 3rd generation mannose-functionalized polyester dendron as well as a mannose-terminated PBD-PEO BCP were prepared (Figure 1.16). As shown in Figure 1.16a, dendritic mannose polymersomes were prepared by the "click" conjugation of the mannose dendron to polymersomes containing 5% azide-functionalized PBD-PEO. Non-dendritic mannose polymersomes were prepared by the assembly of polymersomes from a 50:50 mixture of mannose and hydroxyl-terminated polymers (Figure 1.16b). These quantities were selected in order to provide the same overall mannose content in the dendritic and non-dendritic polymersomes, but displayed in a different manner.
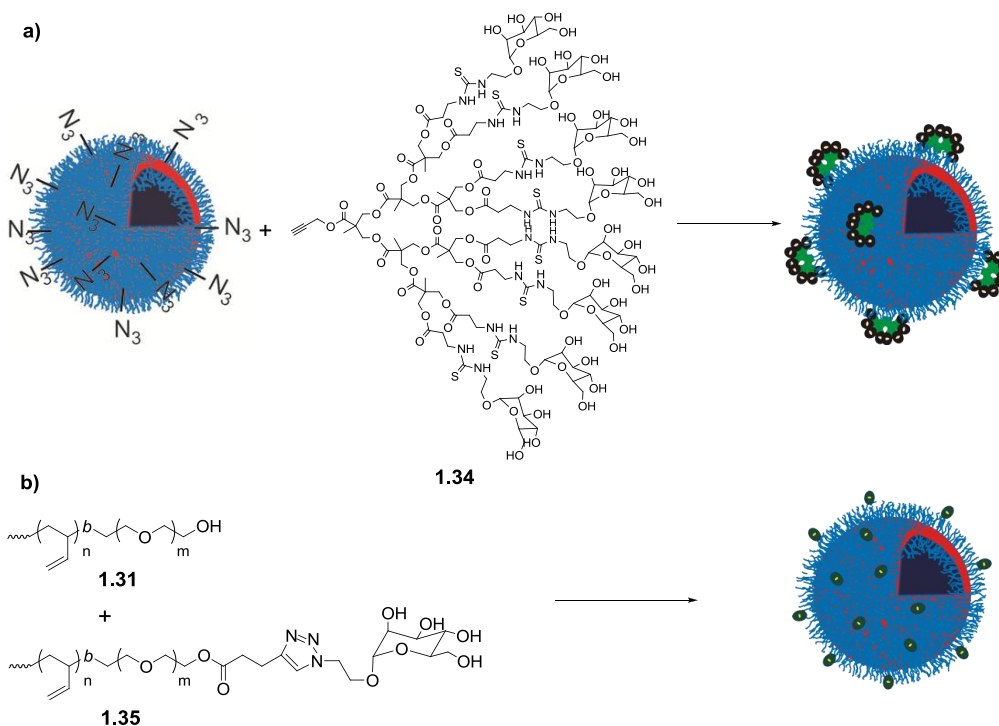
Figure 1.16. Schematic for the preparation of a) dendritic mannose polymersomes; b) non-dendritic mannose polymersomes.

The dendritic and non-dendritic polymersomes were compared using a hemagglutination assay. The results showed that despite their multivalency, the non-

dendritic polymersomes provided only a very modest 3.7-fold enhancement in affinity on a per mannose basis. In contrast, the dendritic mannose functionalized polymersomes provided a much greater 42-fold increase in relative binding affinity. This enhancement relative to the non-dendritic system was attributed to several factors including the relatively rigid display of ligands on the dendritic scaffold resulting in an entropic advantage, the ability of the dendritic scaffold to overcome steric inhibition of binding by the PEO layer, and an enhanced "proximity" effect resulting from the clustered display of ligands on the dendron. Through the preparation of the analogous dendritic and non-dendritic systems on dextran coated superparamagnetic iron oxide nanoparticles, it was demonstrated that these enhancements were generalizable to other nanoparticles and other polymer coatings in addition to PEO.[153] Thus, this study revealed that it is important to consider carefully not only the choice of biological ligand, but also the mode in which it is conjugated to the surface in order to exploit the benefits of nanomaterials. Furthermore, it showed that dendritic scaffolds are an effective means of displaying biological ligands on surfaces.

1.4 Stimuli Responsive Dendrimers

As described above, dendrimers have been explored in a broad range of biomedical applications.[154,155] Despite these advancements, the area of responsive dendrimers (dendrimers that can either disassemble or change their conformation in response to external stimuli) is in its infancy. This field is of a great importance because triggering such behavior in a controlled manner can impart new properties and expand their scope of applications. External stimuli used thus far for the triggering of stimuli-responsive dendrimers include pH,[156,157] light,[158] temperature,[159,160] and redox state.[161,162] In this section, representative examples of each stimulus will be discussed with an emphasis on light-responsive dendrimers. For exhaustive examples of stimuli-responsive dendrimers, readers are referred to review articles published in this field.[163-165]

It is known that tumor cells along with lysosomes and endosomes of healthy cells have a mildly acidic pH. As a result, delivery vehicles that are sensitive to variations in pH can act as smart materials for the selective delivery of drugs in such micro-environments. In a study by Pistolis and coworkers,[156] the peripheral groups of a PPI dendrimer were first

functionalized with quaternary ammonium salts. This positively charged dendrimer was used to physically encapsulate pyrene as a model drug. In the next step, the release behaviour of this system at low pH values was followed by fluorescence studies. It was found that when the pH was decreased from 11 to 2-4 by addition of hydrochloric acid, the fluorescence intensity of the system was enhanced dramatically as a result of pyrene release. It was proposed that such an acidic pH results in protonation of internal secondary and tertiary amine groups of the dendrimer, which in turn increases its hydrophilicity. Such an increase in the hydrophilicity of the system results in the release of the cargo. Although not pointed out by the authors, the increase in the internal volume of the dendrimer as a result of the repulsion between the positive charges of the protonated amines cannot be ignored. In another study by Fréchet and coworkers,[157] the peripheral groups of either polyester or polylysine dendrons were functionalized with hydrophobic groups via highly acid-labile cyclic acetal groups. These dendrons were then functionalized with PEO at the focal point to obtain linear-dendritic BCPs. It was shown that these materials were able to undergo self-assembly to form stable micelles at neutral pH. These micelles were used to encapsulate Nile Red as a model drug in their hydrophobic dendritic core. Upon exposure to mildly acidic pH, Nile Red was released from the micelles as a result of acetal hydrolysis, which results in disintegration of micelles by disturbing the hydrophilic-hydrophobic balance of the system.

Dendrimers that can release their payload in response to temperature are also highly attractive systems as advanced materials. These materials have the potential to be used in thermotherapy. The response often observed as a result of a change in temperature is a change in the solubility of the macromolecule. This can be accomplished by modifying dendrimers with a molecule that exhibits a lower critical solution temperature (LCST). This is a temperature above which a molecule becomes insoluble due to entropic factors. For example, Kimura and coworkers[159] reported the synthesis of a thermoresponsive dendrimer in which the catalytic activity of the encapsulated molecule showed a significant increase upon increasing the temperature of the system from 25-37 °C. The thermoresponsive dendrimer was constructed by first reacting the peripheral amine groups of a 3rd generation PPI dendrimer with 11-(thioacetyl)-undecanoic acid followed by the hydrolysis of the thioacetyl groups to install thiols on the dendrimer. In the second

step, these thiols were used as chain transfer reagents for free radical polymerization of *N*-isopropylacrylamide (NIPAAm). The resulting dendrimer was used to encapsulate a water-soluble cobalt(II) phthalocyanine complex which is a known catalyst for thiol oxidation. It was observed that catalytic activity of this system for the oxidation of mercaptoethanol was only 6% of that with the PPI dendrimer at 25 °C. This implies that PNIPAAm arms effectively restrict the penetration of starting materials (thiols and dioxygen) to the catalytic site inside the dendrimer. However, at a temperature above the LCST of the PNIPAAm arms (34 °C), a dramatic increase in the turnover frequency of the catalyst was observed. The authors concluded that below LCST of the PNIPAAm arms, these chains are soluble and expand over the dendrimer core and sterically hinder substrate penetration. Above the LCST, the PNIPAAm arms phase-separate and shrink which results in accessibility of the catalytic center to substrates. In addition, Kono and coworkers showed that functionalization of the periphery of PAMAM dendrimers with phenylalanine imparts thermoresponsive behaviour to the resulting dendrimers.[160] They were able to show that the LCSTs of such dendrimers were tuneable by the introduction of more hydrophilic amino acid residues, as well as through changes in dendrimer generation and pH.

To prepare redox-responsive materials, McCarley and coworkers took advantage of trimethyl-locked quinones (TLQ) as redox-active moieties. They prepared G1-5 PPI dendrimers functionalized with this redox-active group on their peripheries.[162] Using $Na_2S_2O_4$ as a chemical reducing agent, they demonstrated successful liberation of the peripheral groups from the dendrimers as lactones. Intramolecular reaction of the hydroxyl groups, formed from the quinone reduction, with the amide-containing substituents on the quinone moiety resulted in the liberation of the above-mentioned lactones. Interestingly, this process did not show any generation-dependent rates and reached completion in about 20 minutes (min) for all generations. In a subsequent study by the same group, electrochemical reduction of the same dendrimers was also demonstrated to be an effective way of achieving dendrimer peripheral group cleavage. The authors showed that bulk electrochemical reduction of dendrimers resulted in PPI dendrimers with dianionic TLQ^{2-} peripheral groups which produced the transient hydroquinone intermediates upon protonation with water. These intermediates were

finally liberated from the dendrimers as lactones in the same fashion as the chemically-induced pathway.[161]

In addition to conventional dendrimer backbones mentioned above, non-conventional dendritic backbones such as cascade release dendrimers have also been used as responsive dendrimers. In this case, stimuli such as enzymes and light have been applied to trigger the release of drug molecules. This class of materials has been recently reviewed.[166]

1.4.1 Photodegradable Dendrimers

Among the above-mentioned stimuli, light is of particular interest for the development of smart materials as it can be applied at a specific time and location, with control over its intensity and wavelength. Among the many photocleavable groups that have been investigated, *o*-nitrobenzyl ester derivatives have gained tremendous attention. This photolabile group was initially used as a protecting group in organic synthesis.[167] The mechanism of action for this group is based on the photoisomerization of the *o*-nitrobenzyl ester group into the corresponding *o*-nitrosobenzaldehyde and the release of the corresponding carboxylic acid upon irradiation with UV light (Scheme 1.1). This mechanism has been the subject of in-depth studies recently by Wirz and coworkers.[168] This isomerization and cleavage of the ester bond often occur within minutes upon exposure to 300-360 nm light. The irradiation wavelength can be tuned by including substituents on both the aromatic ring and the benzylic position of the linker.

R' = H, CH₃
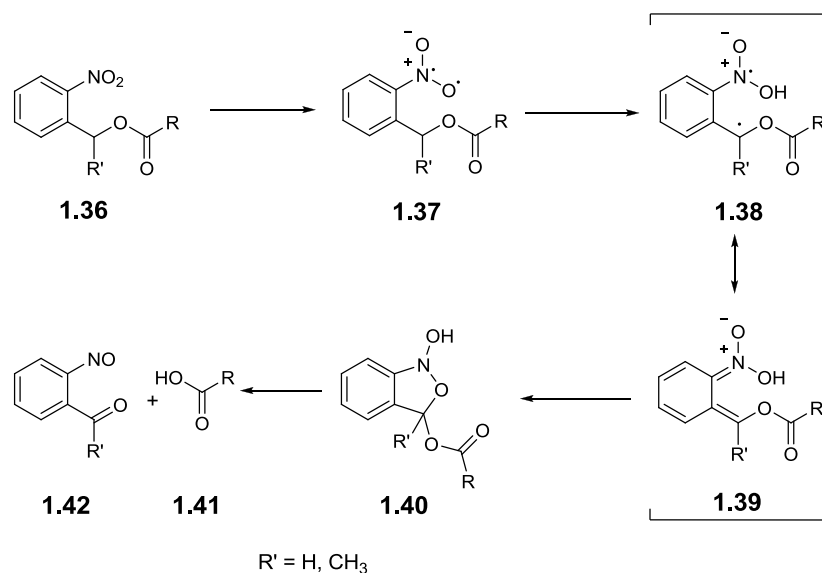
Scheme 1.1. Photoisomerization mechanism for *o*-nitrobenzyl ester derivatives.

Application of the photolabile *o*-nitrobenzyl ester group has not been restricted to organic synthesis and protecting groups. In fact, numerous applications of this moiety in polymer and materials science within different backbones such as BCPs, hydrogels, and dendrimers have been the subject of several reviews.[165,169,170] In the context of dendritic materials, systems have been developed through the incorporation of photodegradable units either at the core of the dendrimer[171] or at the junction between the hydrophobic and hydrophilic portions of amphiphilic dendrons.[158,172]

In an early example, photolabile dendrimers based on *o*-nitrobenzyl ester groups in which the photolabile moieties were installed at the cores of the dendrimers were reported by McGrath and coworker.[171] In this study, first through third generation dendrimers that contained three *o*-nitrobenzyl ester groups at their cores were synthesized. Due to the hydrophobic backbones of the dendrimers, their photolysis was carried out in chloroform. The degradation studies revealed that upon irradiation with 350 nm light, these dendrimers released discrete dendrons as shown in the cartoon in Figure 1.17.
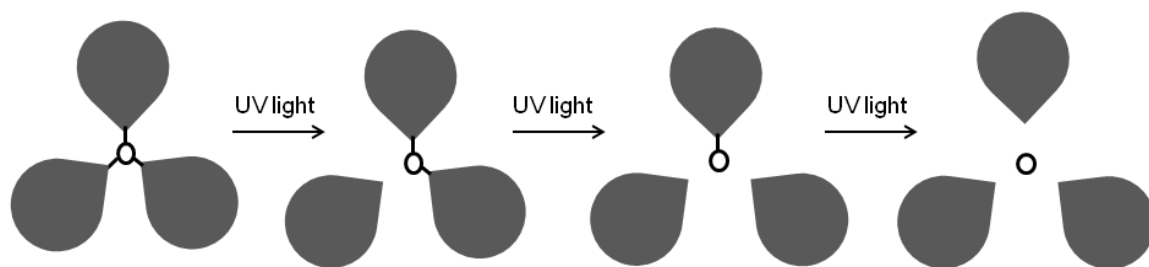
Figure 1.17. Schematic representation of sequential photodegradation of dendrimers functionalized with three *o*-nitrobenzyl ester groups at their core.

In a second study by Kostiainen and coworkers,[172] first and second generation amphiphilic dendrons with hydrophilic spermine peripheral groups and *o*-nitrobenzyl ester groups at the junctions between the hydrophilic and hydrophobic segments were synthesized. The chemical structures of these dendrons are shown in Figure 1.18. The photolytic behaviors of these dendrons were first studied in aqueous media by irradiating dendron solutions at 350 nm. The results showed that the degradation needed only 200 seconds to reach completion. As an application of these optically triggerable dendrons, they were used for complexation of DNA. It was found that both generations of the dendrons were able to effectively bind to DNA with the second generation dendron having slightly higher binding strength compared to the first generation dendron due to the increased multivalent effect at higher generations of dendrons and dendrimers. To release DNA, the complexed samples were irradiated at 350 nm. The authors showed that at a lower NaCl concentration of 9.4 mM, dendrons were able to release the DNA within only 90 seconds, while at higher salt concentration of 150 mM, the release time was decreased. The DNA release behaviour of the dendrons were also confirmed by light scattering, ς-potential, and gel electrophoresis measurements.
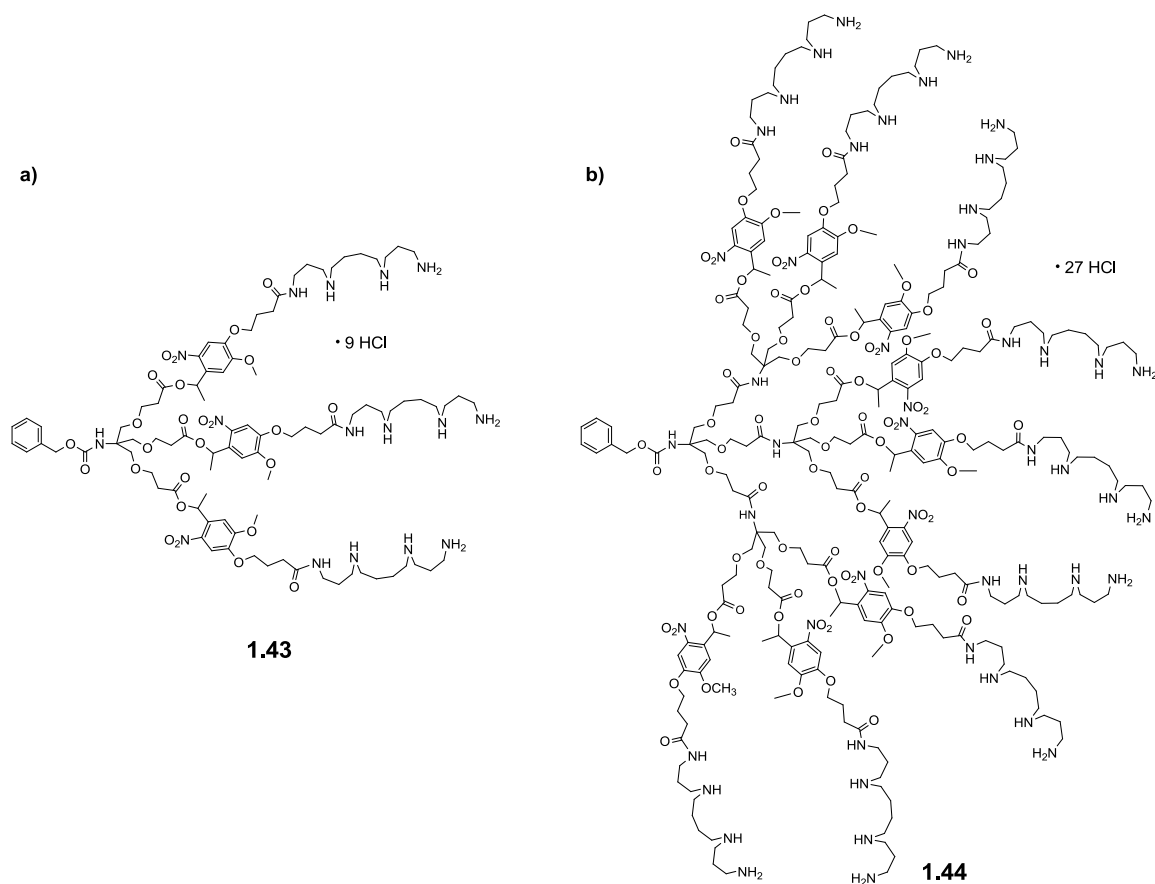
Figure 1.18. Chemical structures of a) first generation and b) second generation photodegradable amphiphilic dendrons used for DNA complexation and release.

More recently, Thayumanavan and coworkers developed nanocontainers comprised of photodegradable amphiphilic dendritic structures that are capable of encapsulation and release of hydrophobic guest molecules.[158] First and second generation dendrons in this study were based on hydrophilic oligo ethylene glycol groups and hydrophobic alkyl chains which were conjugated together through *o*-nitrobenzyl ester linkers (Figure 1.19). It was found that the micellar structures formed by G1 and G2 dendrons in aqueous media were 80 and 85 nm in diameter respectively. In the next step, the micelles were used to encapsulate Nile Red as a model hydrophobic drug within their hydrophobic cores. To study the release of the cargo from the micelles, Nile Red-containing micelles were irradiated with 365 nm light and the release of the organic dye was monitored by fluorescence spectroscopy. The authors showed that after 200 seconds, the G1 dendron

was able to release up to 88% of the loaded guest molecule while this value for the G2 dendron was about 72%, presumably due to the more tightly packed nature of the micelles obtained from the G2 dendron. Moreover, it was observed by dynamic light scattering (DLS) measurements, that the sizes of the assemblies were decreased from about 80 nm down to about 37 nm by irradiating the micellar samples with UV light.
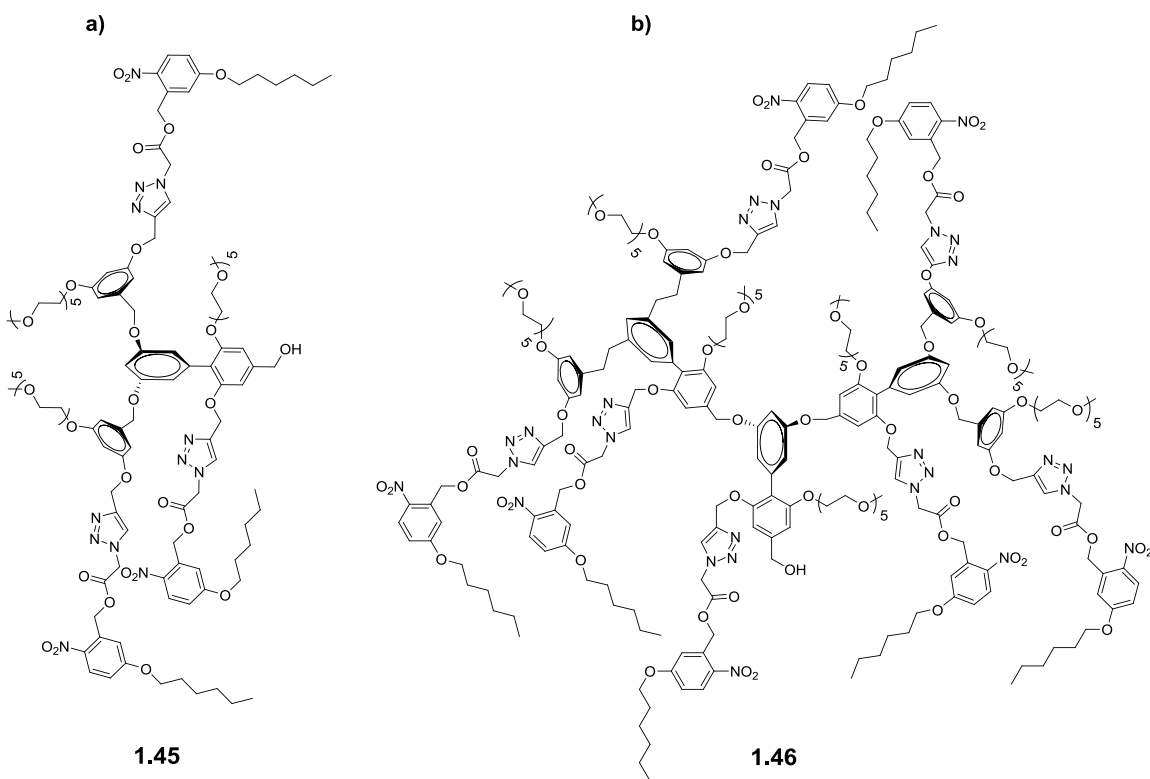
Figure 1.19. Chemical structures of a) first generation and b) second generation amphiphilic photodegradable dendrons used for encapsulation and release of Nile Red.

These examples highlight the potential of such photo-responsive dendrimers for biomedical applications. However, to better achieve this goal, dendrimers that could respond to NIR or visible wavelengths of light are highly desirable. This demands extensive research on developing chromophores that absorb light at higher wavelengths or a combination of dendrimers with metal nanoparticles, such as up-converting nanoparticles, that are capable of absorbing light in NIR or visible region and converting it to UV light. In such an example, Almutairi and coworkers have developed self-immolative dendritic scaffolds caged with a coumarin derivative that are capable of

releasing their terminal groups (in this case L-glutamic acid) in response to two photons of NIR light.[173] The structures of the quinone-methide based dendrimers used in this study are shown in Figure 1.20. NIR light-induced release of the L-glutamic acid terminal groups occurs via a cascade of molecular rearrangements upon the removal of the caging coumarin derivative.
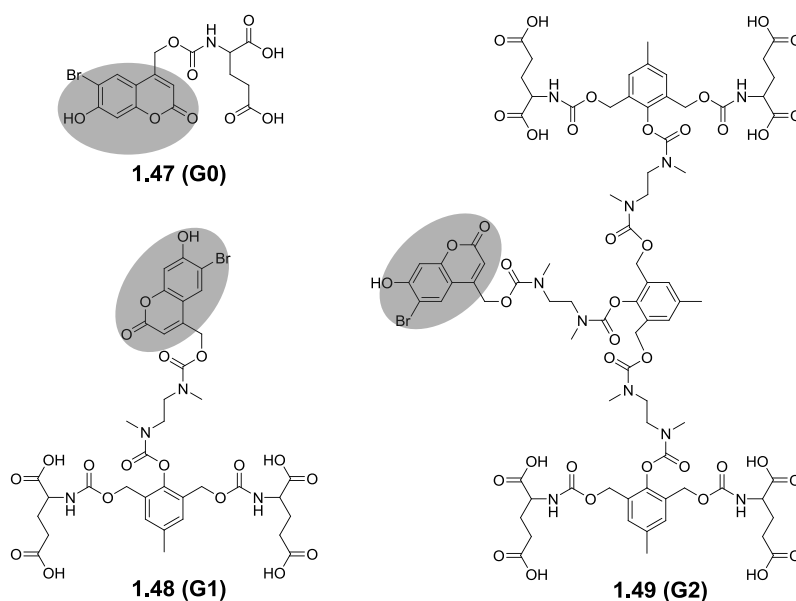
Figure 1.20. Structures of photodegradable dendrimers containing coumarin as NIR light-degrading groups.

1.5 Scope of This Thesis

The main goal of this thesis is to demonstrate the potential of biodegradable and biocompatible polymersomes, conventional and photodegradable dendrimers and dendrons, and polymersome-dendron hybrid materials toward biomedical applications. When work began on this thesis, the concept of dendritic surface functionalization of polymersomes was previously developed by our group. However, based on the fact that in the previous work, non-biodegradable polymersomes with unknown biocompatibilty were used, one of the first goals of this thesis was to develop biocompatible and biodegradable drug delivery systems. Once this was accomplished, several biomedical applications of the system, such as MRI contrast agents and potential antiviral agents, were pursued using these constructs. In addition, a new photodegradable dendritic

backbone was developed with the ultimate goal of constructing dendrimer-based vesicles, known as dendrimersomes, as *smart materials* for the controlled release of drugs.

Chapter two focuses on development of biocompatible and biodegradable polymersomes based on poly(ethylene oxide)-*b*-polycaprolactone (PEO-PCL) BCPs. The synthesis of azide-functionalized PEO-PCL BCPs and their assembly into polymeric micelles and vesicles with activated surface azide groups will be shown. The surface functionalization of these assemblies with both dendritic groups and small molecules will be discussed.

Chapter three will describe the application of PEO-PCL polymersomes as scaffolds for the development of polymersome-dendritic hybrid materials as effective MRI contrast agents. It will be shown how nanoscale components can be readily combined to provide additive enhancements in relaxivity of MRI contrast agents.

Chapter four describes the development of a polymersome-based potential influenza virus inhibitor agent. The synthesis of sialic acid-functionalized polyester dendrons, their installation onto polymersome surfaces, and evaluation of their inhibitory potentials will be shown in this chapter.

Chapter five describes the synthesis of backbone photodegradable dendrons and dendrimers by the incorporation of photodegradable *o*-nitrobenzyl ester moieties into the widely used 2,2-bis(hydroxymethyl) propionic acid (bis-MPA) dendrimer backbone. The photodegradation behaviours of G1-3 dendrimers will also be discussed.

Chapter six will demonstrate the incorporation of photodegradable dendrons into AJDs which will be shown to self-assemble to form dendrimersomes with a photodegradable membrane with the goal of encapsulation and triggered release of hydrophilic and hydrophobic model drugs.

Chapter seven will summarize the key results discussed in previous chapters in the context of the field and will outline the future directions for the ongoing projects.

1.6 References

1. Elias, H. G. *Macromolecules, Volume 1: Chemical Structures and Syntheses*; Wiley-VCH Verlag GmbH & Co. KGaA: Weinheim, 2005.

2. Vert, M. *Biomacromolecules* **2005**, *6*, 538.

3. Zilberman, M.; Eberhart, R. C. *Annu. Rev. Biomed. Eng.* **2006**, *8*, 153.

4. Vainionpaa, S.; Rokkanen, P.; Tormala, P. *Prog. Polym. Sci.* **1989**, *14*, 679.

5. Yaszemski, M. J.; Payne, R. G.; Hayes, W. C.; Langer, R.; Mikos, A. G. *Biomaterials* **1996**, *17*, 175.

6. Zhang, J. Y.; Beckman, E. J.; Piesco, N. P.; Agarwal, S. *Biomaterials* **2000**, *21*, 1247.

7. Aframian, D. J.; Redman, R. S.; Yamano, S.; Nikolovski, J.; Cukierman, E.; Yamada, K. M.; Kriete, M. F.; Swaim, W. D.; Mooney, D. J.; Baum, B. J. *Tissue Eng.* **2002**, *8*, 649.

8. Lee, S. H.; Kim, B. S.; Kim, S. H.; Choi, S. W.; Jeong, S. I.; Kwon, I. K.; Kang, S. W.; Nikolovski, J.; Mooney, D. J.; Han, Y. K.; Kim, Y. H. *J. Biomed. Mater. Res., Part A* **2003**, *66A*, 29.

9. Guan, J. J.; Fujimoto, K. L.; Sacks, M. S.; Wagner, W. R. *Biomaterials* **2005**, *26*, 3961.

10. Ulery, B. D.; Nair, L. S.; Laurencin, C. T. *J. Polym. Sci., Part B: Polym. Phys.* **2011**, *49*, 832.

11. Nicolas, J.; Mura, S.; Brambilla, D.; Mackiewicz, N.; Couvreur, P. *Chem. Soc. Rev.* **2013**, *42*, 1147.

12. Manners, I. *Angew. Chem., Int. Ed.* **2007**, *46*, 1565.

13. Mai, Y.; Eisenberg, A. *Chem. Soc. Rev.* **2012**, *41*, 5969.

14. Aoshima, S.; Kanaoka, S. *Chem. Rev.* **2009**, *109*, 5245.

15. Szwarc, M. *Nature* **1956**, *178*, 1168.

16. Webster, O. W.; Hertler, W. R.; Sogah, D. Y.; Farnham, W. B.; Rajanbabu, T. V. *J. Am. Chem. Soc.* **1983**, *105*, 5706.

17. Wang, J. S.; Matyjaszewski, K. *J. Am. Chem. Soc.* **1995**, *117*, 5614.

18. Matyjaszewski, K.; Xia, J. H. *Chem. Rev.* **2001**, *101*, 2921.

19. Lowe, A. B.; McCormick, C. L. *Prog. Polym. Sci.* **2007**, *32*, 283.

20. Hawker, C. J.; Bosman, A. W.; Harth, E. *Chem. Rev.* **2001**, *101*, 3661.

21. Leitgeb, A.; Wappel, J.; Slugovc, C. *Polymer* **2010**, *51*, 2927.

22. Buchmeiser, M. R. *Chem. Rev.* **2000**, *100*, 1565.

23. Alexandridis, P.; Lindman, B. *Amphiphilic Block Copolymers: Self-Assembly and Applications*; Elsevier: Amsterdam: New York, 2000.

24. Cornelissen, J.; Fischer, M.; Sommerdijk, N.; Nolte, R. J. M. *Science* **1998**, *280*, 1427.

25. Pochan, D. J.; Chen, Z. Y.; Cui, H. G.; Hales, K.; Qi, K.; Wooley, K. L. *Science* **2004**, *306*, 94.

26. Zhang, L. F.; Eisenberg, A. *Science* **1995**, *268*, 1728.

27. Discher, D. E.; Eisenberg, A. *Science* **2002**, *297*, 967.

28. Yan, D. Y.; Zhou, Y. F.; Hou, J. *Science* **2004**, *303*, 65.

29. Cui, H. G.; Chen, Z. Y.; Zhong, S.; Wooley, K. L.; Pochan, D. J. *Science* **2007**, *317*, 647.

30. Blanazs, A.; Armes, S. P.; Ryan, A. J. *Macromol. Rapid Commun.* **2009**, *30*, 267.

31. Ahmed, F.; Photos, P. J.; Discher, D. E. *Drug Dev. Res.* **2006**, *67*, 4.

32. Zhang, S. Y.; Zhao, Y. *J. Am. Chem. Soc.* **2010**, *132*, 10642.

33. Letchford, K.; Burt, H. *Eur. J. Pharm. Biopharm.* **2007**, *65*, 259.

34. Discher, B. M.; Won, Y. Y.; Ege, D. S.; Lee, J. C. M.; Bates, F. S.; Discher, D. E.; Hammer, D. A. *Science* **1999**, *284*, 1143.

35. Kabanov, A. V.; Alakhov, V. Y. *Crit. Rev. Ther. Drug* **2002**, *19*, 1.

36. Zhang, X. C.; Jackson, J. K.; Burt, H. M. *Int. J. Pharm.* **1996**, *132*, 195.

37. Brannan, A. K.; Bates, F. S. *Macromolecules* **2004**, *37*, 8816.

38. Kim, S. Y.; Shin, I. L. G.; Lee, Y. M.; Cho, C. S.; Sung, Y. K. *J. Controlled Release* **1998**, *51*, 13.

39. Luo, L. B.; Eisenberg, A. *J. Am. Chem. Soc.* **2001**, *123*, 1012.

40. Sant, V. P.; Smith, D.; Leroux, J. C. *J. Controlled Release* **2004**, *97*, 301.

41. Meng, F. H.; Hiemstra, C.; Engbers, G. H. M.; Feijen, J. *Macromolecules* **2003**, *36*, 3004.

42. Arifin, D. R.; Palmer, A. F. *Biomacromolecules* **2005**, *6*, 2172.

43. Jin, H.; Huang, W.; Zhu, X.; Zhou, Y.; Yan, D. *Chem. Soc. Rev.* **2012**, *41*, 5986.

44. Tomalia, D. A.; Baker, H.; Dewald, J.; Hall, M.; Kallos, G.; Martin, S.; Roeck, J.; Ryder, J.; Smith, P. *Polym. J.* **1985**, *17*, 117.

45. Tomalia, D. A.; Baker, H.; Dewald, J.; Hall, M.; Kallos, G.; Martin, S.; Roeck, J.; Ryder, J.; Smith, P. *Macromolecules* **1986**, *19*, 2466.

46. Newkome, G. R.; Yao, Z.; Baker, G. R.; Gupta, V. K. *J. Org. Chem.* **1985**, *50*, 2003.

47. de Brabander-van den Berg, E. M. M.; Meijer, E. W. *Angew. Chem., Int. Ed.* **1993**, *32*, 1308.

48. Launay, N.; Caminade, A. M.; Lahana, R.; Majoral, J. P. *Angew. Chem., Int. Ed.* **1994**, *33*, 1589.

49. Hawker, C. J.; Fréchet, J. M. J. *J. Am. Chem. Soc.* **1990**, *112*, 7638.

50. Boas, U.; Heegaard, P. M. H. *Chem. Soc. Rev.* **2004**, *33*, 43.

51. Cheng, Y. Y.; Xu, Z. H.; Ma, M. L.; Xu, T. W. *J. Pharm. Sci.* **2008**, *97*, 123.

52. El Kazzouli, S.; Mignani, S.; Bousmina, M.; Majoral, J. P. *New J. Chem.* **2012**, *36*, 227.

53. Svenson, S.; Tomalia, D. A. *Adv. Drug Deliver. Rev.* **2005**, *57*, 2106.

54. Caminade, A. M.; Laurent, R.; Delavaux-Nicot, B.; Majoral, J. P. *New J. Chem.* **2012**, *36*, 217.

55. Harrington, D. A.; Behanna, H. A.; Tew, G. N.; Claussen, R. C.; Stupp, S. I. *Chem. Biol.* **2005**, *12*, 1085.

56. Yang, M.; Wang, W.; Yuan, F.; Zhang, X. W.; Li, J. Y.; Liang, F. X.; He, B. L.; Minch, B.; Wegner, G. *J. Am. Chem. Soc.* **2005**, *127*, 15107.

57. Luman, N. R.; Grinstaff, M. W. *Org. Lett.* **2005**, *7*, 4863.

58. Yuan, F.; Zhang, X. J.; Yang, M.; Wang, W.; Minch, B.; Lieser, G.; Wegner, G. *Soft Matter* **2007**, *3*, 1372.

59. Yang, M.; Zhang, Z.; Yuan, F.; Wang, W.; Hess, S.; Lienkamp, K.; Lieberwirth, I.; Wegner, G. *Chem.-Eur. J.* **2008**, *14*, 3330.

60. Yang, M.; Wang, W.; Lieberwirth, I.; Wegner, G. *J. Am. Chem. Soc.* **2009**, *131*, 6283.

61. Percec, V.; Wilson, D. A.; Leowanawat, P.; Wilson, C. J.; Hughes, A. D.; Kaucher, M. S.; Hammer, D. A.; Levine, D. H.; Kim, A. J.; Bates, F. S.; Davis, K. P.; Lodge, T. P.; Klein, M. L.; DeVane, R. H.; Aqad, E.; Rosen, B. M.; Argintaru, A. O.; Sienkowska, M. J.; Rissanen, K.; Nummelin, S.; Ropponen, J. *Science* **2010**, *328*, 1009.

62. Peterca, M.; Percec, V.; Leowanawat, P.; Bertin, A. *J. Am. Chem. Soc.* **2011**, *133*, 20507.

63. Stuart, M. A. C.; Huck, W. T. S.; Genzer, J.; Muller, M.; Ober, C.; Stamm, M.; Sukhorukov, G. B.; Szleifer, I.; Tsukruk, V. V.; Urban, M.; Winnik, F.; Zauscher, S.; Luzinov, I.; Minko, S. *Nat. Mater.* **2010**, *9*, 101.

64. Alarcon, C. D. H.; Pennadam, S.; Alexander, C. *Chem. Soc. Rev.* **2005**, *34*, 276.

65. Stiriba, S. E.; Frey, H.; Haag, R. *Angew. Chem., Int. Ed.* **2002**, *41*, 1329.

66. Parida, U. K.; Nayak, A. K.; Nayak, P. L. *Pop. Plast. Packag.* **2011**, *56*, 25.

67. Mishra, B.; Patel, B. B.; Tiwari, S. *Nanomed.-Nanotechnol.* **2010**, *6*, 9.

68. Svenson, S. *Eur. J. Pharm. Biopharm.* **2009**, *71*, 445.

69. Svenson, S. *Mol. Pharm.* **2013**, *10*, 848.

70. Menon, J. U.; Jadeja, P.; Tambe, P.; Vu, K.; Yuan, B. H.; Nguyen, K. T. *Theranostics* **2013**, *3*, 152.

71. Campolongo, M. J.; Tan, S. J.; Xu, J. F.; Luo, D. *Adv. Drug Deliver. Rev.* **2010**, *62*, 606.

72. Terwogt, J. M. M.; Nuijen, B.; Huinink, W. W. T.; Beijnen, J. H. *Cancer Treat. Rev.* **1997**, *23*, 87.

73. Petros, R. A.; DeSimone, J. M. *Nat. Rev. Drug Discov.* **2010**, *9*, 615.

74. Otsuka, H.; Nagasaki, Y.; Kataoka, K. *Adv. Drug Deliver. Rev.* **2003**, *55*, 403.

75. Torchilin, V. P.; Trubetskoy, V. S.; Whiteman, K. R.; Caliceti, P.; Ferruti, P.; Veronese, F. M. *J. Pharm. Sci.* **1995**, *84*, 1049.

76. Choi, H. J.; Montemagno, C. D. *Nano Lett.* **2005**, *5*, 2538.

77. Trubetskoy, V. S.; Torchilin, V. P. *Adv. Drug Deliver. Rev.* **1995**, *16*, 311.

78. Zhang, Z.; Grijpma, D. W.; Feijen, J. *J. Controlled Release* **2006**, *112*, 57.

79. Najer, A.; Wu, D. L.; Vasquez, D.; Palivan, C. G.; Meier, W. *Nanomedicine* **2013**, *8*, 425.

80. Moghimi, S. M.; Hunter, A. C.; Murray, J. C. *Pharmacol. Rev.* **2001**, *53*, 283.

81. Choi, H. S.; Liu, W.; Misra, P.; Tanaka, E.; Zimmer, J. P.; Ipe, B. I.; Bawendi, M. G.; Frangioni, J. V. *Nat. Biotechnol.* **2007**, *25*, 1165.

82. Brinkhuis, R. P.; Stojanov, K.; Laverman, P.; Eilander, J.; Zuhorn, I. S.; Rutjes, F.; van Hest, J. C. M. *Bioconjugate Chem.* **2012**, *23*, 958.

83. Kedar, U.; Phutane, P.; Shidhaye, S.; Kadam, V. *Nanomed.-Nanotechnol.* **2010**, *6*, 714.

84. Torchilin, V. P.; Levchenko, T. S.; Lukyanov, A. N.; Khaw, B. A.; Klibanov, A. L.; Rammohan, R.; Samokhin, G. P.; Whiteman, K. R. *BBA-Biomembranes* **2001**, *1511*, 397.

85. Gabizon, A.; Horowitz, A. T.; Goren, D.; Tzemach, D.; Mandelbaum-Shavit, F.; Qazen, M. M.; Zalipsky, S. *Bioconjugate Chem.* **1999**, *10*, 289.

86. Zhu, S. J.; Qian, L. L.; Hong, M. H.; Zhang, L. H.; Pei, Y. Y.; Jiang, Y. Y. *Adv. Mater.* **2011**, *23*, 84.

87. Kwon, G. S.; Kataoka, K. *Adv. Drug Deliver. Rev.* **2012**, *64*, 237.

88. Duncan, R.; Vicent, M. J. *Adv. Drug Deliver. Rev.* **2013**, *65*, 60.

89. Wei, H.; Zhuo, R.-X.; Zhang, X.-Z. *Prog. Polym. Sci.* **2013**, *38*, 503.

90. Kwon, G. S.; Naito, M.; Yokoyama, M.; Okano, T.; Sakurai, Y.; Kataoka, K. *Pharm. Res.* **1995**, *12*, 192.

91. Hruby, M.; Konak, C.; Ulbrich, K. *J. Controlled Release* **2005**, *103*, 137.

92. LoPresti, C.; Lomas, H.; Massignani, M.; Smart, T.; Battaglia, G. *J. Mater. Chem.* **2009**, *19*, 3576.

93. Brinkhuis, R. P.; Rutjes, F.; van Hest, J. C. M. *Polym. Chem.* **2011**, *2*, 1449.

94. Christian, D. A.; Cai, S.; Bowen, D. M.; Kim, Y.; Pajerowski, J. D.; Discher, D. E. *Eur. J. Pharm. Biopharm.* **2009**, *71*, 463.

95. Meng, F.; Zhong, Z. *J. Phys. Chem. Lett.* **2011**, *2*, 1533.

96. Ahmed, F.; Pakunlu, R. I.; Srinivas, G.; Brannan, A.; Bates, F.; Klein, M. L.; Minko, T.; Discher, D. E. *Mol. Pharm.* **2006**, *3*, 340.

97. Zhang, J. C.; Wu, L. L.; Meng, F. H.; Wang, Z. J.; Deng, C.; Liu, H. Y.; Zhong, Z. Y. *Langmuir* **2012**, *28*, 2056.

98. Li, W.; Li, H. F.; Li, J. F.; Wang, H. J.; Zhao, H.; Zhang, L.; Xia, Y.; Ye, Z. W.; Gao, J.; Dai, J. X.; Wang, H.; Guo, Y. J. *Int. J. Nanomed.* **2012**, *7*, 4661.

99. Christian, N. A.; Milone, M. C.; Ranka, S. S.; Li, G. Z.; Frail, P. R.; Davis, K. P.; Bates, F. S.; Therien, M. J.; Ghoroghchian, P. P.; June, C. H.; Hammer, D. A. *Bioconjugate Chem.* **2007**, *18*, 31.

100. Grull, H.; Langereis, S.; Messager, L.; Castelli, D. D.; Sanino, A.; Torres, E.; Terreno, E.; Aime, S. *Soft Matter* **2010**, *6*, 4847.

101. Ren, T. B.; Liu, Q. M.; Lu, H.; Liu, H. M.; Zhang, X.; Du, J. Z. *J. Mater. Chem.* **2012**, *22*, 12329.

102. De Jesus, O. L. P.; Ihre, H. R.; Gagne, L.; Fréchet, J. M. J.; Szoka, F. C. *Bioconjugate Chem.* **2002**, *13*, 453.

103. Chau, Y.; Dang, N. M.; Tan, F. E.; Langer, R. *J. Pharm. Sci.* **2006**, *95*, 542.

104. Kaminskas, L. M.; McLeod, V. M.; Porter, C. J. H.; Boyd, B. J. *Mol. Pharm.* **2012**, *9*, 355.

105. Kono, K.; Kojima, C.; Hayashi, N.; Nishisaka, E.; Kiura, K.; Wataral, S.; Harada, A. *Biomaterials* **2008**, *29*, 1664.

106. Nicolaou, K. C.; Mitchell, H. J. *Angew. Chem., Int. Ed.* **2001**, *40*, 1576.

107. Mammen, M.; Choi, S. K.; Whitesides, G. M. *Angew. Chem., Int. Ed.* **1998**, *37*, 2755.

108. Chen, Y. A.; Star, A.; Vidal, S. *Chem. Soc. Rev.* **2013**, *42*, 4532.

109. Spinelli, N.; Defrancq, E.; Morvan, F. *Chem. Soc. Rev.* **2013**, *42*, 4557.

110. Eissa, A. M.; Cameron, N. R. In *Bio-Synthetic Polymer Conjugates*; Schlaad, H., Ed.; Springer: 2013; Vol. 253, p 71.

111. Pieters, R. J. *Org. Biomol. Chem.* **2009**, *7*, 2013.

112. Gillies, E. R. In *Engineered Carbohydrate-Based Materials for Biomedical Applications: Polymers, Surfaces, Dendrimers, Nanoparticles, and Hydrogels*; Narain, R., Ed.; John Wiley & Sons, Inc.: 2011, p 261.

113. Roy, R.; Zanini, D.; Meunier, S. J.; Romanowska, A. *J. Chem. Soc., Chem. Commun.* **1993**, 1869.

114. Page, D.; Zanini, D.; Roy, R. *Bioorgan. Med. Chem.* **1996**, *4*, 1949.

115. Zanini, D.; Roy, R. *J. Am. Chem. Soc.* **1997**, *119*, 2088.

116. Meunier, S. J.; Wu, Q. Q.; Wang, S. N.; Roy, R. *Can. J. Chem.* **1997**, *75*, 1472.

117. Matsuoka, K.; Kurosawa, H.; Esumi, Y.; Terunuma, D.; Kuzuhara, H. *Carbohydr. Res.* **2000**, *329*, 765.

118. Sakamoto, J. I.; Koyama, T.; Miyamoto, D.; Yingsakmongkon, S.; Hidari, K.; Jampangern, W.; Suzuki, T.; Suzuki, Y.; Esumi, Y.; Hatano, K.; Terunuma, D.; Matsuoka, K. *Bioorg. Med. Chem. Lett.* **2007**, *17*, 717.

119. Sakamoto, J. I.; Koyama, T.; Miyamoto, D.; Yingsakmongkon, S.; Hidari, K.; Jampangern, W.; Suzuki, T.; Suzuki, Y.; Esumi, Y.; Nakamura, T.; Hatano, K.; Terunuma, D.; Matsuoka, K. *Bioorgan. Med. Chem.* **2009**, *17*, 5451.

120. Clayton, R.; Hardman, J.; LaBranche, C. C.; McReynolds, K. D. *Bioconjugate Chem.* **2011**, *22*, 2186.

121. Zanini, D.; Roy, R. *J. Org. Chem.* **1998**, *63*, 3486.

122. Reuter, J. D.; Myc, A.; Hayes, M. M.; Gan, Z. H.; Roy, R.; Qin, D. J.; Yin, R.; Piehler, L. T.; Esfand, R.; Tomalia, D. A.; Baker, J. R. *Bioconjugate Chem.* **1999**, *10*, 271.

123. Caravan, P.; Ellison, J. J.; McMurry, T. J.; Lauffer, R. B. *Chem. Rev.* **1999**, *99*, 2293.

124. Merbach, A. E.; Toth, E. *The Chemistry of Contrast Agents in Medical Magnetic Resonance Imaging*; John Wiley and Sons: Chichester, 2001.

125. Aime, S.; Botta, M.; Terreno, E. *Adv. Inorg. Chem.* **2005**, *57*, 173.

126. Prince, M. R.; Zhang, H. L.; Roditi, G. H.; Leiner, T.; Kucharczyk, W. *J. Magn. Reson. Imaging* **2009**, *6*, 1298.

127. Terreno, E.; Delli Castelli, D.; Viale, A.; Aime, S. *Chem. Rev.* **2010**, *110*, 3019.

128. Villaraza, A. J. L.; Bumb, A.; Brechbiel, M. W. *Chem. Rev.* **2010**, *110*, 2921.

129. Langereis, S.; Dirkson, A.; Hackeng, T. M.; van Genderen, M. H. P.; Meijer, E. W. *New J. Chem.* **2007**, *31*, 1152.

130. Caravan, P. *Chem. Soc. Rev.* **2006**, *35*, 512.

131. Wiener, E. C.; Brechbiel, M. W.; Brothers, H.; Magin, R. L.; Gansow, O. A.; Tomalia, D. A.; Lauterbur, P. C. *Magn. Res. Med.* **1994**, *31*, 1.

132. Kobayashi, H.; Kawamoto, S.; Jo, S. K.; Bryant, H. L., Jr.; Brechbiel, M. W.; Star, R. A. *Bioconjugate Chem.* **2003**, *14*, 388.

133. Langereis, S.; de Lussanet, Q. G.; van Genderen, M. H. P.; Backes, W. H.; Meijer, E. W. *Macromolecules* **2004**, *37*, 3084.

134. Bryant, L. H.; Brechbiel, M. W.; Wu, C. C.; Bulte, J. W. M.; Herynek, V.; Frank, J. A. *J. Magn. Reson. Imaging* **1999**, *9*, 348.

135. Toth, E.; Pubanz, D.; Vauthey, S.; Helm, L.; Merbach, A. E. *Chem.-Eur. J.* **1996**, *2*, 1607.

136. Rudovsky, J.; Hermann, P.; Botta, M.; Aime, S.; Lukes, I. *Chem. Commun.* **2005**, 2390.

137. Rudovsky, J.; Botta, M.; Hermann, P.; Hardcastle, K. I.; Lukes, I.; Aime, S. *Bioconjugate Chem.* **2006**, *17*, 975.

138. Dong, Q.; Hurst, D. R.; Weinmann, H. J.; Chenevert, T. L.; Londy, F. J.; Prince, M. R. *Invest. Radiol.* **1998**, *33*, 699.

139. Fulton, D. A.; O'Halloran, M.; Parker, D.; Senanayake, K.; Botta, M.; Aime, S. *Chem. Commun.* **2005**, 474.

140. Raymond, K. N.; Pierre, V. C. *Bioconjugate Chem.* **2005**, *16*, 3.

141. Pierre, V. C.; Botta, M.; Raymond, K. N. *J. Am. Chem. Soc.* **2005**, *127*, 504.

142. Floyd, W. C.; Klemm, P. J.; Smiles, D. E.; Kohlgruber, A. C.; Pierre, V. C.; Mynar, J. L.; Fréchet, J. M. J.; Raymond, K. N. *J. Am. Chem. Soc.* **2011**, *133*, 2390.

143. Wiener, E. C.; Konda, S.; Shadron, A.; Brechbiel, M.; Gansow, O. *Invest. Radiol.* **1997**, *32*, 748.

144. Konda, S. D.; Wang, S.; Brechbiel, M.; Wiener, E. C. *Invest. Radiol.* **2002**, *37*, 199.

145. Yang, X. Q.; Grailer, J. J.; Rowland, I. J.; Javadi, A.; Hurley, S. A.; Matson, V. Z.; Steeber, D. A.; Gong, S. Q. *ACS Nano* **2010**, *4*, 6805.

146. Pittet, M. J.; Swirski, F. K.; Reynolds, F.; Josephson, L.; Weissleder, R. *Nat. Protoc.* **2006**, *1*, 73.

147. Pang, Z. Q.; Feng, L. A.; Hua, R. R.; Chen, J.; Gao, H. L.; Pan, S. Q.; Jiang, X. G.; Zhang, P. *Mol. Pharm.* **2010**, *7*, 1995.

148. Rai, P.; Padala, C.; Poon, V.; Saraph, A.; Basha, S.; Kate, S.; Tao, K.; Mogridge, J.; Kane, R. S. *Nat. Biotechnol.* **2006**, *24*, 582.

149. Pawar, P. V.; Gohil, S. V.; Jain, J. P.; Kumar, N. *Polym. Chem.* **2013**, *4*, 3160.

150. Egli, S.; Schlaad, H.; Bruns, N.; Meier, W. *Polymers* **2011**, *3*, 252.

151. Li, B.; Martin, A. L.; Gillies, E. R. *Chem. Commun.* **2007**, 5217.

152. Martin, A. L.; Li, B.; Gillies, E. R. *J. Am. Chem. Soc.* **2009**, *131*, 734.

153. Martin, A. L.; Bernas, L. M.; Rutt, B. K.; Foster, P. J.; Gillies, E. R. *Bioconjugate Chem.* **2008**, *19*, 2375.

154. Astruc, D.; Boisselier, E.; Ornelas, C. *Chem. Rev.* **2010**, *110*, 1857.

155. Mintzer, M. A.; Grinstaff, M. W. *Chem. Soc. Rev.* **2011**, *40*, 173.

156. Pistolis, G.; Malliaris, A.; Tsiourvas, D.; Paleos, C. M. *Chem.-Eur. J.* **1999**, *5*, 1440.

157. Gillies, E. R.; Jonsson, T. B.; Fréchet, J. M. J. *J. Am. Chem. Soc.* **2004**, *126*, 11936.

158. Yesilyurt, V.; Ramireddy, R.; Thayumanavan, S. *Angew. Chem., Int. Ed.* **2011**, *50*, 3038.

159. Kimura, M.; Kato, M.; Muto, T.; Hanabusa, K.; Shirai, H. *Macromolecules* **2000**, *33*, 1117.

160. Tono, Y.; Kojima, C.; Haba, Y.; Takahashi, T.; Harada, A.; Yagi, S.; Kono, K. *Langmuir* **2006**, *22*, 4920.

161. Ong, W.; McCarley, R. L. *Macromolecules* **2006**, *39*, 7295.

162. Ong, W.; McCarley, R. L. *Chem. Commun.* **2005**, 4699.

163. Gingras, M.; Raimundo, J. M.; Chabre, Y. M. *Angew. Chem., Int. Ed.* **2007**, *46*, 1010.

164. Kojima, C. *Expert Opin. Drug Del.* **2010**, *7*, 307.

165. Ramireddy, R. R.; Raghupathi, K. R.; Torres, D. A.; Thayumanavan, S. *New J. Chem.* **2012**, *36*, 340.

166. Wong, A. D.; DeWit, M. A.; Gillies, E. R. *Adv. Drug Deliver. Rev.* **2012**, *64*, 1031.

167. Patchorn.A; Amit, B.; Woodward, R. B. *J. Am. Chem. Soc.* **1970**, *92*, 6333.

168. Il'ichev, Y. V.; Schworer, M. A.; Wirz, J. *J. Am. Chem. Soc.* **2004**, *126*, 4581.

169. Zhao, H.; Sterner, E. S.; Coughlin, E. B.; Theato, P. *Macromolecules* **2012**, *45*, 1723.

170. Thomas, S. W. *Macromol. Chem. Phys.* **2012**, *213*, 2443.

171. Smet, M.; Liao, L. X.; Dehaen, W.; McGrath, D. V. *Org. Lett.* **2000**, *2*, 511.

172. Kostiainen, M. A.; Smith, D. K.; Ikkala, O. *Angew. Chem., Int. Ed.* **2007**, *46*, 7600.

173. Fomina, N.; McFearin, C. L.; Almutairi, A. *Chem. Commun.* **2012**, *48*, 9138.

Chapter 2

2 Dendritic Surface Functionalization of Biodegradable Polymer Assemblies[*]

2.1 Introduction

In solution, amphiphilic BCPs can undergo self-assembly, forming a diverse range of structures from spherical micelles[1] to helical rods,[2] toroids,[3] vesicles,[4,5] tubes,[6] and multicompartment cylinders.[7] In recent years, micelles and vesicles have received significant attention as they can be readily accessed using a wide range of BCPs by controlling the relative volume fractions of the constituent blocks.[8] Relative to their counterparts formed from low MW surfactants,[9] these assemblies typically exhibit much lower critical aggregation concentrations and enhanced thermodynamic and kinetic stabilities.[7,10] Because of these properties, there has been particular interest in biomedical applications of these materials and they have been demonstrated as promising carriers of proteins,[11-13] hydrophilic and hydrophobic drugs,[14-17] and imaging contrast agents.[18-20] Micelles and vesicles are complementary systems in that micelles possess a hydrophobic core that is typically used to encapsulate hydrophobic species, while vesicles possess an aqueous core capable of encapsulating water-soluble species. However, vesicles also possess a hydrophobic membrane that can also encapsulate hydrophobes, making these assemblies multifunctional.

While much research thus far has focused on controlling the assembly and encapsulation properties of BCPs and their corresponding assemblies,[21-23] the functionalization of micelle and vesicle surfaces is emerging as an important area of research. The surfaces of the materials will come into direct contact with biological

---

systems and will therefore play a critical role in determining their properties such as toxicity and biodistribution behaviour.[16] Furthermore, the conjugation of ligands to the surface can potentially lead to targeting of specific tissues such as tumours *in vivo*.[20,24] Our group has recently reported a method for the introduction of dendritic groups to the surfaces of polymer vesicles using the widely applicable Cu(I)-catalyzed click reaction between vesicle azide groups and dendrons bearing focal point alkynes.[25] Owing to the high multivalency of the dendrons, this approach provides a rapid means of controlling the surface functionalities on the assembly. Furthermore, using mannose as a model biological ligand, it was demonstrated that binding to the target receptors was significantly enhanced using a dendritic approach in comparison to the conjugation of small molecules directly to the vesicle surface.[26] This result was also generalizable to polymer functionalized nanoparticles and was attributed to the increased availability of the ligands on the surface of the nanomaterial when presented on the dendritic framework, as well as the clustered nature of ligand display.

Overall, the results of our previous studies suggested that this dendritic surface functionalization approach is highly promising for controlling the surface functionalities of nanomaterials in order to impart specific biological properties and functions such as targeting. However, this initial work was performed on vesicles composed of PEO-PBD BCP, a non-biodegradable polymer with unknown biocompatibility. Furthermore, the micron-scale sizes of these vesicles were unsuitable for *in vivo* circulation.[27] To address these limitations, and thus provide a significant advancement towards biomedical applications, we describe here the application of the dendritic surface functionalization approach to nano-sized PEO-PCL vesicles and micelles. PCL is a well-known biodegradable polymer that is currently Food and Drug Administration (FDA)-approved for uses in tissue engineering[28,29] and drug delivery.[30,31] Although PEO is not biodegradable, it is generally considered non-toxic and is currently used in several FDA-approved products including PEG-INTRON, ONCASPAR, and NEULASTA. Both micelles[32-38] and vesicles[15,38-46] based on PEO-PCL have been previously reported and have been investigated as delivery vehicles for drugs such as DOX,[40] TAX,[15] docetaxel,[36] hemoglobin,[41] dihydrotestosterone,[33] cyclosporine A,[34] and rapamycin.[35] In current work, we describe the synthesis of azide terminated PEO-PCL BCPs, their assembly into

micelles and vesicles, and the conjugation of dendrons bearing different surface functionalities including hydroxyls, amines, and guanidines, as well as a small molecule rhodamine derivative to both vesicles and micelles. The effects of these conjugations on the properties of the assemblies are explored.

2.2 Results and Discussion

2.2.1 Synthesis of Block Copolymers

In order to functionalize polymer assemblies using the previously described azide + alkyne click chemistry approach, new PEO-PCL BCPs bearing terminal azides on the hydrophilic PEO blocks were required. As the polymerization of ε-caprolactone (CL) is generally initiated from small molecule[47,48] or macromolecular alcohols,[49-51] these target copolymers could be most readily derived from asymmetrically functionalized PEOs bearing azide and hydroxyl termini (N_3-PEO-OH). While there are numerous reports describing the asymmetric functionalization of oligo(ethylene glycol)s,[52-54] their higher MW analogues, particularly those lacking charged moieties are more difficult to prepare due to the purification challenges associated with statistical functionalization reactions. For example, in recent work Hillmyer and coworkers did not succeed in purifying their target asymmetrically functionalized PEO, and therefore used the statistical mixture of end-functionalized molecules in the preparation of a BCP.[55] They later separated the resulting copolymers based on their differing solubilities and sizes. On the other hand, Taton and coworkers have recently reported asymmetric PEOs that were obtained directly from the ring-opening polymerization (ROP) of ethylene oxide using *N*-heterocyclic carbenes as catalysts.[56]

In the current work, to obtain the target N_3-PEO-OH, hydroxy-terminated PEO (HO-PEO-OH, **2.1**) with a MW of 2000 g/mol was first reacted with 1.1 equivalent (equiv.) of *p*-toluenesulfonyl chloride (TsCl) in the presence of 4-dimethylaminopyridine (DMAP) as a catalyst and triethylamine (NEt_3) (Scheme 2.1). The crude product was then reacted with sodium azide to obtain the target N_3-PEO-OH (**2.2**) along with the diazide N_3-PEO-N_3 and diol HO-PEO-OH resulting from the statistical functionalization. Although the properties of the three products were quite similar to each other, using very careful

column chromatography it was possible to isolate an 18% yield (out of a possible 50% theoretical yield) of the target compound **2.2** in pure form as evidenced by MALDI-MS (Figure A2.11.). Despite the relatively low yield, the low cost of all of the reagents and starting materials for this chemistry resulted in this being a viable route for the preparation of the required macroinitiator.
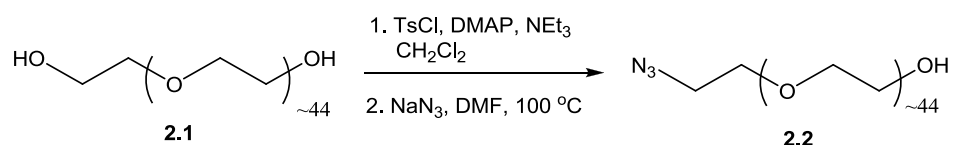
Scheme 2.1. Synthesis of HO-PEO-N$_3$ (**2.2**).

As shown in Scheme 2.2, N$_3$-PEO-OH (**2.2**) was then used as a macroinitiator in the ROP of CL. The commercially available PEO monomethyl ether (MeO-PEO-OH) was also used as a macroinitiator to provide BCPs without terminal azides. These non-functionalized copolymers were required in the preparation of the assemblies to control the number of surface azide groups and thus the degree of functionalization with the dendritic groups. Most reports involving the preparation of PEO-PCL have involved the use of metal catalysts such as tin 2-ethylhexanoate (stannous(II) octanoate),[37,42,44,57] zinc bis[bis(trimethylsilyl)amide],[39] or triethylaluminum.[58,59] For *in vivo* applications, the use of non-metallic catalysts is highly desired in order to minimize the potential toxicity effects. Acids such as hydrochloric acid (HCl),[36,60] trifluoromethanesulfonic acid,[61] and methanesulfonic acid[61] (MSA) have been reported to polymerize CL with small molecule alcohols as initiator. Among these catalysts, MSA was shown to produce PCLs with lower PDIs and in shorter reaction times. For these reasons, MSA was selected as the catalyst for this work and the polymerization was conducted at 30 °C for 2.5-3.5 h. Based on previous reports that PEO-PCL BCPs with monomer ratios of approximately 44:9 to 44:40 assemble into spherical micelles, while those with ratios of 44:82 to 44:105 assemble into vesicles, the four BCPs **2.3 - 2.6** shown in Table 2.1 were synthesized with the aim of preparing both micelles and vesicles from these materials.
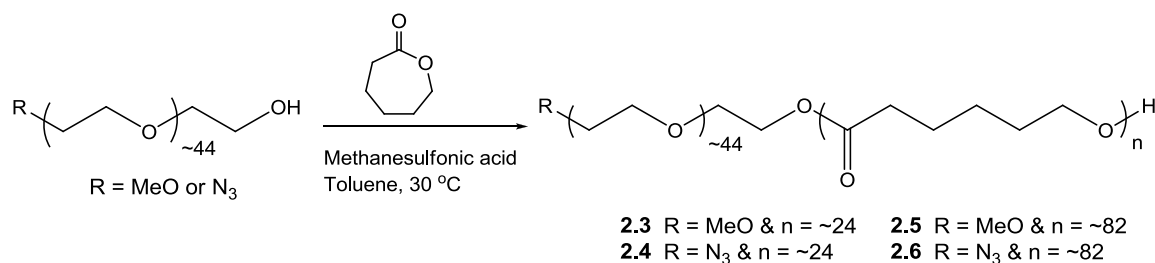
Scheme 2.2. Synthesis of PEO-PCL BCPs.

Table 2.1. MW characteristics of PEO-PCL BCPs. [a]MW expected from the polymerization based on the initiator and monomer ratio. [b]MW determined by ^{1}H NMR spectroscopy in CDCl$_3$. [c]M_w obtained from SEC-MALS. [d]PDI determined from SEC-MALS.

Copolymer	MW$_{expected}$ (g/mol)[a]	MW$_{NMR}$ (g/mol)[b]	M_w (g/mol)[c]	PDI[d]	Experimental Yield
MeO-PEO$_{44}$-PCL$_{24}$ (**2.3**)	4700	4800	5500	1.14	97%
N$_3$-PEO$_{44}$-PCL$_{24}$ (**2.4**)	4700	5000	4600	1.18	97%
MeO-PEO$_{44}$-PCL$_{82}$ (**2.5**)	11300	11300	12400	1.40	95%
N$_3$-PEO$_{44}$-PCL$_{82}$ (**2.6**)	11300	11600	12000	1.19	93%

The MWs of the resulting polymers were determined by ^{1}H NMR spectroscopy and size exclusion chromatography with detection by multi-angle light scattering (SEC-MALS). The MW characteristics of the synthesized BCPs are summarized in Table 2.1 and SEC traces of the polymers are shown in Figure 2.1. It is worth noting that high reaction yields and relatively low PDIs were generally obtained, with the measured MWs in agreement with target monomer ratios.
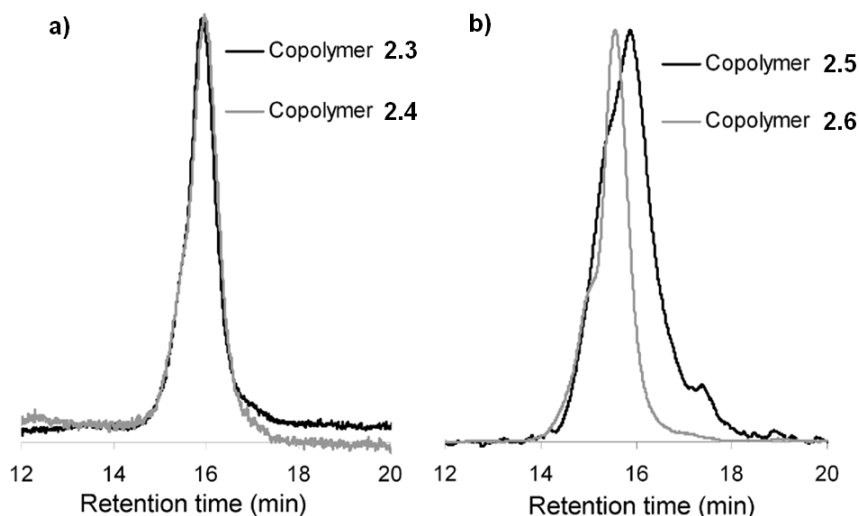
Figure 2.1. SEC traces for copolymers: (a) **2.3** and **2.4** and (b) **2.5** and **2.6**. Detection was based on light scattering (90 ° trace shown).

2.2.2 Synthesis of Alkyne-Functionalized Dendrons

To explore the functionalization of the PEO-PCL vesicles and micelles, two different dendrons with focal point alkynes were initially explored. The third generation dendron **1.33** bearing peripheral amine functional groups and statistically one rhodamine dye per molecule was selected, as this dendron was used in previous work with the PEO-PBD vesicles[25] and would allow comparison between the different vesicle systems. Additionally, to demonstrate that the dendritic surface functionalization approach can impart new functions, the guanidine functionalized dendron **2.8** was prepared by first reacting **1.33**[25] with the *tert*-butoxycarbonyl (Boc)-protected guanidine derivative **2.7**[62] in the presence of *o*-(benzotriazol-1-yl)-*N,N,N′,N′*-tetramethyluronium hexafluorophosphate (HBTU), 1-hydroxybenzotriazole (HOBt), and *N,N*-diisopropylethylamine (DIPEA), then removing the Boc groups by treatment with 1/1 trifluoroacetic acid (TFA)/CH_2Cl_2 (Scheme 2.3). Similar guanidine functionalized dendrons[62] have been demonstrated by our group to have cell penetrating properties comparable to those of the well known HIV Tat peptide,[63,64] and were capable of enhancing the transport of iron oxide nanoparticles into cells.[62] Therefore, they might enhance the capacity of these micelles and vesicles to carry cargo into cells. The molar extinction coefficients (ε) for dendrons **1.33** and **2.8** were determined by UV-visible spectroscopy in order to enable the quantification of their

conjugation yields to the surfaces of the nanoassemblies. Finally, as the conjugation yields for the dendrons can be limited by steric hindrance at the surface of the assembly, it was also of interest to compare these reactions with those of a small molecule alkyne. Thus, the rhodamine derivative **2.9**[65] was reacted with propargyl bromide to provide **2.10** (Scheme 2.4). As the local environment of the dye may alter its extinction coefficient, rhodamine-functionalized derivatives of copolymers **2.4** and **2.6** were also prepared as shown in Scheme 2.5, and the extinction coefficients of the resulting polymers **2.11** and **2.12** were measured in order to enable the accurate quantification of the conjugation yields for **2.10**.
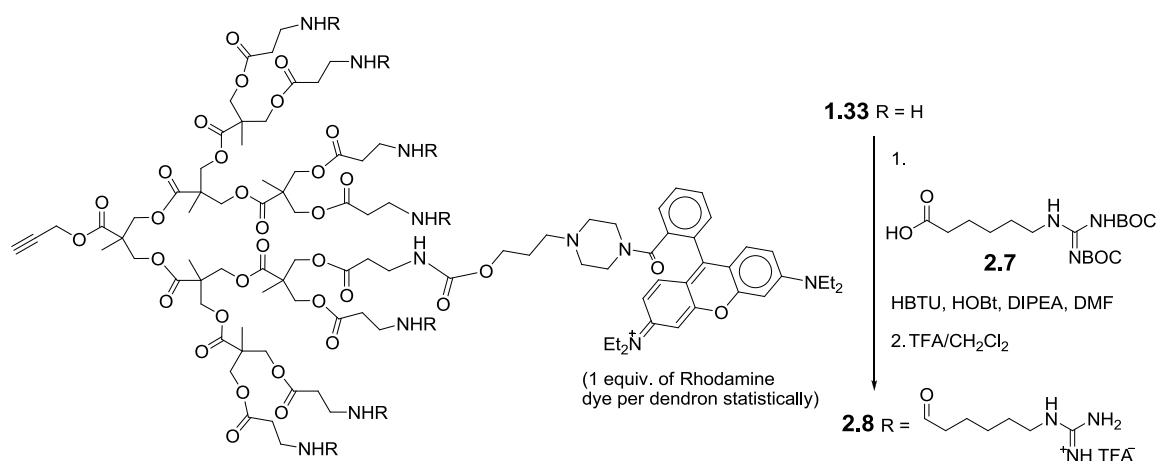
Scheme 2.3. Synthesis of rhodamine-labeled guanidine dendron **2.8**.
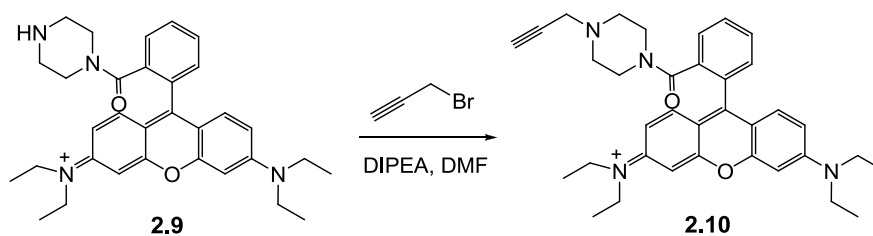
Scheme 2.4. Synthesis of alkyne-functionalized rhodamine **2.10**.
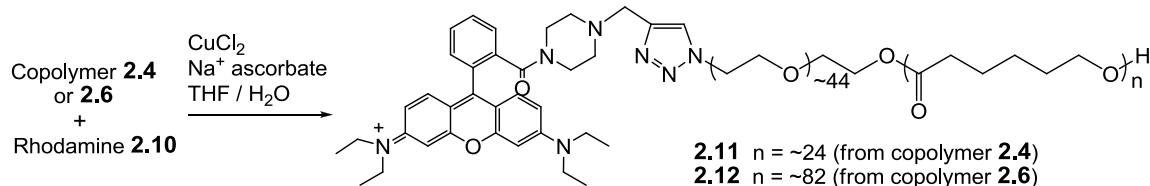
Scheme 2.5. Synthesis of rhodamine-labeled PEO-PCL block copolymers **11** and **12**.

2.2.3 Formation of Nanoassemblies and Surface Functionalization Reactions

PEO-PCL vesicles and micelles can be formed through a number of different methods including rehydration of copolymer thin films on roughened teflon plates[36,43,44] and nanoprecipitation.[38,42,45,46] In our hands, thin film rehydration of copolymers **2.3** and **2.4** provided micelles with diameters on the order of 25 nm. With copolymers **2.5** and **2.6**, rehydration of copolymer thin films on roughened teflon plates resulted in the formation of micron-sized vesicles, accompanied by many aggregates. The large sizes and aggregation were undesirable, so this method was not explored further. On the other hand, using a nanoprecipitation method involving the dissolution of the copolymer in tetrahydrofuan (THF), followed by a gradual addition of water and then dialysis against water to remove the THF, led reproducibly to micelles with diameters of approximately 20 nm (copolymers **2.3** and **2.4**) and vesicles with diameters of approximately 140 nm (copolymers **2.5** and **2.6**) as measured by both DLS (Figure 2.2) and transmission electron microscopy (TEM) (Figure 2.3). As materials smaller than 100 nm are desired for *in vivo* applications, it was demonstrated that the vesicles could be extruded through a 100 nm polycarbonate membrane at 65 ˚C. This resulted in a decrease in the vesicle diameter to about 65 nm.
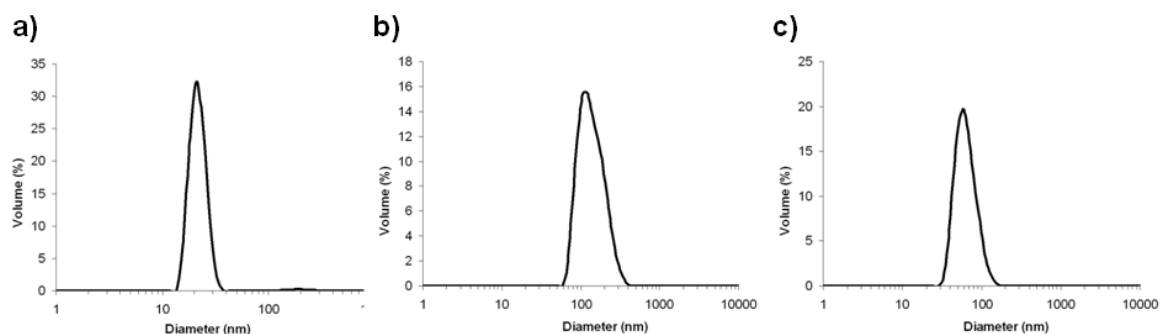
Figure 2.2. Size distribution profiles measured by DLS for: a) micelles prepared from copolymer **2.3**; b) vesicles prepared from copolymer **2.5**; c) extruded vesicles prepared from copolymer **2.5**.
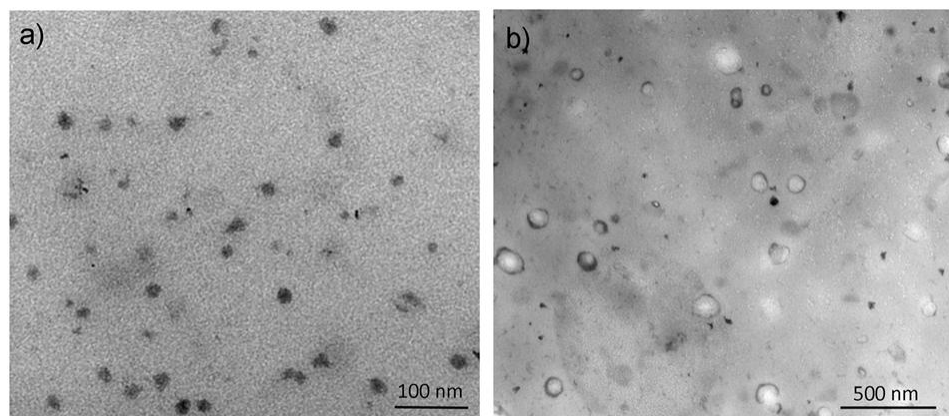
Figure 2.3. TEM images of: a) micelles prepared from copolymer **2.3**; b) vesicles prepared from copolymer **2.5**.

Micelles and vesicles with varying densities of surface azides were prepared from mixtures of copolymers **2.3** and **2.4** or **2.5** and **2.6** respectively using the nanoprecipitation method described above. Click reactions were subsequently performed using $CuCl_2$, sodium ascorbate, and four equivalents of the alkyne **1.33**, **2.8**, or **2.10** relative to the azide (Scheme 2.6). After 18 h, the excess alkyne and other reagents were removed by dialysis. Following the removal of water, the materials resulting from each reaction were dissolved in $CHCl_3$/MeOH (3/2), and their UV-visible absorbances were measured. Using the extinction coefficients measured for **1.33**, **2.8**, **2.11**, and **2.12**, the yields of the alkynes conjugated to the micelle and vesicle surfaces were then calculated.
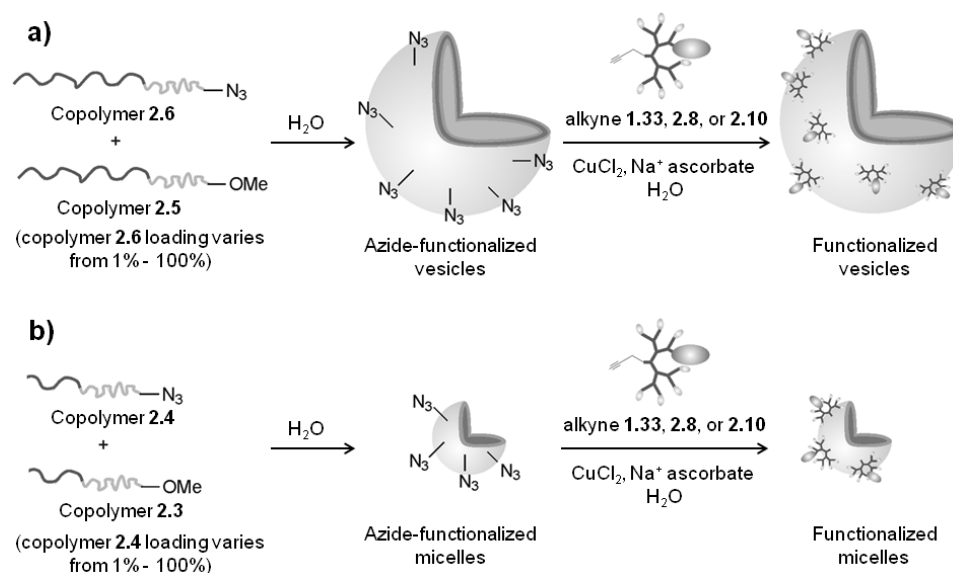
Scheme 2.6. Preparation of functionalized a) vesicles and b) micelles.

The conjugation yields for the vesicles are shown in Figure 2.4a. It was found that the yields for the conjugation of dendron **1.33**, bearing peripheral amines were very similar to those previously obtained with PEO-PBD vesicles.[25] It should be noted that approximately 50% of the azides should be located in the interior of the vesicles, and thus inaccessible to the dendron, which is unlikely to diffuse through the vesicle membrane. Nevertheless, as previously reported,[25] conjugation yields higher than 50% were obtained at low azide loadings. This may be attributed to the dynamic nature of the vesicles, allowing azides from the vesicle interior to migrate to the vesicle surface during the 18 h reaction time and then subsequently react. The slow migration of dendron **1.33** from the reaction solution into the vesicle core also cannot be excluded. As the azide loading increased beyond 20%, the reaction yields decreased. This was likely due to the steric hindrance at the vesicle surface which restricted the conjugation of dendrons. The yields for the conjugation of the guanidine-functionalized dendron **2.8** were consistently lower than those for dendron **1.33**. This result was not surprising considering the larger size of this dendron.
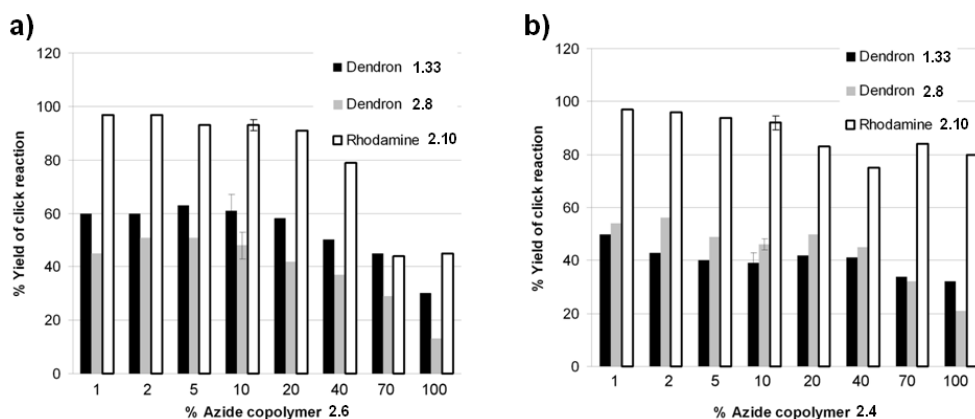
Figure 2.4. Click reaction yields as a function of azide loading on: a) vesicles (remaining copolymer is **2.5**); b) micelles (remaining copolymer is **2.3**).

Yields for the conjugation of the small molecule rhodamine derivative **2.10**, calculated using the extinction coefficient of **2.12**, were consistently greater than 90% for azide loadings of 1% to 40%. In order to ensure that the measured reaction yields accurately reflected covalently conjugated dye, and not simply dye entrapped within the vesicle core or membrane, these yields were determined following not only the usual aqueous dialysis but also a dialysis against DMF, which would disrupt the vesicles and enable the release of any non-covalently bound dye. Indeed these yields are lower than those observed after just the aqueous dialysis, which were consistently greater than 100% (at all azide loadings). Overall, these results suggested that the dye can diffuse across the vesicle membrane during the reaction time and react with azides on the interior membrane surface. Consistent with this hypothesis, we have observed the release of non-covalently encapsulated rhodamine out of vesicle cores over a 24 h period suggesting that the reverse process could also occur given the appropriate concentration gradient. Somewhat surprisingly, the reaction yields even for this small molecule dropped off at higher azide loadings above 20%. This might be attributed to the presence of dye molecules on the membrane disrupting the availability of nearby azides, or perhaps due to diffusion of the rhodamine across the vesicle membrane providing insufficient concentrations of rhodamine to react with all of the azides at the vesicle core. Moreover, the covalent or non-covalent attachment of the substrates to the nanoassemblies was evaluated by performing control experiments. Two PEO-PCL vesicle samples with 0% azide polymer

content were prepared. Both samples were subjected to click reaction condition with either alkyne-functionalized rhodamine dye **2.10** or dye-labled amine dendron **1.33** equal to vesicles containing 10% azide-functionalized PEO-PCL copolymer **2.6**. The vesicle sample with **1.33** was dialyzed only against water and the sample with **2.10** was dialyzed against water followed by dialysis against DMF. Quantification of the samples, with respect to 10% azide-functionalized PEO-PCL copolymer, revealed that 1.3% of the dye-labeled amine dendron **1.33** and 2.3% of the alkyne-functionalized rhodamine dye **2.10** were non-covalently attached to the vesicles samples. Comparing these values with the overall conjugation yields shows that non-covalent attachment of the substrates to nanoassemblies is negligible compared to covalently bonded substrates.

In the conjugation reactions of dendron **1.33** with the micelles, it was expected that the yields would approach 100% at low azide loadings as all of the azides should be available for reaction at the micelles surface. However, as shown in Figure 2.4b, this was not the case, and surprisingly the conjugation yields were consistently lower than those obtained for the vesicles. The reasons for these lower yields are still unclear at this time, but could perhaps be related to the large size of the dendrons relative to the micelles. The yields for the conjugation of the guanidine-functionalized dendron **2.8** were similar to those obtained with dendron **1.33** and were similar to the yields obtained on the vesicles. Like for the vesicles, the conjugation yields for the small molecule rhodamine **2.10** were high, but unlike for the vesicles, these yields did not drop off as significantly at higher azide loadings. This suggests that the decrease in yields observed for the vesicles at high azide loading was more likely due to insufficient quantities of rhodamine **2.10** for reaction with the interior azides due to its limited diffusion across the vesicle membrane, rather than due to the presence of dye molecules hindering the reaction of nearby azides. Furthermore, in the context of the micelles, it suggests that the lower conjugation yields obtained for the dendrons were likely related to their size. It should also be noted that in order to investigate the reproducibility of the conjugation reactions, each reaction combination was repeated three times at the azide loading of 10%. The standard deviations, represented as error bars in Figure 2.4 ranged from $\pm$ 2% to $\pm$ 9%, indicating that the results were quite reproducible.

2.2.4 Effects of Surface Functionalization on the Nanoassemblies

During the conjugation reactions, all of the micelles and vesicles remained well-dispersed and the solutions were clear. As shown in Figures 2.5a and 2.5d, TEM confirmed that the micelles and vesicles remained intact following the click reaction. However, upon removal of the excess alkyne and other reagents by aqueous dialysis, aggregation was observed in some cases. In the case of dendron **1.33** with the vesicles, DLS measurements revealed aggregation, even at low azide loadings (Figure 2.6a), and beyond 10% azide loading, macroscopic aggregates were observed that could not even be measured by DLS. In our previous work with PEO-PBD, vesicle aggregates were observed at azide loadings beyond approximately 20%, but at low loadings the vesicles remained well-dispersed based on fluorescence confocal microscopy images.[25] Thus, the PEO-PCL vesicles appear to be more sensitive to aggregation. In the case of the guanidine dendron **2.8**, the aggregation was even more extensive. The aggregates formed at 2% azide loading were detected by DLS (Figure 2.6a) and were imaged by TEM (Figures 2.5b and c). Based on the TEM images, these aggregates seem to be composed primarily of vesicles. Beyond 2% azide, macroscopic precipitates were formed and unfortunately it was not possible to image these by TEM.
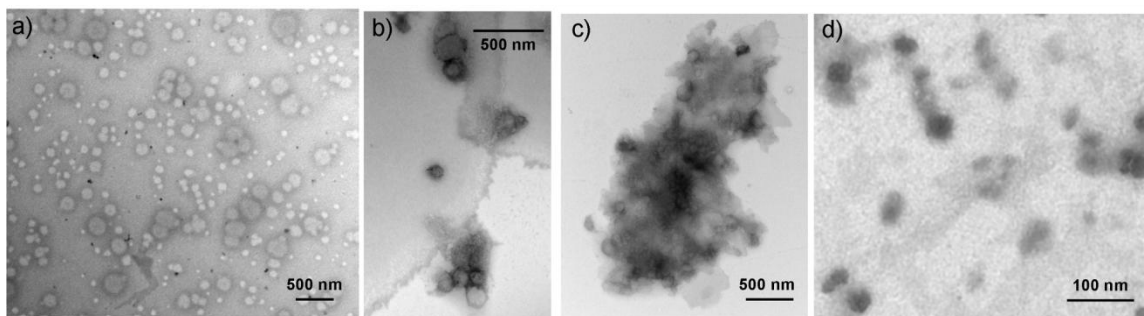
Figure 2.5. TEM images of: a) vesicles with 2% azide loading, following conjugation of dendron **2.8** (prior to dialysis); b) and c) vesicles with 2% azide loading, following conjugation of dendron **2.8** and dialysis, showing aggregation; d) micelles with 20% azide loading, following conjugation of dendron **2.8** and dialysis.
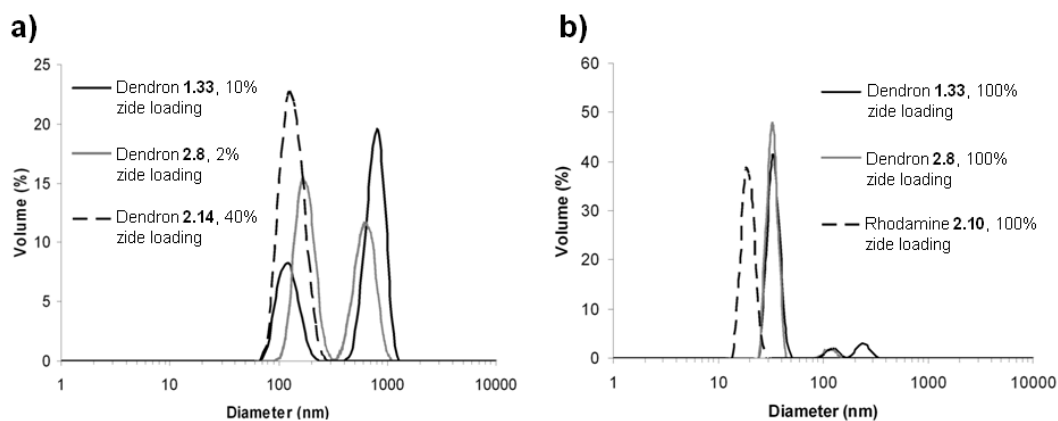
Figure 2.6. Size distribution profiles following click reactions and dialysis, measured by DLS for: a) vesicles and b) micelles.

The high sensitivity of the vesicles to aggregation upon dendron conjugation may be in part due to the resulting linear-dendritic copolymers being architecturally unfavorable for membrane formation. In addition, incorporation of the dendron may disrupt the hydrophilic-hydrophobic balance of the copolymer that is required for vesicle formation. These factors may destabilize the vesicle membrane. Nevertheless, the formation of the aggregates only upon dialysis suggests that these are not the only factors. It is noteworthy that dendrons **1.33** and **2.8** both possess cationic charges and it is possible that the presence of the excess dendrons somehow helps to stabilize the dispersed vesicles through hydrogen bonding or ionic interactions. To further investigate this aggregation phenomenon additional experiments were performed. First, a fourth generation polyester dendron **2.14** with a focal point alkyne was prepared as shown in Scheme 2.7.[66] This dendron was selected as it was estimated to have a size similar to dendron **1.33** but without the cationic charges. Dendron conjugation at azide loadings from 5% to 40% were investigated and no aggregation was detected in any of these cases, even after dialysis (Figure 2.6a). This suggests that the dendritic architecture alone is not sufficient to trigger aggregation in this system, and that the charge of the dendrons was involved. The use of NaCl solutions (0.2 or 0.5 M) rather than pure water for the dialyses was also investigated as a means of controlling the counterion and ionic strength of the medium, but aggregation was still observed. In addition to this, dialysis against buffer solutions at different pH values were also examined. Dialysis of the samples against phosphate buffer

at pH = 6 and acetate buffer at pH = 5 also resulted in the aggregation of the vesicle samples functionalized with amine and guanidine dendrons. The role of the rhodamine dye molecule was also investigated. Vesicles functionalized with alkyne **2.10**, did exhibit some aggregation, likely due to the dye's cationic charge and the tendency of polycyclic aromatic systems to undergo π-π stacking (Figure A2.12).[67] However, the rhodamine was certainly not the only contributor, as the conjugation of previously reported dendrons analogous to dendrons **1.33** and **2.8** but lacking the rhodamine,[25,62] led to the same degree of vesicle aggregation as observed with the dye-labeled dendrons. Therefore, it appears that the PEO-PCL vesicles are sensitive to aggregation, particularly upon conjugation of cationic molecules. On the other hand, uncharged dendritic molecules, despite their architecture, seem to be well-tolerated and will be the focus of future work.
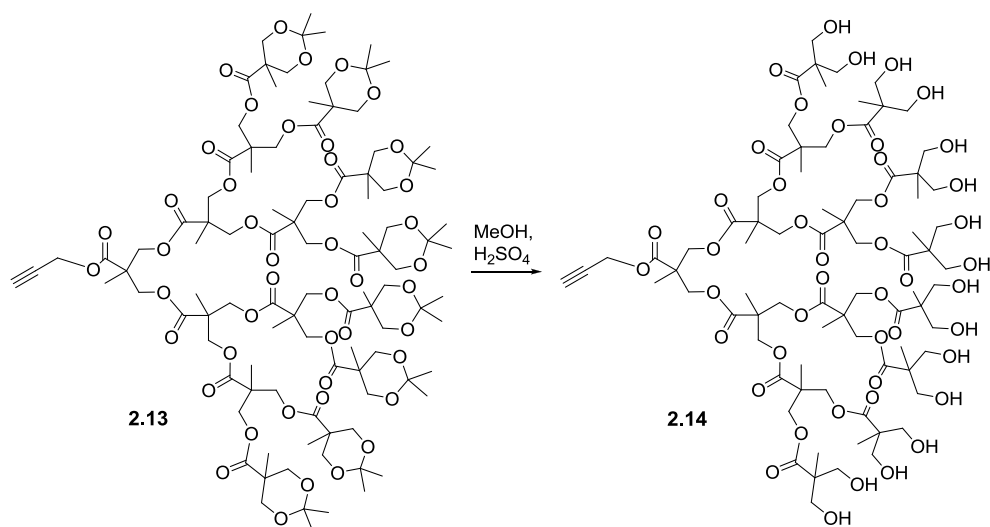
Scheme 2.7. Synthesis of dendron **2.14**.

In the case of dendron conjugation to the micelles, much less aggregation was observed. For example, upon conjugation of amine-functionalized dendron **1.33**, no significant aggregation was observed, even at azide loadings up to 100% (Figure 2.6b). The guanidine dendron **2.8** and the rhodamine **2.10** could also be conjugated at azide loadings up to 100% without significant aggregation (Figure 2.6b). Thus, overall the micelles were much less sensitive to aggregation than the vesicles. Unlike the vesicles, the incorporation of linear-dendritic polymers into micelles is known to be well-tolerated, and there are several examples of micelles comprising linear dendritic copolymers where

the dendritic block is hydrophilic or even hydrophobic.[68-70] Furthermore, micelle formation is generally favored for BCPs possessing hydrophilic volume fractions of >50%.[8] Thus, the formation of micelles may be less affected by the increase in hydrophilic volume fraction imparted by the dendritic groups. The micelles also seem to be able to tolerate the introduction of charged groups much better than the vesicles. This may be attributed to the inherent structural differences between the micelles and vesicles. If the introduction of cationic groups to the vesicle surfaces results in repulsive interactions that destabilize the membrane, the hydrophobic portions of the membranes can perhaps become exposed, triggering the aggregation. In contrast, the micelles posses much shorter hydrophobic blocks that are well-buried at the cores of the micelles. This may make them inherently more resistant to the aggregation phenomena observed in this work.

2.2.5 Cellular Uptake of the Guanidine Dendron-Functionalized Micelles

It has been shown by our group that dextran-coated superparamagnetic iron oxide nanoparticles bearing guanidine-functionalized polyester dendrons exhibit enhanced cell uptake relative to the unfunctionalized nanoparticles or those bearing hydroxyl- or amine-functionalized dendrons.[62] To demonstrate that the dendritic surface functionalization approach can impart new functions to our nanoassemblies, the cellular uptake of micelles bearing guanidine-functionalized dendrons was investigated in HeLa cancer cells. Micelles were prepared from a 70/20/10 ratio of polymers **2.3**/**2.4**/**2.11** as described above (Figure 2.7). This provided an azide loading of 20% and the incorporation of polymer **2.11** provided the rhodamine for visualization of cell uptake. A dendron analogous to **2.8** but with an eighth guanidine in place of the rhodamine[62] was then conjugated to the micelle surface by the click chemistry protocol described above. This approach was used as the presence of the rhodamine dye in **2.8** might alter the transport properties of the dendron. Micelles comprising a 90/10 ratio of copolymers **2.3**/**2.11** were used as a control. Due their high levels of aggregation, even at low azide loadings, guanidine-functionalized vesicles were not included in this experiment.
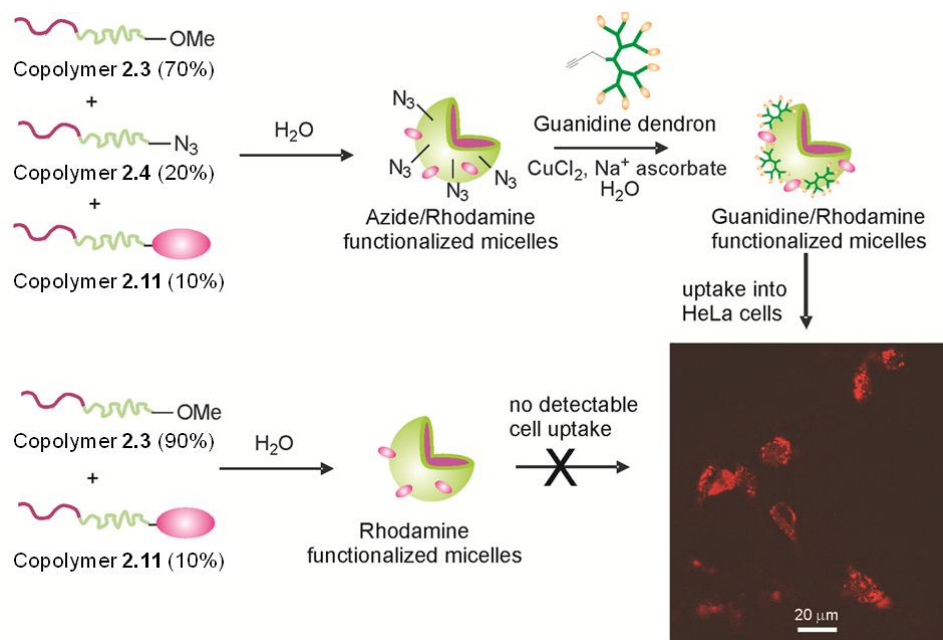
Figure 2.7. Preparation of PEO-PCL micelles functionalized with dendrons having peripheral guanidines, and their uptake into HeLa cells as visualized by fluorescence microscopy (detection of the rhodamine label). In contrast, micelles bearing the rhodamine label, but no dendron exhibited no detectable uptake.

Micelles were incubated with the cells at a concentration of 0.1 mg/mL (estimated 0.2 μM concentration of dendron) for 4 h, and then the cells were fixed and imaged by fluorescence confocal microscopy. As shown in Figure 2.7, cells incubated with the guanidine-functionalized micelles were strongly fluorescent, while no fluorescence was detected in cells incubated with the unfunctionalized micelles using the same microscope settings (Figure A2.13). This suggests that the dendritic surface functionalization approach can be used to impart cell penetrating properties to PEO-PCL micelles, which may allow them to more effectively deliver materials such as drugs, DNA, or labels into cells. Further experimentation will be required to quantify the cell uptake, study the intracellular tracking of these materials, and explore applications of these materials.

2.3 Conclusion

In conclusion, azide- and methoxy-terminated PEO-PCL BCPs with the appropriate relative block lengths for formation of micelles and vesicles were prepared with the aim

of developing surface-functionalized biodegradable assemblies. The azide- and methoxy-terminated copolymers were combined in varying ratios to provide assemblies with varying loadings of surface azide groups. Subsequently, dendrons having focal point alkyne moieties and peripheral amines, guanidines, or hydroxyl groups, as well as a small molecule alkyne derivative of rhodamine were conjugated to the surfaces of the micelles and vesicles using a Cu(I)-catalyzed azide + alkyne cycloaddition reaction. It was found that the conjugation yields for the dendrons on the vesicles were similar to those reported previously for PEO-PBD vesicles, while those for the small molecule were higher, likely due its ability to cross the vesicle membrane. Conjugation yields on the micelle surface were somewhat lower than expected for the dendrons, but were high for the small molecule. While the micelles remained well-dispersed following all conjugation reactions, the vesicles exhibited a propensity to aggregate, particularly upon the conjugation of cationic alkynes. To demonstrate the applicability of the dendritic surface functionalization approach, micelles with conjugated dendritic guanidines were shown to have enhanced cell uptake relative to unfunctionalized micelles.

2.4 Experimental

General Procedures and Materials

Chemicals were purchased from Sigma-Aldrich and were used without further purification unless otherwise noted. Anhydrous DMF, toluene, and CH_2Cl_2 were obtained from a solvent purification system. NEt_3 was distilled from CaH_2. CL was stirred over CaH_2 for 24 h at room temperature and overnight at 60 ˚C and then it was distilled from CaH_2 at reduced pressure under nitrogen immediately prior to polymerization. PEO derivatives were purified by precipitation from CH_2Cl_2 into cold diethyl ether (1:10). The precipitated PEO was then dried by azeotropic distillation ($\times$3) with dry toluene using a Schlenk line system under nitrogen. Unless otherwise stated, all reactions were performed under a N_2 atmosphere using flame or oven dried glassware. Column chromatography was performed using silica gel (0.063-0.200 mm particle size, 70-230 mesh). Dialyses were performed using Spectra/Por regenerated cellulose membranes with either a 12000-14000 g/mol or 3500 g/mol molecular weight cutoff (MWCO). ^{1}H NMR spectra were obtained at 400 MHz and ^{13}C NMR spectra were obtained at 100 MHz.

NMR chemical shifts are reported in ppm and are calibrated against residual solvent signal of CDCl$_3$ (δ 7.26 and 77 ppm), CD$_3$OD (δ 3.34 ppm), or (CD$_3$)$_2$SO (δ 2.50 and 40 ppm). Coupling constants (*J*) are expressed in Hertz (Hz). Infrared spectra (IR) were obtained as films from CH$_2$Cl$_2$ or THF/MeOH on NaCl plates. UV-visible absorption spectroscopy was performed on a Varian Cary 300 Bio UV-Visible Spectrophotometer. SEC was performed in THF using a Waters 515 HPLC pump, Wyatt OptilabRex RI and miniDAWN-TREOS detectors and two ResiPore (300 x 7.5 mm) columns from Polymer Laboratories. Polymer MWs were calculated based on the multi-angle light scattering data using the Wyatt Astra software, with dn/dc values of the polymers determined from the refractive index (RI) detector using Astra. DLS data were obtained using a Zetasizer Nano ZS instrument from Malvern Instruments. MALDI-TOF mass spectrometry data were obtained using a 4700 Proteomics Analyzer, MALDI TOF TOF (Applied Biosystems, Foster City, CA, USA). Reflectron and linear positive ion modes were used. High-resolution mass spectrometry (HRMS) was performed using a Finnigan MAT 8400 electron impact (EI) mass spectrometer. Extinction coefficients (ϵ) of compounds **1.33**, **2.8**, **2.10**, **2.11** and **2.12** were obtained from calibration curves based on the measurement of UV-visible absorbance versus concentration in CHCl$_3$/MeOH (3/2).

Synthesis of N$_3$-PEO-OH (2.2): HO-PEO-OH (**2.1**) with a MW of 2000 g/mol (2.0 g, 1.0 mmol, 1.0 equiv.), TsCl (0.22 g, 1.1 mmol, 1.1 equiv.), and DMAP (0.061 g, 0.50 mmol, 0.50 equiv.) were dissolved in dry CH$_2$Cl$_2$ (30 mL). Dry NEt$_3$ (0.12 g, 1.2 mmol, 1.2 equiv.) was then added via syringe. The resulting mixture was stirred at room temperature for 24 h. Following this, the mixture was washed with cold 1M HCl solution (1×20 mL) and cold brine (1×20 mL). The organic phase was dried over MgSO$_4$. After removal of MgSO$_4$ via filtration, CH$_2$Cl$_2$ was removed under reduced pressure. The residue was taken up in minimal CH$_2$Cl$_2$ and the product was precipitated into cold diethyl ether. This material was then dissolved in dry DMF (15 mL). Sodium azide (0.16 g, 2.5 mmol, 2.5 equiv. relative to **2.1**) was then added and the resulting mixture was stirred at 100 ^{o}C overnight. After cooling to room temperature, distilled water (15 mL) and CH$_2$Cl$_2$ (15 mL) were added. The organic phase was separated. The aqueous phase was extracted with CH$_2$Cl$_2$ (3×10 mL) and the combined CH$_2$Cl$_2$ layers were dried over

MgSO$_4$. After removal of MgSO$_4$ via filtration, the CH$_2$Cl$_2$ was removed under reduced pressure. The residue was taken up in minimal CH$_2$Cl$_2$ and precipitated into cold diethyl ether. Subsequent purification by column chromatography using CH$_2$Cl$_2$/MeOH as eluent (gradient: 19/1 to 14/1) gave compound **2.2** (0.36 g, 0.18 mmol) as a white solid. Overall yield: 18%. ^{1}H NMR (400 MHz, CDCl$_3$): δ 3.42-3.80 (m, 180H), 3.36 (t, 2H, J = 4.0). IR (cm^{-1}): 3445, 2884, 2102. MS calcd. for [M+Na]$^+$ based on functionalization of the starting polymer **2.1** with a peak MW of 1802 g/mol (n = 40): 1827. Found (MALDI-TOF+): 1827.

Synthesis of Copolymer 2.3 and General Procedure for the Preparation of Copolymers 2.3-2.6: Dry MeO-PEO-OH (0.25 g, 0.12 mmol, 1.0 equiv.) was added to a Schlenk flask as a solution in dry toluene (1.5 mL). CL (0.34 g, 3.0 mmol, 24 equiv.) was then added to the macroinitiator and the resulting solution was equilibrated at 30 °C for 10 min. MSA (0.12 mmol, 7.8 μL, 1.0 equiv.) was then added and the reaction mixture was stirred at 30 °C for 2.5 h. After cooling to room temperature, the mixture was treated with Amberlyst® A21 in order to remove the catalyst. The resin was removed by filtration and the product was precipitated in excess cold hexane. The resulting white solid was filtered and dried *in vacuo* to give 0.57 g of the product. Yield = 97%. ^{1}H NMR (400 MHz, CDCl$_3$): δ 4.21 (t, J = 6.0), 4.05 (t, J = 8.0, 50H), 3.46-3.82 (m, 180H), 3.37 (s, 3H), 2.29 (t, J = 8.0, 50H), 1.63 (m, 100H), 1.37 (m, 50H). IR (cm^{-1}): 3436, 2889, 1724. SEC: M_w = 5500 g/mol, PDI = 1.14, dn/dc = 0.086.

Synthesis of Copolymer 2.4: The copolymer was prepared by the same method described above for copolymer **2.3** except that compound **2.2** was used as the macroinitiator. Yield = 97%. ^{1}H NMR (400 MHz, CDCl$_3$): δ 4.21 (t, J = 6.0, 2H), 4.05 (t, J = 8.0, 56H), 3.46-3.82 (m, 180H), 3.37 (t, J = 6.0, 2H), 2.29 (t, J = 8.0, 56H), 1.63 (m, 112H), 1.37 (m, 56H). IR (cm^{-1}): 3438, 2869, 2105, 1724. SEC: M_w = 4600 g/mol, PDI = 1.18, dn/dc = 0.078.

Synthesis of Copolymer 2.5: The copolymer was prepared by the same method described above for copolymer **2.3** except that 82 equiv. of CL were used and the reaction time was 3.5 h. Yield = 95%. ^{1}H NMR (400 MHz, CDCl$_3$): δ 4.19 (t, J = 6.0,

2H), 4.03 (t, J = 8.0, 164H), 3.43-3.79 (m, 180H), 3.35 (s, 3H), 2.28 (t, J = 8.0, 164H), 1.64 (m, 328H), 1.37 (m, 164H). IR (cm^{-1}): 3437, 2867, 1724. SEC: M_w = 12400 g/mol, PDI = 1.40, dn/dc = 0.060.

Synthesis of Copolymer 2.6: The copolymer was prepared by the same method described above for copolymer **2.3** except that compound **2.2** was used as the macroinitiator, 82 equiv. of CL were used, and the reaction time was 3.5 h. Yield = 93%. ^{1}H NMR (400 MHz, CDCl$_3$): δ 4.21 (t, J = 6.0, 2H), 4.05 (t, J = 8.0, 168H), 3.45-3.80 (m, 180H), 3.38 (t, J = 4.0, 2H), 2.30 (t, J = 8.0, 168H), 1.64 (m, 336H), 1.37 (m, 168H). IR (cm^{-1}): 3433, 2866, 2100, 1725. SEC: M_w = 12000 g/mol, PDI = 1.19, dn/dc = 0.080.

Synthesis of Dendron 2.8: Dendron **1.33**[25] (81 mg, 39 μmol, 1.0 equiv.) and the protected guanidine derivative **2.7**[62] (0.20 g, 0.55 mmol, 14 equiv.) were dissolved in anhydrous DMF (7 mL) under a nitrogen atmosphere. HBTU (0.20 g, 0.55 mmol, 14 equiv.) was added, followed by HOBt (73 mg, 0.55 mmol, 14 equiv.) and DIPEA (0.14 mL, 0.78 mmol, 20 equiv.). The reaction mixture was stirred under nitrogen in the dark for 48 h. The product was then purified by dialysis against DMF using a 3500 MWCO membrane for 24 h. After removal of DMF under reduced pressure, the residue was dissolved in 2 mL of 1/1 TFA/CH$_2$Cl$_2$, and the reaction mixture was stirred at room temperature and in dark for 2 h. The solvent was removed under reduced pressure to provide dendron **2.8** (0.11 g) with approximately one chromophore per dendron statistically. Yield: 87%. ^{1}H NMR (400 MHz, CD$_3$OD): δ 7.92 (d, J = 8.0, 1H), 7.84-7.75 (m, 3H), 7.65-7.47 (m, 3H), 7.28 (d, J = 12, 1H), 7.10 (dd, J_1 = 12.0 , J_2 = 4.0, 1H), 7.00 (d, J = 4.0, 1H), 4.84-4.81 (m, 2H), 4.39-4.10 (m, 30H), 3.78-3.65 (m, 8H), 3.55-3.37 (m, 20H), 3.20 (t, J = 8.0, 16H), 3.04 (br s, 1H), 2.76-2.68 (m, 2H), 2.66-2.47 (m, 16H), 2.48-2.21 (m, 20H), 1.81-1.55 (m, 32H), 1.52-1.07 (m, 49H). IR (cm^{-1}): 3282, 3180, 2943, 2125, 1730, 1670, 1590, 1467. ε: 28008 L mol^{-1} cm^{-1} at 563 nm (CHCl$_3$/MeOH, 3/2).

Synthesis of Rhodamine Derivative 2.10: To a solution of **2.9**[65] (0.40 g, 0.73 mmol, 1.0 equiv.) in anhydrous DMF (2 mL) were added propargyl bromide (0.11 g, 0.92 mmol, 1.2 equiv.) and DIPEA (0.16 g, 1.3 mmol, 1.8 equiv.). The reaction mixture was stirred at room temperature in the dark for 24 h. An additional 1.2 equiv. of propargyl bromide and

DIPEA was then added, and the resulting solution was stirred for 2 additional h. The reaction mixture was then partitioned between ethyl acetate and saturated aqueous NaHCO$_3$. The aqueous layer was extracted with isopropanol/CH$_2$Cl$_2$ (1/3). The organic layer was collected, dried over MgSO$_4$, filtered, and concentrated to provide 0.33 g of the desired product. Yield: 82%. ^{1}H NMR (400 MHz, CDCl$_3$): δ 7.69-7.67 (m, 2H), 7.56-7.54 (m, 1H), 7.37-7.35 (m, 1H), 7.28 (s, 1H), 7.25 (s, 1H), 7.05-7.02 (dd, J_1 = 12.0, J_2 = 12.0, 2H), 6.81 (d, J = 4.0, 2H), 3.71-3.61 (m, 8H), 3.46-3.41 (m, 2H), 3.38-3.32 (m, 2H), 3.26 (d, J = 4.0, 2H), 2.41-2.33 (m, 4H), 2.24 (t, J = 4.0, 1H), 1.33 (t, J = 8.0, 12H). ^{13}C NMR (400 MHz, CDCl$_3$): δ 167.2, 157.5, 155.4, 135.2, 131.8, 130.2, 130.0, 129.7, 127.4, 114.0, 113.4, 110.7, 96.1, 73.8, 51.4, 50.7, 47.2, 46.4, 46.0, 41.3, 12.5. HRMS (m/z) calc'd for C$_{35}$H$_{42}$N$_4$O$_2$, 550.3308; found (EI), 550.3221 [M]$^+$. ε: 86201 L mol^{-1} cm^{-1} at 563 nm (CHCl$_3$/MeOH, 3/2).

Preparation of Rhodamine-Labeled Copolymers 2.11 and 2.12: Copolymer **2.4** or **2.6** (1.0 equiv.) and rhodamine derivative **2.10** (5.0 equiv.) were dissolved in THF/H$_2$O (2/1). To the solution were added CuCl$_2$·2H$_2$O (5.0 equiv.) and sodium ascorbate (50 equiv.), and the reaction mixture was stirred in the dark at room temperature for 20 h. The product was purified by first dialysis against distilled water for 24 h followed by dialysis against DMF for an additional 24 h using a 3500 MWCO dialysis membrane. DMF was removed *in vacuo* to give dye-labeled polymers **2.11** (yield: 81%) or **2.12** (yield: 89%), respectively. Due to low intensity of aromatic peaks of the dye compared to the polymer peaks, the integration of the ^{1}H NMR spectrum was not possible. However, completion of the reaction was confirmed by disappearance of the peaks corresponding to the methylene protons adjacent to the azide group in the polymer (Figure A2.8 and Figure A2.9). ε for **2.11**: 22851 L mol^{-1} cm^{-1} at 563 nm (CHCl$_3$/MeOH, 3/2). ε for **2.12**: 19847 L mol^{-1} cm^{-1} at 563 nm (CHCl$_3$/MeOH, 3/2).

Synthesis of Dendron 2.14: Dendron **2.13**[66] (0.42 g, 0.20 mmol) was dissolved in methanol (150 mL) and concentrated sulfuric acid (1.5 mL) was added. The resulting solution was stirred at room temperature for 2 h and then was then neutralized with 7 M NH$_3$ in MeOH to pH 7. The solution was filtered to remove the (NH$_4$)$_2$SO$_4$ precipitate and then the solvent was removed under reduced pressure to provide **2.14** (0.35 g) as a

white solid. Yield: 99%. ^{1}H NMR (400 MHz, DMSO-$d6$): δ 7.35-6.80 (br s, 16H), 4.72 (d, J = 7.8, 2H), 4.70-4.50 (m, 12H), 4.21-4.07 (m, 16H), 3.49-3.30 (m, 32H), 2.42 (t, J = 7.0, 1H), 1.22 (s, 3H), 1.18 (s, 6 H), 1.15 (s, 12H), 1.00 (s, 24H). ^{13}C NMR (400 MHz, DMSO-$d6$): δ 174.5, 172.2, 171.8, 171.7, 78.3, 78.2, 64.8, 64.1, 53.3, 50.6, 46.7, 46.6, 33.7, 25.7, 24.9, 17.8, 17.6, 17.3, 17.1. MS (m/z) calc'd for $C_{78}H_{124}NaO_{46}$, 1820; found (MALDI-TOF), 1820 [M+Na]$^{+}$.

General Procedure for the Preparation of PEO-PCL Micelles and Vesicles: The BCP (5 mg) was dissolved in THF (0.5 mL). Distilled water (2 mL) was added dropwise over 10 min with vigorous stirring. After the addition was complete, the resulting nanoassembly suspension was stirred for 10 min and then dialyzed against 2 liters of distilled water, using a 12000-14000 MWCO dialysis membrane, with multiple changes for at least 36 h to remove THF. The vesicles were extruded ten times through a 0.1 μm polycarbonate membrane at 65 ˚C using a pressure driven Lipex Thermobarrel Extruder (1.5 mL capacity, Northern Lipids).

General Procedure for Surface Functionalization of Micelles and Vesicles: Micelles or vesicles were prepared as described above using mixtures of copolymers **2.3** and **2.4** (micelles) or **2.5** and **2.6** (vesicles) in varying ratios (Scheme 2.6). To the assemblies were added CuCl$_2$·2H$_2$O (0.40 equiv. relative to total polymer), sodium ascorbate (4.0 equiv. relative to total polymer), and dye labeled dendron **1.33**, **2.8**, or dye **2.10** (4.0 equiv. relative azides) in sequence and the reaction mixture was stirred at room temperature for 18 h and then dialyzed against distilled water for 24 h using a 12000-14000 MWCO or 3500 MWCO dialysis membrane.

Quantification of Surface Dendritic Groups: Following dialysis, the samples were lyophilized in order to remove water and were then taken up in about 2 mL of CHCl$_3$/methanol 3/2. The solutions were centrifuged at 4500 rpm for 4 h to remove any insoluble material. Finally, the absorbance was measured at 563 nm. The degree of functionalization was calculated using the measured ε for the dye-labeled dendron **1.33**, dye-labeled guanidine dendron **2.8**, or rhodamine-functionalized polymers **2.11** or **2.12** in the same solvent.

Transmission Electron Microscopy: The suspension of micelles or vesicles (20 μL, 0.1 mg/mL) was placed on a carbon formvar grid and was left to stand for 5 min. The excess solution was then blotted off using a piece of filter paper. The resulting sample was dried in air overnight before imaging. Imaging was performed using a Phillips CM10 microscope operating at 80 kV with a 40 μm aperture.

Uptake of Micelles into HeLa Cells: HeLa cells were maintained at 37 ^{o}C and 5% CO_2 in Dulbecco's Modified Eagle Medium (DMEM) (Invitrogen) supplemented with 10% fetal bovine serum (FBS, Invitrogen). Sterilized microscope glass cover slips (22mm × 22mm) were placed in the wells of a 6-well plate and 1.5×10^5 cells per well were seeded onto each cover slip. The cells were allowed to adhere for 24 h. The culture medium was then aspirated and replaced with fresh serum free medium containing control or functionalized micelles at a concentration of 0.1 mg/mL of polymer. The experiments were completed in triplicate. The cells were incubated at 37 ^{o}C for 4 h. They were then washed 3 times with phosphate buffered saline (PBS) then fixed with 10% paraformaldehyde solution for 10 min. The cells were washed again with PBS, and then the cover slips were placed face down onto microscope slides for confocal microscopy. Confocal images were obtained using a confocal laser scanning microscope (LSM 510, Carl Zeiss Inc.) using a 63× (N.A. = 1.4) oil immersion objective and an excitation wavelength of 543 nm (He-Ne laser).

2.5 References

1. Alexandridis, P.; Lindman, B. *Amphiphilic Block Copolymers: Self-Assembly and Applications*; Elsevier: Amsterdam: New York, 2000.

2. Cornelissen, J.; Fischer, M.; Sommerdijk, N.; Nolte, R. J. M. *Science* **1998**, *280*, 1427.

3. Pochan, D. J.; Chen, Z. Y.; Cui, H. G.; Hales, K.; Qi, K.; Wooley, K. L. *Science* **2004**, *306*, 94.

4. Zhang, L. F.; Eisenberg, A. *Science* **1995**, *268*, 1728.

5. Discher, D. E.; Eisenberg, A. *Science* **2002**, *297*, 967.

6. Yan, D. Y.; Zhou, Y. F.; Hou, J. *Science* **2004**, *303*, 65.

7. Cui, H. G.; Chen, Z. Y.; Zhong, S.; Wooley, K. L.; Pochan, D. J. *Science* **2007**, *317*, 647.

8. Ahmed, F.; Photos, P. J.; Discher, D. E. *Drug Dev. Res.* **2006**, *67*, 4.

9. Photos, P. J.; Bacakova, L.; Discher, B.; Bates, F. S.; Discher, D. E. *J. Controlled Release* **2003**, *90*, 323.

10. Zhang, S. Y.; Zhao, Y. *J. Am. Chem. Soc.* **2010**, *132*, 10642.

11. Ranquin, A.; Versees, W.; Meier, W.; Steyaert, J.; Van Gelder, P. *Nano Lett.* **2005**, *5*, 2220.

12. Toti, U. S.; Guru, B. R.; Grill, A. E.; Panyam, J. *Mol. Pharm.* **2010**, *7*, 1108.

13. Liu, G. J.; Ma, S. B.; Li, S. K.; Cheng, R.; Meng, F. H.; Liu, H. Y.; Zhong, Z. Y. *Biomaterials* **2010**, *31*, 7575.

14. Harada, A.; Togawa, H.; Kataoka, K. *Eur. J. Pharm. Sci.* **2001**, *13*, 35.

15. Ahmed, F.; Pakunlu, R. I.; Srinivas, G.; Brannan, A.; Bates, F.; Klein, M. L.; Minko, T.; Discher, D. E. *Mol. Pharm.* **2006**, *3*, 340.

16. Yang, X. Q.; Grailer, J. J.; Rowland, I. J.; Javadi, A.; Hurley, S. A.; Matson, V. Z.; Steeber, D. A.; Gong, S. Q. *ACS Nano* **2010**, *4*, 6805.

17. Yang, X. Q.; Grailer, J. J.; Rowland, I. J.; Javadi, A.; Hurley, S. A.; Steeber, D. A.; Gong, S. Q. *Biomaterials* **2010**, *31*, 9065.

18. Ghoroghchian, P. P.; Frail, P. R.; Susumu, K.; Blessington, D.; Brannan, A. K.; Bates, F. S.; Chance, B.; Hammer, D. A.; Therien, M. J. *P. Natl. Acad. Sci. USA.* **2005**, *102*, 2922.

19. Guthi, J. S.; Yang, S. G.; Huang, G.; Li, S. Z.; Khemtong, C.; Kessinger, C. W.; Peyton, M.; Minna, J. D.; Brown, K. C.; Gao, J. M. *Mol. Pharm.* **2010**, *7*, 32.

20. Pang, Z. Q.; Feng, L. A.; Hua, R. R.; Chen, J.; Gao, H. L.; Pan, S. Q.; Jiang, X. G.; Zhang, P. *Mol. Pharm.* **2010**, *7*, 1995.

21. Blanazs, A.; Armes, S. P.; Ryan, A. J. *Macromol. Rapid Commun.* **2009**, *30*, 267.

22. LoPresti, C.; Lomas, H.; Massignani, M.; Smart, T.; Battaglia, G. *J. Mater. Chem.* **2009**, *19*, 3576.

23. Letchford, K.; Burt, H. *Eur. J. Pharm. Biopharm.* **2007**, *65*, 259.

24. Pittet, M. J.; Swirski, F. K.; Reynolds, F.; Josephson, L.; Weissleder, R. *Nat. Protoc.* **2006**, *1*, 73.

25. Li, B.; Martin, A. L.; Gillies, E. R. *Chem. Commun.* **2007**, 5217.

26. Martin, A. L.; Li, B.; Gillies, E. R. *J. Am. Chem. Soc.* **2009**, *131*, 734.

27. Shi, M.; Lu, J.; Shoichet, M. S. *J. Mater. Chem.* **2009**, *19*, 5485.

28. Lam, C. X. F.; Teoh, S. H.; Hutmacher, D. W. *Polym. Int.* **2007**, *56*, 718.

29. Jenkins, M. J.; Harrison, K. L.; Silva, M.; Whitaker, M. J.; Shakesheff, K. M.; Howdle, S. M. *Eur. Polym. J.* **2006**, *42*, 3145.

30. Sinha, V. R.; Bansal, K.; Kaushik, R.; Kumria, R.; Trehan, A. *Int. J. Pharm.* **2004**, *278*, 1.

31. Chandra, R.; Rustgi, R. *Prog. Polym. Sci.* **1998**, *23*, 1273.

32. Allen, C.; Yu, Y. S.; Maysinger, D.; Eisenberg, A. *Bioconjugate Chem.* **1998**, *9*, 564.

33. Allen, C.; Han, J. N.; Yu, Y. S.; Maysinger, D.; Eisenberg, A. *J. Controlled Release* **2000**, *63*, 275.

34. Aliabadi, H. M.; Mahmud, A.; Sharifabadi, A. D.; Lavasanifar, A. *J. Controlled Release* **2005**, *104*, 301.

35. Forrest, M. L.; Won, C. Y.; Malick, A. W.; Kwon, G. S. *J. Controlled Release* **2006**, *110*, 370.

36. Mikhail, A. S.; Allen, C. *Biomacromolecules* **2010**, *11*, 1273.

37. Azzam, T.; Eisenberg, A. *Langmuir* **2007**, *23*, 2126.

38. Adams, D. J.; Kitchen, C.; Adams, S.; Furzeland, S.; Atkins, D.; Schuetz, P.; Fernyhough, C. M.; Tzokova, N.; Ryan, A. J.; Butler, M. F. *Soft Matter* **2009**, *5*, 3086.

39. Meng, F. H.; Hiemstra, C.; Engbers, G. H. M.; Feijen, J. *Macromolecules* **2003**, *36*, 3004.

40. Ahmed, F.; Discher, D. E. *J. Controlled Release* **2004**, *96*, 37.

41. Rameez, S.; Alosta, H.; Palmer, A. F. *Bioconjugate Chem.* **2008**, *19*, 1025.

42. Pang, Z. Q.; Lu, W.; Gao, H. L.; Hu, K. L.; Chen, J.; Zhang, C. L.; Gao, X. L.; Jiang, X. G.; Zhu, C. Q. *J. Controlled Release* **2008**, *128*, 120.

43. Katz, J. S.; Zhong, S.; Ricart, B. G.; Pochan, D. J.; Hammer, D. A.; Burdick, J. A. *J. Am. Chem. Soc.* **2010**, *132*, 3654.

44. Ghoroghchian, P. P.; Li, G. Z.; Levine, D. H.; Davis, K. P.; Bates, F. S.; Hammer, D. A.; Therien, M. J. *Macromolecules* **2006**, *39*, 1673.

45. Sachl, R.; Uchman, M.; Matejicek, P.; Prochazka, K.; Stepanek, M.; Spirkova, M. *Langmuir* **2007**, *23*, 3395.

46. Johnston, A. H.; Dalton, P. D.; Newman, T. A. *J. Nanopart. Res.* **2010**, *12*, 1997.

47. Labet, M.; Thielemans, W. *Chem. Soc. Rev.* **2009**, *38*, 3484.

48. Oshimura, M.; Takasu, A. *Macromolecules* **2010**, *43*, 2283.

49. Chang, K. Y.; Lee, Y. D. *Acta Biomater.* **2009**, *5*, 1075.

50. Wang, G. W.; Huang, J. L. *J. Polym. Sci., Part A: Polym. Chem.* **2008**, *46*, 1136.

51. Xu, X. W.; Huang, J. L. *J. Polym. Sci., Part A: Polym. Chem.* **2006**, *44*, 467.

52. Canaria, C. A.; Smith, J. O.; Yu, C. J.; Fraser, S. E.; Lansford, R. *Tetrahedron Lett.* **2005**, *46*, 4813.

53. Uyeda, H. T.; Medintz, I. L.; Jaiswal, J. K.; Simon, S. M.; Mattoussi, H. *J. Am. Chem. Soc.* **2005**, *127*, 3870.

54. Bouzide, A.; Sauve, G. *Org. Lett.* **2002**, *4*, 2329.

55. Petersen, M. A.; Yin, L. G.; Kokkoli, E.; Hillmyer, M. A. *Polym. Chem.* **2010**, *1*, 1281.

56. Raynaud, J.; Absalon, C.; Gnanou, Y.; Taton, D. *J. Am. Chem. Soc.* **2009**, *131*, 3201.

57. Luo, L. B.; Tam, J.; Maysinger, D.; Eisenberg, A. *Bioconjugate Chem.* **2002**, *13*, 1259.

58. Vangeyte, P.; Gautier, S.; Jerome, R. *Colloids Surf., A* **2004**, *242*, 203.

59. Zupancich, J. A.; Bates, F. S.; Hillmyer, M. A. *Macromolecules* **2006**, *39*, 4286.

60. Liu, J. B.; Zeng, F. Q.; Allen, C. *Eur. J. Pharm. Biopharm.* **2007**, *65*, 309.

61. Gazeau-Bureau, S.; Delcroix, D.; Martin-Vaca, B.; Bonrissou, D.; Navarro, C.; Magnet, S. *Macromolecules* **2008**, *41*, 3782.

62. Martin, A. L.; Bernas, L. M.; Rutt, B. K.; Foster, P. J.; Gillies, E. R. *Bioconjugate Chem.* **2008**, *19*, 2375.

63. Josephson, L.; Tung, C. H.; Moore, A.; Weissleder, R. *Bioconjugate Chem.* **1999**, *10*, 186.

64. Lewin, M.; Carlesso, N.; Tung, C. H.; Tang, X. W.; Cory, D.; Scadden, D. T.; Weissleder, R. *Nat. Biotechnol.* **2000**, *18*, 410.

65. Nguyen, T.; Francis, M. B. *Org. Lett.* **2003**, *5*, 3245.

66. Wu, P.; Malkoch, M.; Hunt, J. N.; Vestberg, R.; Kaltgrad, E.; Finn, M. G.; Fokin, V. V.; Sharpless, K. B.; Hawker, C. J. *Chem. Commun.* **2005**, 5775.

67. Chou, T. C.; Lin, K. C.; Wu, C. A. *Tetrahedron* **2009**, *65*, 10243.

68. Peng, S. M.; Chen, Y.; Hua, C.; Dong, C. M. *Macromolecules* **2009**, *42*, 104.

69. Hua, C.; Peng, S. M.; Dong, C. M. *Macromolecules* **2008**, *41*, 6686.

70. Gillies, E. R.; Jonsson, T. B.; Fréchet, J. M. J. *J. Am. Chem. Soc.* **2004**, *126*, 11936.

Chapter 3

3 Biodegradable Dendritic Polymersomes as Modular, High Relaxivity MRI Contrast Agents[*]

3.1 Introduction

The early detection and diagnosis of disease is currently one of the major challenges in medicine. Clinical imaging plays a significant role in this process. Among the various imaging modalities, MRI has become a well-established and powerful tool, due to its excellent spatial resolution and soft tissue contrast. To aid in the differentiation between healthy and diseased tissues, small molecule Gd(III) chelates such as Magnevist[®] are used in approximately 50% of MRI scans. While the availability of these agents has enabled significant developments in MRI, they do suffer from some significant limitations. For example, they typically possess longitudinal relaxivities (r_1) in the range of 3 - 5 mM^{-1}s^{-1}, only a small fraction of the theoretically possible values.[1] This results in the requirement for very large doses of these agents and also limits their applicability in molecular imaging.[2] In addition, most of these agents are non-targeted and have very short circulation half-lives in the blood.

To address these limitations, Gd(III) complexes have been conjugated to a wide variety of macromolecular scaffolds including dendrimers,[3,4] linear polymers,[5] proteins,[6] viral particles,[7] micelles,[8,9] liposomes,[10,11] and polymersomes.[12-14] This can result in improvements in r_1 values due to the slower tumbling rates of macromolecules and the resulting increases in the rotational correlation times of the Gd(III).[15,16] In addition, macromolecular systems can exhibit prolonged blood circulation times, enabling the targeting of tissues either passively or actively through the conjugation of targeting ligands. Among the available macromolecular assemblies, BCP vesicles, commonly referred to as polymersomes, have attracted significant attention due to their potential

multifunctionality. They possess an aqueous core capable of encapsulating water-soluble species, a hydrophobic membrane that can encapsulate hydrophobes, and a surface to which specific targeting ligands or other species can be conjugated. Thus far, there are very few reports of polymersome-based MRI contrast agents.[12-14] Cheng et al. have investigated porous polymersomes containing Gd(III)-labeled dendrimers within their aqueous cores, and have obtained an r_1 of 7.5 mM^{-1}s^{-1} (60 MHz, 40 ˚C) on per Gd basis.[12,13] More recently, Grüll et al. incorporated Gd(III)-labeled lipids into a polymersome membrane, resulting in an r_1 of 22 mM^{-1}s^{-1} (20 MHz, 25 ˚C).[14]

Our group has developed approaches for the functionalization of polymersome surfaces with dendritic groups.[17,18] It was shown that this is an effective method for tuning the surface chemistries of polymersomes in a single step, resulting in properties such as enhanced target binding and cell uptake.[19,20] For the current work, it was proposed that polymersome-immobilized dendrons functionalized with Gd(III) complexes may serve as highly efficient MRI contrast agents. While conjugation of Gd(III) complexes to high generation dendrimers is known to enhance their relaxivities,[3,4] immobilization on the polymersome surface should provide further enhancements, at the same time opening the possibility to exploit the multifunctional properties of polymersomes. We describe here the preparation of the dendron and polymersome components, and studies of their relaxivities. It is demonstrated how nanoscale components can be readily combined to provide additive enhancements in relaxivity.

3.2 Results and Discussion

3.2.1 Design and Synthesis

Figure 3.1 depicts the general approach for the preparation of the polymersome MRI contrast agents. PCL-PEO BCPs were selected due to the biodegradability of the PCL block and the well demonstrated biocompatibility of PEO in various applications.[21] Methoxy- (**2.5**) and azide-terminated (**2.6**) PCL-PEO were prepared as previously reported and were assembled into azide-functionalized vesicles.[22] The z-average diameter of the polymersomes was 140 nm, as measured by DLS.
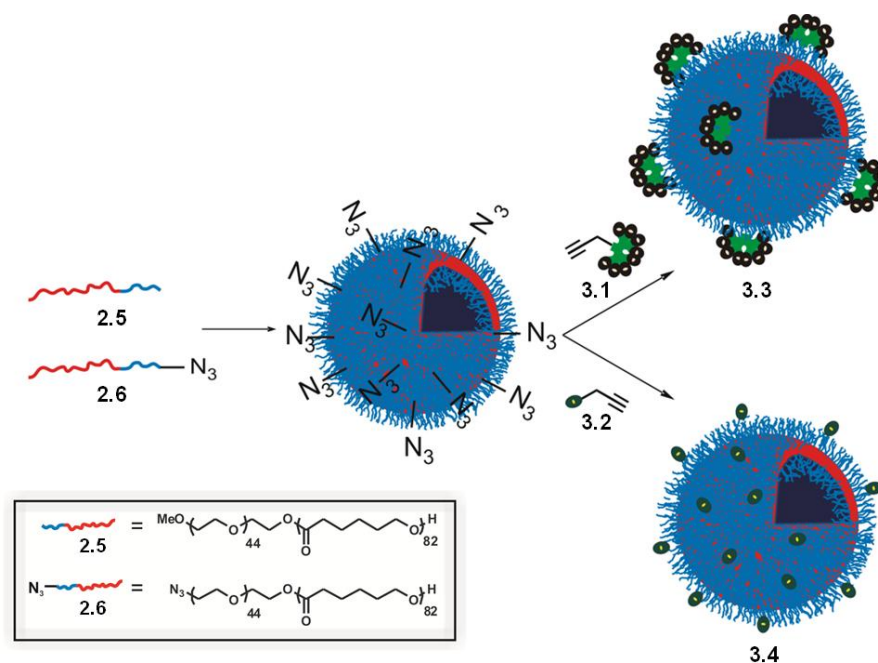
Figure 3.1. Schematic for the preparation of dendritic and non-dendritic Gd(III)-functionalized polymersomes.

Gd(III)-functionalized dendron **3.1**, having a focal point alkyne, was prepared starting from the third generation polyester dendron **3.5**.[17] As shown in Scheme 3.1, the peripheral amine groups of **3.5** were reacted with the commercially available DTPA isothiocyanate derivative **3.6**. The resulting dendron **3.7** was then treated with GdCl$_3$ to provide the target dendron **3.1**.

As shown in Figure 3.1, in order to determine the contribution of the dendron versus polymersome to the relaxivity, it was also desirable to prepare a non-dendritic alkyne derivative of the Gd(III) chelate (**3.2**). As shown in Scheme 3.2, this was accomplished by the reaction of propargyl amine with **3.6** to provide **3.8**, followed by chelation of Gd(III) to obtain the target compound **3.2**.
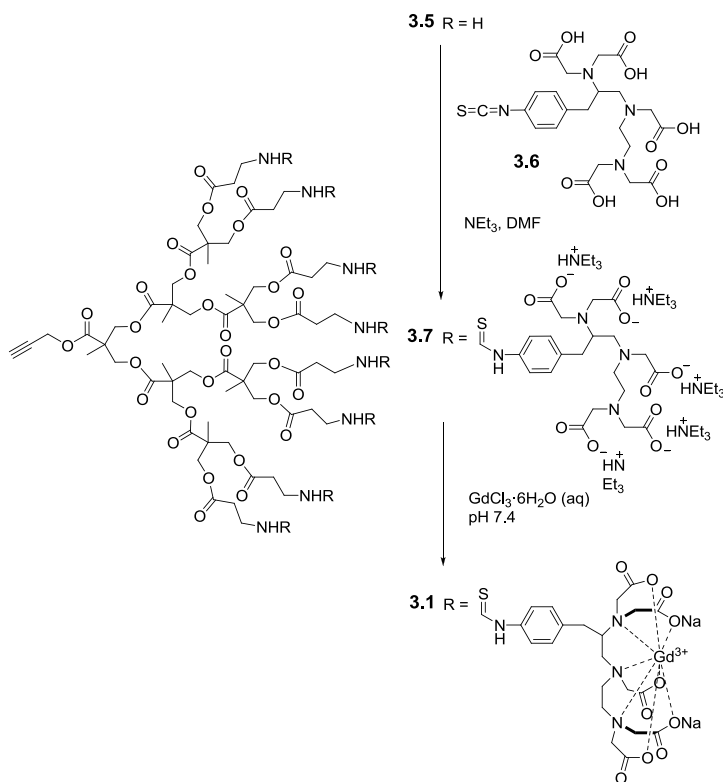
Scheme 3.1. Synthesis of Gd(III)-functionalized dendron **3.1**.
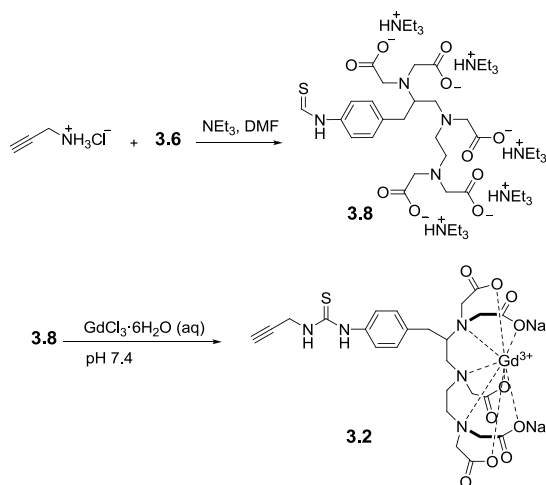
Scheme 3.2. Synthesis of Gd(III) complex **3.2**.

Prior to Gd(III) insertion, compounds **3.7** and **3.8** were characterized by ^{1}H and ^{13}C NMR spectroscopy. In addition, IR spectroscopy was informative for this class of

compounds. For example, upon conversion of dendron **3.5** to **3.7**, the absence of the characteristic C=S stretch of the isothiocyanate functional group that was present in compound **3.6** confirmed the successful removal of excess **3.6** (Figure A3.1). After insertion of Gd(III), NMR spectroscopic analysis was no longer possible due to the paramagnetic nature of the Gd(III) ion. However, inductively coupled plasma mass spectrometry (ICP-MS) was performed, confirming the successful insertion of Gd(III) into dendron **3.1** and compound **3.2**. In addition, IR spectroscopy demonstrated that the peaks corresponding to the C=O stretches of the ligand shifted to significantly lower frequencies in compounds **3.1** and **3.2** relative to **3.7** and **3.8** respectively (Figure A3.1 and Figure A3.2). This is also an indication of successful coordination of the carboxylate groups to Gd(III).[23]

3.2.2 Functionalization of Polymersome Surfaces with Dendritic and Non-Dendritic Contrast Agents

The next step was to conjugate **3.1** and **3.2** to the polymersome surfaces. This was accomplished by a Cu(I)-mediated 3+2 "click" cycloaddition to provide the dendritic Gd(III)-functionalized polymersomes **3.3**, and non-dendritic Gd(III)-functionalized polymersomes, **3.4**, respectively. Unreacted **3.1** and **3.2** were removed by dialysis. ICP-MS measurements were performed on the products and the results indicated that 38% of the azide groups were functionalized in polymersomes **3.3** and 26% in polymersomes **3.4**. The sizes and morphologies of the resulting polymersomes were evaluated by DLS and TEM. As shown in Figure 3.2, small increases in the z-average diameters to 158 and 156 nm were found for vesicles **3.3** and **3.4** respectively. It should be mentioned that the shoulder observed at higher molecular weight region in polymersomes **3.3** (Figure 3.2c) suggests the existence of a small degree of aggregation upon conjugation of the bulky dendron **3.1** to the polymersome surfaces. Moreover, TEM showed that the vesicular morphology was preserved and the contrast was enhanced upon incorporation of the Gd(III) in both dendritic and non-dendritic polymersomes (Figure 3.3).
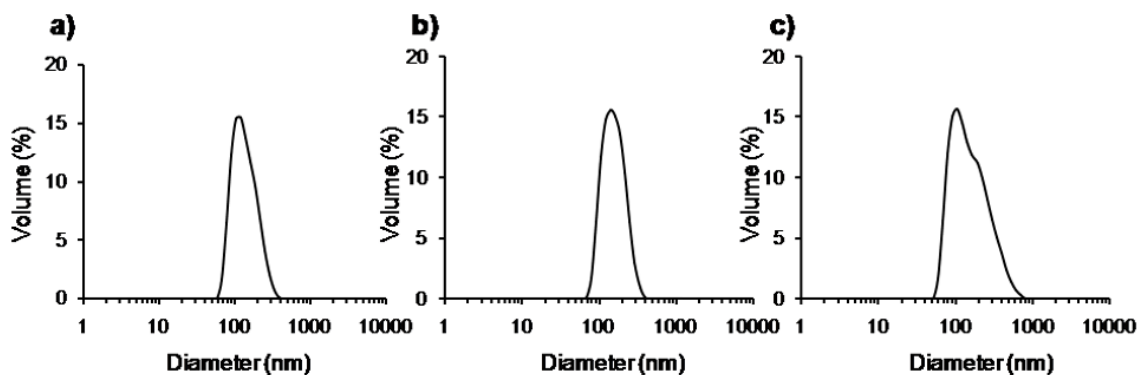
Figure 3.2. Size distribution profiles for: a) naked polymersome; non-dendritic polymersome **3.4**; c) dendritic polymersome **3.3**.
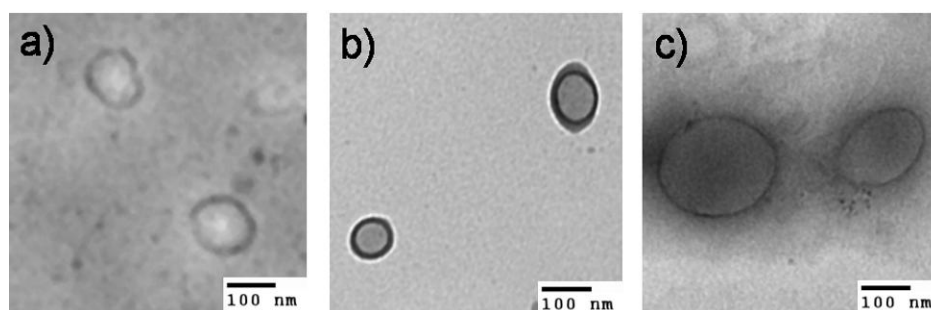
Figure 3.3. TEM images of (a) naked polymersome; (b) dendritic Gd(III)-functionalized polymersomes **3.3**; (c) non-dendritic Gd(III)-functionalized polymersomes **3.4**.

3.2.3 Evaluation of the Relaxivity Properties of the Contrast Agents

The properties of the three newly developed contrast agents (**3.1**, **3.3**, and **3.4**) were assessed in phosphate buffer (0.1 M, pH 7.4) at 298K (Figure 3.4) and 310 K (Figure A3.3) between 0.01 and 42 MHz using a field cycling relaxometer. On a per Gd(III) basis, dendron **3.1** and polymersomes **3.3** and **3.4** exhibited r_1 values of 12.1 ± 0.3, 26.1 ± 1.2, and 10.6 ± 0.4 mM^{-1}s^{-1}, respectively (20 MHz, 298 K). In comparison with the clinical agent Magnevist® (Gd(III)-DTPA) which has a reported relaxivity of 4.6 mM^{-1}s^{-1} under the same conditions[24], this corresponds to 2.6-, 5.7-, and 2.3-fold increases in r_1 for dendron **3.1**, and polymersome **3.3** and **3.4** respectively. All of the systems exhibit an r_1 versus frequency curve shape that is characteristic of restricted tumbling motion of the Gd(III) complex.[1]
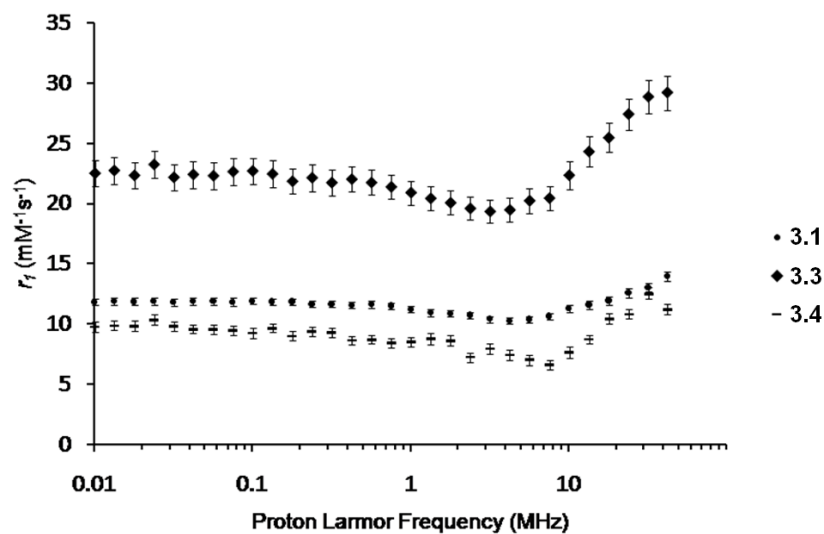
Figure 3.4. Longitudinal relaxivity (r_1) of dendron **3.1**, polymersome **3.3**, and polymersome **3.4** in phosphate buffer (0.1 M, pH 7.4) as a function of field strength at 298 K.

While polyester dendrons such as **3.1** have not previously been investigated as MRI contrast agents, the r_1 value of 12.1 mM^{-1}s^{-1} is within the range expected for a third generation dendrimer.[3,4] As with other dendrimers, this enhancement can likely be attributed to the crowded nature of the dendron periphery, which inhibits the free rotation of the Gd(III) complexes. The enhanced r_1 value of 10.6 mM^{-1}s^{-1} obtained for the non-dendritic polymersomes **3.4** is also likely a result of the hindered motion of the Gd(III) complexes at the vesicle surface, as well as the slow tumbling rate of the entire vesicle system. This r_1 value is lower than the value of 22 mM^{-1}s^{-1} at (20 MHz, 25 °C) obtained by Grüll et al. with lipid functionalized Gd(III) chelates incorporated into polymersomes. This is probably because their chelates were attached directly to the lipids, rather than through a long linker. The PEO chains in the current work introduce flexibility, which can decrease the rotational correlation time. PEO surrounding the chelate may also slow water exchange. However, r_1 is higher than for the system reported by Cheng et al. which contained Gd(III) complexes within the polymersomes.[12,13] This can be attributed to our selective attachment of the chelates to the periphery, where they are easily accessible to bulk water.

When both the dendritic component and the polymersome component are combined in polymersome **3.3**, the resulting r_1 of 26.1 mM^{-1}s^{-1} is the highest reported relaxivity for a polymersome system. This additive effect can result from the availability of chelates at the vesicle surface for water exchange, hindered motion of the Gd(III) complexes imparted by the dendron at a local level, as well as the large size and slow tumbling rate of the polymersome at the nanoscale level. Thus, this work elegantly demonstrates that different components can be combined through rational design to obtain additive effects on the relaxivity. An additional feature of the current system relative to those previously reported is the biodegradability imparted by the PCL block of the copolymer and the polyester dendron which is known to break down over a period of several days in physiological conditions.[25] This should enable the release of low MW Gd(III) complexes and polymer products from the body, an important consideration for MRI contrast agents.

3.3 Conclusion

In conclusion, through the synthesis of dendritic and non-dendritic Gd(III) chelates and their conjugation to polymersome surfaces, three new MRI contrast agents were developed. Using these systems, the effects of the dendritic and polymersome components on the relaxivities of the agents were elucidated. They were found to have an additive effect, resulting in the highest currently reported r_1 for a polymersome system. In addition, this system possesses the advantage of being composed of PEO and biodegradable polyester components. Future work will be aimed at exploring the biodegradability and *in vivo* properties of the system as well as exploiting the multifunctional capabilities of polymersomes.

3.4 Experimental

General Procedures and Materials

Compound **3.6** was purchased from Macrocyclics (Dallas, USA). All the other chemicals were purchased from Sigma-Aldrich and were used without further purification unless otherwise noted. Anhydrous DMF was obtained from a solvent purification system using aluminum oxide columns. NEt$_3$ was distilled from CaH$_2$. Ultrapure water was obtained

from a Barnstead EASYpure II system. Unless otherwise stated, all reactions were performed under a nitrogen atmosphere using flame or oven dried glassware. Dialyses were performed using Spectra/Por regenerated cellulose membranes with either a 1000, 3500, or 50000 g/mol MWCO. ^{1}H NMR spectra were obtained at 400 MHz, and ^{13}C NMR spectra were obtained at 100 MHz. NMR chemical shifts are reported in ppm and are calibrated against the residual solvent signal of CD$_3$OD (δ 3.31 and 50.41 ppm), or (CD$_3$)$_2$SO (δ 2.50 and 40.45 ppm). J values are expressed in Hz. IR spectra were obtained as NaCl pellets using a Bruker Tensor 27 instrument. HRMS was performed using a Finnigan MAT 8400 electron impact mass spectrometer. DLS data were obtained using a Zetasizer NanoZS instrument from Malvern Instruments. ICP-MS analysis was performed at the Environmental Analytical Laboratories of the Saskatchewan Research Council. Relaxation rate measurements were performed on a Stelar Spinmaster FFC2000 1T C/DC relaxometer at 298 and 310 K using 100 mM pH 7.4 phosphate buffer as solvent. Error measurements on the relaxivity are based on the combined uncertainties of the relaxometer measurements and the Gd(III) concentrations in the solutions.

Synthesis of Dendron 3.7: Dendron **3.5**[17] (49 mg, 22 μmol, 1.0 equiv.) and DTPA derivative **3.6** (0.11 g, 0.18 mmol, 8.0 equiv.) were dissolved in anhydrous DMF (2 mL) with sonication. Anhydrous NEt$_3$ (0.4 mL) was then added and the reaction mixture was stirred at room temperature overnight. An additional portion of **3.6** (0.11 g, 0.18 mmol, 8.0 equiv.) was added the next morning and the mixture was stirred for another 12 h at room temperature. Distilled water (1 mL) was then added to dissolve the resulting solid and the solution was dialyzed against distilled water (2 L) using a 3500 g/mol MWCO membrane for 24 h. The sample was lyophilized to provide dendron **3.7** as a light yellow fluffy solid (0.12 g, 73%). ^{1}H NMR (CD$_3$OD): δ 7.54-7.35 (m, 16H), 7.32-7.19 (m, 16H), 4.79 (br s, 2H), 4.40-4.16 (m, 28H), 3.89-3.40 (m, 112H), 3.24-2.94 (m, 296H), 2.80-2.68 (m, 16H), 1.27 (t, 384H, J = 8). ^{13}C NMR (CD$_3$OD): δ 180.7, 174.6, 171.7, 169.9, 169.4, 158.4, 138.2, 129.3, 124.1, 123.6, 62.3, 57.2, 55.6, 54.3, 53.9, 53.8, 52.5, 45.8, 39.6, 38.6, 38.4, 37.8, 33.4, 32.0, 25.4, 24.7, 17.1, 17.0, 7.9. IR (cm^{-1}): 3444, 2976, 2939, 2678, 2495, 1740, 1628.

Synthesis of Dendron 3.1: Dendron **3.7** (30 mg, 3.9 μmol, 1.0 equiv.) was dissolved in ultrapure water (4 mL). Using 0.1 M NaOH (in ultrapure water), the pH of the dendron solution was carefully adjusted to 7.4. $GdCl_3 \cdot 6H_2O$ (46 mg, 0.12mmol, 32 equiv.) was then added as a solution in ultrapure water. The pH of the solution was again adjusted to 7.4 using the 0.1M NaOH. The resulting solution was stirred at room temperature for 20 h. After this period of time, the mixture was transferred to a 1000 g/mol MWCO membrane and dialyzed against ultrapure water for 24 h. The sample was centrifuged at 5000 rpm for 30 min to remove any insoluble species. Finally, the sample was lyophilized to give the target Dendron **3.1** as a fluffy white solid (19 mg, 65%). IR (cm^{-1}): 3421, 2924, 1735, 1602.^{1}H and ^{13}C NMR of this compound could not be obtained because of paramagnetic Gd(III) ions. ICP-MS: mass of dendron analyzed: 2.4 mg; mass of Gd(III) expected: 0.43 mg; mass of Gd(III) found: 0.42 ± 0.01 mg. This suggests that all eight positions at the periphery of dendron **3.1** were functionalized with the DTPA derivative and these successfully chelated Gd(III).

Synthesis of compound 3.8: Compound **3.6** (21 mg, 33 μmol, 1.0 equiv.) and propargylamine hydrochloride (2.7 mg, 30 μmol, 0.90 equiv.) were dissolved in anhydrous DMF (0.5 mL) and anhydrous NEt$_3$ (0.4 mL). The mixture was stirred at room temperature overnight. The solvents were removed under reduced pressure and the obtained target molecule **3.8** was used without further purification (quantitative yield). ^{1}H NMR (DMSO-d_6): δ 7.45 (d, 2H, $J = 8$), 7.10 (d, 2H, $J = 8$), 5.21 (d, 2H, $J = 16$), 4.74 (s, 1H), 3.63 (br s, 2H), 3.52-3.18 (m, 12H), 3.12-2.91 (m, 5H), 2.88-2.75 (m, 5H), 2.47-2.40 (m, 1H), 1.18 (br s, 9H). ^{13}C NMR (DMSO-d_6): δ 189.6, 162.7, 153.2, 132.2, 129.7, 118.6, 78.0, 77.6, 74.4, 45.6, 37.0, 31.2, 31.2, 28.5, 8.8. IR (cm^{-1}): 3422, 2978, 2676, 2495, 2125, 1637. HRMS: calcd [M]$^+$ ($C_{25}H_{33}N_5O_{10}SNa$): 618.1846 Found: (EI) 618.1830.

Synthesis of compound 3.2: Compound **3.8** (23 mg, 21 μmol, 1.0 equiv.) was dissolved in ultrapure water (3 mL). Using 0.1 M NaOH (in ultrapure water) the pH of the solution was carefully adjusted to 7.4. $GdCl_3 \cdot 6H_2O$ (12 mg, 31 μmol, 1.5 equiv.) was then added as a solution in ultrapure water. The pH of the solution was again adjusted to 7.4 using 0.1 M NaOH. The resulting solution was stirred at room temperature for 20 h. The

sample was centrifuged at 5000 rpm for 30 min to remove any insoluble species. Finally, the sample was lyophilized to give the target molecule **5** as a white solid (12 mg, 70%). IR (cm^{-1}): 3412, 2924, 1603. ^{1}H and ^{13}C NMR of this compound could not be obtained because of paramagnetic Gd (III) ions. ICP-MS: mass of sample analyzed: 0.51 mg; mass of Gd(III) expected: 0.10 mg; mass of Gd(III) found: 0.16 ± 0.01 mg. The higher amount of Gd(III) found for this sample was expected as no purification was performed on compound **3.2**. However, this is not problematic as the relaxivity of this molecule will not be evaluated and the excess Gd(III) will subsequently be removed during dialysis of polymersomes **3.4**.

Preparation of dendritic Gd(III)-functionalized polymersomes 3.3: PCL-PEO polymersomes (2 mg/mL, 5 mL) containing an 80:20 ratio of methoxy-terminated PCL-PEO (**2.5**): azide-terminated PCL-PEO-N$_3$ (**2.6**) were prepared in ultrapure water as previously reported.[18] To the vesicle suspension was then added **3.1** (5.1 mg, 0.70 µmol, 4.0 equiv. relative to azide polymer) dissolved in minimal ultrapure water. Separately, CuCl$_2$·2H$_2$O (0.34 mg, 2.0 µmol, 2.3 equiv. relative to total polymer) and bathophenanthrolinedisulfonic acid (2.4 mg, 4.0 µmol, 4.6 equiv. relative to total polymer) were combined in ultrapure water (0.2 mL) for 15 min and then the resulting complex was added to the vesicle suspension followed by addition of sodium ascorbate (4.0 mg, 20 µmol, 23 equiv. relative to total polymer). The resulting mixture was stirred at room temperature for 18 h and then dialyzed against phosphate buffer (0.10 M, pH 7.4) for 24 h using a 50000 g/mol MWCO dialysis membrane. ICP-MS of the sample prepared for relaxivity measurement: mass of Gd(III) expected for 100% functionalization of **2.6**: 220 µg; mass of Gd(III) found: 83 ± 4 µg, which corresponds to 38% functionalization of polymer **2.6** in the polymersomes with dendron **3.1**. To exclude the possibility of presence of any free Gd, Xylenol orange test[26] was performed and it was found that less than 0.01% of the Gd(III) present was unchelated. Moreover, ICP-MS results showed that > 94% of the copper used for reaction was successfully removed by dialysis.

Preparation of non-dendritic Gd(III)-functionalized polymersomes 3.4: PCL-PEO polymersomes (2 mg/mL, 5 mL) containing a 50:50 ratio of methoxy-terminated PCL-

PEO (**2.5**): azide-terminated PCL-PEO-N$_3$ (**2.6**) were prepared in ultrapure water as previously reported.[18] To the vesicle suspension was then added **3.2** (1.4 mg, 1.7 μmol, 4.0 equiv. relative to azide polymer) dissolved in minimal ultrapure water. Separately, CuCl$_2$·2H$_2$O (0.34 mg, 2.0 μmol, 2.3 equiv. relative to total polymer) and bathophenanthrolinedisulfonic acid (2.4 mg, 4.0 μmol, 4.6 equiv. relative to total polymer) were combined in ultrapure water (0.2 mL) for 15 min and then the resulting complex was added to the vesicle suspension followed by the addition of sodium ascorbate (4.0 mg, 20 μmol, 23 equiv. relative to total polymer). The resulting mixture was stirred at room temperature for 18 h and then dialyzed against phosphate buffer (0.10 M, pH 7.4) for 24 h using a 50000 g/mol MWCO dialysis membrane. ICP-MS of the sample prepared for relaxivity measurement: mass of Gd(III) expected for 100% functionalization of **2.6**: 68 μg; mass of Gd(III) found: 18 ± 1 μg, which corresponds to 26% functionalization of polymer **2.6** in the polymersomes with compound **3.2**. Xylenol orange test showed that only 0.06% of the of the Gd(III) present was unchelated. In addition, ICP-MS results confirmed successful removal of more than 97% of the copper used for the reaction by dialysis.

*Note: The reason why a different composition of **2.5**:**2.6** was used for polymersome formation here than for polymersomes **3.3** is to account for the higher loading of Gd that was introduced by each dendron **3.1**, because each dendron can potentially introduce eight Gd ions while each of molecule **3.2** can only introduce one Gd ion.

Transmission electron microscopy: A small portion of the vesicle suspension was dialyzed against distilled water to remove any salts from the phosphate buffer. The suspension (20 μL, 0.1 mg/mL) was then placed on a Carbon/Formvar® grid and was left to stand for 5 min. The excess solution was then blotted off using a piece of filter paper. The resulting sample was dried in air overnight before imaging. Imaging was performed using a Phillips CM10 microscope operating at 80 kV with a 40 μm aperture.

3.5 References

1. Caravan, P. *Chem. Soc. Rev.* **2006**, *35*, 512.

2. Prince, M. R.; Zhang, H. L.; Roditi, G. H.; Leiner, T.; Kucharczyk, W. *J. Magn. Reson. Imaging* **2009**, *6*, 1298.

3. Langereis, S.; de Lussanet, Q. G.; van Genderen, M. H. P.; Backes, W. H.; Meijer, E. W. *Macromolecules* **2004**, *37*, 3084.

4. Cyran, C. C.; Fu, Y.; Raatschen, H.-J.; Rogut, V.; Chaopathomkul, B.; Shames, D. M.; Wendland, M. F.; Yeh, B. M.; Brasch, R. C. *J. Magn. Reson. Imaging* **2008**, *27*, 581.

5. Allen, M. J.; Raines, R. T.; Kiessling, L. L. *J. Am. Chem. Soc.* **2006**, *128*, 6534.

6. Caravan, P.; Cloutier, N. J.; Greenfield, M. T.; McDermid, S. A.; Dunham, S. U.; Bulte, J. W. M.; Amedio, J. C.; Looby, R. J.; Supkowski, R. M.; Horrocks, W. D.; McMurry, T. J.; Lauffer, R. B. *J. Am. Chem. Soc.* **2002**, *124*, 3152.

7. Prasuhn, D. E.; Yeh, R. M.; Obenaus, A.; Manchester, M.; Finn, M. G. *Chem. Commun.* **2007**, 1269.

8. Accardo, A.; Tesauro, D.; Roscigno, P.; Gianolio, E.; Paduano, L.; D'Errico, G.; Pedone, C.; Morelli, G. *J. Am. Chem. Soc.* **2004**, *126*, 3097.

9. Schühle, D. T.; Polášek, M.; Lukeš, I.; Chauvin, T.; Tóth, É.; Schatz, J.; Hanefield, U.; Stuart, M. C. A.; Peters, J. A. *Dalton Trans.* **2010**, *39*, 185.

10. Schühle, D. T.; van Rijn, P.; Laurent, S.; Vander Elst, L.; Muller, R. N.; Stuart, M. C. A.; Schatz, J.; Peters, J. A. *Chem. Commun.* **2010**, *46*, 4399.

11. Kielar, F.; Tei, L.; Terreno, E.; Botta, M. *J. Am. Chem. Soc.* **2010**, *132*, 7836.

12. Cheng, Z. L.; Tsourkas, A. *Langmuir* **2008**, *24*, 8169.

13. Cheng, Z. L.; Thorek, D. L. J.; Tsourkas, A. *Adv. Funct. Mater.* **2009**, *19*, 3753.

14. Grull, H.; Langereis, S.; Messager, L.; Castelli, D. D.; Sanino, A.; Torres, E.; Terreno, E.; Aime, S. *Soft Matter* **2010**, *6*, 4847.

15. Strandberg, E.; Westlund, P. O. *J. Magn. Reson. A* **1996**, *122*, 179.

16. Villaraza, A. J. L.; Bumb, A.; Brechbiel, M. W. *Chem. Rev.* **2010**, *110*, 2921.

17. Li, B.; Martin, A. L.; Gillies, E. R. *Chem. Commun.* **2007**, 5217.

18. Nazemi, A.; Amos, R. C.; Bonduelle, C. V.; Gillies, E. R. *J. Polym. Sci., Part A: Polym. Chem.* **2011**, *49*, 2546.

19. Amos, R. C.; Nazemi, A.; Bonduelle, C. V.; Gillies, E. R. *Soft Matter* **2012**, *8*, 5947.

20. Martin, A. L.; Li, B.; Gillies, E. R. *J. Am. Chem. Soc.* **2009**, *131*, 734.

21. Lam, C. X. F.; Teoh, S. H.; Hutmacher, D. W. *Polym. Int.* **2007**, *56*, 718.

22. Nazemi, A.; Amos, R. C.; Bonduelle, C. V.; Gillies, E. R. *J. Polym. Sci., Part A: Polym. Chem.* **2011**, *49*, 2546.

23. Konings, M. S.; Dow, W. C.; Love, D. B.; Raymond, K. N.; Quay, S. C.; Rocklage, S. M. *Inorg. Chem.* **1990**, *29*, 1488.

24. Laurent, S.; Botteman, F.; Elst, L. V.; Muller, R. N. *Magn. Reson. Mater. Phys. Biol. Med.* **2004**, *16*, 235.

25. Gillies, E. R.; Dy, E.; Fréchet, J. M. J.; Szoka, F. C. *Mol. Pharm.* **2005**, *2*, 129.

26. Barge, A.; Cravotto, G.; Gianolio, E.; Fedeli, F. *Contrast Media Mol. I.* **2006**, *1*, 184.

Chapter 4

4 Multifunctional Dendritic Sialopolymersomes as Potential Antiviral Agents: Their Lectin Binding and Drug Release Properties[*]

4.1 Introduction

Amphiphilic BCPs have been demonstrated to undergo self-assembly in solution to form a wide range of structures including spherical micelles,[1] helical rods,[2] toroids,[3] vesicles,[1,4] tubes,[5] and multicompartment cylinders.[6] In recent years, polymer vesicles, commonly referred to as polymersomes, have garnered significant attention.[7-9] They are attractive materials because they can be readily accessed using a wide range of BCPs, and relative to their counterparts formed from low MW surfactants, polymersomes typically exhibit much lower critical aggregation concentrations and enhanced thermodynamic and kinetic stabilities.[6,10] In addition, they are potentially multifunctional, possessing an aqueous core capable of encapsulating water-soluble molecules, a hydrophobic membrane that can encapsulate hydrophobic species, and a surface to which specific targeting ligands or other moieties can be conjugated. Based on these properties, there has been particular interest in biomedical applications of polymersomes and they have been employed as carriers for proteins,[11,12] hydrophilic drugs,[13,14] and imaging contrast agents.[15]

Influenza viruses are highly contagious viruses known to cause widespread seasonal epidemics as well as potentially catastrophic pandemics. The two glycoproteins hemagglutinin (HA) and neuraminidase (NA) on the virus are responsible for the initiation and sustenance of the infection process. *N*-Acetylneuraminic acid (Neu5Ac) is the most abundant sialic acid found in mammalian cells. It is known that all types of influenza viruses interact with Neu5Ac residues on the host cell surface through their HA, and this is followed by endocytosis of the virus into the cell.[16-18] Release of the

progeny virus from the infected cell is then triggered by NA-catalyzed cleavage of the terminal Neu5Ac.[16] Most of the effort in developing anti-influenza drugs has been devoted to the design of drugs that can cease the release of progeny virus after cell infection. Drugs in this category include the proton channel *M2* targeting drugs such as amantadine and rimantadine,[19] and NA inhibitors such as zanamivir and oseltamivir.[20] However, it has been proposed that various influenza strains are prone to the development of resistance to these drugs.[19] An alternative approach involves the inhibition of the initial adhesion of the virus HA glycoprotein to Neu5Ac moieties on target cells and thus prevention of the initial cell infection. Monomeric Neu5Ac can inhibit this interaction, but only at millimolar concentrations.[19] In order to achieve inhibition at lower concentrations, Neu5Ac has been conjugated to various scaffolds to obtain multivalent displays. In this context, polymers,[17,18,21-24] dendrimers,[25-30] liposomes,[31-33] gold nanoparticles,[34,35] nanogels,[36] and polymer nanoparticles[37] functionalized with Neu5Ac have been proposed as potential inhibitors of influenza virus infection.

Because of their high multivalency, multifunctional capabilities, tunable size, and morphological resemblance to mammalian cells, polymersomes are attractive scaffolds for the study of carbohydrate-protein interactions[38-44] and for the potential development of therapeutics and vaccines.[38-45] However, to the best of our knowledge there are currently no examples of carbohydrate-functionalized polymersomes capable of interacting with viral proteins. Our group has recently developed approaches for the introduction of dendritic groups to the surfaces of polymersomes.[46,47] Owing to the high multivalency of dendrons, this approach provides a means of tuning the polymersome's surface chemistry using a single synthetic step.[48] Furthermore, using mannose as a model biological ligand, it was demonstrated that binding to the target protein Con A was significantly enhanced using the dendritic approach in comparison with the conjugation of small molecule mannose derivatives directly to the polymersome surface.[42] This was attributed to the increased availability of the dendritic mannose in comparison to the small molecule mannose derivatives on the polymersome surface, as well as a cluster effect resulting from the dendritic ligand display. This suggested the promise of dendritic

polymersomes for the development of new therapeutic inhibitors based on multivalent carbohydrate displays.

Here we exploit the multivalent and multifunctional capabilities of polymersomes in a dendritic sialopolymersome system designed to interact with the influenza virus at two different stages in the infection process. First, the preparation of biodegradable PEO-PCL polymersomes functionalized with dendritic Neu5Ac is described, and their binding affinities to the sialic acid-binding lectin *Limax flavus* agglutinin (LFA) were compared with those of a small-molecule Neu5Ac derivative as well as dendritic Neu5Ac in an enzyme-linked lectin inhibition assay (ELLA). Second, it is demonstrated that in addition to the Neu5Ac at the polymersome surface, which is designed to interact with HA, preventing uptake of the virus into the host cells, it is also possible to encapsulate the drug zanamivir, an NA inhibitor, into the aqueous core of the polymersomes. Release of this drug in the vicinity of infected cells, should further hinder the spread of viral infection through a synergistic effect. The release rates of the drug from both naked and dendritic sialopolymersomes are studied and compared.

4.2 Results and Discussion

4.2.1 Sialodendron Synthesis

To obtain the desired Neu5Ac-functionalized dendron for conjugation to the polymersome surface, a polyester dendron (**3.5**) based on bis-MPA (Scheme 4.1) was selected due to its demonstrated biocompatibility and ease of synthesis.[46,49] It was envisioned that as previously reported, the focal point alkyne moiety would enable conjugation to azide functionalized vesicles via Cu(I)-catalyzed azide + alkyne "click" cycloaddition chemistry, [46,47] while peripheral amine groups would provide sites for the conjugation to an Neu5Ac derivative. This dendron was prepared as previously reported.[46] An isothiocyanate derivative of Neu5Ac was selected because an unprotected Neu5Ac isothiocyanate can be prepared and selectively reacted with the dendritic amines to provide a stable thiourea linkage, without the need for deprotection of the carbohydrate once on the polyester dendron backbone. To prepare the target Neu5Ac derivative, the amine-functionalized Neu5Ac **4.1** was first synthesized in five steps starting form

commercially available Neu5Ac according to previously published procedures.[29,50] Next, upon reacting **4.1** with thiophosgene, the isothiocyanate group was successfully installed to obtain the target molecule **4.2** in quantitative yield (Scheme 4.1). Dendron **3.5** was then reacted with Neu5Ac derivative **4.2** in the presence of NEt$_3$ to obtain the target Neu5Ac-functionalized dendron **4.3** in good yield.
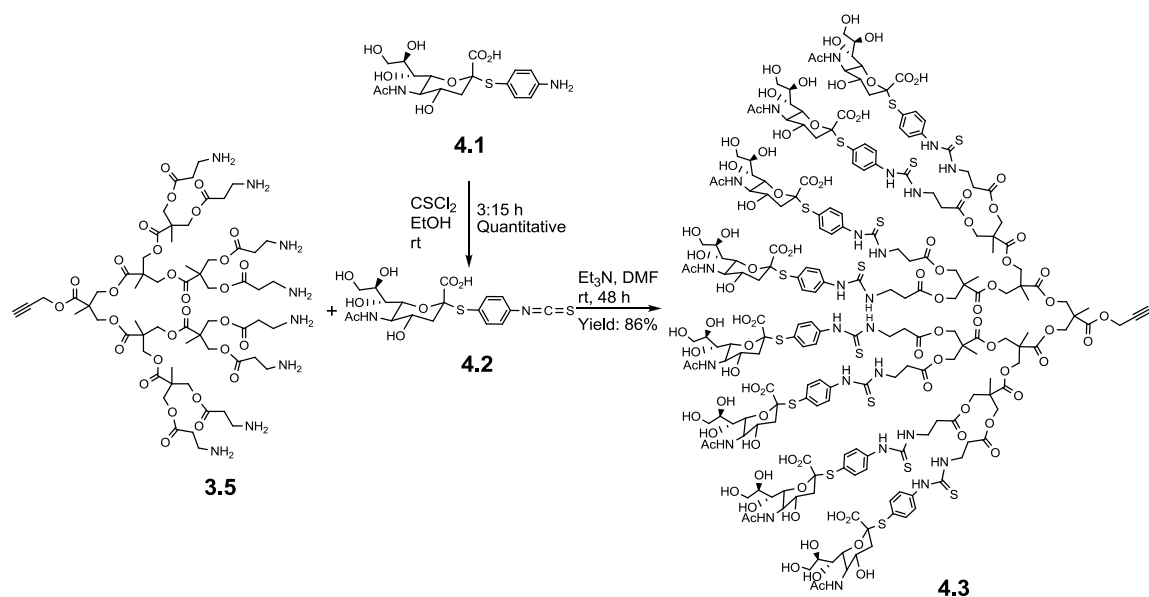
Scheme 4.1. Synthesis of sialodendron **4.3**.

To quantify the functionalization of the polymersomes with the Neu5Ac-functionalized dendron, it was necessary to tag the sialodendron with a chromophore for quantification using UV-visible absorption spectroscopy. This approach has proven to be reliable for the quantification of polymersome surface functionalization with dendritic groups.[46-48,51] For this purpose, the third generation dendron **1.33**[46] bearing peripheral amine functional groups and statistically one rhodamine dye per molecule was reacted with Neu5Ac derivative **4.2** under the same reaction conditions used for the synthesis of **4.3**, to obtain the rhodamine-labeled sialodendron **4.4** (Scheme 4.2). ε for **4.4** was then measured in MeOH/DMF (10/1) to be 43980 L·mol^{-1}cm^{-1} at 563 nm.
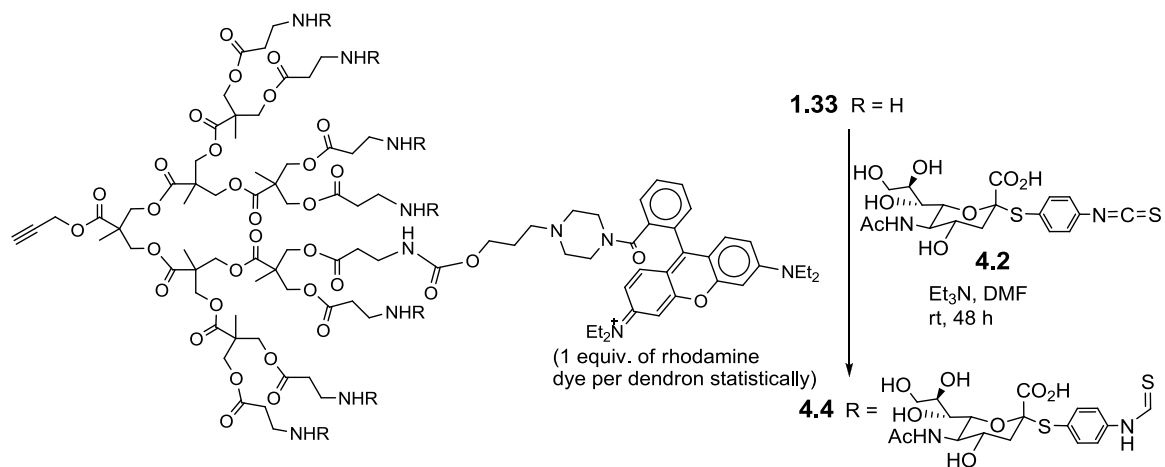
Scheme 4.2. Synthesis of rhodamine-labeled sialodendron **4.4**.

4.2.2 Functionalization of Polymersomes with Sialodendrons

To functionalize PEO-PCL polymersomes with sialodendrons, polymersomes with varying densities of surface azides were first prepared from mixtures of methoxy- (**2.5**) and azide-terminated (**2.6**) PEO-PCL BCPs as previously reported.[47] With the aim of quantifying the conjugation yields at different azide densities, azide + alkyne "click" reactions were then performed using $CuCl_2$, sodium ascorbate, and four equivalents of dendron **6** relative to the azide (Scheme 4.3). The reaction mixtures were stirred at room temperature in the dark overnight and then the unreacted dendrons and other reagents were removed by dialysis. After water was removed by lyophilization, the product of each reaction was dissolved in DMF/MeOH (10/1), and the UV–visible absorbance was measured. Using the ε measured for dendron **4.4**, the yield of the conjugation reaction on polymersome surface was calculated.
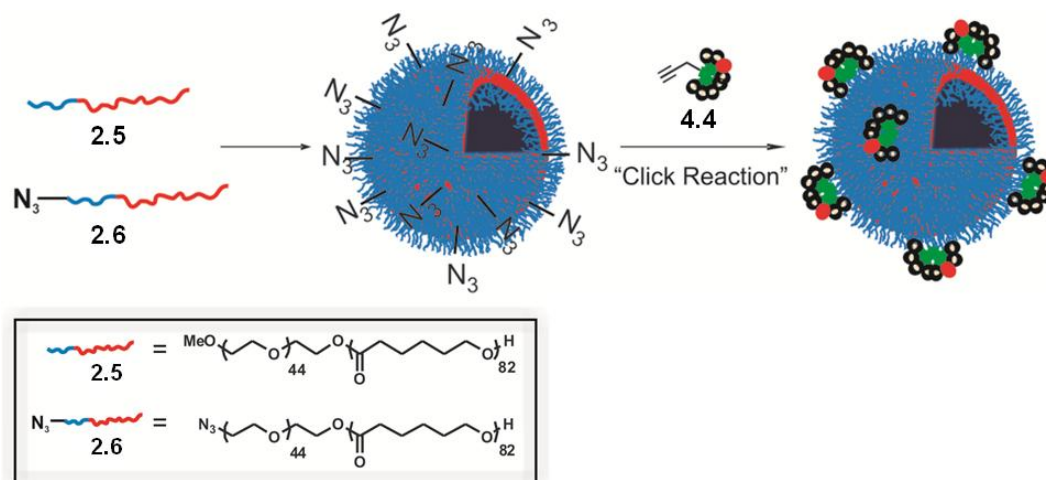
Scheme 4.3. Preparation of dendritic sialopolymersomes.

The conjugation yields for the reaction of polymersomes with the rhodamine-labeled sialodendron **4.4** are shown in Figure 4.1. Consistent with our previous studies, the yields were higher than 50% at lower loadings of azide-terminated copolymer.[42,46,47] It should be noted that approximately 50% of the azides should be located in the interior of the vesicles, and thus inaccessible to the dendron, which is unlikely to diffuse through the vesicle membrane. As a result, this observation may be attributed to the dynamic nature of the vesicles, allowing azides from the vesicle interior to migrate to the vesicle surface during the reaction time and then subsequently react. To ensure that the high reaction yields were not the result of noncovalently immobilized dendron remaining after dialysis, a control experiment was also performed on polymersomes composed entirely of methoxy-terminated copolymer **2.5** but with the same excess of dendron and other reaction and purification conditions used for vesicles containing 20 wt% copolymer **2.6**. In this case, the apparent ''yield'' was less than ~5%, indicating that no significant amount of noncovalently immobilized dendron remained after dialysis. The reproducibity of the conjugation was assessed by performing the conjugation experiment in triplicate on polymersomes composed of 20 wt% copolymer **2.6** and it was found that the standard deviation was less than 6%.
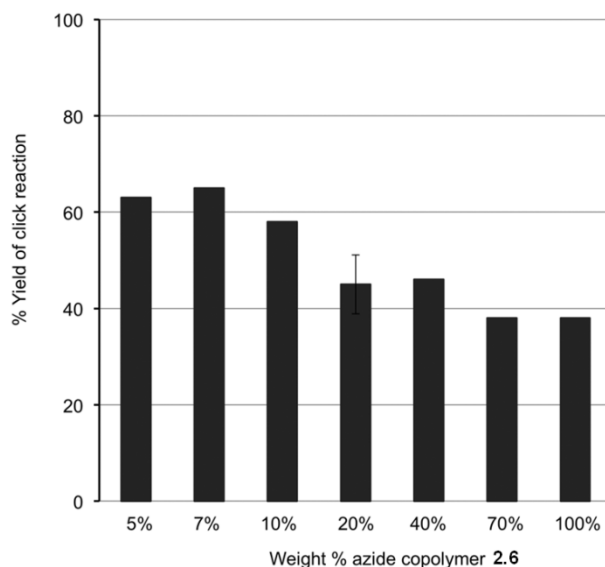
Figure 4.1. Yields for the azide + alkyne "click" conjugation reaction between dendron **4.4** and PEO-PCL polymersomes having varying percentages of azide-terminated copolymer **2.6** (remaining percentage is methoxy-terminated PEO-PCL **2.5**). Note that the error bar on the 20 wt% copolymer **2.6** measurement represents the standard deviation of triplicate experiments designed to assess the reproducibility of the conjugation.

These polymersomes were also characterized by DLS. The initial PEO-PCL polymersomes had a z-average diameter of 140 nm and a low PDI of 0.11. After conjugation with dendron **4.4**, no significant changes were observed at lower percentages of azide-functionalized copolymer **2.6**. Beyond 40 wt% copolymer **2.6**, some aggregation was observed (Figure A4.2). This can be explained by taking into account that the linear-dendritic architecture of the resulting triBCPs as well as the newly imparted hydrophilic-hydrophobic balance might be unfavourable for polymersome formation at high degrees of dendritic functionalization.

4.2.3 Evaluation of Inhibitory Potencies Using an Enzyme-Linked Lectin Inhibition Assay

On the basis of the quantification of sialodendron conjugation to the polymersomes, as well as the aggregation observed at the highest degrees of dendritic functionalization, two dendritic sialopolymersome samples based on 20 wt% and 40 wt% azide-functionalized copolymer **2.6** were prepared in order to evaluate their lectin binding potencies using an

ELLA. These polymersomes were prepared as described above but using fully sialylated dendron **4.3** rather than dendron **4.4**. As shown in Figure 4.2a, for the volume distribution, DLS showed no change in the size of polymersomes after reaction with dendron **4.3**. The intensity distribution was very similar, with no aggregation detected (Figure A4.3). Although a modest increase in polymersome hydrodynamic diameter might be expected upon dendron conjugation, this has generally not been observed in our previous work.[47,60] It is possible that the hydrophobic backbone may be able to integrate itself to some extent into the polymersome membrane, mainly leaving the hydrophilic surface groups exposed to the aqueous solution, and also that the modest size change may be difficult to reliably detect by DLS. TEM was also used to confirm that the polymersomes retained their integrity after their reaction with dendron **4.3** and their diameters were in agreement with those measured by DLS. This result, as well as the TEM image of the naked polymersomes, are shown in parts b and c, respectively, of Figure 4.2.
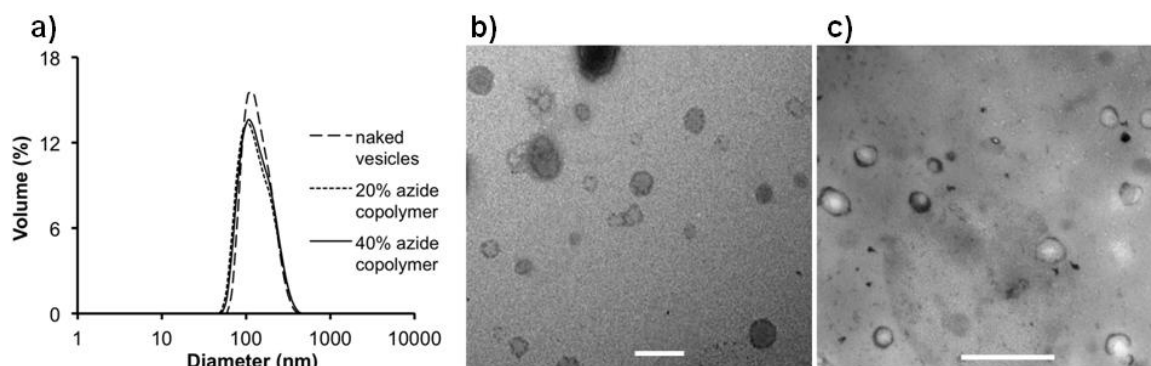
Figure 4.2. a) Size distribution profiles for naked polymersomes and polymersomes composed of different percentages of azide-functionalized copolymer **2.6** following "click" conjugation of dendron **4.3**; b) TEM image of polymersomes prepared from 40 wt% copolymer **2.6** following conjugation of dendron **4.3**; c) TEM image of naked polymersomes prepared from 100 wt% copolymer **2.5**. Scale bars are 500 nm.

With the dendritic sialopolymersomes in hand, their protein binding properties were then evaluated using an ELLA. In this assay, the polymersomes were compared to dendron **4.3** and to a monovalent Neu5Ac derivative phenyl 2-thio-α-sialoside (**4.5**)[50]. LFA has been shown to be a specific lectin for Neu5Ac and *N*-glycolylneuraminic acid

with a much greater binding affinity towards Neu5Ac. This has made it a good candidate to study Neu5Ac-protein binding.[52] The ELLA was performed as reported by Roy and coworkers,[28,29] where the inhibition of the binding of horseradish peroxidase-labeled LFA (HRP-LFA) to human α_1-acid glycoprotein (coating antigen) was studied.

The results of the ELLA are shown in Figure 4.3. In general, the inhibition did not reach 100%, which has commonly been observed in such assays with Neu5Ac[28] and other sugars.[53,54] For the monovalent Neu5Ac derivative **4.5**, the concentration required for 50% inhibition of LFA binding to the coating antigen (IC_{50}) was 4.0 ± 1.0 mM. In contrast, dendron **4.3** having 8 Neu5Ac moieties exhibited an IC_{50} value of 30 ± 5 μM (240 μM per sialoside moiety), which means that it was approximately 17 times more potent than the monovalent sialoside **4.5** on a per sialoside basis. This result is comparable with the results obtained previously by Roy and coworkers for dendritic sialosides.[28] When this dendron was conjugated to the polymersome surface, the resulting materials exhibited a much stronger potency towards the inhibition of LFA binding to human α_1-acid glycoprotein. For instance, when dendritic sialopolymersomes prepared from 20 wt% and 40 wt% azide-terminated copolymer **2.6** were tested, IC_{50} values of 0.24 ± 0.10 μM and 0.28 ± 0.12 μM were obtained respectively on a per dendron basis (1.92 μM and 2.24 μM per sialoside respectively). This means that the sialopolymersomes exhibit a greater than 100-fold increase in LFA binding inhibition potency compared to dendron **4.3** and almost 2000-fold enhanced potency relative to monovalent compound **4.5** on per sialoside basis. This can perhaps be attributed to the increased ability of the larger polymersome systems to span the two Neu5Ac binding sites on LFA in comparison with the relatively small and compact dendrons on their own. The two different polymersome systems exhibit very similar IC_{50} values on a per dendron (or per sialoside) basis relative to one another, indicating that in this range of dendron densities there is no further increase in multivalent effect to be gained from increased Neu5Ac density at the polymersome surface, though the sialopolymersomes prepared from 40 wt% copolymer **2.6** would exhibit higher potency on a per polymersome basis. Such plateauing of multivalent effects is commonly observed with dendrimeric and polymeric sialosides and has been attributed to factors such as lack of involvement of some of the glycoside residues in binding due to conformation constraints.[28,55-60]
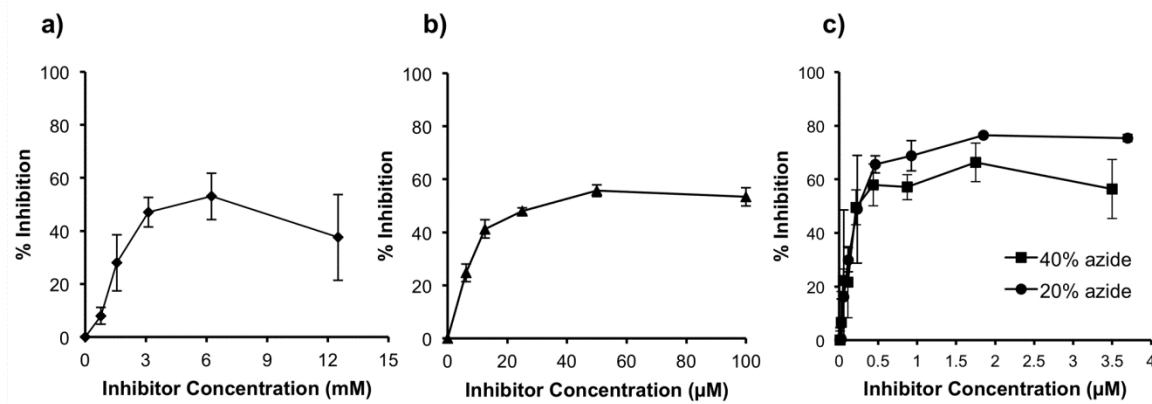
Figure 4.3. Inhibition of binding of LFA to human α_1-acid glycoprotein by a) monovalent Neu5Ac derivative **4.5**; b) sialodendron **4.3**; c) dendritic sialopolymersomes prepared from the conjugation of sialodendron **4.3** to polymersomes prepared from 20 wt% and 40 wt% azide-functionalized copolymer **2.6**. Note that in b) and c) the inhibitor concentration corresponds to the dendron concentration.

4.2.4 Encapsulation and Release of Zanamivir by Naked Polymersomes and Dendritic Sialopolymersomes

While the binding properties of the sialopolymersomes to LFA were promising on their own, a key advantage of polymersomes over other macromolecular systems that have previously been used to display multivalent Neu5Ac, is their potential to simultaneously perform multiple functions by also exploiting their hydrophobic membrane domains and/or their aqueous core to encapsulate other bioactive molecules. To demonstrate this, the water-soluble antiviral drug zanamivir was selected for encapsulation into the polymersome's aqueous core. Zanamivir is a dehydrated neuraminic acid derivative in which a guanidinyl group has been substituted for the hydroxyl group on carbon 4. The presence of the alkene group in the molecular framework mimics the geometry of the transition state in the enzymatic reaction and the guanidinyl functional group enhances its interaction with enzyme's active site.[20] Zanamivir is a highly specific inhibitor for influenza NA and causes viral replication to cease. Currently there is one prior report involving the preparation of polymers with both Neu5Ac and zanamivir covalently conjugated and these were found to be potent inhibitors of wild-type influenza virus, suggesting the promise of the approach.[61] The encapsulation of zanamivir into the

polymersome core should lead to sustained release of drug, which may prolong and enhance its therapeutic efficacy, while the binding of the sialopolymersomes to the virus may target the release to occur in the vicinity of the virus.

To prepare the multifunctional system, dendritic sialopolymersomes prepared from the conjugation of dendron **4.3** to polymersomes composed of 20 wt% azide-terminated copolymer **2.6** were selected. To encapsulate the drug, a solution of zanamivir in distilled water was added to a THF solution of copolymers **2.5** and **2.6**. After removal of THF through evaporation, sialodendron **4.3** was conjugated to the vesicle surface by the Cu(I)-catalyzed cycloaddition reaction. Finally, nonencapsulated drug, unreacted **4.3**, and click reaction reagents were removed by rapid dialysis against pH 7.4 phosphate buffer using Slide-A-Lyser dialysis cassette at room temperature for 3.5 h. That 3.5 h was sufficient for removal of unencapsulated drug was determined in a separate control experiment where the free drug was dialyzed in the absence of polymersomes under the same conditions. After 3.5 h, the sample was transferred to fresh phosphate buffer at 37 °C. The release of the drug was then evaluated by measuring the UV-visible absorption of the dialysate at 234 nm, until no further changes in absorbance were observed. To verify that complete release had been achieved, the polymersomes were disrupted by the addition of THF. After the THF was removed under reduced pressure, the aqueous solutions were returned to the dialysis cassette and dialyzed for an additional 24 h. No absorption peak was detected in the dialysate, confirming that all drug had been previously released. The release of zanamivir from naked polymersomes was also evaluated to investigate the effect of the dendritic groups on the encapsulation and release properties of the polymers. These polymersomes were prepared in the same manner described above for the dendritic sialopolymersomes except that no dendron conjugation was performed. The release experiment was performed following the same protocol.

As shown in Figure 4.4a, approximately 50% of the zanamivir was released from the naked polymersomes over the first day, and complete release was observed after about 6 days. The dendritic sialopolymersomes also released about 50% of the drug over the first day, and complete release required approximately 4 days (Figure 4.4b). This suggests that the release rates were quite similar for the naked and dendritic polymersomes, though the

data suggests that there was a small increase in the release rate of drug imparted by the dendritic functionalization, perhaps due to the effect of the large dendritic groups on polymersome stability. Examination of the DLS and TEM data for polymersomes after the release was complete suggested that the polymersomes were still intact and that drug release likely occurred through diffusion across the polymersome membrane (Figure A4.5). Overall, the polymersome systems exhibit a sustained release of zanamivir, which could be beneficial for its therapeutic effect.
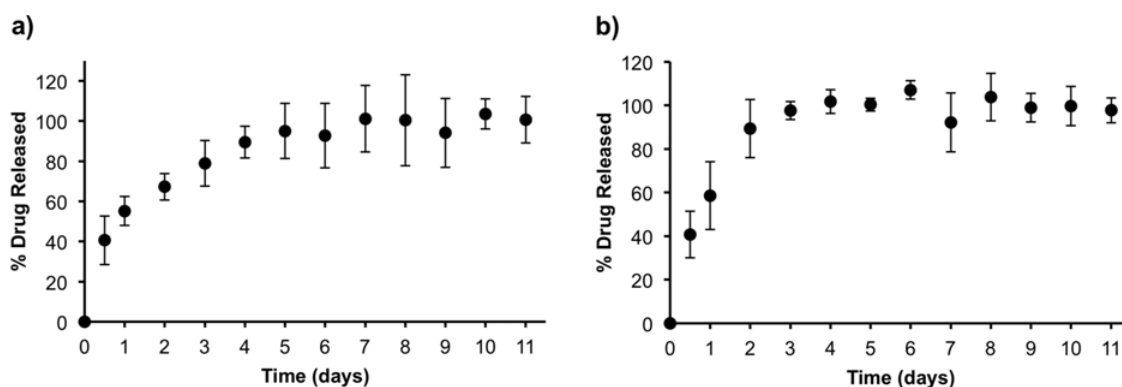

Figure 4.4. Release profiles of zanamivir from a) naked PEO-PCL polymersomes and b) dendritic sialopolymersomes. All experiments were performed in triplicate.

Using the drug release data as well as the measured extinction coefficient for zanamivir in phosphate buffer ($\varepsilon = 6540$ L·mol^{-1}cm^{-1}) the amount of encapsulated drug in each polymersome system was determined, allowing the loading efficiency (mass of drug in loaded polymersomes relative to mass of initial drug used for sample preparation) and drug content (mass of drug in loaded polymersomes relative to mass of polymer) to be calculated. The naked polymersomes were found to have a loading efficiency of 8% ± 1% and a drug content of 31% ± 5% and the dendritic sialopolymersomes had a loading efficiency of 8.8% ± 0.2% and a drug content of 35% ± 1%. The relatively low loading efficiencies are intrinsic to the loading method as the drug is expected to partition equally between the polymersome cores and external solution, and the external solution constitutes a much greater volume than the polymersome cores. However, the drug content in these systems is high, which is a desirable property for their application.

4.3 Conclusion

In summary, we have developed for the first time, a multifunctional polymersome system with the potential to interfere with the viral infection process at two levels. First dendritic Neu5Ac incorporated onto the polymersome surface was designed to inhibit the binding of the influenza virus HA to Neu5Ac moieties on mammalian host cells. Secondly, the antiviral drug zanamivir was incorporated into the polymersome core with the aim of also inhibiting influenza virus NA, thus preventing the release of progeny virus from host cells. In this study, we showed that sialodendrons based on a polyester backbone could be synthesized, and their conjugation to biodegradable PEO-PCL polymersomes was demonstrated and quantified using a rhodamine-labeled dendron. Using an ELLA with a model sialic acid binding lectin, LFA, it was found that incorporation of Neu5Ac onto the dendritic scaffold led to a 17-fold enhancement in binding on a per-Neu5Ac basis in comparison to a small molecule analogue. Incorporation of the dendritic Neu5Ac onto the polymersome surface led to an almost 2000-fold enhancement, showing the advantage of the polymersome system for enhancing binding. The antiviral drug zanamivir was encapsulated in the aqueous core of the dendritic sialopolymersomes during their preparation and the drug release behavior was studied and compared to that of naked polymersomes encapsulating the same drug. Sustained release of drug was observed for both systems with release occurring over a period of several days. Furthermore the drug content was high (30-35 wt%) for these systems. Combined, this work demonstrates how polymer self-assembly can serve as a promising approach for enhancing interactions with biological targets, with an additive effect on target binding imparted by the different nanoscale components of the system including the dendron and the polymersome, and with different components of the polymersome performing different functions including target binding and drug release. Future work will involve an evaluation of this multifunctional system in *in vitro* and *in vivo* models to demonstrate how the combined functions of the drug loaded dendritic sialopolymersomes can lead to potent inhibition of viral infection.

4.4 Experimental

General Procedures and Materials

Compounds **3.5**[51], **4.1**[29,50] and **1.33**[46] were synthesized according to previously published procedures. Neu5Ac was purchased from RIA International LLC. HRP-LFA was purchased from E-Y Laboratories. α_1-acid glycoprotein from human plasma was purchased from Sigma-Aldrich. All the other chemicals were purchased from Sigma-Aldrich or Alfa Aesar and were used without further purification unless otherwise noted. Anhydrous DMF was obtained from a solvent purification system using aluminum oxide columns. NEt$_3$ was distilled from CaH$_2$. Unless otherwise stated, all reactions were performed under a nitrogen atmosphere using flame or oven dried glassware. Dialyses were performed using Spectra/Por regenerated cellulose membranes with a 1,000 g/mol, 3500 g/mol, or 25,000 g/mol MWCO. ^{1}H NMR spectra were obtained at 400 MHz, and ^{13}C NMR spectra were obtained at 100 MHz. NMR chemical shifts are reported in ppm and are calibrated against the residual solvent signal of (CD$_3$)$_2$SO (δ 2.50 and 39.52 ppm), or CD$_3$OD (δ 3.31 and 49.00 ppm). *J* values are expressed in Hz. IR spectra were obtained as NaCl pellets using a Bruker Tensor 27 instrument. HRMS was performed using a Finnigan MAT 8400 electron impact mass spectrometer. UV–visible absorption spectroscopy was performed on a Varian Cary 300 Bio UV–visible spectrophotometer. DLS was performed using a Zetasizer Nano ZS instrument from Malvern Instruments, at a polymer concentration of 0.05 mg·mL^{-1}. Nunclon (Delta) microtiter 96-well plates were purchased from Thermo Scientific and were used for the incubation of inhibitors and Horseradish peroxidase-conjugated LFA. Nunc Immuno 96-well plates with flat bottom, Maxi Sorp, Pinchbar 400 µL/well were purchased from Fisher Scientific and were used for intigen coating. Absorbances of each well were measured at 410 nm and 570 nm using a plate reader (Tecan Safire).

Synthesis of Neu5Ac derivative 4.2: Compound **4.1**[29,50] (0.43 g, 1.0 mmol, 1.0 equiv.) was dissolved in ethanol (80%, 50 mL). Thiophosgene (0.17 mL, 2.3 mmol, 2.2 equiv.) was then added and the resulting solution was stirred at room temperature for 3 h. The solvent was then removed under reduced pressure. The remaining residue was then azeotroped with toluene to remove all traces of water and HCl byproducts (3×20 mL). The target compound **4.2** was obtained as a light orange solid in quantitative yield (0.47 g). ^{1}H NMR (CD$_3$OD) δ: 7.63 (d, *J* = 8.0, 2H), 7.27 (d, *J* = 8.0, 2H), 3.82-3.66 (m, 4H),

3.58 (dd, J_1 = 16.0, J_2 = 8.0, 1H), 3.47 (dd, J_1 = 8.0, J_2 = 4.0, 1H), 3.38 (dd, J_1 = 8.0, J_2 = 4.0, 1H), 2.87 (dd, J_1 = 16.0, J_2 = 8.0, 1H), 2.00 (s, 3H), 1.85 (dd, J_1 = 12.0, J_2 = 4.0, 1H). ^{13}C NMR ((CD$_3$)$_2$SO) δ: 172.0, 170.1, 137.0, 134.9, 131.2, 129.2, 126.2, 86.2, 76.2, 72.0, 68.6, 66.7, 63.0, 52.2, 48.6, 22.7. IR (film from THF/MeOH, cm^{-1}): 3348, 3085, 2930, 2859, 2090, 1716, 1635, 1558, 1271, 1128. HRMS: calcd for [M+Na]$^+$ (C$_{18}$H$_{22}$N$_2$O$_8$S$_2$Na): 481.0715. Found: (EI) 481.0710.

Synthesis of dendron 4.3: Dendron **3.5**[51] (40 mg, 17 μmol, 1.0 equiv.) was dissolved in DMF (5 mL). Neu5Ac derivative **4.2** (0.12 g, 0.27 mmol, 16 equiv.) and NEt$_3$ (0.5 mL) were then added and the resulting solution was stirred at room temperature for 48 h. The mixture was then dialyzed against distilled water using a 1000 g/mol MWCO membrane for 24 h with multiple dialysate changes. Target dendron **4.3** was obtained in 86% yield by lyophilization as a light yellow fluffy solid (75 mg, 15 μmol). ^{1}H NMR ((CD$_3$)$_2$SO) δ: 10.16 (br s, 8H), 8.10 (br s, 8H), 7.70-7.25 (br m, 32H), 5.14 (br s, 8H), 4.72 (br s, 10 H), 4.43-4.04 (br m, 28H), 3.86-3.06 (br m, 104H), 2.80-2.51 (br m, 25H), 1.86 (s, 24H), 1.61-1.44 (br m, 8H), 1.32-1.04 (br m, 21H). ^{13}C NMR ((CD$_3$)$_2$SO) δ: 180.1, 172.0, 171.8, 171.4, 171.3, 171.1, 171.0, 140.5, 135.6, 124.3, 121.6, 87.6, 87.4, 86.0, 77.9, 75.7, 71.7, 68.6, 67.2, 64.9, 63.0, 52.3, 46.2, 46.0, 45.5, 41.4, 36.6, 34.3, 32.9 (2), 22.6, 17.3, 17.0, 8.6. IR (film from THF/MeOH, cm^{-1}): 3340, 3066, 2923, 2855, 2102, 1733, 1652, 1541, 1251, 1126.

Synthesis of rhodamine-labeled dendron 4.4: Dendron **1.33**[46] (17 mg, 8.4 μmol, 1.0 equiv.) and Neu5Ac derivative **4.2** (54 mg, 0.12 mmol, 14 equiv.) were dissolved in DMF (2 mL). NEt$_3$ (0.2 mL) was then added and the resulting solution was stirred at room temperature in dark for 48 h. The resulting material was dialyzed first against DMF, then against distilled water using a 3500 g/mol MWCO membrane. Dendron **4.4** was obtained in 81% yield (36 mg, 6.8 mmol) by lyophilization. ^{1}H NMR ((CD$_3$)$_2$SO) δ: 10.07 (br s, 7H), 9.10 (s, 1H), 8.18-8.05 (m, 5H), 7.72 (m, 1H), 7.66-7.22 (m, 28H), 7.16-7.03 (m, 2H), 6.93 (s, 1H), 6.70 (s, 1H), 5.13 (br s, 7H), 4.80-4.60 (m, 9H), 4.40-4.00 (m, 28H), 3.89 (br s, 2H), 3.78-3.08 (m, 93H), 2.71-2.59 (m, 23H), 2.48-2.32 (m, 10H), 2.26 (s, 7H), 1.86 (s, 21H), 1.59-1.45 (m, 7H), 1.29-0.98 (m, 33H). IR (film from THF/MeOH,

cm^{-1}): 3309, 3076, 2923, 2852, 2127, 1735, 1649, 1591, 1541, 1247, 1131. ε: 43979 L·mol^{-1}cm^{-1} at 563 nm (DMF/MeOH, 10/1).

General procedure for dendritic surface functionalization of polymersomes: Azide-functionalized PEO-PCL polymersomes were prepared as described previously using BCPs **2.5** and **2.6** to obtain a final polymer concentration of 2 mg/mL in distilled water.[47] Dendron **4.3** or **4.4** (4.0 equiv. relative to azide polymer), CuCl$_2$·2H$_2$O (0.40 equiv. relative to total polymer), and sodium ascorbate (4.0 equiv. relative to total polymer) were added in sequence to the aqueous suspension of polymersomes and the resulting reaction mixture was stirred at room temperature and in dark overnight. After this time, the mixture was dialyzed against distilled water (dendron **4.3** for TEM analysis and dendron **4.4**) or against 10 mM pH 7.3 phosphate buffer (dendron **4.3** for ELLA) for 24 h using a 25,000 g/mol MWCO membrane to remove excess dendrons and reagents required for click reaction. We have previously shown by ICP-MS measurements that this dialysis method effectively removes copper ions up to 97% from the reaction mixture.[62] Therefore, no extra purification methods were applied to remove copper as trace levels should not interfere with the ELLA assay.

Quantification of click reaction yields on polymersome surfaces: The functionalized polymersomes were prepared as described above. After dialysis, the samples were lyophilized to remove water. The resulting residues were then taken up in about 2 mL of DMF/MeOH (10/1) and were centrifuged at 4500 rpm for 4 h to remove any insoluble material. Next, the absorbance was measured at 563 nm. The reaction yields were then calculated using the measured ε for the rhodamine-labeled dendron **4.4** in the same solvent.

Transmission Electron Microscopy: The suspension of polymersomes (10 μL, 0.05 mg·mL^{-1}) was placed on a carbon formvar grid and was left to dry overnight. Imaging was performed using a Phillips CM10 microscope operating at 80 kV with a 40 μm aperture.

Enzyme-linked lectin assay: The procedure developed by Roy and coworkers was adopted for this assay.[28,29] The detailed description of this assay is as follows: A stock

solution of human α₁-acid glycoprotein in phosphate buffer (10 mM, pH 7.3) was first prepared at a concentration of 10 µg/mL. Nunc Immuno 96-well plates were then coated with this solution overnight. A phosphate buffer (10 mM, pH 7.3) solution containing 0.05% (v/v) Tween 20 (PBST) was then used to wash the wells (3 × 300 µL/well). This PBST solution was used to wash the wells after each incubation periods throughout the assay. In the next step, the wells were blocked with phosphate buffer (10 mM, pH 7.3) containing 1% bovine serum alumin (150 µL/well) for 1 h at 37°C. After washing with PBST, the inhibitor/HRP-LFA solutions were added to wells (100 µL/well) following by another 1 h incubation at 37°C. These inhibitor solutions were premade in Nunclon (Delta) microtiter 96-well plates as follows: The inhibitor (dendritic sialopolymersomes, sialodendron **4.3**, or sialoside **4.5**) solutions in PBS were added in serial 2-fold dilutions to each well (60 µ/well). To these was then added HRP-LFA solution in PBS (60 μL/well of 100-fold dilution of a 1 mg/mL stock solution of HRP-LFA in PBS) and incubated at 37 °C for 1 h. The inhibitor/HRP-LFA solutions (100 μL/well) were then transferred to the blocked antigen-coated plate and incubated for 1 h at 37 °C. After washing with PBST, 2,2'-azinobis(3-ethylbenzothiazoline-6-sulfonic acid) diammonium salt solution (1 mg/mL) in citrate-phosphate buffer (0.2 M, pH 4.0 with 0.015% H_2O_2) was added to each well (50 μL/well) which causes the reaction with the enzyme. After 20 min, the reaction was stopped by adding 1 M sulfuric acid solution (50 μL/well). Finally, the optical density was measured at 410 nm relative to 570 nm using plate reader. The percent inhibition was calculated using the following equation:

$$\% \text{ inhibition} = [(A_{\text{no inhibitor}} - A_{\text{with inhibitor}})/A_{\text{no inhibitor}}]\times100$$

In this assay, the concentration of sialopolymersomes was calculated based on initial loading of azide copolymer **2.6** in the polymersome formation (described above), the conjugation yield of sialodendron on the polymersome surface at each azide loading, calculated by UV-visible measurement, as described above, and the total volume of polymersome solution added in the assay.

Preparation of zanamivir-loaded dendritic sialopolymersomes: To a solution of polymers **2.5** (4 mg) and **2.6** (1 mg) in THF (0.5 mL) was added zanamivir solution (2

mL, 10 mg/mL) in distilled water with vigorous stirring. The resulting mixture was stirred at room temperature overnight with an open cap to remove THF by evaporation. The click reaction was then performed with dendron **4.3** as described above. The sample was then transferred to a Slide-A-Lyzer dialysis cassette with a MWCO of 20,000 g/mol and dialyzed against phosphate buffer (10 mM, pH 7.4) at room temperature for 3.5 h to remove the unencapsulated drug and other reagents required for click reaction. The time required for the removal of free drug was determined by performing the same dialysis using a cassette containing the same concentration of only free zanamivir and waiting until the absorbance of the drug in the dialysate reached equilibrium as measured by UV-visible spectroscopy at 234 nm. This time was measured to be 3.5 h.

Preparation of zanamivir-loaded naked polymersomes: To a solution of polymer **2.5** (5 mg) in THF (0.5 mL) was added zanamivir solution (2 mL, 10 mg/mL) in phosphate buffer (10 mM, pH 7.4) with vigorous stirring. The resulting mixture was stirred at room temperature with an open cap to remove THF by evaporation. The sample was then transferred to a Slide-A-Lyzer dialysis cassette with a MWCO of 20,000 g/mol and dialyzed against phosphate buffer (10 mM, pH 7.4) at room temperature to remove the unencapsulated drug.

Measurement of zanamivir release from the polymersomes: After the removal of free drug, the Slide-A-Lyzer dialysis cassette containing the loaded polymersomes was transferred to phosphate buffer (400 mL, 10 mM, pH 7.4) preheated to 37 °C. This point was taken as t = 0. At certain time points, 3 mL aliquots of the dialysate were taken for UV-visible measurement. The aliquots were placed back in the dialysate immediately after measurements. An average of the absorption intensities at 234 nm of aliquots where the release had clearly plateaued was defined as 100% release and the percent release at other time points was calculated relative to this value. Moreover, to ensure that complete release had been achieved, the individual polymersome solutions were mixed with THF (4 mL) to disrupt the assemblies and release any potential remaining drug. The THF was removed under reduced pressure and the aqueous solution was returned to the dialysis cassette and allowed to stir for another 24 h in fresh buffer. At this point, the UV-visible

spectrum of the dialysate was measured and did not show any absorption peak at 234 nm. The release experiments were performed in triplicate.

4.5 References

1. Zhang, L. F.; Eisenberg, A. *Science* **1995**, *268*, 1728.

2. Cornelissen, J.; Fischer, M.; Sommerdijk, N.; Nolte, R. J. M. *Science* **1998**, *280*, 1427.

3. Pochan, D. J.; Chen, Z. Y.; Cui, H. G.; Hales, K.; Qi, K.; Wooley, K. L. *Science* **2004**, *306*, 94.

4. Discher, D. E.; Eisenberg, A. *Science* **2002**, *297*, 967.

5. Yan, D. Y.; Zhou, Y. F.; Hou, J. *Science* **2004**, *303*, 65.

6. Cui, H. G.; Chen, Z. Y.; Zhong, S.; Wooley, K. L.; Pochan, D. J. *Science* **2007**, *317*, 647.

7. Brinkhuis, R. P.; Rutjes, F.; van Hest, J. C. M. *Polym. Chem.* **2011**, *2*, 1449.

8. LoPresti, C.; Lomas, H.; Massignani, M.; Smart, T.; Battaglia, G. *J. Mater. Chem.* **2009**, *19*, 3576.

9. Meng, F. H.; Zhong, Z. Y.; Feijen, J. *Biomacromolecules* **2009**, *10*, 197.

10. Zhang, S. Y.; Zhao, Y. *J. Am. Chem. Soc.* **2010**, *132*, 10642.

11. Ranquin, A.; Versees, W.; Meier, W.; Steyaert, J.; Van Gelder, P. *Nano Lett.* **2005**, *5*, 2220.

12. Arifin, D. R.; Palmer, A. F. *Biomacromolecules* **2005**, *6*, 2172.

13. Ahmed, F.; Pakunlu, R. I.; Srinivas, G.; Brannan, A.; Bates, F.; Klein, M. L.; Minko, T.; Discher, D. E. *Mol. Pharm.* **2006**, *3*, 340.

14. Brown, M. D.; Schatzlein, A.; Brownlie, A.; Jack, V.; Wang, W.; Tetley, L.; Gray, A. I.; Uchegbu, I. F. *Bioconjugate Chem.* **2000**, *11*, 880.

15. Ghoroghchian, P. P.; Frail, P. R.; Susumu, K.; Blessington, D.; Brannan, A. K.; Bates, F. S.; Chance, B.; Hammer, D. A.; Therien, M. J. *P. Natl. Acad. Sci. USA.* **2005**, *102*, 2922.

16. Webster, R. G.; Bean, W. J.; Gorman, O. T.; Chambers, T. M.; Kawaoka, Y. *Microbiol. Rev.* **1992**, *56*, 152.

17. Lees, W. J.; Spaltenstein, A.; Kingery-Wood, J. E.; Whitesides, G. M. *J. Med. Chem.* **1994**, *37*, 3419.

18. Mammen, M.; Choi, S. K.; Whitesides, G. M. *Angew. Chem., Int. Ed.* **1998**, *37*, 2755.

19. Carlescu, I.; Scutaru, D.; Popa, M.; Uglea, C. V. *Med. Chem. Res.* **2009**, *18*, 477.

20. Gubareva, L. V.; Kaiser, L.; Hayden, F. G. *Lancet* **2000**, *355*, 827.

21. Reuter, J. D.; Myc, A.; Hayes, M. M.; Gan, Z. H.; Roy, R.; Qin, D. J.; Yin, R.; Piehler, L. T.; Esfand, R.; Tomalia, D. A.; Baker, J. R. *Bioconjugate Chem.* **1999**, *10*, 271.

22. Spaltenstein, A.; Whitesides, G. M. *J. Am. Chem. Soc.* **1991**, *113*, 686.

23. Mammen, M.; Dahmann, G.; Whitesides, G. M. *J. Med. Chem.* **1995**, *38*, 4179.

24. Tuzikov, A. B.; Chinarev, A. A.; Gambaryan, A. S.; Oleinikov, V. A.; Klinov, D. V.; Matsko, N. B.; Kadykov, V. A.; Ermishov, M. A.; Demin, I. y. V.; Demin, V. V.; Rye, P. D.; Bovin, N. V. *ChemBioChem* **2003**, *4*, 147.

25. Roy, R.; Zanini, D.; Meunier, S. J.; Romanowska, A. *J. Chem. Soc., Chem. Commun.* **1993**, 1869.

26. Zanini, D.; Roy, R. *J. Org. Chem.* **1996**, *61*, 7348.

27. Llinares, M.; Roy, R. *Chem. Commun.* **1997**, 2119.

28. Zanini, D.; Roy, R. *J. Am. Chem. Soc.* **1997**, *119*, 2088.

29. Zanini, D.; Roy, R. *J. Org. Chem.* **1998**, *63*, 3486.

30. Sashiwa, H.; Shigemasa, Y.; Roy, R. *Macromolecules* **2000**, *33*, 6913.

31. Kingerywood, J. E.; Williams, K. W.; Sigal, G. B.; Whitesides, G. M. *J. Am. Chem. Soc.* **1992**, *114*, 7303.

32. Spevak, W.; Nagy, J. O.; Charych, D. H.; Schaefer, M. E.; Gilbert, J. H.; Bednarski, M. D. *J. Am. Chem. Soc.* **1993**, *115*, 1146.

33. Reichert, A.; Nagy, J. O.; Spevak, W.; Charych, D. *J. Am. Chem. Soc.* **1995**, *117*, 829.

34. Zhang, L.; Wei, G. H.; Do, Y. G. *Carbohydr. Res.* **2009**, *344*, 2083.

35. Papp, I.; Sieben, C.; Ludwig, K.; Roskamp, M.; Bottcher, C.; Schlecht, S.; Herrmann, A.; Haag, R. *Small* **2010**, *6*, 2900.

36. Papp, I.; Sieben, C.; Sisson, A. L.; Kostka, J.; Bottcher, C.; Ludwig, K.; Herrmann, A.; Haag, R. *ChemBioChem* **2011**, *12*, 887.

37. Bondioli, L.; Costantino, L.; Ballestrazzi, A.; Lucchesi, D.; Boraschi, D.; Pellati, F.; Benvenuti, S.; Tosi, G.; Vandelli, M. A. *Biomaterials* **2010**, *31*, 3395.

38. Kim, B. S.; Hong, D. J.; Bae, J.; Lee, M. *J. Am. Chem. Soc.* **2005**, *127*, 16333.

39. Kim, B. S.; Yang, W. Y.; Ryu, J. H.; Yoo, Y. S.; Lee, M. *Chem. Commun.* **2005**, 2035.

40. Dai, X.-H.; Dong, C.-M. *J. Polym. Sci., Part A: Polym. Chem.* **2008**, *46*, 817.

41. Pasparakis, G.; Alexander, C. *Angew. Chem., Int. Ed.* **2008**, *47*, 4847.

42. Martin, A. L.; Li, B.; Gillies, E. R. *J. Am. Chem. Soc.* **2009**, *131*, 734.

43. Huang, J.; Bonduelle, C.; Thevenot, J.; Lecommandoux, S.; Heise, A. *J. Am. Chem. Soc.* **2012**, *134*, 119.

44. Zhou, W.; Dai, X.-H.; Dong, C.-M. *Macromol. Biosci.* **2008**, *8*, 268.

45. Quer, C. B.; Marsden, H. R.; Romeijn, S.; Zope, H.; Kros, A.; Jiskoot, W. *Polym. Chem.* **2011**, *2*, 1482.

46. Li, B.; Martin, A. L.; Gillies, E. R. *Chem. Commun.* **2007**, 5217.

47. Nazemi, A.; Amos, R. C.; Bonduelle, C. V.; Gillies, E. R. *J. Polym. Sci., Part A: Polym. Chem.* **2011**, *49*, 2546.

48. Amos, R. C.; Nazemi, A.; Bonduelle, C. V.; Gillies, E. R. *Soft Matter* **2012**, *8*, 5947.

49. De Jesus, O. L. P.; Ihre, H. R.; Gagne, L.; Fréchet, J. M. J.; Szoka, F. C. *Bioconjugate Chem.* **2002**, *13*, 453.

50. Rothermel, J.; Faillard, H. *Biol. Chem. Hoppe-Seyler* **1989**, *370*, 1077.

51. Martin, A. L.; Bernas, L. M.; Rutt, B. K.; Foster, P. J.; Gillies, E. R. *Bioconjugate Chem.* **2008**, *19*, 2375.

52. Miller, R. L.; Collawn, J. F.; Fish, W. W. *J. Biol. Chem.* **1982**, *257*, 7574.

53. Page, D.; Roy, R. *Bioconjugate Chem.* **1997**, *8*, 714.

54. Andre, S.; Ortega, P. J. C.; Perez, M. A.; Roy, R.; Gabius, H. J. *Glycobiology* **1999**, *9*, 1253.

55. Roy, R.; Laferriere, C. A.; Gamian, A.; Jennings, H. J. *J. Carbohydr. Chem.* **1987**, *6*, 161.

56. Roy, R.; Laferriere, C. A. *Carbohydr. Res.* **1988**, *177*, c1.

57. Byramova, N. E.; Mochalova, L. V.; Belyanchikov, I. M.; Matrosovich, M. N.; Bovin, N. V. *J. Carbohydr. Chem.* **1991**, *10*, 691.

58. Gamian, A.; Chomik, M.; Laferriere, C. A.; Roy, R. *Can. J. Microbiol.* **1991**, *37*, 233.

59. Roy, R.; Andersson, F. O.; Harms, G.; Kelm, S.; Schauer, R. *Angew. Chem., Int. Ed.* **1992**, *31*, 1478.

60. Sigal, G. B.; Mammen, M.; Dahmann, G.; Whitesides, G. M. *J. Am. Chem. Soc.* **1996**, *118*, 3789.

61. Haldar, J.; de Cienfuegos, L. A.; Tumpey, T. M.; Gubareva, L. V.; Chen, J. Z.; Klibanov, A. M. *Pharm. Res.* **2010**, *27*, 259.

62. Nazemi, A.; Martinez, F.; Scholl, T. J.; Gillies, E. R. *RSC Adv.* **2012**, *2*, 7971.

Chapter 5

5 Synthesis and Degradation of Backbone Photodegradable Polyester Dendrimers[*]

5.1 Introduction

Dendrimers are highly branched macromolecules with exact MWs or very low PDIs resulting from their step-wise synthesis. Higher generation dendrimers possess large numbers of functional groups on their peripheries and often adopt globular conformations with internal cavities. These properties have led to much research in the application of dendrimers for light-harvesting,[1,2] organic light-emitting diodes,[3,4] catalysis,[5,6] and numerous biomedical areas.[7-9] The development of dendrimers that are responsive to specific stimuli is also of significant interest as this can impart new properties and further expand their scope of applications. For example, the breakdown of a dendrimer in response to a stimulus can provide a means of releasing encapsulated cargo or fragmenting assemblies of dendritic materials.

The first reports on cleavable dendrimers emerged less than two decades ago.[10,11] Since then, a number of examples of dendrimers that cleave in response to stimuli such as pH change,[12-14] light,[15-24] transition metals,[25,26] catalytic antibodies,[27,28] and reducing agents[29,30] have been developed. Among these stimuli, light is of particular interest for the development of smart materials as it can be applied at a specific time and location with control over its intensity and wavelength. Thus far, several photodegradable dendrimer systems have been developed through the incorporation of photodegradable units either at the core of the dendrimer[15,19] or at the junction between the hydrophobic and hydrophilic portions of amphiphilic dendrons.[16,20,22,23] The limitation of these approaches is that following photodegradation, in most cases large residual fragments of

the dendrimer remain, limiting the application of these materials. For example, residual hydrophobic fragments may undergo aggregation in aqueous solutions. Self-immolative dendrons that fragment in response to the cleavage of a photoresponsive focal point moiety have also been developed.[17,18,24] However, due to the inherent design of these materials they have been limited to dendrons rather than dendrimers and are thus far limited to a very select set of backbone monomers that are derivatives of dihydroxybenzylalcohols.

Photodegradable linkages have not previously been incorporated throughout the backbones of dendrimers or dendrons at each monomer unit. This approach would allow for a rapid, simultaneous cleavage of multiple linkages through the dendrimer backbone, and is potentially applicable to various dendrimer backbones. However, the incorporation of photodegradable moieties throughout the dendrimer backbone is a significant synthetic challenge due to the requirement for extremely clean and efficient chemistry in dendrimer synthesis. Despite the multitude of reports on dendrimer synthesis over the last few decades, only a limited number of dendrimer backbones have emerged as widely accessible synthetically, and minor modifications to the monomer units can dramatically alter the synthetic process and results. We report here the incorporation of photodegradable *o*-nitrobenzyl ester moities[31,32] into the widely used bis-MPA dendrimer backbone and photodegradation studies of the resulting materials.

5.2 Results and Discussion

5.2.1 Design and Synthesis

Our synthetic strategy, an adaptation of the polyester dendrimer synthesis developed by Ihre et al.,[33] involved the divergent synthesis of first, second, and third generation (G1-G3) dendrons with alkyne focal points followed by an azide + alkyne "click" conjugation of the dendrons onto a trifunctional azide core to obtain the target G1-G3 dendrimers. Due to the photosensitivity of the target molecules and intermediates, all reaction flasks were protected from light using aluminum foil, but no special measures were required during the isolation and purification steps. 4-Bromomethyl-3-nitrobenzoic acid (**5.1**) was used as the starting material in the synthesis (Scheme 5.1). First, it was necessary to mask

the carboxylic acid group on **5.1** using a protecting group that would not require acidic or basic conditions for deprotection as these conditions would cause complications in subsequent steps of the synthesis. Thus, an allyl ester was installed by reaction with allyl alcohol using *N,N'*-dicyclohexylcarbodiimide (DCC) to provide **5.2**. Bis-MPA (**5.3**) was then introduced in the presence of Cs_2CO_3 in DMF to provide **5.4** in quantitative yield. Finally, the principle monomer for dendrimer growth (**5.5**) was synthesized by deprotection of the allyl group in **5.4** using $Pd(PPh_3)_4$ and piperidine.

With the key monomer in hand, the next step was the synthesis of the G1-G3 dendrons. As an alkyne focal point was desired for the eventual dendron coupling to the core, the synthesis of the G1 dendron was carried out in a manner similar to that described above for monomer **5.5**, but using propargyl alcohol instead of allyl alcohol. This provided first the propargyl ester derivative **5.6**, followed by the bis-MPA derivative **5.7** (Scheme 5.1). Another key difference was that instead of cleaving the focal point propargyl alcohol on **5.7**, this was left intact and instead the acetonide protecting group was removed using H_2SO_4 in MeOH to provide the G1 dendron **5.8** in high yield overall.
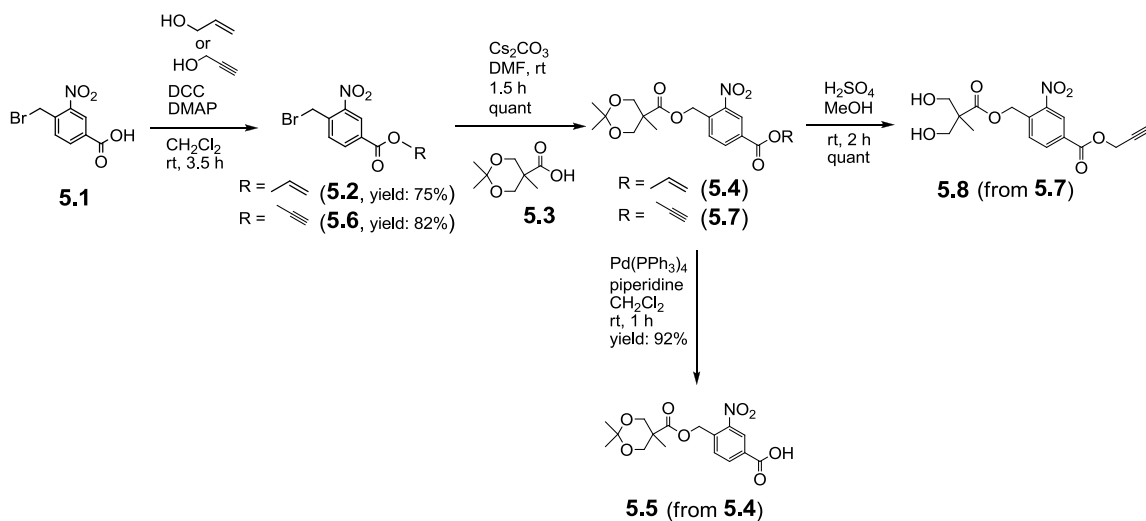
Scheme 5.1. Synthesis of monomer **5.5** and G1 dendron **5.8.**

Synthesis of the G2 dendron was accomplished by coupling monomer **5.5** to the deprotected G1 dendron **5.8** using EDC·HCl to provide **5.9** (Scheme 5.2). Removal of the

acetonide groups under acidic conditions provided **5.10**. Repetition of this coupling and deprotection sequence provided G3 dendron **5.12** in high yield.
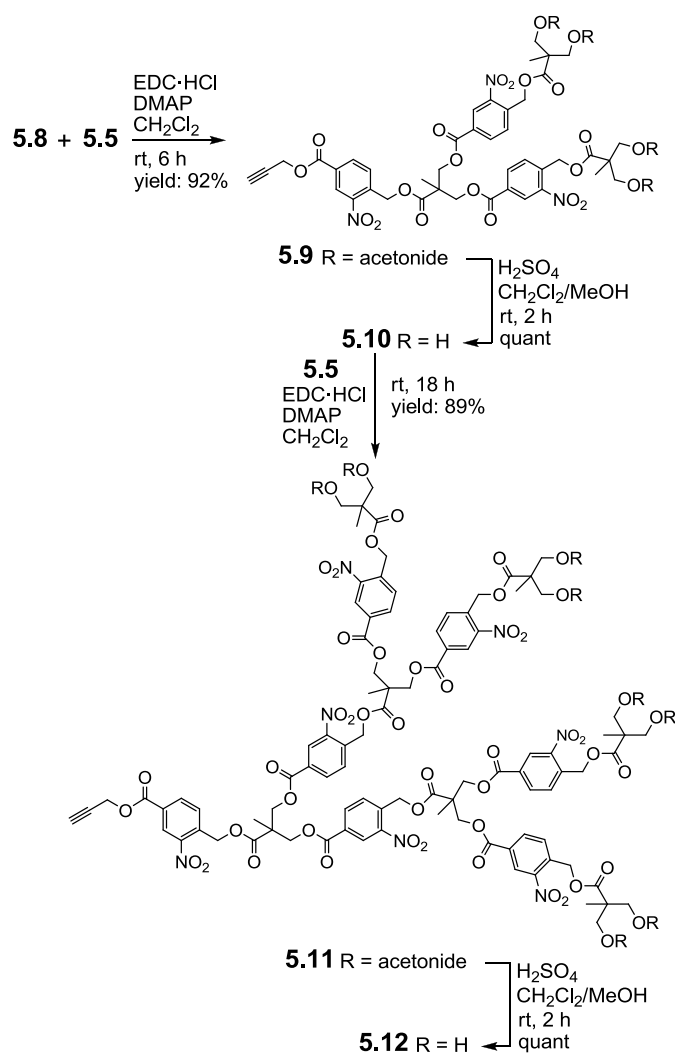
Scheme 5.2. Synthesis of G2 dendron **5.10** and G3 dendron **5.12**.

   In order to construct the target photodegradable G1-G3 dendrimers, dendrons **5.8**, **5.10**, and **5.12** were attached to a trifunctional azide core molecule **5.13**[34] via a copper(I)-catalyzed alkyne-azide cycloaddition reaction (Scheme 5.3). It should be noted that **5.13** was handled with care as organic polyazides can be potentially explosive. While heating the reaction vessel in an oil bath at 70 °C overnight resulted in low dendrimer yields, likely due to breakdown of ester linkages under these conditions, the reaction proceeded smoothly under microwave conditions at 120 °C in 20 min.[35] Follow-up

studies showed that the catalyst was still essential under these conditions and that microwave irradiation played a significant role in accelerating the reaction, even at this temperature.
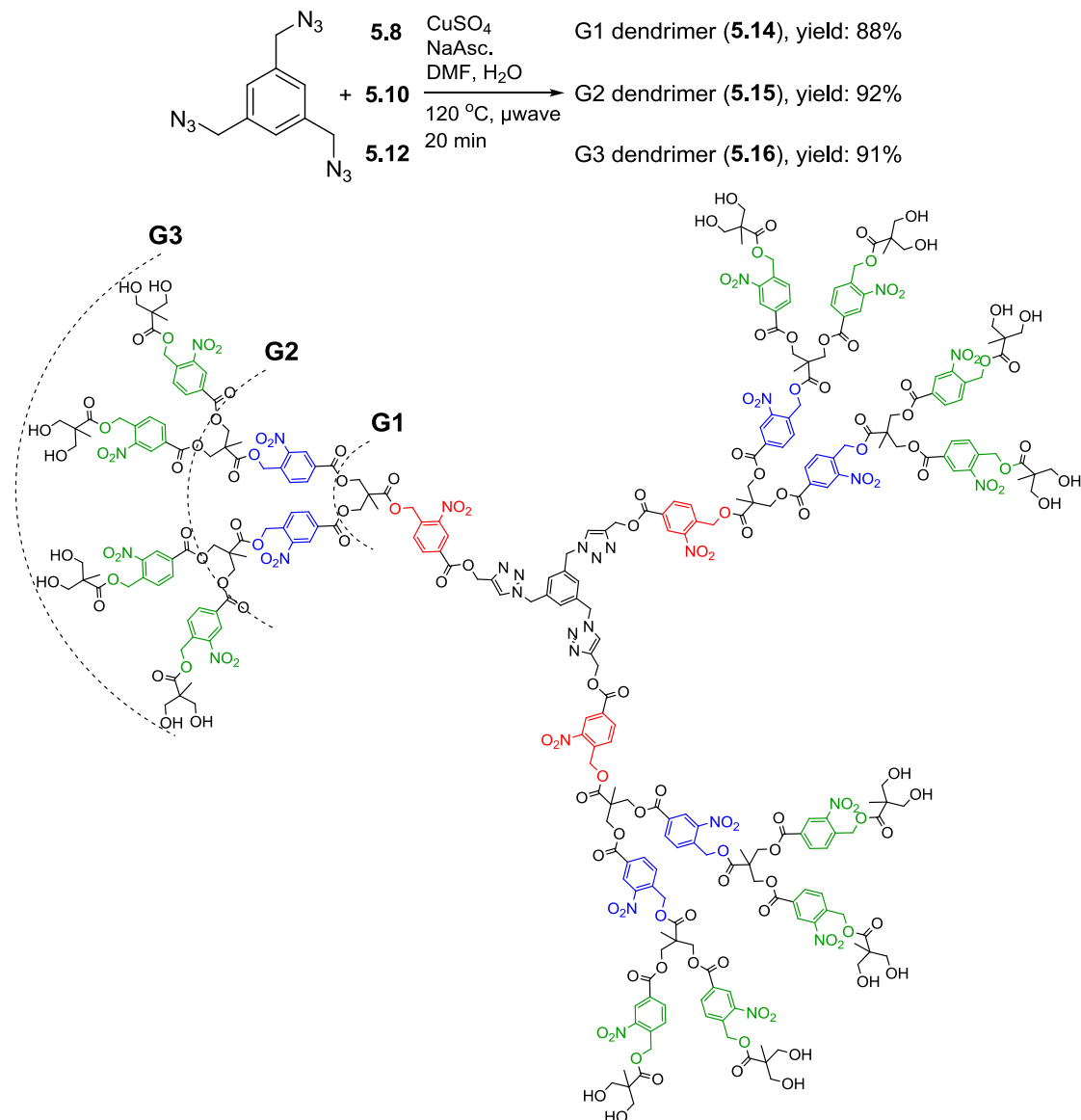
Scheme 5.3. Synthesis of G1-G3 dendrimers **5.14** - **5.16**.

The resulting dendrimers were characterized by ^{1}H and ^{13}C NMR spectroscopy, MALDI mass spectrometry, IR spectroscopy, and SEC. As shown in SEC traces (Figure 5.1), the resulting dendrimers exhibited monomodal molecular weight distribution

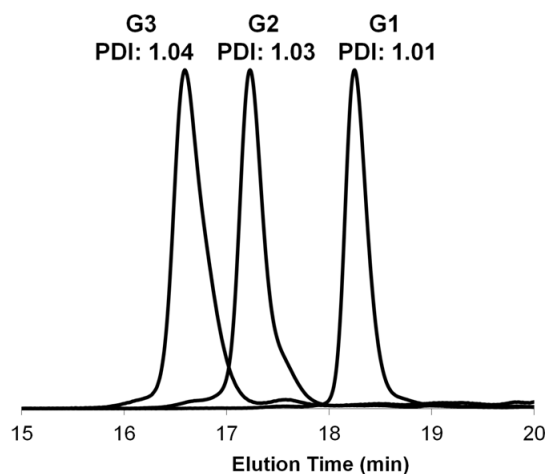profiles with the expected increases in hydrodynamic volume with each generation, as well as very narrow PDIs.

Figure 5.1. SEC traces of G1 (**5.14**), G2 (**5.15**), and G3 (**5.16**) dendrimers with their corresponding PDIs.

5.2.2 Photodegradation Study of the Dendrimers

Having the three dendrimers in hand, their photodegradation behaviors were then studied. First, ~20 µg/mL solutions of each dendrimer in THF were irradiated with UV light for 1 h and the UV-visible absorption spectra of the solutions were recorded in 2 min intervals for the first 10 min, followed by 5 min intervals for the remaining 50 min. The results for the G3 dendrimer (**5.16**) are shown in Figure 5.2a. A decrease in absorbance was observed for the peak at 225 nm while increases in absorbance were observed at 305 and 350 nm, along with corresponding red shifts in their absorption maxima. The results for photolysis of G1 (**5.14**) and G2 (**5.15**) dendrimers are shown in Figure A5.1. These observations are in accordance with the results obtained by other groups for this photolabile group.[15,16,20] The absorption band at 350 nm is attributed to *o*-nitrosobenzaldehyde, which is a product of *o*-nitrobenzyl ester photolysis, and exhibits a weak absorption band at 350-360 nm that is solvent dependent.[16] ^{1}H NMR spectroscopy was also used to study the photodegradation of the dendrimers. A 10 mg/mL solution of the dendrimer in $(CD_3)_2SO$ was irradiated with UV light in a quartz NMR tube for 1 h and ^{1}H NMR spectra were collected in 10 min intervals. The results for the photodegradation of G3 dendrimer (**5.16**) are shown in Figure 5.2b. The results for

photolysis of G1 (**5.14**) and G2 (**5.15**) dendrimers as well as extensive peak assignments for the degradation of all three dendrimers are shown in Figure A5.2, Figure A5.3 and Figure A5.4.
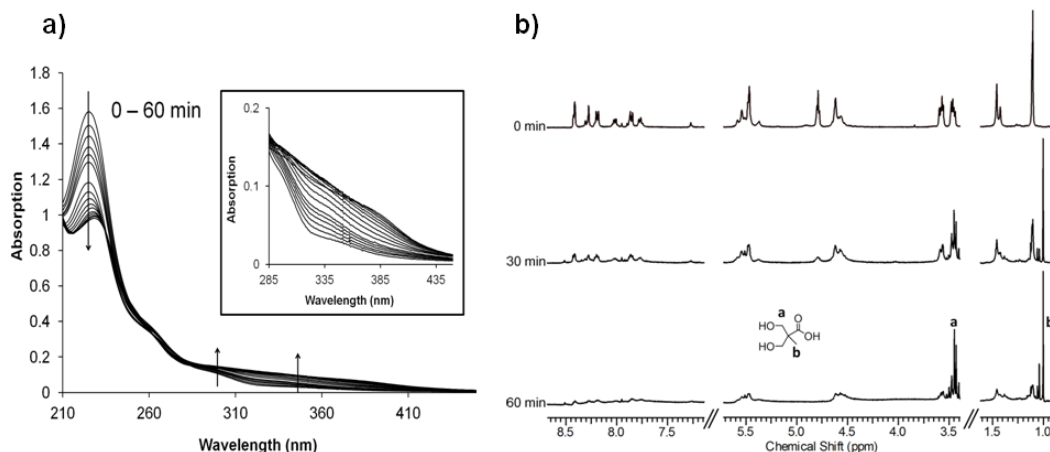

Figure 5.2. a) UV-visible spectra for G3 dendrimer (**5.16**) upon irradiation with UV light for 60 min. Inset shows the expanded region between 285-450 nm. b) Evolution of ^{1}H NMR spectra during the photolysis of a 10 mg/mL sample of G3 dendrimer (**5.16**) in $(CD_3)_2SO$.

As shown for the G3 dendrimer (**5.16**) in Figure 5.2b, the multiplets at 3.57 and 3.46 ppm, corresponding to the methylene groups of bis-MPA in the dendrimer backbone decrease as irradiation time increases. At the same time, a new sharp multiplet at 3.45 ppm appears, corresponding to the same methylene groups in the released product bis-MPA, a starting material for the dendrimer synthesis. The peak intensities of the methyl groups in the dendrimer backbone at 1.46, 1.42, and 1.10 ppm also decrease and a single methyl peak at 1.00 ppm corresponding to the released bis-MPA compound increases in intensity. The appearance of other smaller multiplets in the region of 3.45 ppm and singlets in the region of 1.00 ppm can result from the expected release of other bis-MPA derivatives containing the photocleavable aromatic groups. In addition, a general trend of peak broadening in the aromatic region was observable, which can be attributed to formation of different aromatic species after photodegradation, as nitroso compounds are known to be unstable and undergo side reactions to form other aromatic species such as diazo compounds.[31] However, if the aromatic region is expanded and increased in

intensity, it is possible to see that the peaks at 7.27 and 8.31 ppm, corresponding to the core molecule and triazole ring respectively, are still present after 1 h as they do not participate in degradation process. Moreover, SEC traces of the degraded ^{1}H NMR samples showed that only small molecules were present, demonstrating the successful full degradation of the dendrimers (Figure A5.5).

5.3 Conclusion

In summary, we have successfully designed and synthesized a new series of dendrons and dendrimers that are able for the first time to undergo complete backbone photodegradation to small molecules. We expect that the incorporation of these dendrons and dendrimers into new materials will impart new photoresponsive properties and functions. In addition, tuning of their optical properties by changing the photochemically responsive group or through the incorporation of other photophysical processes in such a way that they can undergo photodegradation in the visible or nearinfrared region can potentially open up new opportunities to access materials with fully photodegradable hydrophobic blocks suitable for biological or other applications.

5.4 Experimental

General Procedures and Materials

Compounds **5.3**[36] and **5.13**[35] were synthesized according to the previously published procedures. All the other chemicals were purchased from Sigma-Aldrich or Alfa Aesar and were used without further purification unless otherwise noted. Anhydrous DMF was obtained from a solvent purification system using aluminum oxide columns. Dichloromethane was distilled from CaH_2. Unless otherwise stated, all reactions were performed under a nitrogen atmosphere using flame or oven dried glassware. For the reactions that were mentioned to be stirred in dark, aluminum foil was used to isolate the reaction flasks from light. No special precautions regarding light, were taken during purification or isolation of these compounds. For long term storage the isolated materials were stored in freezer. However no degradation issues were encountered when materials were stored in the dark at ambient temperature. ^{1}H NMR spectra were obtained at 400

MHz, and ^{13}C NMR spectra were obtained at 100 MHz. NMR chemical shifts are reported in ppm and are calibrated against the residual solvent signal of CDCl$_3$ (δ 7.26 and 77.16 ppm), (CD$_3$)$_2$SO (δ 2.50 and 39.52 ppm), or (CD$_3$)$_2$CO (δ 2.05 and 29.84 ppm). *J* values are expressed in Hz. IR spectra were obtained as films from CH$_2$Cl$_2$ or THF on NaCl plates using a Bruker Tensor 27 instrument. HRMS was performed using a Finnigan MAT 8400 electron impact mass spectrometer. Electrospray mass spectrometry (ESI) was performed using a PE-Sciex API 365 mass spectrometer. Melting points (m.p.) were determined using a Gallenkamp variable heater. UV–visible absorption spectroscopy was performed on a Varian Cary 300 Bio UV–visible spectrophotometer. MALDI-TOF mass spectrometry data were obtained using a 4700 Proteomics Analyzer, MALDI TOF (Applied Biosystems, Foster City, CA). Reflectron and linear positive ion modes were used. 2-(4'-Hydroxybenzeneazo)benzoic acid (HABA) was used as the matrix for the measurements. Dialyses were performed using Spectra/Por regenerated cellulose membranes with either a 12,000–14,000 g/mol or 6000-8000 g/mol MWCO. SEC instrument was equipped with a Viscotek GPC Max VE2001 solvent module. Samples were analyzed using the Viscotek VE3580 RI detector operating at 30 °C. The separation technique employed a Polypore guard column (50x7.5mm) and two Agilent Polypore (300x7.5mm) columns connected in series. Samples were dissolved in THF (glass distilled grade) at approximately 5 mg/mL concentrations and filtered through 0.22 µm syringe filters. Samples were injected using a 100 µL loop. The THF eluent was filtered and eluted at 1 ml/min for a total of 30 min. A calibration curve was obtained from polystyrene standards with MWs ranging from 1,540-1,126,000 g/mol. Microwave reactions were performed in a Biotage® Initiator Microwave Synthesizer. The light source used for the photochemical reactions was either a Hanovia medium pressure mercury lamp (PC 451050/616750, 450 Wage) or a model LZC-4X Luzchem Photoreactor equipped with Luzchem LZC-UVB lamps.

Note: Triazide **5.13** has been reported to be relatively insensitive to heat and shock.[35,37] However, due to the explosive nature of organic polyazides, this compound was handled with care. A blast shield was used during concentrating its solution on rotary evaporator and during further drying under high vacuum.

Synthesis of compound 5.2: Compound **5.1** (0.50 g, 1.9 mmol, 1.0 equiv.) and allyl alcohol (2.2 g, 38 mmol, 20 equiv.) were dissolved in CH_2Cl_2 (14 mL). DCC (0.68 g, 3.3 mmol, 1.7 equiv.) and DMAP (0.12 g, 0.96 mmol, 0.50 equiv.) were then added. The resulting solution was stirred at room temperature in dark while the course of the reaction was monitored by thin layer chromatography (TLC) (ethyl acetate (EtOAc):cyclohexane, 1:2). TLC showed that the reaction was complete after 3.5 h. At this point, the solution was filtered and the filtrate was washed with 1 M $KHSO_4$ (1×50 mL), distilled water (3×50 mL), and brine (1×50 mL). The organic solution was dried over magnesium sulfate, filtered, and concentrated under reduced pressure. The product was purified by column chromatography (EtOAc:cyclohexane, 1:6). Compound **5.2** (0.43 g, 1.4 mmol) was obtained in 75% yield as a yellow oil. ^1H NMR ($CDCl_3$) δ: 8.68 (s, 1H), 8.26 (d, $J = 8.0$, 1H), 7.68 (d, $J = 8.0$, 1H), 6.09-5.99 (m, 1H), 5.46-5.41 (m, 1H), 5.36-5.32 (m, 1H), 4.87 (dd, $J_1 = 8.0$, $J_2 = 4.0$, 2H), 4.85 (s, 2H). ^{13}C NMR ($CDCl_3$) δ: 163.8, 148.2, 137.3, 134.3, 133.0, 131.9, 131.6, 126.7, 119.5, 66.7, 28.0. IR (cm^{-1}, film from CH_2Cl_2): 3093, 2931, 2858, 2106, 1730, 1539, 1351, 1263, 1131. HRMS: calcd for $[M]^+$ ($C_{11}H_{10}BrNO_4$): 298.9793. Found: (EI) 298.9798.

Synthesis of compound 5.4: Compound **5.2** (0.90 g, 3.0 mmol, 1.0 equiv.) was dissolved in DMF (25 mL). Compound **5.3** (1.0 g, 6.0 mmol, 2.0 equiv.) and cesium carbonate (2.9 g, 9.0 mmol, 3.0 equiv.) were then added. The resulting mixture was stirred at room temperature in dark while the course of the reaction was monitored by TLC (EtOAc:cyclohexane, 1:4). TLC showed that the reaction was complete after 1.5 h. At this point, the mixture was diluted with EtOAc (100 mL), washed with distilled water (1×100 mL), 1M $KHSO_4$ (1×100 mL), 1M Na_2CO_3 (2×100 mL), and brine (1×100 mL). The organic layer was dried over $MgSO_4$, filtered, and concentrated under reduced pressure. The product **5.4** (1.2 g, 3.0 mmol) was obtained in quantitative yield as a light orange solid that did not require further purification. ^1H NMR ($CDCl_3$) δ: 8.76 (d, $J = 4.0$, 1H), 8.30 (dd, $J_1 = 8.0$, $J_2 = 4.0$, 1H), 7.86 (d, $J = 8.0$, 1H), 6.09-5.99 (m, 1H), 5.67 (s, 1H), 5.45-5.40 (m, 1H), 5.35-5.32 (m, 1H), 4.88-4.86 (m, 2H), 4.28 (d, $J = 12.0$, 2H), 3.72 (d, $J = 12.0$, 2H), 1.47 (s, 3H), 1.40 (s, 3H), 1.17 (s, 1H). ^{13}C NMR ($CDCl_3$) δ: 173.8, 164.0, 147.3, 137.3, 134.4, 131.6, 131.1, 129.1, 126.3, 119.3, 98.4, 66.6, 66.4, 63.3, 42.6, 26.8, 20.8, 18.4. IR (cm^{-1}, film from CH_2Cl_2): 3096, 2994, 2932, 2877, 1728,

1625, 1539, 1373, 1350, 1257, 1158. HRMS: calcd for $[M+H]^+$ ($C_{19}H_{24}NO_8$): 394.1502. Found: (CI) 394.1499. m. p.: 79.3-81.1 °C.

Synthesis of monomer 5.5: Compound **5.4** (1.1 g, 2.7 mmol, 1.0 equiv.) and tetrakis(triphenylphosphine)palladium(0) (0.16 g, 0.14 mmol, 0.050 equiv.) were dissolved in CH_2Cl_2 (20 mL). Piperidine (0.40 mL, 4.0 mmol, 1.5 equiv.) was added and the resulting solution was stirred at room temperature in dark while the course of the reaction was monitored by TLC (EtOAc:cyclohexane, 1:1). TLC showed that the reaction was complete after 1 h. At this point, CH_2Cl_2 was removed under reduced pressure. The residue was dissolved in EtOAc (100 mL). The organic solution was washed with 1 M $KHSO_4$ (3×100 mL), brine (1×100 mL), dried over $MgSO_4$, filtered, and concentrated under reduced pressure. The product was purified by column chromatography using a gradient of EtOAc:cyclohexane (1:1) to pure EtOAc. Compound **5.5** (0.87 g, 2.5 mmol) was obtained in 92% yield as a light yellow solid. ^{1}H NMR ($CDCl_3$) δ: 8.80 (d, J = 4.0, 1H), 8.32 (dd, J_1 = 8.0, J_2 = 4.0, 1H), 7.90 (d, J = 8.0, 1H), 5.69 (s, 2H), 4.31 (d, J = 12.0, 2H), 3.75 (d, J = 12.0, 2H), 1.49 (s, 3H), 1.42 (s, 3H), 1.18 (s, 3H). ^{13}C NMR ($CDCl_3$) δ: 173.9, 168.9, 147.4, 138.0, 134.9, 134.8, 129.2, 126.8, 98.6, 66.4, 63.3, 42.6, 27.0, 20.6, 18.4. IR (cm^{-1}, film from CH_2Cl_2): 3460, 3249, 2995, 2933, 2887, 2104, 1737, 1625, 1541, 1352, 1222, 1157. HRMS: calcd for $[M+H]^+$ ($C_{16}H_{20}NO_8$): 354.1189. Found: (CI) 354.1198. m. p.: 146.1-148.8 °C.

Synthesis of compound 5.6: Compound **5.1** (0.50 g, 1.9 mmol, 1.0 equiv.) and propargyl alcohol (2.2 g, 38 mmol, 20 equiv.) were dissolved in CH_2Cl_2 (14 mL). DCC (0.68 g, 3.3 mmol, 1.7 equiv.) and DMAP (0.12 g, 0.96 mmol, 0.50 equiv.) were then added. The resulting solution was stirred at room temperature in dark while the course of the reaction was monitored by TLC (EtOAc:cyclohexane, 1:2). TLC showed that the reaction was complete after 3.5 h. At this point, the solution filtered and the filtrate was washed with 1 M $KHSO_4$ (1×50 mL), distilled water (3×50 mL), and brine (1×50 mL). The organic solution was dried over magnesium sulfate, filtered, and concentrated under reduced pressure. The product was purified by column chromatography (EtOAc:cyclohexane, 1:4). Compound **5.6** (0.47 g, 1.6 mmol) was obtained in 82% yield as light yellow solid. ^{1}H NMR ($CDCl_3$) δ: 8.70 (d, J = 4.0, 1H), 8.28 (dd, J_1 = 8.0, J_2 = 4.0, 1H), 7.70 (d, J =

8.0, 1H), 4.98 (d, J = 4.0, 2H), 4.85 (s, 2H), 2.56 (t, J = 4.0, 1H). ^{13}C NMR (CDCl$_3$) δ: 163.4, 148.2, 137.7, 134.4, 133.1, 131.2, 126.9, 77.0, 76.0, 53.5, 28.0. IR (cm^{-1}, film from CH$_2$Cl$_2$): 3296, 3096, 2959, 2917, 2131, 1733, 1621, 1537, 1350, 1262, 1132. HRMS: calcd for [M]$^+$ (C$_{11}$H$_8$BrNO$_4$): 296.9637. Found: (EI) 296.9641. m. p.: 54.8-56.5 °C.

Synthesis of protected G1 dendron 5.7: Compounds **5.6** (0.64 g, 2.1 mmol, 1.0 equiv.), **5.3** (0.74 g, 4.3 mmol, 2.0 equiv.), and cesium carbonate (2.1 g, 6.4 mmol, 3.0 equiv.) were dissolved in DMF (20 mL). The resulting mixture was stirred at room temperature in dark while the course of the reaction was monitored by TLC (EtOAc:cyclohexane, 1:4). TLC showed that the reaction was complete after 1.5 h. At this point, the mixture was diluted with EtOAc (100 mL), washed with distilled water (1×100 mL), 1M KHSO$_4$ (1×100 mL), 1M sodium carbonate (Na$_2$CO$_3$) (2×100 mL), and brine (1×100 mL). The organic layer was dried over MgSO$_4$, filtered, and concentrated under reduced pressure. The product **5.7** was obtained in quantitative yield (0.82 g, 2.1 mmol) as an orange solid that did not require any further purification. ^{1}H NMR (CDCl$_3$) δ: 8.78 (d, J = 4.0, 1H), 8.31 (dd, J_1 = 8.0, J_2 = 4.0, 1H), 7.88 (d, J = 8.0, 1H), 5.67 (s, 2H), 4.97 (d, J = 4.0, 2H), 4.28 (d, J = 12.0, 2H), 4.72 (d, J = 12.0, 2H), 2.56 (t, J = 4.0, 1H), 1.47 (s, 3H), 1.41 (s, 3H), 1.17 (s, 3H). ^{13}C NMR (CDCl$_3$) δ: 173.8, 163.6, 147.4, 137.7, 134.6, 130.4, 129.2, 126.4, 98.4, 77.1, 75.9, 66.4, 63.2, 53.4, 42.6, 26.9, 20.8, 18.4. IR (cm^{-1}, film from CH$_2$Cl$_2$): 3291, 3097, 2994, 2967, 2878, 2133, 1738, 1625, 1539, 1373, 1370, 1254, 1154. HRMS: calcd for [M+H]$^+$ (C$_{19}$H$_{22}$NO$_8$): 392.1345. Found: (CI) 392.1346. m. p.: 88.4-89.8 °C.

Synthesis of deprotected G1 dendron 5.8: Compound **5.7** (0.79 g, 2.0 mmol) was dissolved in methanol (50 mL) and CH$_2$Cl$_2$ (5 mL). Concentrated sulfuric acid (0.40 mL) was added and the resulting solution was stirred at room temperature in dark while the course of the reaction was monitored by TLC (EtOAc:cyclohexane, 1:2). TLC showed that the reaction was complete after 2 h. At this point, the solution was concentrated to one-third of its initial volume. EtOAc (50 mL) was added and the organic solution was washed with 1M Na$_2$CO$_3$ (2×50 mL) and brine (1×50 mL). The organic layer was dried over MgSO$_4$, filtered, and concentrated under reduced pressure. The product **5.8** was obtained in quantitative yield as an orange solid that did not require any further

purification. ^{1}H NMR (CDCl$_3$) δ: 8.76 (d, J = 4.0, 1H), 8.33 (dd, J_1 = 8.0, J_2 = 4.0, 1H), 7.84 (d, J = 8.0, 1H), 5.66 (s, 2H), 4.97 (d, J = 4.0, 2H), 4.00 (d, J = 12.0, 2H), 8.79 (d, J = 12.0, 2H), 2.56 (t, J = 4.0, 1H), 1.12 (s, 3H). ^{13}C NMR (CDCl$_3$) δ: 175.3, 163.6, 147.5, 137.1, 134.7, 130.5, 129.4, 126.4, 77.1, 75.9, 68.8, 63.4, 53.4, 49.7, 17.3. IR (cm^{-1}, film from CH$_2$Cl$_2$): 3421, 3299, 3097, 2953, 2888, 2126, 1742, 1625, 1541, 1433, 1352, 1249, 1131. HRMS: calcd for [M+H]$^+$ (C$_{16}$H$_{18}$NO$_8$): 352.1032. Found: (CI) 352.1039. m. p.: 76.4-77.0 °C.

Synthesis of protected G2 dendron 5.9: Compounds **5.8** (0.30 g, 0.85 mmol, 1.0 equiv.) and **5.5** (0.91 g, 2.6 mmol, 3.0 equiv.) were dissolved in CH$_2$Cl$_2$ (20 mL). EDC·HCl (0.74 g, 3.8 mmol, 4.5 equiv) and DMAP (0.10 g, 0.85 mmol, 1.0 equiv.) were added in one portion and the resulting solution was stirred at room temperature in dark while the course of the reaction was monitored by TLC (EtOAc:cyclohexane, 1:1). TLC showed that the reaction was complete after 7 h. At this point, CH$_2$Cl$_2$ was removed under reduced pressure. The remaining residue was dissolved in EtOAc (50 mL) and washed with 1M KHSO$_4$ (3×100 mL), 1M Na$_2$CO$_3$ (3×100 mL), and brine (1×100 mL). The organic layer was dried was dried over MgSO$_4$, filtered, and concentrated under reduced pressure. The product was purified by column chromatography (EtOAc:cyclohexane, 1:1). Compound **5.9** (0.80 g, 0.78 mmol) was obtained in 91% yield as a fluffy off white solid. ^{1}H NMR (CDCl$_3$) δ: 8.63 (d, J = 4.0, 1H), 8.62 (d, J = 4.0, 2H), 8.20-8.15 (m, 3H), 7.84 (d, J = 8.0, 2H), 7.64 (d, J = 8.0, 1H), 5.66 (s, 4H), 5.62 (s, 2H), 4.96 (d, J = 4.0, 2H), 4.63 (s, 4H), 4.28 (d, J = 12.0, 4H), 3.73 (d, J = 12.0, 4H), 2.56 (t, J = 4.0, 1H), 1.50 (s, 3H), 1.47 (s, 6H), 1.39 (s, 6H), 1.18 (s, 6H). ^{13}C NMR (CDCl$_3$) δ: 173.7, 171.6, 163.5, 163.2, 147.8, 147.2, 137.7, 135.6, 134.3, 134.2, 130.9, 130.1, 130.0, 129.1, 126.3, 126.0, 98.3, 77.0, 76.0, 66.6, 66.2, 63.8, 63.0, 53.4, 47.1, 42.5, 26.7, 20.7, 18.3, 18.0. IR (cm^{-1}, film from CH$_2$Cl$_2$): 3269, 2999, 2885, 2137, 1730, 1652, 1539, 1257, 1122. HRMS: calcd [M+Na]$^+$ (C$_{48}$H$_{51}$N$_3$O$_{22}$Na): 1044.2862. Found: (ESI) 1044.2867.

Synthesis of deprotected G2 dendron 5.10: Compound **5.9** (0.22 g, 0.21 mmol) was dissolved in a mixture of methanol (40 mL) and CH$_2$Cl$_2$ (4 mL). Concentrated sulfuric acid (0.40 mL) was added and the resulting solution was stirred at room temperature in dark while the course of the reaction was monitored by TLC (EtOAc:cyclohexane, 1:1).

TLC showed that the reaction was complete after 2 h. At this point, the solution was concentrated to one-third of its initial volume. EtOAc (50 mL) was added and the organic solution was washed with 1M Na_2CO_3 (2×50 mL) and brine (1×50 mL). The organic layer was dried over $MgSO_4$, filtered, and concentrated under reduced pressure. The product **5.10** (0.20 g, 0.21 mmol) was obtained in quantitative yield as a fluffy light orange solid that did not require any further purification. ^{1}H NMR (CDCl$_3$) δ: 8.61 (d, J = 4.0, 1H), 8.56 (d, J = 4.0, 2H), 8.17-8.14 (m, 3H), 7.80 (d, J = 8.0,, 2H), 7.65 (d, J = 8.0, 1H), 5.64 (s, 4H), 5.63 (s, 2H), 4.96 (d, J = 4.0, 2H), 4.64 (s, 4H), 4.00 (d, J = 12.0, 4H), 3.80 (d, J = 12.0, 4H), 2.93 (br s, 4H), 2.58 (t, J = 4.0, 1H), 1.49 (s, 3H), 1.13 (s, 6H). ^{13}C NMR (CDCl$_3$) δ: 175.0, 171.8, 163.6, 163.3, 147.8, 147.1, 137.3, 135.7, 134.3 (2), 130.8, 130.1 (2), 129.2, 126.2, 126.0, 77.0, 76.1, 67.4, 66.8, 63.8, 63.1, 53.4, 49.8, 47.0, 18.1, 17.2. IR (cm^{-1}, film from CH$_2$Cl$_2$): 3440, 3300, 3087, 2932, 2859, 2133, 1737, 1623, 1539, 1352, 1257, 1125. HRMS: calcd [M+Na]$^+$ (C$_{42}$H$_{43}$N$_3$O$_{22}$Na): 964.2236. Found: (ESI) 964.2266.

Synthesis of protected G3 dendron 5.11: Compounds **5.10** (55 mg, 58 µmol, 1.0 equiv.) and **5.5** (0.12 g, 0.35 mmol, 6.0 equiv.) were dissolved in CH$_2$Cl$_2$ (10 mL). EDC·HCl (0.11 g, 0.52 mmol, 9.0 equiv) and DMAP (15 mg, 0.12 mmol, 2.0 equiv.) were added and the resulting solution was stirred at room temperature in dark overnight. CH$_2$Cl$_2$ was removed under reduced pressure. The remaining residue was dissolved in EtOAc (50 mL) and washed with 1M KHSO$_4$ (3×100 mL), 1M Na$_2$CO$_3$ (3×100 mL), and brine (1×100 mL). The organic layer was dried was dried over MgSO$_4$, filtered, and concentrated under reduced pressure. The product was purified by dialysis against DMF (300 mL) using a 3500 MWCO membrane. The solvent was then removed under reduced pressure. Dendron **5.11** (0.12 g, 50 µmol) was obtained in 86% yield as a fluffy off-white solid. ^{1}H NMR (CDCl$_3$) δ: 8.60-8.59 (m, 5H), 8.49-8.48 (m, 2H), 8.20 (dd, J_1 = 8.0, J_2 = 4.0, 4H), 8.16 (dd, J_1 = 8.0, J_2 = 4.0, 1H), 8.10 (dd, J_1 = 8.0, J_2 = 4.0, 2H), 7.85 (d, J = 8.0, 4H), 7.67-7.63 (m, 3H), 5.64 (s, 8H), 5.61 (br s, 6H), 4.94 (d, J = 4.0, 2H), 4.64 (s, 8H), 4.62 (s, 4H), 4.27 (d, J = 12.0, 8H), 3.72 (d, J = 12.0, 8H), 2.57 (t, J = 4.0, 1H), 1.50 (s, 6H), 1.49 (s, 3H), 1.46 (s, 12H), 1.38 (s, 12H), 1.17 (s, 12H). ^{13}C NMR (CDCl$_3$) δ: 173.7, 171.6, 163.6, 163.3, 163.2, 147.9, 147.8, 147.2, 137.8, 135.7, 135.6, 134.3 (2), 134.1, 130.9, 130.8, 130.2, 130.1 (2), 129.1, 126.3, 126.1, 126.0, 98.3, 77.0, 76.0, 66.7, 66.6,

66.2, 63.9, 63.1, 53.4, 47.1, 47.0, 42.5, 41.8, 26.7, 20.7, 18.3, 18.1, 18.0. IR (cm^{-1}, film from CH$_2$Cl$_2$): 3300, 3097, 2989, 2879, 2131, 1739, 1625, 1539, 1352, 1249, 1122. HRMS: calcd [M+Na]$^+$ (C$_{106}$H$_{111}$N$_7$O$_{50}$Na): 2304.6256. Found: (ESI) 2304.6218.

Synthesis of deprotected G3 dendron 5.12: Compound **5.11** (0.10 g, 44 µmol) was dissolved in methanol (30 mL) and CH$_2$Cl$_2$ (15 mL). Concentrated sulfuric acid (0.50 mL) was added and the resulting solution was stirred at room temperature in dark while the course of the reaction was monitored by TLC (EtOAc:cyclohexane, 4:1). TLC showed that the reaction was complete after 2 h. At this point, the solution was concentrated to one-third of its initial volume. EtOAc (50 mL) was added and the organic solution was washed with 1M Na$_2$CO$_3$ (2×50 mL) and brine (1×50 mL). The organic layer was dried over MgSO$_4$, filtered, and concentrated under reduced pressure. The product **5.12** was further purified by dialysis against DMF (300 mL) using a 3500 MWCO membrane. The solvent was then removed under reduced pressure. Dendron **5.12** was obtained in quantitative yield (93 mg, 44 µmol) as a fluffy off-white solid. ^{1}H NMR (CDCl$_3$) δ: 8.59 (d, $J = 4.0$, 1H), 8.51 (d, $J = 4.0$, 4H), 8.34 (d, $J = 4.0$, 2H), 8.16-8.14 (m, 5H), 8.06-8.01 (m, 2H), 7.78 (d, $J = 8.0$, 4H), 7.66-7.62 (m, 3H), 5.63-5.60 (m, 14H), 4.94 (d, $J = 4.0$, 2H), 4.64 (s, 8H), 4.61 (s, 4H), 3.96 (d, $J = 12.0$, 8H), 3.78 (d, $J = 12.0$, 8H), 3.03 (br s, 8H), 2.58 (t, $J = 4.0$, 1H), 1.50 (s, 6H), 1.48 (s, 3H), 1.12 (s, 12H). ^{13}C NMR ((CD$_3$)$_2$SO) δ: 174.3, 171.7, 171.6, 163.3, 163.1, 162.9, 147.5, 147.4, 146.9, 137.5, 135.8, 135.6, 134.0, 133.8 (2), 130.6, 130.5, 130.0, 129.8, 129.6, 129.2, 125.3, 125.2, 125.1, 78.4, 77.8, 66.6, 66.5, 64.0, 63.3 (2), 63.2, 62.0, 53.3, 50.7, 46.6, 17.3 (2), 16.9. IR (cm^{-1}, film from CH$_2$Cl$_2$): 3440, 3290, 3109, 2931, 2854, 2129, 1731, 1623, 1537, 1346, 1255, 1122. HRMS: calcd [M+Na]$^+$ (C$_{94}$H$_{95}$N$_7$O$_{50}$Na): 2144.5004. Found: (ESI) 2144.5006.

Synthesis of G1 dendrimer 5.14: Compound **5.13** (7.0 mg, 29 µmol, 1 equiv.), dendron **5.8** (36 mg, 0.10 mmol, 3.6 equiv.), copper sulfate (CuSO$_4$) (2.8 mg, 17 µmol, 0.60 equiv.), and sodium ascorbate (14 mg, 69 µmol, 2.4 equiv.) were dissolved in DMF/water (4:1) mixture (2 mL). The reaction vessel was sealed and irradiated in a Biotage microwave at 120 °C for 20 min. The reaction content was then partitioned between brine (50 mL) and EtOAc (50 mL). The organic layer was separated and the aqueous layer was

extracted with EtOAc (3×50 mL). The organic layers were combined, dried over $MgSO_4$, filtered, and concentrated under reduced pressure. The product was purified by column chromatography (acetone:CH_2Cl_2, 2:1). Dendrimer **5.14** (33 mg, 25 µmol) was obtained in 88% yield as a fluffy off-white solid. ^{1}H NMR ($(CD_3)_2SO$) δ: 8.52 (d, J = 4.0, 3H), 8.32 (s, 3H), 8.26 (dd, J_1 = 8.0, J_2 = 4.0, 3H), 7.91 (d, J = 8.0, 3H), 7.26 (s, 3H), 5.61 (s, 6H), 5.50 (s, 6H), 5.43 (s, 6H), 4.79 (t, J = 6.0, 6H), 3.60-3.56 (m, 6H), 3.48-3.44 (m, 6H), 1.11 (s, 9H). ^{13}C NMR ($(CD_3)_2CO$) δ: 175.3, 164.6, 148.2, 143.2, 138.6, 138.2, 134.9, 131.2, 130.2, 128.7, 126.3, 125.6, 65.8, 63.1, 59.6, 53.7, 51.5, 17.4. IR (cm^{-1}, film from THF): 3406, 3155, 2960, 2883, 1730, 1623, 1537, 1350, 1259, 1124. HRMS: calcd [M+Na]$^+$ ($C_{57}H_{60}N_{12}O_{24}Na$): 1319.3741. Found: (ESI) 1319.3728 and (MALDI-TOF) 1319.4. SEC data: M_n = 1700 gmol^{-1}, PDI: 1.01.

Synthesis of G2 dendrimer 5.15: Compound **5.13** (4.0 mg, 16 µmol, 1 equiv.), dendron **5.10** (56 mg, 59 µmol, 3.6 equiv.), $CuSO_4$ (1.6 mg, 9.8 µmol, 0.60 equiv.), and sodium ascorbate (7.8 mg, 39 µmol, 2.4 equiv.) were dissolved in DMF/water (4:1) (2 mL). The reaction vessel was sealed and irradiated in a Biotage microwave reactor at 120 °C for 20 min. The product was purified by dialysis against DMF (300 mL) using a 6000-8000 MWCO membrane. The target dendrimer **5.15** (45 mg, 15 µmol) was obtained in 92% yield as a fluffy off-white solid. ^{1}H NMR ($(CD_3)_2SO$) δ: 8.42 (d, J = 4.0, 6H), 8.33 (d, J = 4.0, 3H) 8.29 (s, 3H), 8.19 (dd, J_1 = 8.0, J_2 = 4.0, 6H), 8.06 (dd, J_1 = 8.0, J_2 = 4.0, 3H), 7.86 (d, J = 8.0, 6H), 7.79 (d, J = 8.0, 3H), 7.26 (s, 3H), 5.60 (s, 6H), 5.54 (s, 6H), 5.49 (s, 12H), 5.39 (s, 6H), 4.80 (t, J = 6, 12H), 4.64-4.57 (m, 12H), 3.61-3.57 (m, 12H), 3.49-3.45 (m, 12H), 1.45 (s, 9H), 1.12 (18H). ^{13}C NMR ($(CD_3)_2SO$) δ: 174.4, 174.3, 171.6, 163.3, 147.5, 146.9, 141.6, 137.5, 137.1, 135.5, 133.9, 133.8, 130.7, 130.2, 129.5, 129.2, 127.6, 125.3, 125.2, 125.1, 66.5, 64.0, 63.2, 62.0, 58.6, 52.4, 50.7, 46.6, 17.3, 16.9. IR (cm^{-1}, film from THF): 3396, 3101, 2958, 2879, 1731, 1623, 1537, 1346, 1251, 1120. HRMS: calcd [M+Na]$^+$ ($C_{135}H_{138}N_{18}O_{66}Na$): 3089.7893. Found: (ESI) 3089.7893 and (MALDI-TOF) 3089.9. SEC data: M_n = 3700 gmol^{-1}, PDI: 1.03.

Synthesis of G3 dendrimer 5.16: Compound **5.13** (1.9 mg, 8.0 µmol, 1 equiv.), dendron **5.12** (61 mg, 29 µmol, 3.6 equiv.), $CuSO_4$ (1.6 mg, 9.8 µmol, 1.2 equiv.), and sodium ascorbate (7.8 mg, 39 µmol, 4.9 equiv.) were dissolved in DMF/water (4:1) mixture (2

mL). The reaction vessel was sealed and irradiated in a Biotage microwave reactor at 120 °C for 20 min. The product was purified by dialysis against DMF (300 mL) using a 12000-14000 MWCO membrane. The target dendrimer **5.16** (48 mg, 7.3 µmol) was obtained in 91% yield as a fluffy off-white solid. ^{1}H NMR ((CD$_3$)$_2$SO) δ: 8.44-8.39 (m, 12H), 8.33-8.25 (m, 12H), 8.19 (d, J = 8.0, 12H), 8.02(d, J = 8.0, 9H), 7.90 (s, 3H), 7.88-7.83 (m, 9H), 7.81-7.73 (m, 9H), 7.27 (s, 3H), 5.61-5.32 (m, 54H), 4.84-4.72 (m, 24H), 4.70-4.49 (m, 36H), 3.61-3.53 (m, 24H), 3.50-3.42 (m, 24H), 1.46 (s, 18H), 1.42 (s, 9H), 1.10 (s, 36H). ^{13}C NMR ((CD$_3$)$_2$SO) δ: 174.3, 171.6 (3), 163.3, 163.0, 147.4, 146.8, 137.5, 137.1, 137.0, 135.6, 135.5 (2), 133.9, 133.8 (2), 133.7, 130.5, 130.4, 130.2, 130.1, 130.0, 129.5, 129.2, 125.2, 125.1 (2), 66.5, 66.4, 64.0, 63.2 (2), 62.0, 54.8, 53.1, 50.7, 46.6, 46.5, 17.3, 17.2, 16.8. IR (cm^{-1}, film from THF): 3429, 3097, 2927, 2854, 1731, 1623, 1537, 1350, 1253, 1122. MS: calcd [M+Na]$^+$ (C$_{291}$H$_{294}$N$_{30}$O$_{150}$Na): 6633.6. Found (MALDI-TOF) 6634.3. SEC data: M_n = 6000 gmol^{-1}, PDI: 1.04.

General Procedure for Monitoring Dendrimer Degradation by UV-visible Spectroscopy: Dendrimer solutions were prepared at the concentration of 23 µM in spectroscopic grade THF. 3 mL of solution was transferred to a quartz cuvette and irradiated with 313 nm UV light in a Luzchem Photoreactor for 1 h. UV-visible absorption spectra were collected every 2 min for the first 10 min and then every 5 min for the remaining 50 min.

General Procedure for Monitoring Dendrimer Degradation by ^{1}H NMR Spectroscopy: Dendrimer solutions were prepared at the concentration of 10 mg/mL in (CD$_3$)$_2$SO. The solutions were transferred to a quartz NMR tube and irradiated with UV light using a Hanovia medium pressure mercury lamp (PC 451050/616750, 450 Wage) light box for 1 h. ^{1}H NMR spectra were collected every 10 min.

5.5 References

1. Adronov, A.; Gilat, S. L.; Fréchet, J. M. J.; Ohta, K.; Neuwahl, F. V. R.; Fleming, G. R. *J. Am. Chem. Soc.* **2000**, *122*, 1175.

2. Vijayalakshmi, N.; Maitra, U. *Macromolecules* **2006**, *39*, 7931.

3. Huang, C.; Zhen, C.-G.; Su, S. P.; Loh, K. P.; Chen, Z.-K. *Org. Lett.* **2005**, *7*, 391.

4. Ma, C. Q.; Mena-Osteritz, E.; Debaerdemaeker, T.; Wienk, M. M.; Janssen, R. A. J.; Bauerle, P. *Angew. Chem., Int. Ed.* **2007**, *46*, 1679.

5. Oosterom, G. E.; Reek, J. N. H.; Kamer, P. C. J.; van Leeuwen, P. *Angew. Chem., Int. Ed.* **2001**, *40*, 1828.

6. Helms, B.; Liang, C. O.; Hawker, C. J.; Fréchet, J. M. J. *Macromolecules* **2005**, *38*, 5411.

7. Wolinsky, J. B.; Grinstaff, M. W. *Adv. Drug Deliver. Rev.* **2008**, *60*, 1037.

8. Astruc, D.; Boisselier, E.; Ornelas, C. *Chem. Rev.* **2010**, *110*, 1857.

9. Mintzer, M. A.; Grinstaff, M. W. *Chem. Soc. Rev.* **2011**, *40*, 173.

10. Seebach, D.; Herrmann, G. F.; Lengweiler, U. D.; Bachmann, B. M.; Amrein, W. *Angew. Chem., Int. Ed.* **1996**, *35*, 2795.

11. Tang, M. X.; Redemann, C. T.; Szoka, F. C. *Bioconjugate Chem.* **1996**, *7*, 703.

12. Gillies, E. R.; Jonsson, T. B.; Fréchet, J. M. J. *J. Am. Chem. Soc.* **2004**, *126*, 11936.

13. Gillies, E. R.; Fréchet, J. M. J. *Bioconjugate Chem.* **2005**, *16*, 361.

14. Grayson, S. M.; Fréchet, J. M. J. *Org. Lett.* **2002**, *4*, 3171.

15. Smet, M.; Liao, L. X.; Dehaen, W.; McGrath, D. V. *Org. Lett.* **2000**, *2*, 511.

16. Yesilyurt, V.; Ramireddy, R.; Thayumanavan, S. *Angew. Chem., Int. Ed.* **2011**, *50*, 3038.

17. Amir, R. J.; Pessah, N.; Shamis, M.; Shabat, D. *Angew. Chem., Int. Ed.* **2003**, *42*, 4494.

18. Szalai, M. L.; McGrath, D. V. *Tetrahedron* **2004**, *60*, 7261.

19. Kevwitch, R. M.; McGrath, D. V. *New J. Chem.* **2007**, *31*, 1332.

20. Kostiainen, M. A.; Smith, D. K.; Ikkala, O. *Angew. Chem., Int. Ed.* **2007**, *46*, 7600.

21. Park, C.; Lim, J.; Yun, M.; Kim, C. *Angew. Chem., Int. Ed.* **2008**, *47*, 2959.

22. Kostiainen, M. A.; Kasyutich, O.; Cornelissen, J.; Nolte, R. J. M. *Nature Chem.* **2010**, *2*, 394.

23. Kostiainen, M. A.; Kotimaa, J.; Laukkanen, M. L.; Pavan, G. M. *Chem.-Eur. J.* **2010**, *16*, 6912.

24. Fomina, N.; McFearin, C. L.; Almutairi, A. *Chem. Commun.* **2012**, *48*, 9138.

25. Li, S.; Szalai, M. L.; Kevwitch, R. M.; McGrath, D. V. *J. Am. Chem. Soc.* **2003**, *125*, 10516.

26. Szalai, M. L.; Kevwitch, R. M.; McGrath, D. V. *J. Am. Chem. Soc.* **2003**, *125*, 15688.

27. Shamis, M.; Lode, H. N.; Shabat, D. *J. Am. Chem. Soc.* **2004**, *126*, 1726.

28. Haba, K.; Popkov, M.; Shamis, M.; Lerner, R. A.; Barbas, C. F.; Shabat, D. *Angew. Chem., Int. Ed.* **2005**, *44*, 716.

29. Ong, W.; McCarley, R. L. *Chem. Commun.* **2005**, 4699.

30. Ong, W.; McCarley, R. L. *Macromolecules* **2006**, *39*, 7295.

31. Reichmanis, E.; Smith, B. C.; Gooden, R. *J. Polym. Sci., Part A: Polym. Chem.* **1985**, *23*, 1.

32. Zhao, H.; Sterner, E. S.; Coughlin, E. B.; Theato, P. *Macromolecules* **2012**, *45*, 1723.

33. Ihre, H.; Hult, A.; Fréchet, J. M. J.; Gitsov, I. *Macromolecules* **1998**, *31*, 4061.

34. Garrett, T. M.; McMurry, T. J.; Hosseini, M. W.; Reyes, Z. E.; Hahn, F. E.; Raymond, K. N. *J. Am. Chem. Soc.* **1991**, *113*, 2965.

35. Song, Y.; Kohlmeir, E. K.; Meade, T. J. *J. Am. Chem. Soc.* **2008**, *130*, 6662.

36. Malkoch, M.; Malmstrom, E.; Hult, A. *Macromolecules* **2002**, *35*, 8307.

37. Van Wuytswinkel, G.; Verheyde, B.; Compernolle, F.; Toppet, S.; Dehaen, W. *J. Chem. Soc. Perk. T. 1* **2000**, 1337.

Chapter 6

6 Photodegradable Amphiphilic Janus Dendrimers and Dendrimersomes as Potential Smart Drug Delivery Vehicles

6.1 Introduction

As discussed in Chapters 2 and 5, dendrimers are a major class of macromolecules that are well-known for their three-dimensional globular architecture. Dendrimers are structurally perfect dendritic structures with a single or very narrow molar weight distribution. They comprise three structural regions: a core, layers of branching repeat units comprising the backbone, where each layer typically results from one stage of growth and is termed a "generation", and a peripheral layer. Based on their unique properties such as their very defined chemical structures, branched architectures, and existence of multiple peripheral groups for conjugation of functional moieties, dendrimers and dendrimer assemblies have received significant interest in the area of biomedical applications.[1-4]

In addition to conventional dendrimers, Janus dendrimers have also become the focus of intense research in the past two decades. These are dendrimers with well-defined but asymmetric architectures of two chemically distinct dendrons on opposite sides with different chemical compositions, peripheral groups, and/or polarities. They are also known as ''surface-block'' dendrimers, diblock dendrimers, codendrimers, diblock co-dendrimers, or bow-tie dendrimers.[5] In comparison with conventional dendrimers with uniform chemical structures, the presence of two or more chemically distinct regions in the backbone of Janus dendrimers can impart additional novel properties to these molecules.

To develop dendrimer-based vehicles capable of encapsulating drugs and delivering them to the organs of interest, amphiphilicity needs to be imparted to dendrimers. This can be achieved by having both hydrophobic and hydrophilic dendrons in their

backbones. Such dendrimers, commonly known as "Amphiphilic Janus dendrimers (AJD)", are capable of undergoing phase segregation to form well-defined morphologies owing to different phase behaviour of their dendritic blocks.[5,6] To date, AJDs with a variety of dendritic backbones have been synthesized. The first example of such AJD synthesis dates back only to twenty years ago where Fréchet and coworkers synthesized an asymmetric dendrimer based on 3,5-dihydroxybenzyl alcohol repeat unit, known as Fréchet-type dendrimers, with phenyl and carboxy peripheral groups.[7] Since then, many examples of AJDs and their potential as drug delivery vehicles have been reported in the literature. A few examples of these materials are discussed below.

As PAMAM dendrimers are leading dendrimer types in biomaterials, their incorporation into AJD architectures has also been frequently reported.[8] In an early work by Okada and coworkers,[9] PAMAM-based AJDs were prepared in which the periphery of one wedge of the dendrimer was decorated with the hydrophilic maltono lactone carbohydrate while the surface amine groups of the other wedge were reacted with phthalic anhydride in order to impart the required hydrophobic properties. Although the self-assembly behavior of this dendrimer was not investigated, its molecular recognition potential was evaluated using concanavalin A lectin. In another study by the same group, a library of third and fourth generation PAMAM-based AJDs with various surface functionalities were prepared. These include dendrimers with amino and *n*-hexyl (amino/hexyl) peripheral groups, hydroxyl and *n*-hexyl (hydroxyl/hexyl) peripheral groups, and *N*-acetyl-D-glucosamine and *n*-hexyl (glucosamine/hexyl) peripheries.[10] The authors then studied the adlayer (the layer formed by the adsorption of AJDs on the solid substrate) formation capabilities of these dendrimers on solid substrates. More recently, effective synthesis of AJDs based on PAMAM and Fréchet-type dendrons have also been reported.[11] To efficiently construct such dendrimers, PAMAM dendrons (G1-4) with alkyne functionalities at their focal point and Fréchet-type dendrons (G1-4) with azide focal groups were ligated together employing the high-yielding Cu(I)-catalyzed alkyne-azide click reaction to obtain various generations of such AJDs. In addition to PAMAM-based AJDs, amino acid-based AJDs,[12-15] ones incorporating aliphatic polyethers,[16-18] fullerene-containing AJDs,[19,20] polymerized AJDs,[21] and ones based on PEG have been reported.[22]

AJDs in which at least one dendritic block incorporates bis-MPA-based polyester dendrons in its backbone are among the most widely reported dendrimers of this type.[23-38] For instance, Fréchet and coworkers have developed "bow-tie" dendritic systems in which both dendritic blocks are bis-MPA-based polyester dendrons.[23,25,26] In these examples, the periphery of one dendritic block was used for the conjugation of PEG chains with varying MWs to enhance their water solubility and the other wedge of the dendrimer was used for the conjugation of therapeutics.[23,25,26] In another example, Wegner and coworkers have synthesized a third generation AJD consisting of Fréchet-type and polyester dendrons and studied its self-assembly behavior.[30] It was shown that in water-immiscible organic solvents containing water droplets this AJD undergoes a topological transformation from sphere to button structures.

More recently, Percec and coworkers have synthesized a total number of 107 amphiphilic Janus dendrimers, with different backbones and generation numbers, and screened their self-assembly behaviour in aqueous media.[37,38] The authors showed that when such materials are dispersed in water, they can undergo self-assembly to form a wide range of morphologies including vesicles (named as dendrimersomes), cubosomes, disks, tubular vesicles, and helical ribbons. Similar to polymersomes, dendrimersomes are of significant interest as they can potentially be multifunctional by encapsulating both hydrophilic and hydrophobic species. As a result, they were investigated in more depth in these reports. The authors concluded that dendrimersomes not only exhibit stability and mechanical strength of polymersomes, but also have the advantages of superior size uniformity, ease of formation, and chemical modification.

The development of drug delivery vehicles that are responsive to specific stimuli is also of significant interest as this can impart new properties and further expand their scope of applications. To date, several types of nanomaterials responsive to a wide variety of external stimuli have been developed.[39-43] Among various stimuli, light is of particular interest for the development of smart materials as it can be applied at a specific time and location with control over its intensity and wavelength. In the context of vesicular drug delivery systems that are capable of photolytic degradation, there are limited number of reported examples.[44-48] In these examples, which are mostly

polymersome-based systems, a photodegradable moiety, often an *o*-nitrobenzyl ester moiety, is placed at the junction between the hydrophilic and hydrophobic blocks of the BCPs. Upon irradiation with UV light, the BCPs undergo degradation resulting in disruption of the vesicular structure. However, as pointed out by other scientists, in these cases there is a high chance for the released hydrophobic chains to either aggregate to form macroscopic precipitates or undergo rearrangement to form other sorts of assemblies.[49] Both these events can potentially reduce their drug delivery efficiencies.

We have recently reported the synthesis and photodegradation behavior of dendrons and dendrimers (G1-3) with an entire photodegradable backbone.[50] We have shown that these dendrimers are capable of undergoing complete photolytic backbone cleavage without producing any macromolecular byproducts. In this chapter, the progress towards the incorporation of these photodegradable dendrons into AJD structures, their self-assembly to nanomaterials including photodegradable dendrimersomes, and their photolytic cargo release will be discussed. It is noteworthy that the photodegradable dendrimersomes described in this chapter are the first example of any vesicular architecture (including polymersomes, dendrimersomes, and small amphiphile-based vesicles) that are capable of complete photolytic membrane degradation to release their encapsulated model drugs.

6.2 Results and Discussion

6.2.1 Synthesis of Photodegradable Amphiphilic Janus Dendrimers

The synthetic strategy to incorporate our recently developed photodegradable dendrons[50] into AJD structure involves the divergent growth of the dendrimers from the focal point of the hydrophilic dendritic block (Scheme 6.1).
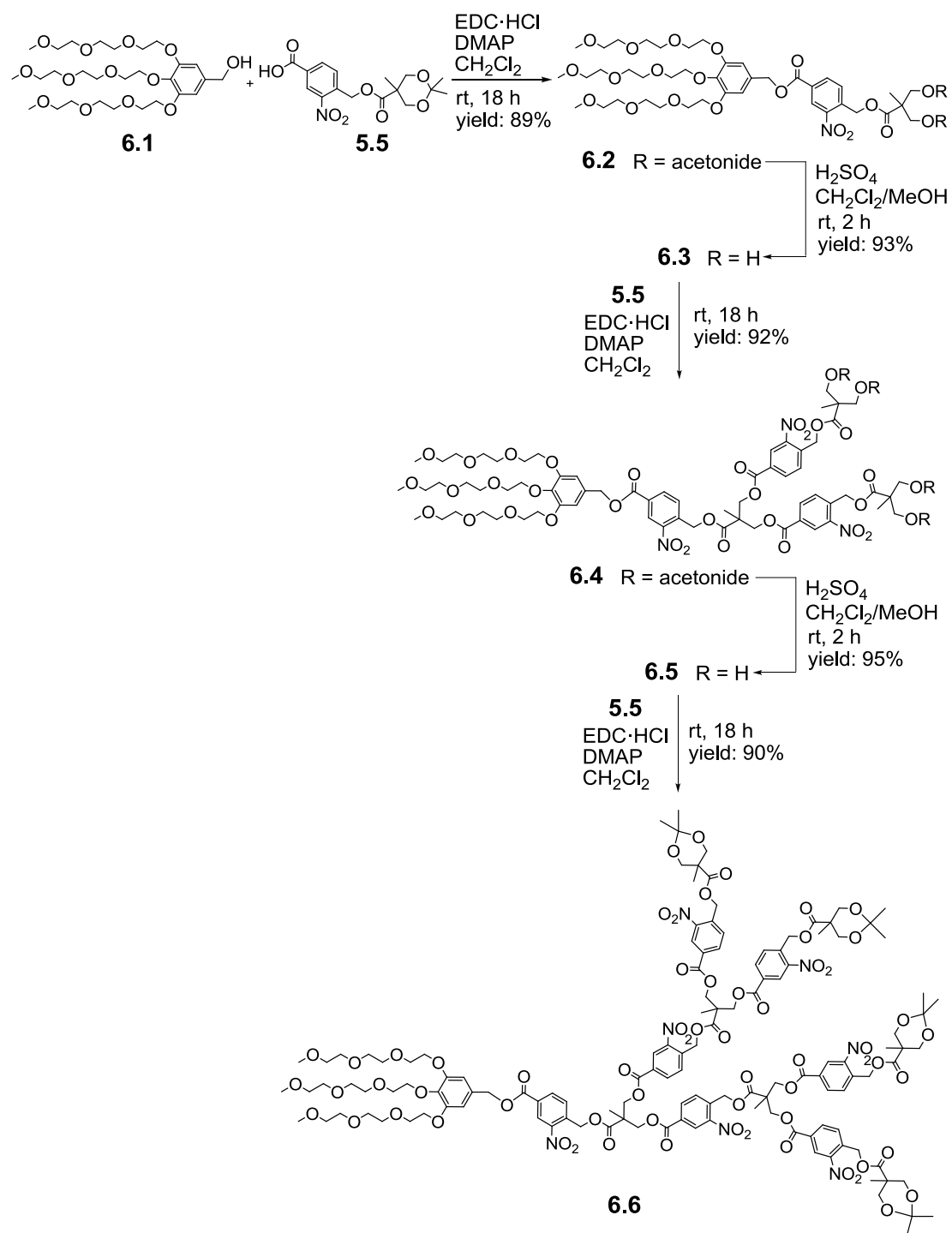
Scheme 6.1. Synthesis of G1-3 AJDs.

For the hydrophilic block, a dendritic backbone based on triethylene glycol (TEG) and gallic acid, **6.1**, was synthesized with a benzyl alcohol focal point.[51,52] As shown in Scheme 6.1, the hydroxyl focal point was then reacted with our previously reported

photodegradable monomer **5.5** under EDC-coupling conditions to provide protected G1 dendrimer **6.2** in high yield. The acetonide protecting group was then removed under acidic condition to obtain unprotected G1 AJD **6.3**. Repetition of this coupling and deprotection sequence provided protected G2, **6.4,** and G3, **6.6**, dendrimers in high yields.

The resulting dendrimers were characterized by ^{1}H and ^{13}C NMR spectroscopy, HRMS, IR spectroscopy, and SEC. SEC traces of the protected AJDs are depicted in Figure 6.1a with their corresponding SEC data shown in Figure 6.1b.

a)

b)

AJD	MW (g/mol)[a]	M_n (g/mol)[b]	PDI[c]
G1 (**6.2**)	930.0	1200	1.01
G2 (**6.4**)	1560.6	1900	1.01
G3 (**6.6**)	2821.7	3200	1.01
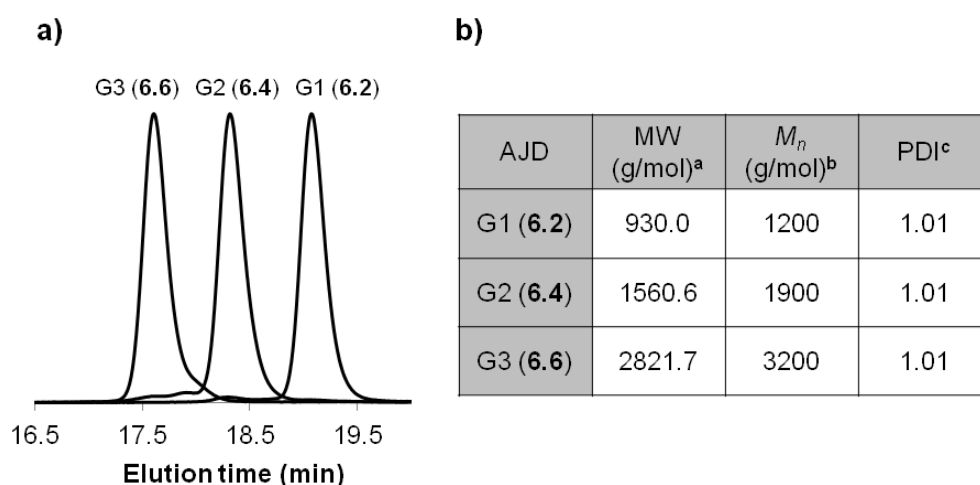
Figure 6.1. a) SEC traces and b) MW and PDI characteristics of AJDs **6.2**, **6.4**, and **6.6**. [a] Molecular weight calculated based on chemical structures of the dendrimers, [b] M_n obtained from SEC, and [c] PDI was determined from SEC.

As shown in the SEC traces (Figure 6.1a), the resulting dendrimers exhibit monomodal MW distribution profiles with the expected increases in hydrodynamic volume with each generation, as well as very narrow PDIs (Figure 6.1b).

6.2.2 Self-Assembly of Amphiphilic Janus Dendrimers in Aqueous Media

Having the protected AJDs **6.2**, **6.4**, and **6.6** in hand, their self-assembly behaviors in mixed organic-aqueous system were then investigated. For this purpose, an 8 mg/mL solution of each dendrimer in THF (0.25 mL) was first prepared in a vial and distilled water (1.25 mL) was then added dropwise with vigorous stirring. The samples were then

stirred overnight with their caps left open to remove most of the THF. The samples were dialyzed against distilled water to further remove the residual THF.

The samples were first analyzed by DLS measurements to gain insight into the sizes of the materials obtained. In the case of the 1st generation dendrimer **6.2**, no meaningful DLS data was obtained. As a result, it was speculated that the hydrophobic block of this AJD was too small compared to the hydrophilic block to induce any self-assembly events and the molecule was essentially water-soluble. On the other hand, it was found that 2nd and 3rd generation AJDs **6.4** and **6.6** were able to form assemblies with average sizes (z-average) of about 270 nm and 450 nm, respectively (Figure 6.2).
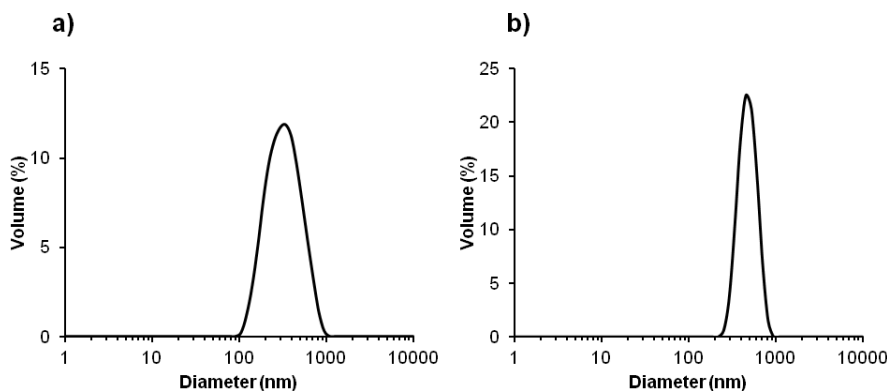
Figure 6.2. Size distribution profiles measured by DLS for assemblies formed by a) 2nd generation AJD **6.4** and b) 3rd generation AJD **6.6**.

In addition to DLS, TEM imaging revealed additional information regarding the morphologies of the resulting assemblies. As shown in Figure 6.3a, it was found that particles formed by dendrimer **6.4** had a core-shell structure with a photodegradable hydrophobic core and a shell of TEG chains. On the other hand, 3rd generation dendrimer **6.6** underwent self-assembly to form well-defined dendrimersomes in which the photodegradable hydrophobic dendritic block constituted their membranes and the TEG chains pointing towards the interior and exterior aqueous media (Figure 6.3b). Further TEM analysis revealed that dendrimersomes have a membrane thickness of roughly 10 nm which is within the range of values obtained for other dendrimersomes formed by a variety of other AJDs in the literature.[37]
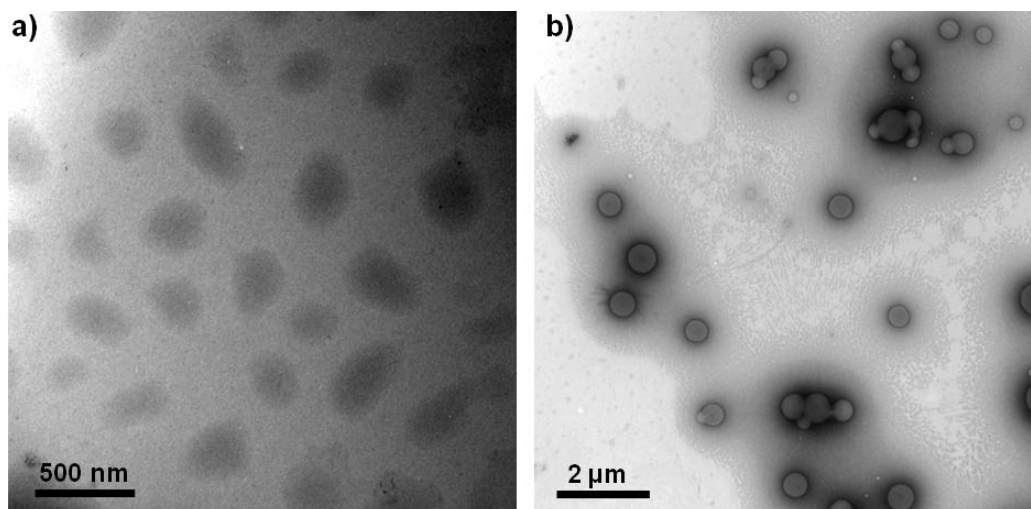
Figure 6.3. TEM images of a) particles prepared from AJD **6.4** and b) dendrimersomes formed by AJD **6.6**.

6.2.3 Photodegradation Study of the Dendrimersomes

As the main focus of this project was to develop dendrimersomes with photodegradable membranes, photodegradation studies of the above-mentioned assemblies did not involve the particles obtained from dendrimer **6.4**.

Prior to the photolysis of the dendrimersomes, it was essential to study the photodegradation behavior of AJD **6.6** in the solution state and compare the results to those previously obtained for our photodegradable dendrimers.[50] For this purpose, a ~30 µg/mL solution of G3 dendrimer **6.6** in THF was irradiated with 300 - 400 nm UV light at with a receiving power of about 25 mW·cm^{-2} over a period of 30 min and the UV-visible absorption spectra of the solution were recorded in 2 min intervals. As shown in Figure 6.4a, the result obtained is in accordance with our previously obtained data for photodegradable hydrophobic dendrimers.[50] A decrease in absorbance was observed for the peaks at 225 and 265 nm while increases in absorbance were observed at 300 and 340 nm, along with corresponding red shifts in their absorption maxima. As mentioned earlier, these observations are in accordance with the results obtained by other groups for this photolabile group. The absorption band at 350 nm is attributed to *o*-nitrosobenzaldehyde, which is a product of *o*-nitrobenzyl ester photolysis, and exhibits a weak absorption band at 350-360 nm that is solvent dependent. In addition, spectral

change behavior of this dendrimer was also investigated when it was self-assembled into vesicular structure in aqueous media. For the data to be consistent with the solution state, the dendrimersome sample was prepared at the concentration of ~30 µg/mL and was irradiated with the same lamp settings and time intervals described above. As shown in Figure 6.4b, a general trend of decrease in the peak intensities was observed for the dendrimersomes. It should be noted that as the chemical environments of dendrimer **6.6** in THF versus in self-assembled state in water are quite different and the suspension of the dendrimersomes scatters light significantly, differences in their spectral profiles were expected. Nevertheless, the change in the UV-visible spectra of the dendrimersomes upon UV irradiation does suggest a change in the spectroscopic state of their photodegradable hydrophobic membrane.
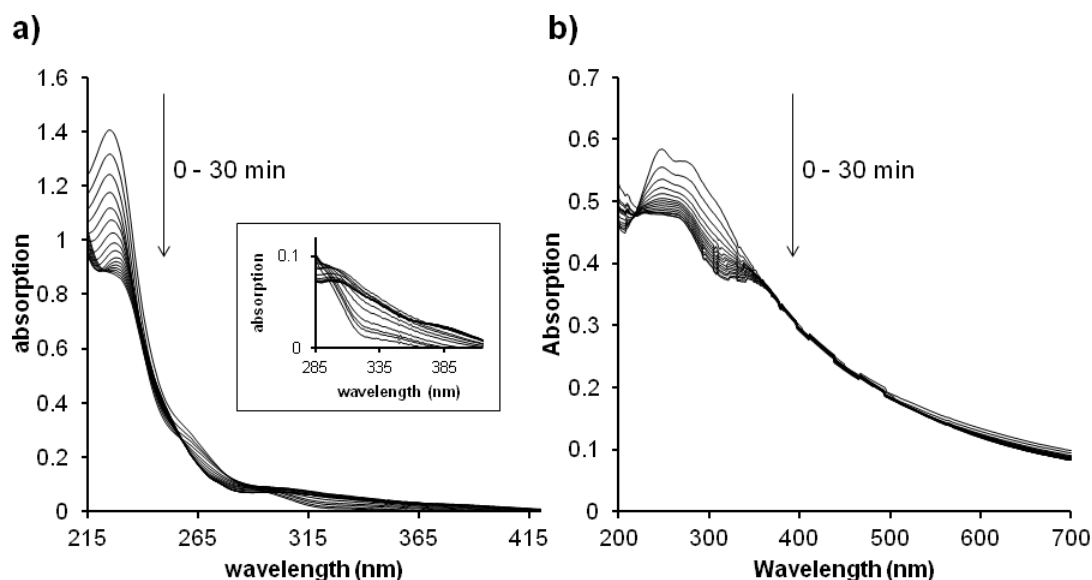
Figure 6.4. UV-visible spectra for G3 AJD **6.6** a) as THF solution and b) as self-assembled dendrimersomes in water upon irradiation with UV light for 30 min. Inset shows the expanded region between 285-415 nm.

DLS analysis was also employed to study the photolysis of the dendrimersomes. For this purpose, suspension of dendrimersomes with the concentration of 0.1 mg/mL were placed in a quartz cuvette, irradiated with UV light, and DLS measurements were performed at the given time points. As a result, there was no change in the overall concentration of the dendrimer **6.6** throughout the experiment in the system. At each time

point, three measurements of 150 s each were performed. As shown in Figure 6.5a, upon irradiating dendrimersome for a course of 210 min, a dramatic decrease in the mean count rate from about 240 to 9 kcps was observed. It has been demonstrated that a decrease in the count rate (intensity of the scattered light) can stem from three factors: 1) a decrease in the total concentration of particles in the system, 2) a decrease in the size of the particles in the system, and 3) a combination of the former two factors.[45] Taking into account that no precipitation was observed during the photolysis of the dendrimersomes, we conclude that the total concentration of particles did not change. As a result, the observed decrease in the mean count rate can be explained by the decrease in the size of the particles in the system. In fact, as shown in Figure 6.5b, it was demonstrated that after irradiating the sample for 210 min, dendrimersomes were completely disrupted and new objects with diameters of 2 nm were formed, likely small molecule degradation products. However, due to the very low degree of light scattering, it should be noted that the quality of DLS data obtained at this point was marginal.
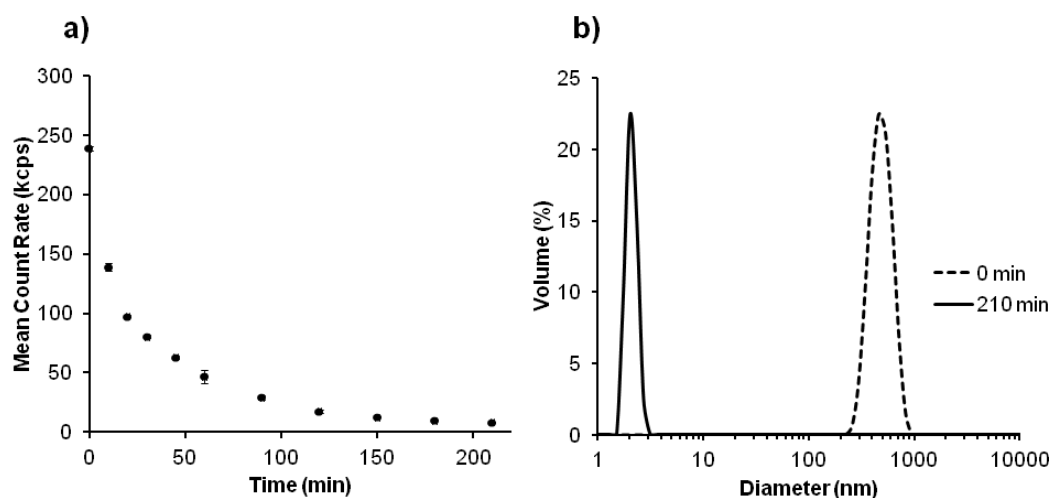
Figure 6.5. DLS measurements for the photolysis of dendrimersomes: a) plot of mean count rate versus irradiation time and b) size distribution profile of the dendrimersome sample before and after UV irradiation.

As described above, while there was no precipitate formation during the experiment, this decrease in the mean count rate can be attributed to very small size of the photolysis byproducts which were out of the detection limit of the instrument. As a result, it was concluded that, upon photolysis, the membranes of the dendrimersomes were completely

fragmented to small molecules and the remaining hydrophilic dendritic blocks were unable to undergo self-assembly to form any further meaningful morphologies. In fact, this hypothesis was further supported by TEM imaging of the photodegraded sample. As shown in Figure 6.6, no distinct self-assembled material was observed in these images. In a similar observation by Zhao and coworkers, 60 nm polymeric micelles with a backbone photodegradable hydrophobic core were shown to undergo photodegradation to a point where no clear morphology was observable.[53]
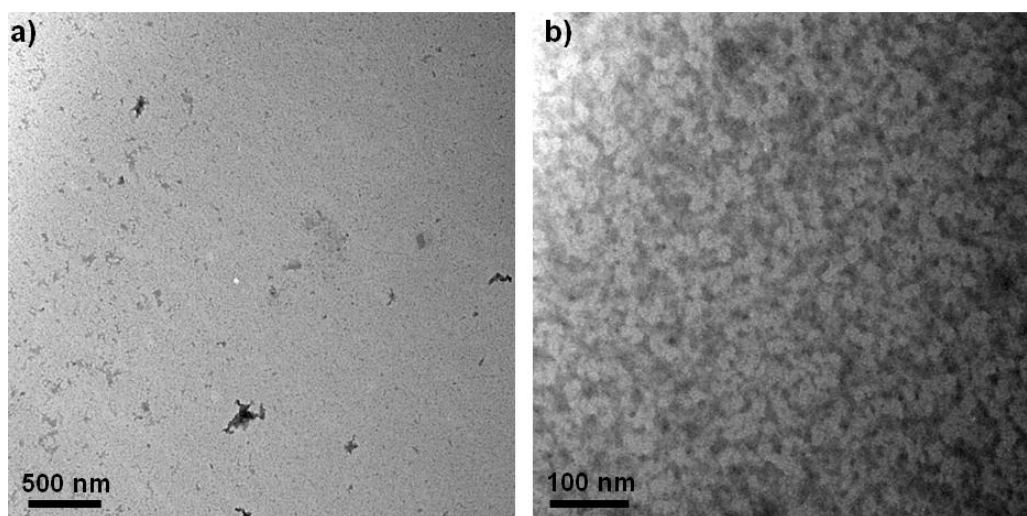
Figure 6.6. TEM images of the UV-irradiated dendrimersome sample after 210 min.

As a result of this complete photolytic membrane degradation, this system offers significant advantage over the currently reported photodegradable vesicular drug delivery systems. As previously discussed, while it has been shown that photolysis of polymersomes, comprised of BCPs with a single photodegradable group at the junction between the hydrophilic and hydrophobic blocks, results either in the precipitation of the detached hydrophobic block or morphological transformation to smaller size particles as micelles, our photodegradable dendrimersome system represents the first example of this class of drug delivery vehicles in which complete degradation of the hydrophobic block is achieved. This is expected to result in significant enhancement in release efficiency of vesicular drug delivery systems.

6.3 Conclusion

In summary, a small library of AJDs (G1-3) with backbone photodegradable hydrophobic dendritic blocks were successfully synthesized and fully characterized. 3rd generation AJD **6.6** was shown to undergo self-assembly to form well-defined dendrimersomes with an average size of about 450 nm. Upon irradiation with UV light (300-400 nm, 25 mW·cm^{-2}), the dendrimersomes' membranes were effectively disrupted to disintegrate these assemblies with no sign of precipitation or morphological change to smaller assemblies. Studies are currently underway to evaluate the photolytic release behavior of these smart dendrimersomes with regards to both hydrophilic and hydrophobic model drug molecules.

6.4 Experimental

General Procedures and Materials

Compounds **6.1**[51,52] and **5.5**[50] were synthesized according to the previously published procedures. All the other chemicals were purchased from Sigma-Aldrich or Alfa Aesar and were used without further purification unless otherwise noted. Anhydrous DMF was obtained from a solvent purification system using aluminum oxide columns. Dichloromethane was distilled from calcium hydride. Unless otherwise stated, all reactions were performed under a nitrogen atmosphere using flame or oven dried glassware. For the reactions that were stirred in dark, aluminum foil was used to isolate the reaction flasks from light. No special precautions regarding light, were taken during purification or isolation of these compounds. For long term storage, the isolated materials were stored in freezer. However no degradation issues were encountered when materials were stored in the dark at ambient temperature. ^{1}H NMR spectra were obtained at 400 MHz, and ^{13}C NMR spectra were obtained at 100 MHz. NMR chemical shifts are reported in ppm and are calibrated against the residual solvent signal of CDCl$_3$ (δ 7.26 and 77.16 ppm). *J* values are expressed in Hz. IR spectra were obtained as films from CH$_2$Cl$_2$ on NaCl plates using a Bruker Tensor 27 instrument. HRMS was performed using a Finnigan MAT 8400 electron impact mass spectrometer. ESI was performed using a PE-Sciex API 365 mass spectrometer. UV−visible absorption spectroscopy was

performed on a Varian Cary 300 Bio UV–visible spectrophotometer. Dialyses were performed using Spectra/Por regenerated cellulose membranes with either a 2,000 g/mol or 3500 g/mol MWCO. SEC instrument was equipped with a Viscotek GPC Max VE2001 solvent module. Samples were analyzed using the Viscotek VE3580 RI detector operating at 30 °C. The separation technique employed a Polypore guard column (50 x 7.5mm) and two Agilent Polypore (300 x 7.5 mm) columns connected in series. Samples were dissolved in THF (glass distilled grade) at approximately 5 mg/mL concentrations and filtered through 0.22 µm syringe filters. Samples were injected using a 100 µL loop. The THF eluent was filtered and eluted at 1 ml/min for a total of 30 minutes. A calibration curve was obtained from polystyrene standards with molecular weights ranging from 1,540-1,126,000 g/mol. The light source used for the photochemical reactions was a Hanovia medium pressure mercury lamp (PC 451050/616750, 450 Wage) with an emitting wavelength of 300-400 nm and a power of 25 mW·cm^{-2} at 10 cm from the lamp where the samples were irradiate. DLS data were obtained using a Zetasizer NanoZS instrument from Malvern Instruments.

Synthesis of Protected G1 AJD 6.2: Hydrophilic dendritic block **6.1** (0.55 g, 0.92 mmol, 1.0 equiv.) and monomer **5.5** (0.49 g, 1.4 mmol, 1.5 equiv.) were dissolved in CH_2Cl_2 (30 mL). EDC·HCl (0.40 g, 2.1 mmol, 2.2 equiv.) and DMAP (0.11 g, 0.92 mmol, 1.0 equiv.) were added in one portion and the resulting solution was stirred at room temperature in dark for 18 h. At this point, CH_2Cl_2 was removed under reduced pressure. The residue was dissolved in DMF and the product was purified by dialysis against DMF using 2000 MWCO membrane for 24 h. The solvent was then removed under reduced pressure to give dendrimer **6.2** (0.76 g, 0.82 mmol) in 89% yield. ^{1}H NMR (CDCl$_3$) δ: 8.76 (d, J = 4.0, 1H), 8.30 (dd, J_1 = 8.0, J_2 = 4.0, 1H), 7.85 (d, J = 8.0, 1H), 6.67 (s, 2H), 5.66 (s, 2H), 5.27 (s, 2H), 4.28 (d, J = 12.0, 2H), 4.19-4.13 (m, 6H), 3.85 (t, J = 4.0, 4H), 3.73 (t, J = 4.0, 2H), 3.75-3.69 (m, 8H), 3.68-3.62 (m, 12H), 3.56-3.52 (m, 6H), 3.37 (s, 9H), 1.47 (s, 3H), 1.40 (s, 3H), 1.17 (s, 3H). ^{13}C NMR (CDCl$_3$) δ: 173.6, 163.9, 152.7, 147.1, 138.7, 137.1, 134.3, 130.8, 130.4, 128.9, 126.1, 108.3, 98.1, 72.2, 71.8, 71.8, 70.7, 70.6, 70.4, 70.4, 69.6, 68.9, 67.6, 66.1, 63.0, 58.9, 42.3, 26.5, 20.7, 18.2. IR (cm^{-1}, film from CH_2Cl_2): 3097, 2939, 2881, 1731, 1623, 1539, 1351, 1249, 1122.

HRMS: calcd [M+Na]$^+$ (C$_{44}$H$_{67}$NO$_{20}$Na): 952.4154. Found: (ESI) 952.4114. SEC data: M_n = 1200 gmol^{-1}, PDI: 1.01.

Synthesis of Deprotected G1 AJD 6.3: Dendrimer **6.2** (0.26 g, 0.28 mmol) was dissolved in methanol (25 mL) and CH$_2$Cl$_2$ (5 mL). Concentrated sulfuric acid (0.30 mL) was added and the resulting solution was stirred at room temperature in dark for 2 h. At this point, ^{1}H NMR showed the completion of the reaction. The solution was diluted by the addition of CH$_2$Cl$_2$ (50 mL). Organic solution was then washed with 1M Na$_2$CO$_3$ (2×100 mL) and brine (1×100 mL). The organic layer was dried over MgSO$_4$, filtered, and concentrated under reduced pressure to give dendrimer **6.3** (0.23 g, 0.26 mmol) in 93% yield. ^{1}H NMR (CDCl$_3$) δ: 8.75 (d, J = 4.0, 1H), 8.31 (dd, J_1 = 8.0, J_2 = 4.0, 1H), 7.83 (d, J = 8.0, 1H), 6.68 (s, 2H), 5.65 (s, 2H), 5.27 (s, 2H), 4.18-4.14 (m, 6H), 3.98 (d, J = 8.0, 2H), 3.85 (t, J = 4.0, 4H), 3.80-3.77 (m, 4H), 3.73-3.70 (m, 6H), 3.66-3.62 (m, 12H), 3.55-3.52 (m, 6H), 3.36 (s, 9H), 2.81 (br s, 2H), 1.12 (s, 3H). ^{13}C NMR (CDCl$_3$) δ: 174.8, 163.8, 152.6, 147.1, 138.5, 136.8, 134.3, 130.8, 130.4, 129.0, 125.9, 108.2, 72.2, 71.7, 70.6, 70.5, 70.4, 70.3, 69.6, 68.8, 67.6, 66.9, 62.8, 58.8, 49.6, 17.1. IR (cm^{-1}, film from CH$_2$Cl$_2$): 3415, 3089, 2906, 2879, 1730, 1623, 1535, 1350, 1253, 1112. HRMS: calcd [M+Na]$^+$ (C$_{41}$H$_{63}$NO$_{20}$Na): 912.3841. Found: (ESI) 912.3821. SEC data: M_n = 1200 gmol^{-1}, PDI: 1.01.

Synthesis of Protected G2 AJD 6.4: Dendrimer **6.3** (0.21 g, 0.24 mmol, 1.0 equiv.) and monomer **5.5** (0.26 g, 0.72 mmol, 3.0 equiv.) were dissolved in CH$_2$Cl$_2$ (45 mL). EDC·HCl (0.21 g, 1.1 mmol, 4.5 equiv.) and DMAP (59 mg, 0.48 mmol, 2.0 equiv.) were added in one portion and the resulting solution was stirred at room temperature in dark for 18 h. At this point, CH$_2$Cl$_2$ was removed under reduced pressure. The residue was dissolved in DMF and product was purified by dialysis against DMF using 3500 MWCO membrane for 24 h. The solvent was then removed under reduced pressure to give dendrimer **6.4** (0.31 g, 0.20 mmol) in 83% yield. ^{1}H NMR (CDCl$_3$) δ: 8.64-8.58 (m, 3H), 8.23-8.16 (m, 3H), 7.85 (d, J = 8.0, 2H), 7.63 (d, J = 8.0, 1H), 6.68 (s, 2H), 5.65 (s, 4H), 5.60 (s, 2H), 5.26 (s, 2H), 4.67-4.59 (m, 4H), 4.28 (d, J = 12.0, 4H), 4.19-4.13 (m, 6H), 3.85 (t, J = 4.0, 4H), 3.73 (t, J = 4.0, 2H), 3.75-3.69 (m, 10H), 3.67-3.61 (m, 12H), 3.56-3.51 (m, 6H), 3.36 (s, 9H), 1.49 (s, 3H), 1.47 (s, 6H), 1.39 (s, 6H), 1.18 (s, 6H). ^{13}C NMR

(CDCl$_3$) δ: 173.6, 171.5, 163.6, 163.4, 152.7, 147.8, 147.1, 138.7, 137.6, 135.0, 134.2, 131.6, 130.4, 130.0, 129.0, 129.0, 126.1, 126.0, 126.0, 108.4, 98.2, 72.3, 71.9, 71.8, 70.7, 70.6, 70.4, 69.6, 68.9, 67.8, 66.4, 66.1, 63.8, 63.0, 58.9, 47.0, 42.4, 26.6, 20.6, 18.2, 17.9. IR (cm^{-1}, film from CH$_2$Cl$_2$): 3091, 2918, 2875, 1733, 1623, 1535, 1348, 1249, 1116. HRMS: calcd [M+Na]$^+$ (C$_{73}$H$_{97}$N$_3$O$_{34}$Na): 1582.5851. Found: (ESI) 1582.5857. SEC data: M_n = 1900 gmol^{-1}, PDI: 1.01.

Synthesis of Deprotected G2 AJD 6.5: Dendrimer **6.4** (0.20 g, 0.13 mmol) was dissolved in methanol (50 mL) and CH$_2$Cl$_2$ (10 mL). Concentrated sulfuric acid (0.60 mL) was added and the resulting solution was stirred at room temperature in dark for 2 h. At this point, ^{1}H NMR showed the completion of the reaction. The solution was diluted by the addition of CH$_2$Cl$_2$ (50 mL). Organic solution was then washed with 1M Na$_2$CO$_3$ (2×100 mL) and brine (1×100 mL). The organic layer was dried over MgSO$_4$, filtered, and concentrated under reduced pressure to give dendrimer **6.5** (0.18 g, 0.12 mmol) in 95% yield. ^{1}H NMR (CDCl$_3$) δ: 8.60-8.51 (m, 3H), 8.20- 8.09 (m ,3H), 7.79 (d, J = 8.0, 2H), 7.62 (d, J = 8.0, 1H), 6.68 (s, 2H), 5.61 (s, 6H), 5.25 (s, 2H), 4.63 (s, 4H), 4.21-4.12 (m, 6H), 4.02-3.94 (m, 4H), 3.85 (t, J = 4.0, 4H), 3.83-3.76 (m, 6H), 3.75-3.69 (m, 6H), 3.68-3.61 (m, 12H), 3.56-3.51 (m, 6H), 3.36 (s, 9H), 2.98 (t, J = 8.0, 4H), 1.49 (s, 3H), 1.13 (s, 6H). ^{13}C NMR (CDCl$_3$) δ: 175.0, 171.7, 163.8, 163.5, 152.7, 147.8, 147.1, 138.6, 137.4, 135.2, 134.2, 134.2, 131.5, 130.4, 130.2, 130.0, 129.2, 126.1, 125.9, 108.4, 72.3, 71.9 (2), 70.7, 70.6, 70.4, 69.7, 68.9, 67.9, 67.3, 67.3, 66.8, 63.8, 62.9, 59.0, 49.7, 47.0, 18.1, 17.2. IR (cm^{-1}, film from CH$_2$Cl$_2$): 3394, 3082, 2927, 2883, 1726, 1625, 1537, 1350, 1255, 1114. HRMS: calcd [M+Na]$^+$ (C$_{67}$H$_{89}$N$_3$O$_{34}$Na): 1502.5225. Found: (ESI) 1502.5205. SEC data: M_n = 1900 gmol^{-1}, PDI: 1.02.

Synthesis of Protected G3 AJD 6.6: Dendrimer **6.5** (0.14 g, 0.10 mmol, 1.0 equiv.) and monomer **5.5** (0.21 g, 0.60 mmol, 6.0 equiv.) were dissolved in CH$_2$Cl$_2$ (35 mL). EDC·HCl (0.17 g, 0.90 mmol, 9.0 equiv.) and DMAP (49 mg, 0.40 mmol, 4.0 equiv.) were added in one portion and the resulting solution was stirred at room temperature in dark for 18 h. At this point, CH$_2$Cl$_2$ was removed under reduced pressure. The residue was dissolved in DMF and product was purified by dialysis against DMF using 3500 MWCO membrane for 24 hrs. The solvent was then removed under reduced pressure to

give dendrimer **6.6** (0.25 g, 90 μmol) in 90% yield. ^{1}H NMR (CDCl$_3$) δ: 8.61-8.57 (m, 5H), 8.51-8.48 (m ,2H), 8.22-8.16 (m, 5H), 8.12-8.08 (m, 2H), 7.85 (d, J = 8.0, 4H), 7.65 (d, J = 8.0, 3H), 6.67 (s, 2H), 5.64 (s, 8H), 5.61 (s, 4H), 5.59 (s, 2H), 5.25 (s, 2H), 4.67-4.58 (m, 12H), 4.27 (d, J = 12.0, 8H), 4.20-4.12 (m, 6H), 3.85 (t, J = 4.0, 4H), 3.73 (t, J = 4.0, 2H), 3.75-3.68 (m, 14H), 3.67-3.61 (m, 12H), 3.56-3.51 (m, 6H), 3.36 (s, 9H), 1.50 (s, 6H), 1.48 (s, 3H), 1.46 (s, 12H), 1.38 (s, 12H), 1.17 (s, 12H). ^{13}C NMR (CDCl$_3$) δ: 173.7, 171.6, 171.6, 163.8, 163.6, 163.3, 152.8, 147.9, 147.8, 147.2, 138.9, 137.7, 135.7, 135.2, 134.3, 134.1, 131.7, 130.9, 130.4, 130.3, 130.1, 129.1, 126.2, 126.1, 126.0, 114.8, 108.5, 98.3, 72.4, 72.0 (2), 70.8, 70.7, 70.6, 70.5, 69.8, 69.0, 67.9, 66.6, 66.5, 66.2, 64.0, 63.9, 63.9, 63.1, 59.0, 47.1, 47.0, 42.5, 26.7, 20.7, 18.3, 18.1, 18.0. IR (cm^{-1}, film from CH$_2$Cl$_2$): 3084, 2927, 2879, 1731, 1623, 1539, 1346, 1255, 1118. HRMS: calcd [M+Na]$^+$ (C$_{131}$H$_{157}$N$_7$O$_{62}$Na): 2842.9251. Found: (ESI) 2842.9245. SEC data: M_n = 3200 gmol^{-1}, PDI: 1.01.

General Procedure for the Preparation of Dendrimer Assemblies: Dendrimer assemblies were prepared by first dissolving each AJD dendrimer (2 mg) in spectroscopic grade THF (0.25 mL) in a vial followed by dropwise addition of distilled water (1.25 mL) with vigorous stirring. The resulting assembly samples were stirred overnight with their vial caps left open to remove most of the THF. The residual THF was removed by dialyzing the samples against distilled water using 3500 MWCO membrane for 24 h.

General Procedure for Monitoring Dendrimer Degradation by UV-visible Spectroscopy: Dendrimer sample was prepared at the concentration of 30 μg/mL in either spectroscopic grade THF or as dendrimersomes in distilled water. 3 mL of solution was transferred to a quartz cuvette and irradiated with UV light for 30 min. UV-visible absorption spectra were collected every 2 min.

General Procedure for Monitoring Dendrimersome Degradation by DLS analysis: Dendrimesome sample was prepared at the concentration of 0.1 mg/mL of dendrimer **6.6** in distilled water. 2 mL of this sample was transfered to a quartz cuvette and irradiated with UV light for 210 min. DLS measurements were performed at the given time points on the same sample. For each time point three measurements each for 150 s were

performed. Mean count rates reported in Figure 6.5a are the average values obtained for each time point with their relevant error bars.

Transmission Electron Microscopy: The suspension of the dendrimer assemblies (5 μL, 0.05 mg/mL) was placed on a carbon formvar grid and was left to dry in air in dark for 6 h. Imaging was performed using a Phillips CM10 microscope operating at 80 kV with a 40 μm aperture.

6.5 References

1. Boas, U.; Heegaard, P. M. H. *Chem. Soc. Rev.* **2004**, *33*, 43.

2. Cheng, Y. Y.; Xu, Z. H.; Ma, M. L.; Xu, T. W. *J. Pharm. Sci.* **2008**, *97*, 123.

3. El Kazzouli, S.; Mignani, S.; Bousmina, M.; Majoral, J. P. *New J. Chem.* **2012**, *36*, 227.

4. Svenson, S.; Tomalia, D. A. *Adv. Drug Deliver. Rev.* **2005**, *57*, 2106.

5. Caminade, A. M.; Laurent, R.; Delavaux-Nicot, B.; Majoral, J. P. *New J. Chem.* **2012**, *36*, 217.

6. Park, C.; Lee, J.; Kim, C. *Chem. Commun.* **2011**, *47*, 12042.

7. Hawker, C. J.; Wooley, K. L.; Fréchet, J. M. J. *J. Chem. Soc. Perk. T. 1* **1993**, 1287.

8. Ornelas, C.; Pennell, R.; Liebes, L. F.; Weck, M. *Org. Lett.* **2011**, *13*, 976.

9. Aoi, K.; Itoh, K.; Okada, M. *Macromolecules* **1997**, *30*, 8072.

10. Ito, M.; Imae, T.; Aoi, K.; Tsutsumiuchi, K.; Noda, H.; Okada, M. *Langmuir* **2002**, *18*, 9757.

11. Lee, J. W.; Kim, B. K.; Kim, J. H.; Shin, W. S.; Jin, S. H. *J. Org. Chem.* **2006**, *71*, 4988.

12. Harrington, D. A.; Behanna, H. A.; Tew, G. N.; Claussen, R. C.; Stupp, S. I. *Chem. Biol.* **2005**, *12*, 1085.

13. Bayele, H. K.; Sakthivel, T.; O'Donell, M.; Pasi, K. J.; Wilderspin, A. F.; Lee, C. A.; Toth, I.; Florence, A. T. *J. Pharm. Sci.* **2005**, *94*, 446.

14. Pan, J. Z.; Guo, L.; Ouyang, L.; Yin, D. Q.; Zhao, Y. *Synlett* **2012**, 1937.

15. Pan, J. Z.; Wen, M.; Yin, D. Q.; Jiang, B.; He, D. S.; Guo, L. *Tetrahedron* **2012**, *68*, 2943.

16. Grayson, S. M.; Fréchet, J. M. J. *J. Am. Chem. Soc.* **2000**, *122*, 10335.

17. Yang, M.; Zhang, Z.; Yuan, F.; Wang, W.; Hess, S.; Lienkamp, K.; Lieberwirth, I.; Wegner, G. *Chem.-Eur. J.* **2008**, *14*, 3330.

18. Yang, M.; Wang, W.; Lieberwirth, I.; Wegner, G. *J. Am. Chem. Soc.* **2009**, *131*, 6283.

19. Nierengarten, J. F.; Eckert, J. F.; Rio, Y.; Carreon, M. D.; Gallani, J. L.; Guillon, D. *J. Am. Chem. Soc.* **2001**, *123*, 9743.

20. Zhang, S.; Rio, Y.; Cardinali, F.; Bourgogne, C.; Gallani, J. L.; Nierengarten, J. F. *J. Org. Chem.* **2003**, *68*, 9787.

21. Bo, Z. S.; Rabe, J. P.; Schluter, A. D. *Angew. Chem., Int. Ed.* **1999**, *38*, 2370.

22. Acton, A. L.; Fante, C.; Flatley, B.; Burattini, S.; Hamley, I. W.; Wang, Z. W.; Greco, F.; Hayes, W. *Biomacromolecules* **2013**, *14*, 564.

23. Gillies, E. R.; Fréchet, J. M. J. *J. Am. Chem. Soc.* **2002**, *124*, 14137.

24. Gillies, E. R.; Fréchet, J. M. J. *J. Org. Chem.* **2004**, *69*, 46.

25. Gillies, E. R.; Dy, E.; Fréchet, J. M. J.; Szoka, F. C. *Mol. Pharm.* **2005**, *2*, 129.

26. Lee, C. C.; Gillies, E. R.; Fox, M. E.; Guillaudeu, S. J.; Fréchet, J. M. J.; Dy, E. E.; Szoka, F. C. *P. Natl. Acad. Sci. USA.* **2006**, *103*, 16649.

27. Ropponen, J.; Nummelin, S.; Rissanen, K. *Org. Lett.* **2004**, *6*, 2495.

28. Wu, P.; Malkoch, M.; Hunt, J. N.; Vestberg, R.; Kaltgrad, E.; Finn, M. G.; Fokin, V. V.; Sharpless, K. B.; Hawker, C. J. *Chem. Commun.* **2005**, 5775.

29. Yuan, F.; Wang, W.; Yang, M.; Zhang, X. J.; Li, J. Y.; Li, H.; He, B. L. *Macromolecules* **2006**, *39*, 3982.

30. Yuan, F.; Zhang, X. J.; Yang, M.; Wang, W.; Minch, B.; Lieser, G.; Wegner, G. *Soft Matter* **2007**, *3*, 1372.

31. Tuuttila, T.; Lipsonen, J.; Lahtinen, M.; Huuskonen, J.; Rissanen, K. *Tetrahedron* **2008**, *64*, 10590.

32. Tuuttila, T.; Lahtinen, M.; Kuuloja, N.; Huuskonen, J.; Rissanen, K. *Thermochim. Acta* **2010**, *497*, 101.

33. Tuuttila, T.; Lahtinen, M.; Huuskonen, J.; Rissanen, K. *Thermochim. Acta* **2010**, *497*, 109.

34. Ledin, P. A.; Friscourt, F.; Guo, J.; Boons, G. J. *Chem.-Eur. J.* **2011**, *17*, 839.

35. Giustini, M.; Bellinazzo, C.; Galantini, L.; Mallardi, A.; Palazzo, G.; Sennato, S.; Bordi, F.; Rissanen, K. *Colloid. Surface. A* **2012**, *413*, 38.

36. Liu, B.; Yang, M.; Xia, N.; Zheng, P.; Wang, W.; Burger, C. *Soft Matter* **2012**, *8*, 9545.

37. Percec, V.; Wilson, D. A.; Leowanawat, P.; Wilson, C. J.; Hughes, A. D.; Kaucher, M. S.; Hammer, D. A.; Levine, D. H.; Kim, A. J.; Bates, F. S.; Davis, K. P.; Lodge, T. P.; Klein, M. L.; DeVane, R. H.; Aqad, E.; Rosen, B. M.; Argintaru, A. O.; Sienkowska, M. J.; Rissanen, K.; Nummelin, S.; Ropponen, J. *Science* **2010**, *328*, 1009.

38. Peterca, M.; Percec, V.; Leowanawat, P.; Bertin, A. *J. Am. Chem. Soc.* **2011**, *133*, 20507.

39. Katz, J. S.; Burdick, J. A. *Macromol. Biosci.* **2010**, *10*, 339.

40. Meng, F. H.; Zhong, Z. Y.; Feijen, J. *Biomacromolecules* **2009**, *10*, 197.

41. Timko, B. P.; Dvir, T.; Kohane, D. S. *Adv. Mater.* **2010**, *22*, 4925.

42. Jochum, F. D.; Theato, P. *Chem. Soc. Rev.* **2013**, *42*, 7468.

43. Ramireddy, R. R.; Raghupathi, K. R.; Torres, D. A.; Thayumanavan, S. *New J. Chem.* **2012**, *36*, 340.

44. Katz, J. S.; Zhong, S.; Ricart, B. G.; Pochan, D. J.; Hammer, D. A.; Burdick, J. A. *J. Am. Chem. Soc.* **2010**, *132*, 3654.

45. Cabane, E.; Malinova, V.; Menon, S.; Palivan, C. G.; Meier, W. *Soft Matter* **2011**, *7*, 9167.

46. Dong, J. M.; Zeng, Y.; Xun, Z. Q.; Han, Y. B.; Chen, J. P.; Li, Y. Y.; Li, Y. *Langmuir* **2012**, *28*, 1733.

47. Cabane, E.; Malinova, V.; Meier, W. *Macromol. Chem. Phys.* **2010**, *211*, 1847.

48. Yang, H.; Jia, L.; Wang, Z. F.; Di-Cicco, A.; Levy, D.; Keller, P. *Macromolecules* **2011**, *44*, 159.

49. Yan, Q.; Han, D.; Zhao, Y. *Polym. Chem.* **2013**, *4*, 5026.

50. Nazemi, A.; Schon, T. B.; Gillies, E. R. *Org. Lett.* **2013**, *15*, 1830.

51. Oar, M. A.; Serin, J. A.; Dichtel, W. R.; Fréchet, J. M. J. *Chem. Mater.* **2005**, *17*, 2267.

52. Li, W.; Zhang, A.; Feldman, K.; Walde, P.; Schluter, A. D. *Macromolecules* **2008**, *41*, 3659.

53. Han, D. H.; Tong, X.; Zhao, Y. *Macromolecules* **2011**, *44*, 437.

Chapter 7

Conclusions and Future Directions

The research described in this thesis demonstrated not only the application of dendron-functionalized biodegradable and biocompatible PEO-PCL polymersome system as a novel scaffold for various biomedical applications, but also took a significant step towards the biomedical applications of photo-responsive materials by developing backbone photodegradable dendrimers and dendrimer assemblies as potential drug delivery vehicles. These contributions are of importance in the area of biomaterials as researchers are always seeking materials with new and improved properties and functions, as well as an enhanced understanding of the interactions of materials with biological systems.

The initial focus of this research was to develop a biodegradable and biocompatible polymersome-based system that could be used in different areas of biomedical research. Work by our group had shown that dendritic surface functionalization of materials, including polymersomes, is a highly promising approach for controlling their surface functionalities and imparting specific biological properties. However, the polymersomes used in these studies were micron-sized and were composed of nonbiodegradable PEO-PBD BCPs with unknown biocompatibility. To address these limitations, and thus provide a significant advancement toward biomedical applications, this work was extended to nano-sized biodegradable and biocompatible polymer assemblies, namely micelles and polymersomes, constructed by the self-assembly of PEO-PCL BCPs. Having decorated their surfaces with azide groups, the conjugation of 3rd generation polyester dendrons bearing alkyne functionalities at their focal points and either amine or guanidine peripheral groups as well as a clickable small molecule rhodamine dye were evaluated by performing Cu(I)-catalyzed alkyne-azide click reaction at the surfaces of the assemblies. To demonstrate the applicability of the dendritic surface functionalization approach, micelles with conjugated dendritic guanidines were shown to have enhanced cell uptake by HeLa cancer cells relative to unfunctionalized micelles.

To enhance the longitudinal relaxivity of clinically used MRI contrast agents, Gd(III) complexes have been conjugated to a wide variety of macromolecular and material-based scaffolds. Among such scaffolds, there are very few reports of polymersome-based MRI contrast agents. Cheng et al. have investigated porous polymersomes containing Gd(III)-labeled dendrimers within their aqueous cores, and have obtained an r_1 of 7.5 mM^{-1} s^{-1} (60MHz, 40 °C) on a per Gd basis. More recently, Grull et al. incorporated Gd(III)-labeled lipids into a polymersome membrane, resulting in an r_1 of 22 mM^{-1} s^{-1} (20 MHz, 25 °C). To improve these values, in Chapter 3, we designed and synthesized dendritic and non-dendritic polymersome-based MRI contrast agents. In this design, both alkyne-functionalized non-dendritic and dendritic Gd(III)-based contrast agents were first synthesized and then installed onto the surface of azide-decorated PEO-PCL polymersomes. The effects of the dendritic and polymersome components on the relaxivities of the agents were elucidated. They were found to have an additive effect, resulting in the highest currently reported r_1 for a polymersome system. In addition, this system possesses the advantage of being composed of PEO and biodegradable polyester components. Therefore, this study not only enhanced the performance of the contrast agents in terms of relaxivity, it also contributed to the fundamental understanding of the contribution of different nano-scale components to enhancing this relaxivity.

To show the versatility of this functionalization approach and to demonstrate the multifunctional potential of polymersomes, in Chapter 4, a multifunctional polymersome system with the potential to interfere with the viral infection process at two levels was developed. In this study, a 3rd generation polyester dendron decorated with Neu5Ac was introduced to the surface of PEO-PCL polymersomes to inhibit the binding of influenza virus hemagglutinin to Neu5Ac moieties on mammalian host cells. In addition, the antiviral drug zanamivir was incorporated into the polymersome core with the aim of also inhibiting influenza virus neuraminidase, thus preventing the release of progeny virus from host cells. Using an enzyme-linked lectin inhibition assay, it was shown that incorporation of the dendritic Neu5Ac onto the polymersome surface led to a nearly 2000-fold enhancement in binding affinity, showing the advantage of the polymersome system for enhancing binding. Sustained release of the drug was also observed for this system, with release occurring over a period of several days. This work represents the

first multifunctional polymersome system with the potential to interfere with the viral infection process.

The development of smart dendrimers that can respond to external stimuli is of significant interest as this can impart new properties and further expand their scope of applications. Among various stimuli, light is of particular interest as it can be applied at a specific time and location with control over its intensity and wavelength. The examples of photodegradable dendrimer systems in the literature have been limited to dendrimers in which the photodegradable units were either at the core of the dendrimer or at the junction between the hydrophobic and hydrophilic portions of amphiphilic dendrons. The limitation of these approaches is that following photodegradation, in most cases residual hydrophobic fragments may undergo aggregation in aqueous solutions. To address this drawback, in Chapter 5, a new series of dendrons and dendrimers that are able for the first time to undergo complete backbone photodegradation to small molecules was designed and synthesized. This was done through the incorporation of photodegradable *o*-nitrobenzyl esters into a new dendrimer monomer based on bis-MPA. Dendrons were synthesized using a divergent approach, and were subsequently coupled to a core molecule in the final step *via* the microwave-assisted Cu(I)-catalyzed alkyne-azide click reaction in high yields. Photolysis of these dendrimers were tracked using techniuqes such as UV-visible and ^{1}H NMR spectroscopy as well as SEC and it was demonstrated that the dendrimers degrade to release the small molecule bis-MPA.

Incorporation of the photodegradable dendrons described in Chapter 5 into AJDs and their self-assembly to different morphologies were discussed in Chapter 6. A small library of AJDs (G1-3) with backbone photodegradable hydrophobic dendritic blocks and hydrophilic blocks based on TEG and gallic acid were successfully synthesized. It was shown that a 3rd generation AJD was able to undergo self-assembly to form well-defined dendrimersomes with an average size of about 450 nm. Upon irradiation with UV light (300-400 nm, 25 mW·cm^{-2}), the dendrimersomes' membranes were effectively disrupted to disintegrate these assemblies with no sign of precipitation or morphological change to smaller assemblies. This result is of significant interest because the photodegradable dendrimersomes described in this chapter are the first example of any vesicular

architecture (including polymersomes, dendrimersomes, and small amphiphile-based vesicles) that are capable of complete photolytic membrane degradation to release their encapsulated model drugs without creation of any smaller size micelles or precipitate.

Future investigations in the area of PEO-PCL polymersome-based biomaterials involves evaluation of their actual antiviral potential against various strains of influenza virus. This can be accomplished by initiating collaborative project with research groups at the Department of Microbiology and Immunology at Western University. Moreover, the concept of biodegradable and biocompatible polymersomes can be extended to biodegradable and biocompatible dendrimersomes with activated azide surface groups by synthesizing third or fourth generation AJDs constructed by bis-MBA-based hydrophobic dendrons and TEG/gallic acid-based hydrophilic dendritic blocks. Given the higher order of monodispersity that is offered by dendrimers compared to linear polymers, this can potentially result in the development of the first example of a dendrimersome system with activated surface groups that can readily be functionalized with various ligands of interest.

In the context of backbone photodegradable dendrimers and dendrimer assemblies, encapsulation and release behavior of these dendrimersomes with respect to both hydrophilic and hydrophobic model drugs needs be investigated in a near future. In longer term, tuning of their optical properties by changing the photochemically responsive group or through the incorporation of other photophysical processes in such a way that they can undergo photodegradation in the visible or NIR region can potentially open up new opportunities to access materials with fully photodegradable hydrophobic blocks suitable for biological or other applications. In addition, it would be interesting to investigate to see whether or not it is possible to fine-tune the release rate of an encapsulate model drug from photodegradable dendrimersomes. This can be done through the selective incorporation of the photodegradable unit at specific generations (G1, G2, or G3) of the AJDs. To accomplish this, a small library of three 3rd generation AJDs with the photodegradable monomer unit incorporated at either the first, second, or the third generation layer needs to be synthesized and their self-assembly to dendrimersomes followed by their cargo release rates needs to be investigated.

Appendix 1: Permission to Reuse Copyrighted Material

RSC | Advancing the Chemical Sciences

Royal Society of Chemistry
Thomas Graham House
Science Park
Milton Road
Cambridge
CB4 0WF

Tel: +44 (0)1223 420 066
Fax: +44 (0)1223 423 623
Email: contracts-copyright@rsc.org

www.rsc.org

Acknowledgements to be used by RSC authors

Authors of RSC books and journal articles can reproduce material (for example a figure) from the RSC publication in a non-RSC publication, including theses, without formally requesting permission providing that the correct acknowledgement is given to the RSC publication. This permission extends to reproduction of large portions of text or the whole article or book chapter when being reproduced in a thesis.

The acknowledgement to be used depends on the RSC publication in which the material was published and the form of the acknowledgements is as follows:

- For material being reproduced from an article in *New Journal of Chemistry* the acknowledgement should be in the form:

  o [Original citation] - Reproduced by permission of The Royal Society of Chemistry (RSC) on behalf of the Centre National de la Recherche Scientifique (CNRS) and the RSC

- For material being reproduced from an article *Photochemical & Photobiological Sciences* the acknowledgement should be in the form:

  o [Original citation] - Reproduced by permission of The Royal Society of Chemistry (RSC) on behalf of the European Society for Photobiology, the European Photochemistry Association, and RSC

- For material being reproduced from an article in *Physical Chemistry Chemical Physics* the acknowledgement should be in the form:

  o [Original citation] - Reproduced by permission of the PCCP Owner Societies

- For material reproduced from books and any other journal the acknowledgement should be in the form:

  o [Original citation] - Reproduced by permission of The Royal Society of Chemistry

The acknowledgement should also include a hyperlink to the article on the RSC website.

The form of the acknowledgement is also specified in the RSC agreement/licence signed by the corresponding author.

Except in cases of republication in a thesis, this express permission does not cover the reproduction of large portions of text from the RSC publication or reproduction of the whole article or book chapter.

A publisher of a non-RSC publication can use this document as proof that permission is granted to use the material in the non-RSC publication.

VAT Registration Number: GB 342 1764 71   Registered Charity Number: 207890

JOHN WILEY AND SONS LICENSE
TERMS AND CONDITIONS

Sep 30, 2013

This is a License Agreement between Ali Nazemi ("You") and John Wiley and Sons ("John Wiley and Sons") provided by Copyright Clearance Center ("CCC"). The license consists of your order details, the terms and conditions provided by John Wiley and Sons, and the payment terms and conditions.

All payments must be made in full to CCC. For payment instructions, please see information listed at the bottom of this form.

License Number	3239000171547
License date	Sep 30, 2013
Licensed content publisher	John Wiley and Sons
Licensed content publication	Journal of Polymer Science Part A: Polymer Chemistry
Licensed content title	Dendritic surface functionalization of biodegradable polymer assemblies
Licensed copyright line	Copyright © 2011 Wiley Periodicals, Inc.
Licensed content author	Ali Nazemi,Ryan C. Amos,Colin V. Bonduelle,Elizabeth R. Gillies
Licensed content date	Apr 14, 2011
Start page	2546
End page	2559
Type of use	Dissertation/Thesis
Requestor type	Author of this Wiley article
Format	Electronic
Portion	Full article
Will you be translating?	No
Total	**0.00 USD**
Terms and Conditions	

TERMS AND CONDITIONS

This copyrighted material is owned by or exclusively licensed to John Wiley & Sons, Inc. or one of its group companies (each a "Wiley Company") or a society for whom a Wiley Company has exclusive publishing rights in relation to a particular journal (collectively "WILEY"). By clicking "accept" in connection with completing this licensing transaction, you agree that the following terms and conditions apply to this transaction (along with the billing and payment terms and conditions established by the Copyright Clearance Center Inc., ("CCC's Billing and Payment terms and conditions"), at the time that you opened your RightsLink account (these are available at any time at http://myaccount.copyright.com).

Terms and Conditions

1. The materials you have requested permission to reproduce (the "Materials") are protected by copyright.

2.You are hereby granted a personal, non-exclusive, non-sublicensable, non-transferable, worldwide, limited license to reproduce the Materials for the purpose specified in the licensing process. This license is for a one-time use only with a maximum distribution equal to the number that you identified in the licensing process. Any form of republication granted by this license must be completed within two years of the date of the grant of this license (although copies prepared before may be distributed thereafter). The Materials shall not be used in any other manner or for any other purpose. Permission is granted subject to an appropriate acknowledgement given to the author, title of the material/book/journal and the publisher. You shall also duplicate the copyright notice that appears in the Wiley publication in your use of the Material. Permission is also granted on the understanding that nowhere in the text is a previously published source

acknowledged for all or part of this Material. Any third party material is expressly excluded from this permission.

3. With respect to the Materials, all rights are reserved. Except as expressly granted by the terms of the license, no part of the Materials may be copied, modified, adapted (except for minor reformatting required by the new Publication), translated, reproduced, transferred or distributed, in any form or by any means, and no derivative works may be made based on the Materials without the prior permission of the respective copyright owner. You may not alter, remove or suppress in any manner any copyright, trademark or other notices displayed by the Materials. You may not license, rent, sell, loan, lease, pledge, offer as security, transfer or assign the Materials, or any of the rights granted to you hereunder to any other person.

4. The Materials and all of the intellectual property rights therein shall at all times remain the exclusive property of John Wiley & Sons Inc or one of its related companies (WILEY) or their respective licensors, and your interest therein is only that of having possession of and the right to reproduce the Materials pursuant to Section 2 herein during the continuance of this Agreement. You agree that you own no right, title or interest in or to the Materials or any of the intellectual property rights therein. You shall have no rights hereunder other than the license as provided for above in Section 2. No right, license or interest to any trademark, trade name, service mark or other branding ("Marks") of WILEY or its licensors is granted hereunder, and you agree that you shall not assert any such right, license or interest with respect thereto.

5. NEITHER WILEY NOR ITS LICENSORS MAKES ANY WARRANTY OR REPRESENTATION OF ANY KIND TO YOU OR ANY THIRD PARTY, EXPRESS, IMPLIED OR STATUTORY, WITH RESPECT TO THE MATERIALS OR THE ACCURACY OF ANY INFORMATION CONTAINED IN THE MATERIALS, INCLUDING, WITHOUT LIMITATION, ANY IMPLIED WARRANTY OF MERCHANTABILITY, ACCURACY, SATISFACTORY QUALITY, FITNESS FOR A PARTICULAR PURPOSE, USABILITY, INTEGRATION OR NON-INFRINGEMENT AND ALL SUCH WARRANTIES ARE HEREBY EXCLUDED BY WILEY AND ITS LICENSORS AND WAIVED BY YOU.

6. WILEY shall have the right to terminate this Agreement immediately upon breach of this Agreement by you.

7. You shall indemnify, defend and hold harmless WILEY, its Licensors and their respective directors, officers, agents and employees, from and against any actual or threatened claims, demands, causes of action or proceedings arising from any breach of this Agreement by you.

8. IN NO EVENT SHALL WILEY OR ITS LICENSORS BE LIABLE TO YOU OR ANY OTHER PARTY OR ANY OTHER PERSON OR ENTITY FOR ANY SPECIAL, CONSEQUENTIAL, INCIDENTAL, INDIRECT, EXEMPLARY OR PUNITIVE DAMAGES, HOWEVER CAUSED, ARISING OUT OF OR IN CONNECTION WITH THE DOWNLOADING, PROVISIONING, VIEWING OR USE OF THE MATERIALS REGARDLESS OF THE FORM OF ACTION, WHETHER FOR BREACH OF CONTRACT, BREACH OF WARRANTY, TORT, NEGLIGENCE, INFRINGEMENT OR OTHERWISE (INCLUDING, WITHOUT LIMITATION, DAMAGES BASED ON LOSS OF PROFITS, DATA, FILES, USE, BUSINESS OPPORTUNITY OR CLAIMS OF THIRD PARTIES), AND WHETHER OR NOT THE PARTY HAS BEEN ADVISED OF THE POSSIBILITY OF SUCH DAMAGES. THIS LIMITATION SHALL APPLY NOTWITHSTANDING ANY FAILURE OF ESSENTIAL PURPOSE OF ANY LIMITED REMEDY PROVIDED HEREIN.

9. Should any provision of this Agreement be held by a court of competent jurisdiction to be illegal, invalid, or unenforceable, that provision shall be deemed amended to achieve as nearly as possible the same economic effect as the original provision, and the legality, validity and enforceability of the remaining provisions of this Agreement shall not be affected or impaired thereby.

10. The failure of either party to enforce any term or condition of this Agreement shall not constitute a waiver of either party's right to enforce each and every term and condition of this Agreement. No breach under this agreement shall be deemed waived or excused by either party unless such waiver or consent is in writing signed by the party granting such waiver or consent. The waiver by or consent of a party to a breach of any provision of this Agreement shall not operate or be construed as a waiver of or consent to any other or subsequent breach by such other party.

11. This Agreement may not be assigned (including by operation of law or otherwise) by you without WILEY's prior written consent.

12. Any fee required for this permission shall be non-refundable after thirty (30) days from receipt

13. These terms and conditions together with CCC's Billing and Payment terms and conditions (which are incorporated herein) form the entire agreement between you and WILEY concerning this licensing transaction and (in the absence of fraud) supersedes all prior agreements and representations of the parties, oral or written. This Agreement may not be amended except in writing signed by both parties. This Agreement shall be binding upon and inure to the benefit of the parties' successors, legal representatives, and authorized assigns.

14. In the event of any conflict between your obligations established by these terms and conditions and those established by CCC's Billing and Payment terms and conditions, these terms and conditions shall prevail.

15. WILEY expressly reserves all rights not specifically granted in the combination of (i) the license details provided by you and accepted in the course of this licensing transaction, (ii) these terms and conditions and (iii) CCC's Billing and Payment terms and conditions.

16. This Agreement will be void if the Type of Use, Format, Circulation, or Requestor Type was misrepresented during the

licensing process.

17. This Agreement shall be governed by and construed in accordance with the laws of the State of New York, USA, without regards to such state's conflict of law rules. Any legal action, suit or proceeding arising out of or relating to these Terms and Conditions or the breach thereof shall be instituted in a court of competent jurisdiction in New York County in the State of New York in the United States of America and each party hereby consents and submits to the personal jurisdiction of such court, waives any objection to venue in such court and consents to service of process by registered or certified mail, return receipt requested, at the last known address of such party.

Wiley Open Access Terms and Conditions

Wiley publishes Open Access articles in both its Wiley Open Access Journals program [http://www.wileyopenaccess.com/view/index.html] and as Online Open articles in its subscription journals. The majority of Wiley Open Access Journals have adopted the Creative Commons Attribution License (CC BY) which permits the unrestricted use, distribution, reproduction, adaptation and commercial exploitation of the article in any medium. No permission is required to use the article in this way provided that the article is properly cited and other license terms are observed. A small number of Wiley Open Access journals have retained the Creative Commons Attribution Non Commercial License (CC BY-NC), which permits use, distribution and reproduction in any medium, provided the original work is properly cited and is not used for commercial purposes.

Online Open articles - Authors selecting Online Open are, unless particular exceptions apply, offered a choice of Creative Commons licenses. They may therefore select from the CC BY, the CC BY-NC and the Attribution-NoDerivatives (CC BY-NC-ND). The CC BY-NC-ND is more restrictive than the CC BY-NC as it does not permit adaptations or modifications without rights holder consent.

Wiley Open Access articles are protected by copyright and are posted to repositories and websites in accordance with the terms of the applicable Creative Commons license referenced on the article. At the time of deposit, Wiley Open Access articles include all changes made during peer review, copyediting, and publishing. Repositories and websites that host the article are responsible for incorporating any publisher-supplied amendments or retractions issued subsequently. Wiley Open Access articles are also available without charge on Wiley's publishing platform, **Wiley Online Library** or any successor sites.

Conditions applicable to all Wiley Open Access articles:

- The authors' moral rights must not be compromised. These rights include the right of "paternity" (also known as "attribution" - the right for the author to be identified as such) and "integrity" (the right for the author not to have the work altered in such a way that the author's reputation or integrity may be damaged).

- Where content in the article is identified as belonging to a third party, it is the obligation of the user to ensure that any reuse complies with the copyright policies of the owner of that content.

- If article content is copied, downloaded or otherwise reused for research and other purposes as permitted, a link to the appropriate bibliographic citation (authors, journal, article title, volume, issue, page numbers, DOI and the link to the definitive published version on Wiley Online Library) should be maintained. Copyright notices and disclaimers must not be deleted.
    - Creative Commons licenses are copyright licenses and do not confer any other rights, including but not limited to trademark or patent rights.

- Any translations, for which a prior translation agreement with Wiley has not been agreed, must prominently display the statement: "This is an unofficial translation of an article that appeared in a Wiley publication. The publisher has not endorsed this translation."

Conditions applicable to non-commercial licenses (CC BY-NC and CC BY-NC-ND)

For non-commercial and non-promotional purposes individual non-commercial users may access, download, copy, display and redistribute to colleagues Wiley Open Access articles. In addition, articles adopting the CC BY-NC may be adapted, translated, and text- and data-mined subject to the conditions above.

Use by commercial "for-profit" organizations

Use of non-commercial Wiley Open Access articles for commercial, promotional, or marketing purposes requires further explicit permission from Wiley and will be subject to a fee. Commercial purposes include:

    - Copying or downloading of articles, or linking to such articles for further redistribution, sale or licensing;

    - Copying, downloading or posting by a site or service that incorporates advertising with such content;

- The inclusion or incorporation of article content in other works or services (other than normal quotations with an appropriate citation) that is then available for sale or licensing, for a fee (for example, a compilation produced for marketing purposes, inclusion in a sales pack)

- Use of article content (other than normal quotations with appropriate citation) by for-profit organizations for promotional purposes

- Linking to article content in e-mails redistributed for promotional, marketing or educational purposes;

- Use for the purposes of monetary reward by means of sale, resale, license, loan, transfer or other form of commercial exploitation such as marketing products

- Print reprints of Wiley Open Access articles can be purchased from: corporatesales@wiley.com

   The modification or adaptation for any purpose of an article referencing the CC BY-NC-ND License requires consent which can be requested from RightsLink@wiley.com .

   Other Terms and Conditions:

   BY CLICKING ON THE "I AGREE..." BOX, YOU ACKNOWLEDGE THAT YOU HAVE READ AND FULLY UNDERSTAND EACH OF THE SECTIONS OF AND PROVISIONS SET FORTH IN THIS AGREEMENT AND THAT YOU ARE IN AGREEMENT WITH AND ARE WILLING TO ACCEPT ALL OF YOUR OBLIGATIONS AS SET FORTH IN THIS AGREEMENT.

   v1.8

Copyright Clearance Center

RightsLink®

Home | Account Info | Help

ACS Publications
High quality. High impact.

Title: Multifunctional Dendritic Sialopolymersomes as Potential Antiviral Agents: Their Lectin Binding and Drug Release Properties

Author: Ali Nazemi, S. M. Mansour Haeryfar, and Elizabeth R. Gillies

Publication: Langmuir

Publisher: American Chemical Society

Date: May 1, 2013

Copyright © 2013, American Chemical Society

PERMISSION/LICENSE IS GRANTED FOR YOUR ORDER AT NO CHARGE

This type of permission/license, instead of the standard Terms & Conditions, is sent to you because no fee is being charged for your order. Please note the following:

- Permission is granted for your request in both print and electronic formats, and translations.
- If figures and/or tables were requested, they may be adapted or used in part.
- Please print this page for your records and send a copy of it to your publisher/graduate school.
- Appropriate credit for the requested material should be given as follows: "Reprinted (adapted) with permission from (COMPLETE REFERENCE CITATION). Copyright (YEAR) American Chemical Society." Insert appropriate information in place of the capitalized words.
- One-time permission is granted only for the use specified in your request. No additional uses are granted (such as derivative works or other editions). For any other uses, please submit a new request.

BACK | CLOSE WINDOW

Copyright Clearance Center

RightsLink®

Home   Account Info   Help

ACS Publications
High quality. High impact.

Title: Synthesis and Degradation of Backbone Photodegradable Polyester Dendrimers

Author: Ali Nazemi, Tyler B. Schon, and Elizabeth R. Gillies

Publication: Organic Letters

Publisher: American Chemical Society

Date: Apr 1, 2013

Copyright © 2013, American Chemical Society

Logged in as:
Ali Nazemi
Account #:
3000702125

LOGOUT

PERMISSION/LICENSE IS GRANTED FOR YOUR ORDER AT NO CHARGE

This type of permission/license, instead of the standard Terms & Conditions, is sent to you because no fee is being charged for your order. Please note the following:

- Permission is granted for your request in both print and electronic formats, and translations.
- If figures and/or tables were requested, they may be adapted or used in part.
- Please print this page for your records and send a copy of it to your publisher/graduate school.
- Appropriate credit for the requested material should be given as follows: "Reprinted (adapted) with permission from (COMPLETE REFERENCE CITATION). Copyright (YEAR) American Chemical Society." Insert appropriate information in place of the capitalized words.
- One-time permission is granted only for the use specified in your request. No additional uses are granted (such as derivative works or other editions). For any other uses, please submit a new request.

BACK   CLOSE WINDOW

Appendix 2: Supporting Information for Chapter 2
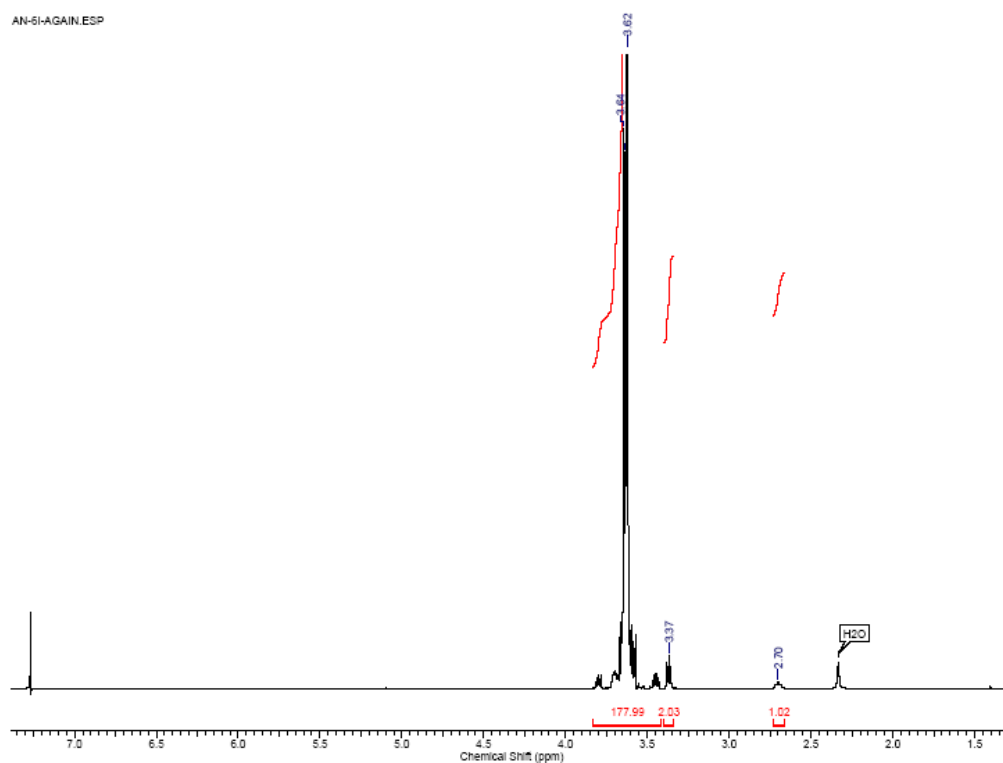
Figure A2.1. ^{1}H NMR spectrum of N$_3$-PEO-OH (**2.2**) (400 MHz, CDCl$_3$).
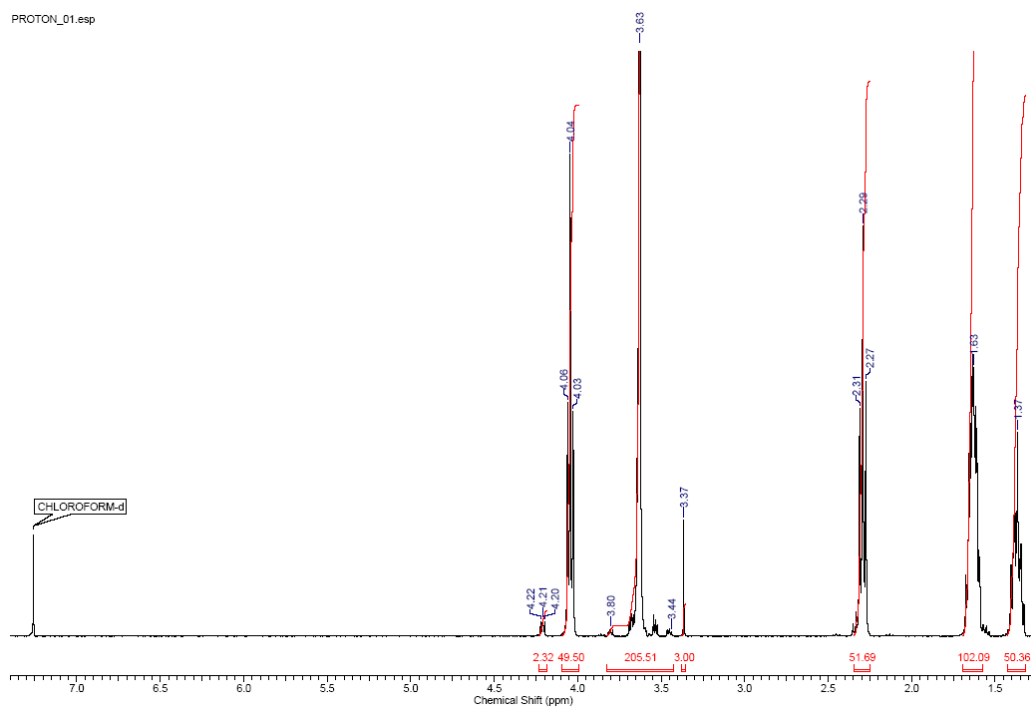
Figure A2.2. ^{1}H NMR spectrum of copolymer **2.3** (400 MHz, CDCl$_3$).
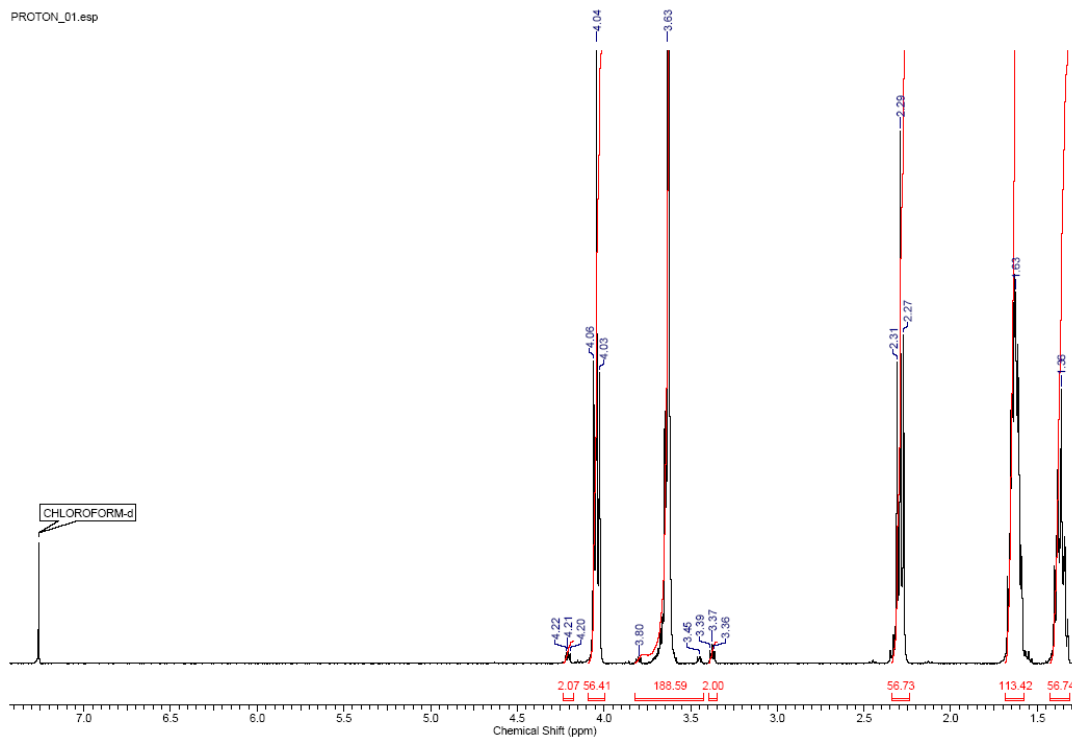
Figure A2.3. ^{1}H NMR spectrum of copolymer **2.4** (400 MHz, CDCl$_3$).
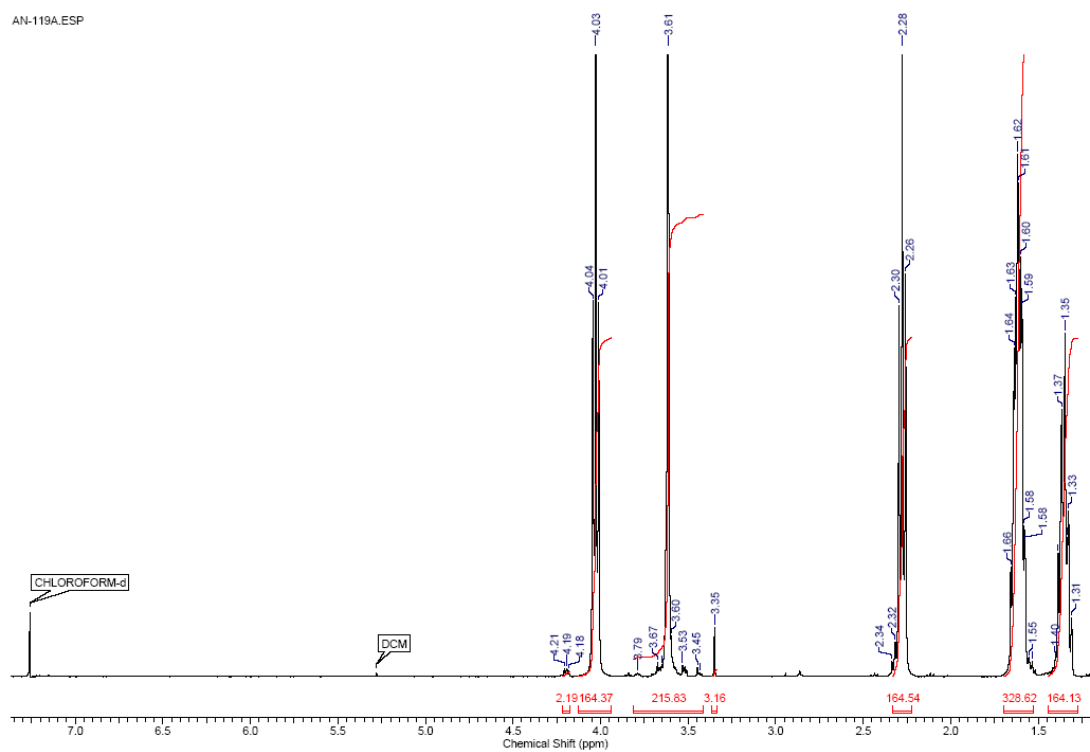
Figure A2.4. ^{1}H NMR spectrum of copolymer **2.5** (400 MHz, CDCl$_3$).
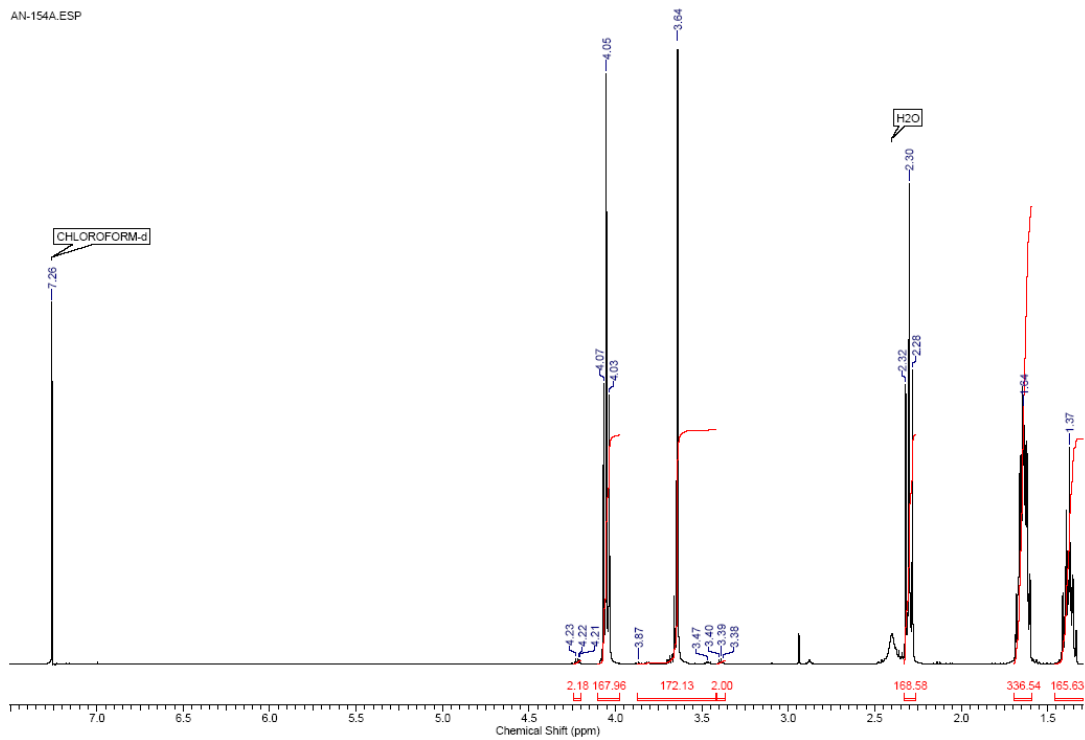
Figure A2.5. ^{1}H NMR spectrum of copolymer **2.6** (400 MHz, CDCl$_3$).
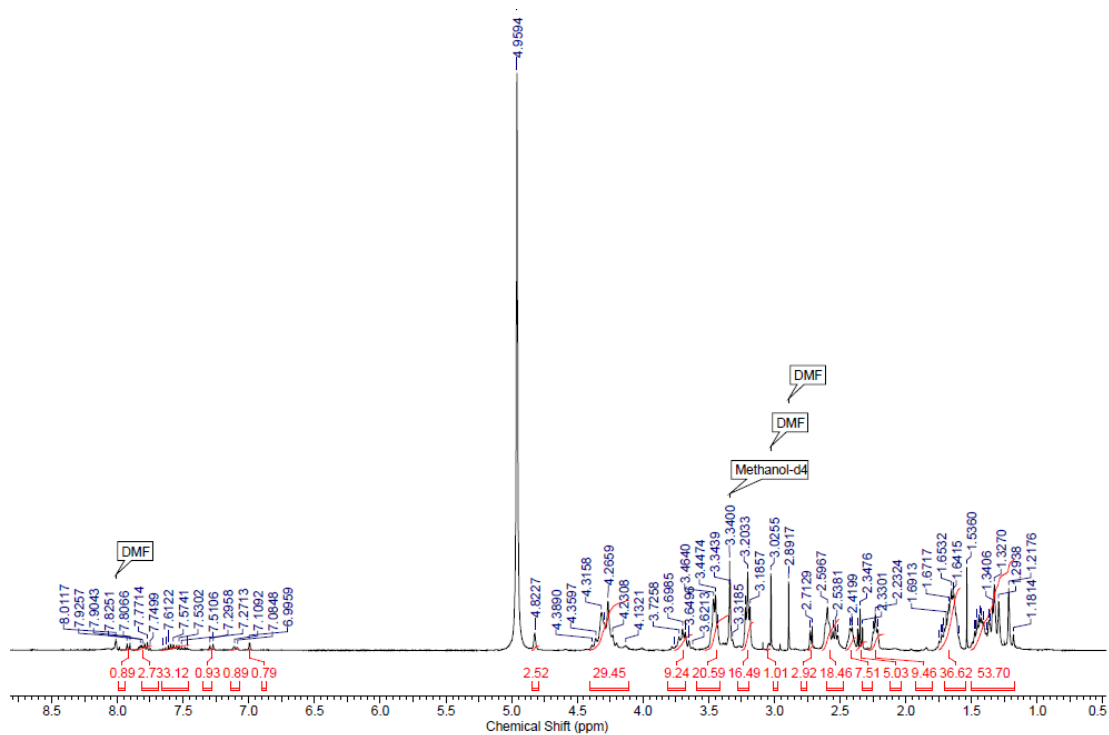
Figure A2.6. ^{1}H NMR spectrum of rhodamine-labeled guanidine-functionalized dendron **2.8** (400 MHz, CD$_3$OD).
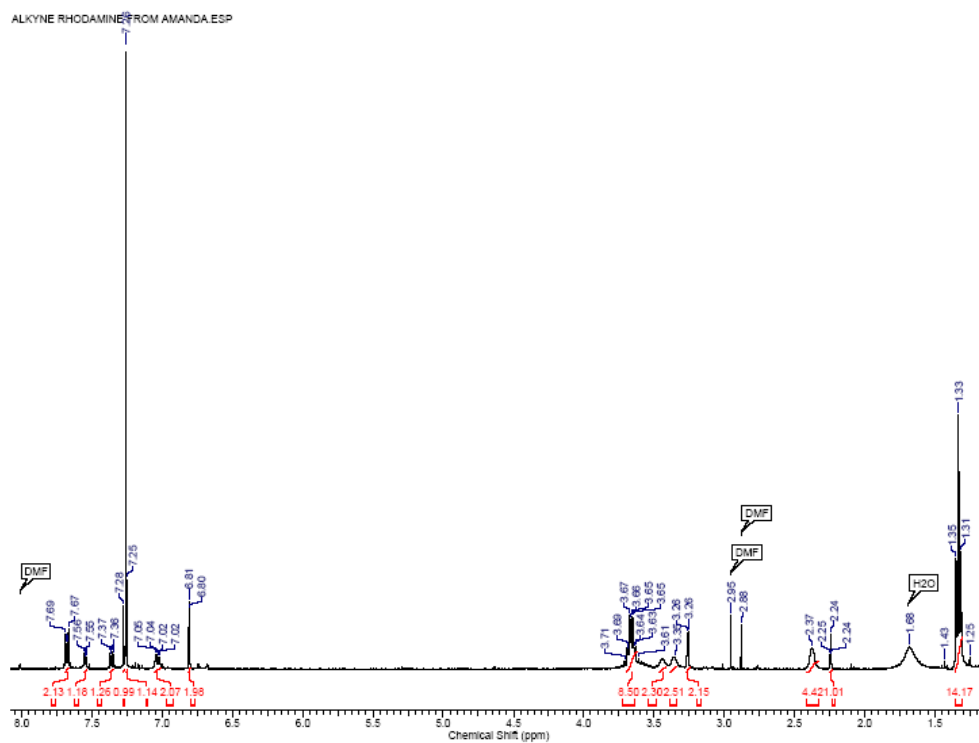
Figure A2.7. ^{1}H NMR spectrum of rhodamine derivative **2.10** (400 MHz, CDCl$_3$).
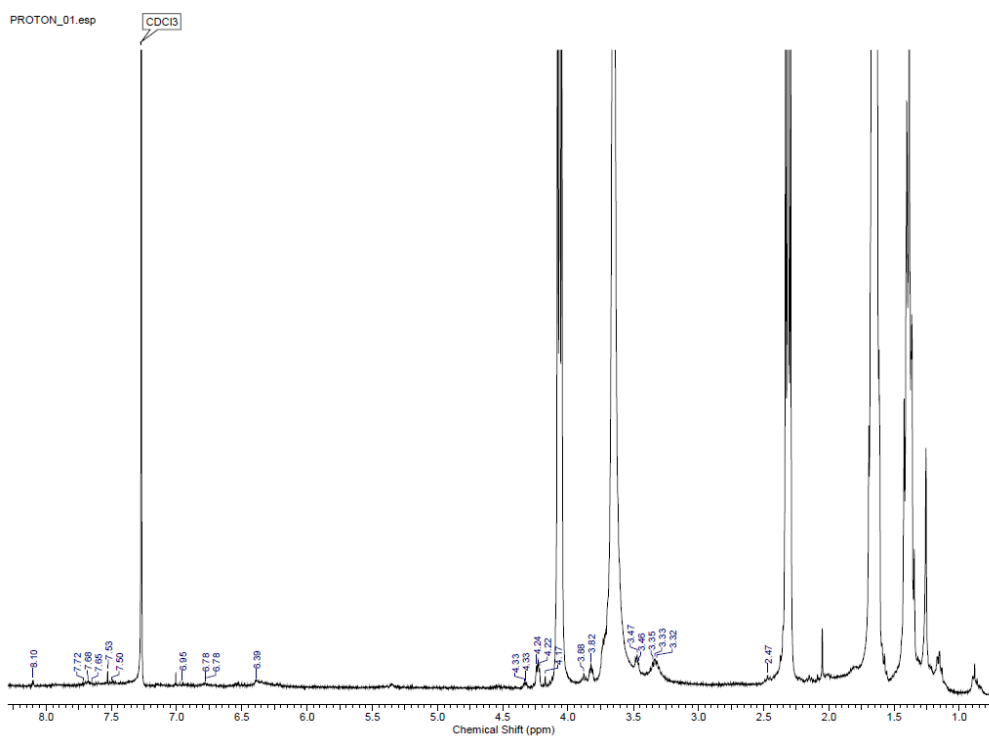
Figure A2.8. ^{1}H NMR spectrum of rhodamine-labeled copolymer **2.11** (400 MHz, CDCl$_3$).
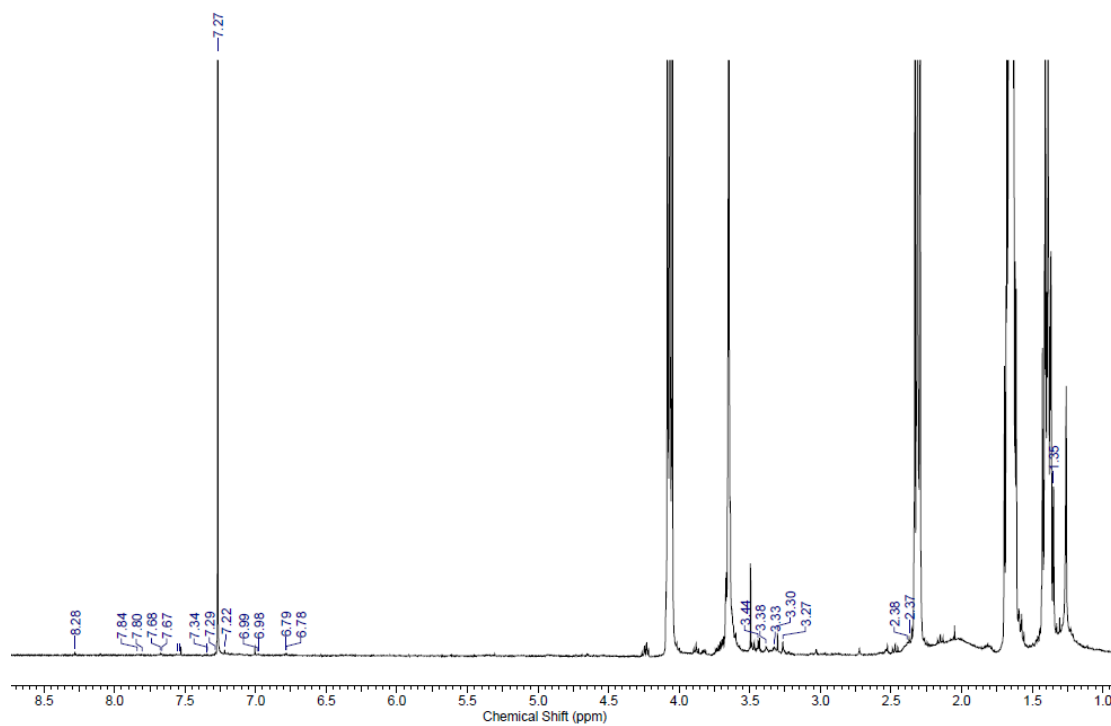
Figure A2.9. ^{1}H NMR spectrum of rhodamine-labeled copolymer **2.12** (400 MHz, CDCl$_3$).
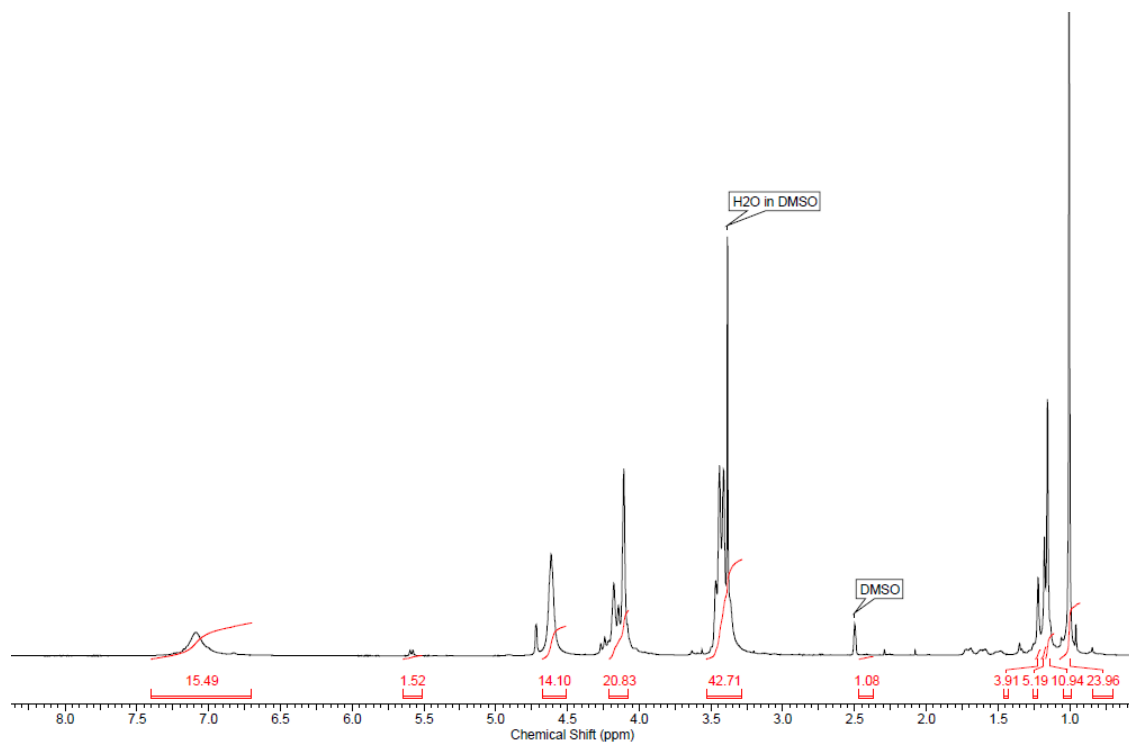
Figure A2.10. ^{1}H NMR spectrum of dendron **2.14** (400 MHz, (CD$_3$)$_2$SO).
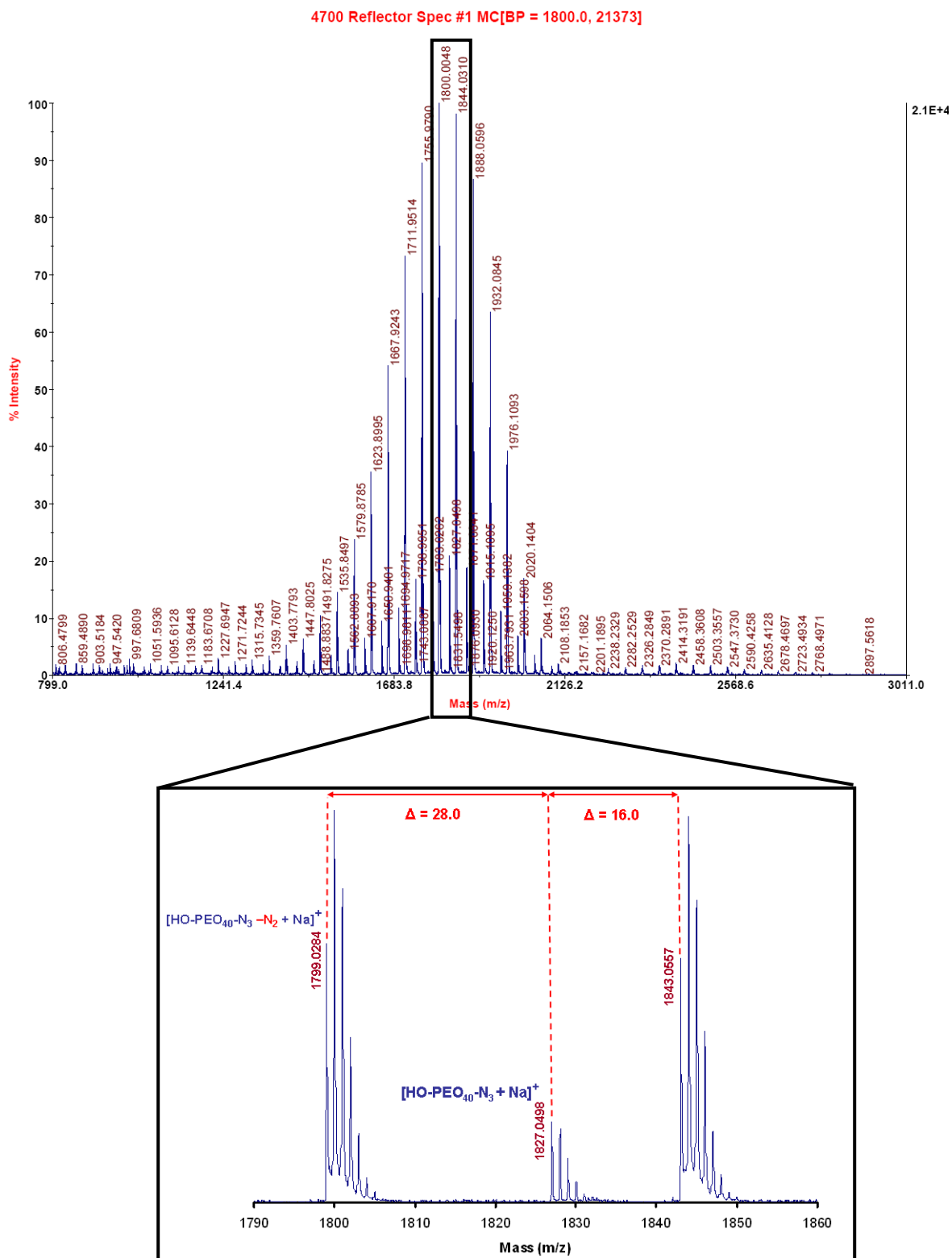
Figure A2.11. MALDI-TOF mass spectrum of compound **2.2**.
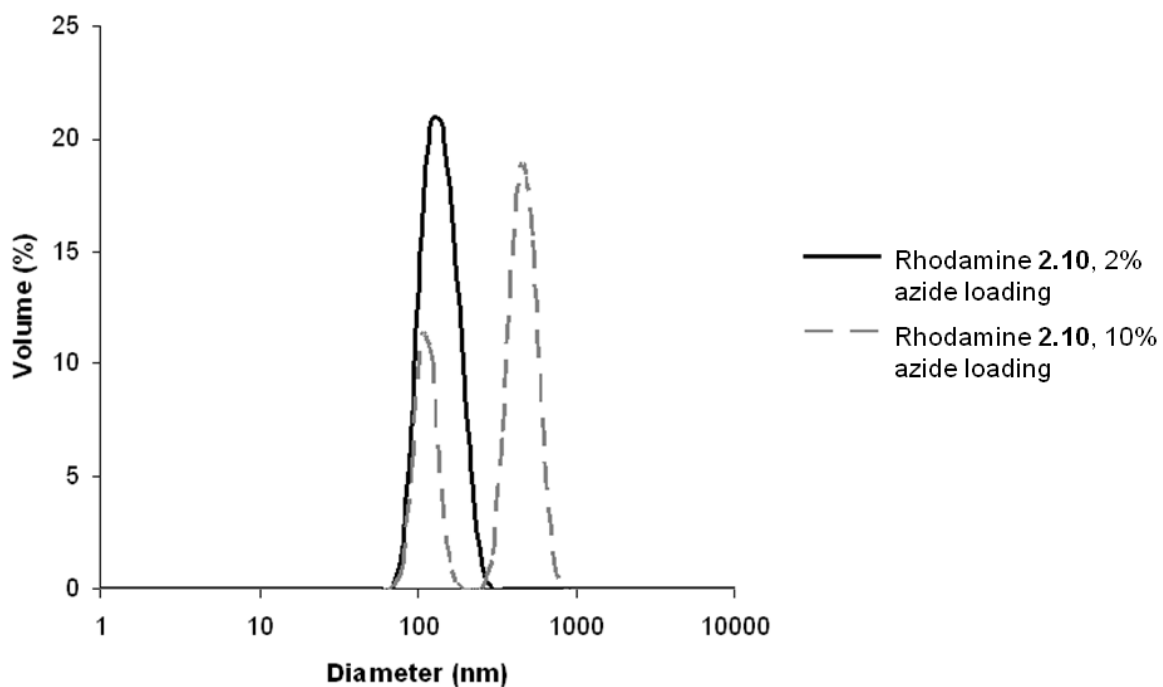
Figure A2.12. Size distribution profiles following click reaction of rhodamine **2.10** on vesicles.
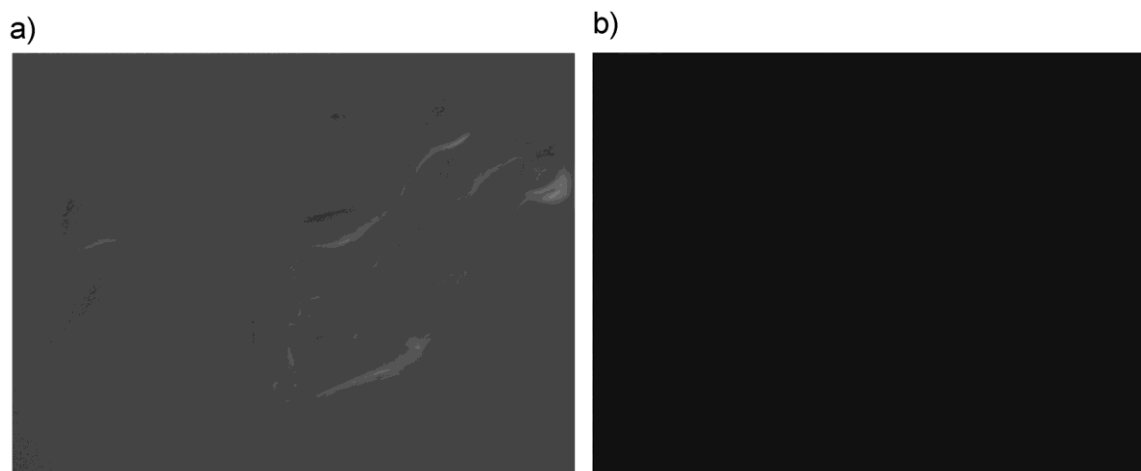
Figure A2.13. Confocal microscopy of HeLa cells after incubation for 4 h with control PEO-PCL micelles (rhodamine functionalization only): a) Differential interference contrast image verifying the presence of cells in the field of view; b) Fluorescence image taken using the same microscope settings used for the image in Figure 2.7 shows no detectable uptake.

Appendix 3: Supporting Information for Chapter 3
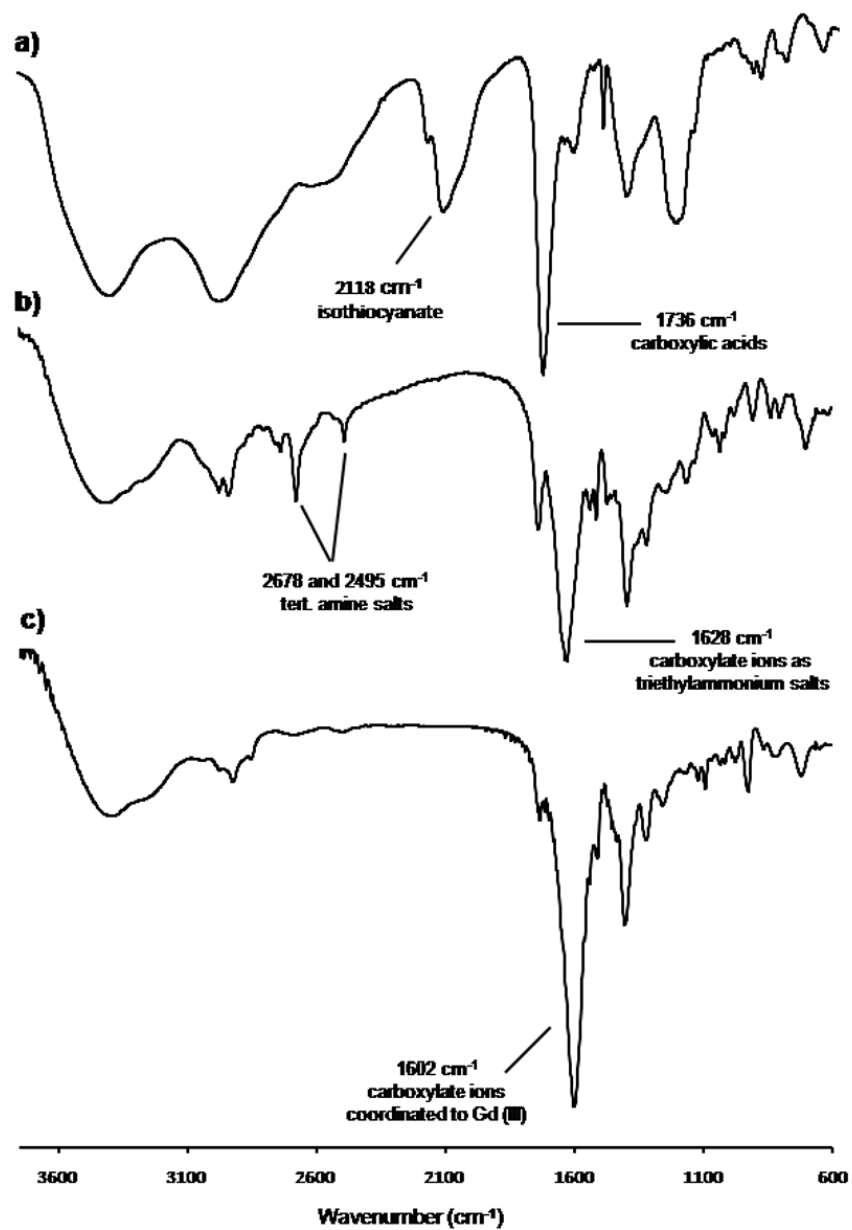
Figure A3.1. IR spectra for: a) DTPA derivative **3.6**; b) dendron **3.7**; c) dendron **3.1**.
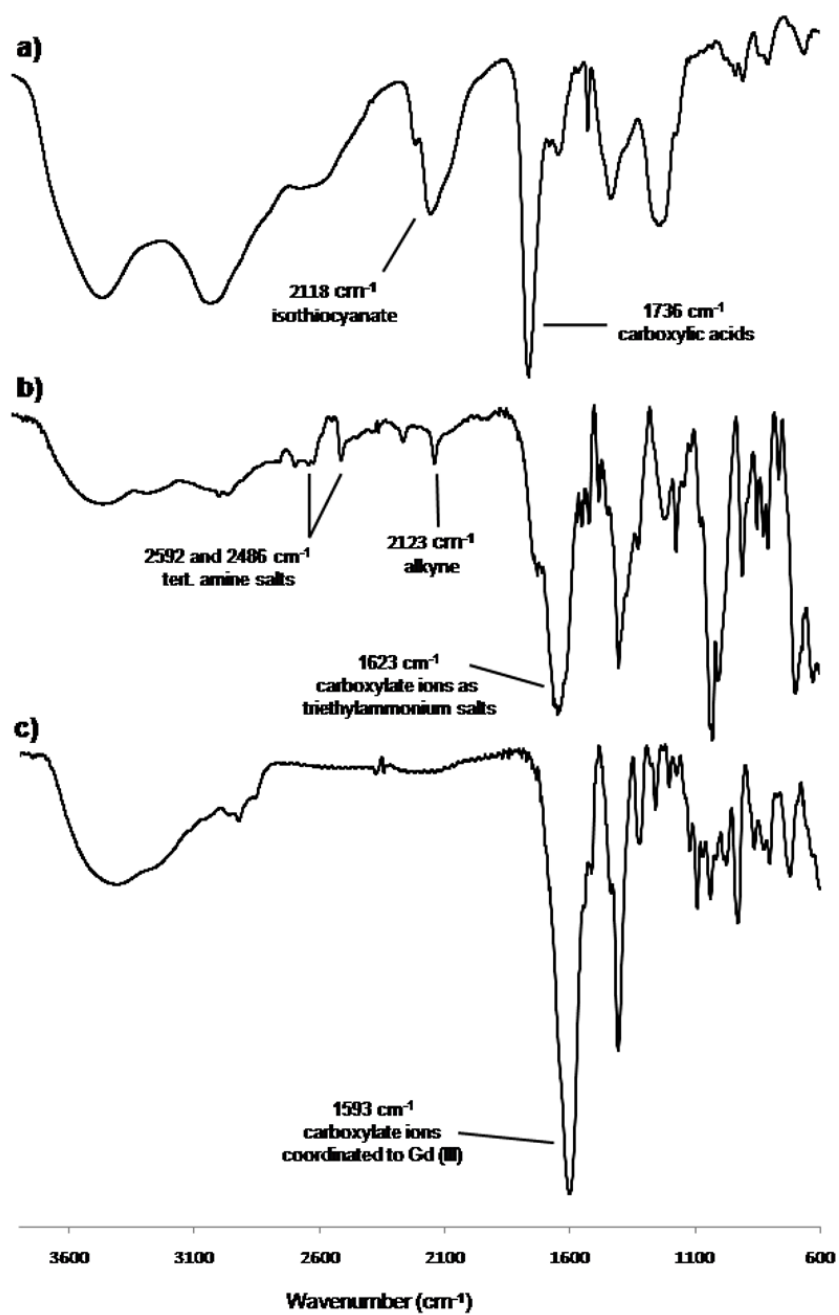
Figure A3.2. IR spectra for: a) DTPA derivative **3.6**; b) compound **3.8**; c) compound **3.2**.
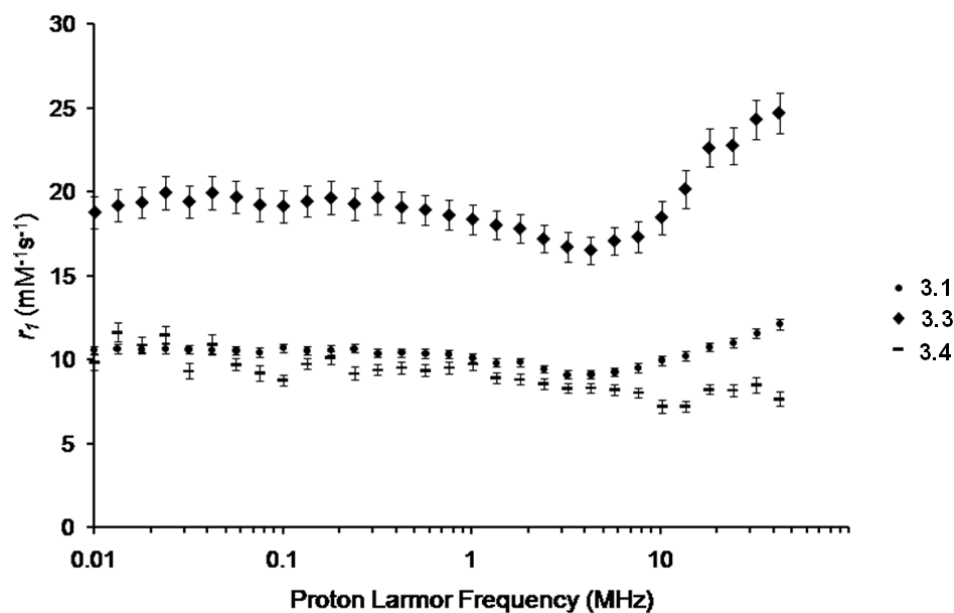
Figure A3.3. Longitudinal relaxivity (r_1) of dendron **3.1**, polymersome **3.3**, and polymersome **3.4** in phosphate buffer (0.1 M, pH 7.4) as a function of field strength at 310 K.
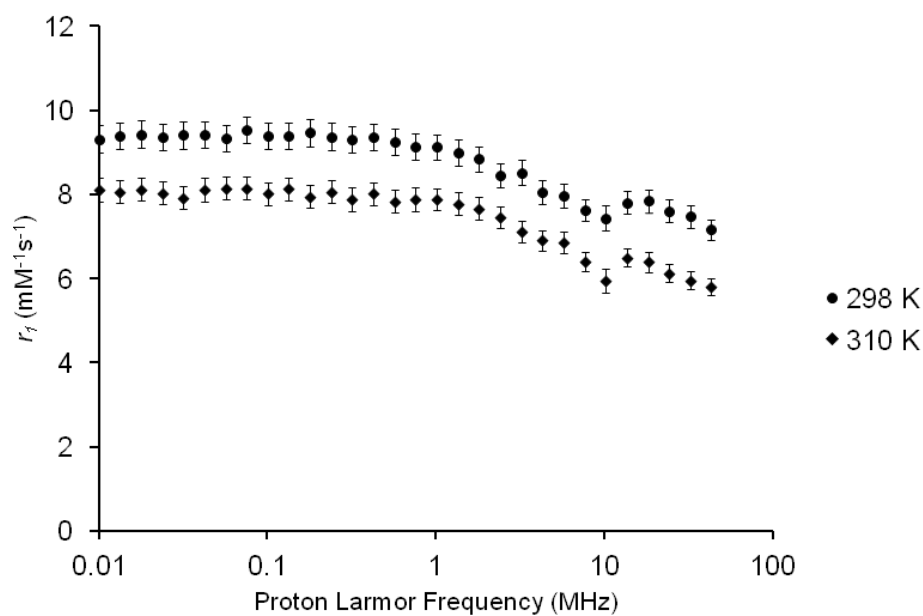
Figure A3.4. Longitudinal relaxivity (r_1) of unpurified **3.2** in phosphate buffer (0.1 M, pH 7.4) as a function of field strength at 310 K. Note that the presence of excess Gd(III) likely present as $Gd(III)(H_2O)_8$ increases the relaxivity.

Table A3.1. NMRD data for **3.1**, **3.3**, and **3.4** at 298 K.

Frequency (MHz)	Dendron **3.1** r_1 (mM^{-1}s^{-1})	$\pm$ error (mM^{-1}s^{-1})	Polymersome **3.3** r_1 (mM^{-1}s^{-1})	$\pm$ error (mM^{-1}s^{-1})	Polymersome **3.4** r_1 (mM^{-1}s^{-1})	$\pm$ error (mM^{-1}s^{-1})
42.485	13.9468	0.35583	29.1871	1.42059	11.2262	0.4526
32.226	13.0277	0.34114	28.8367	1.37637	12.532	0.47005
24.151	12.5703	0.35946	27.3942	1.3068	10.8241	0.39216
18.095	11.9149	0.31532	25.4439	1.21532	10.4419	0.39374
13.56	11.5797	0.37432	24.2906	1.23797	8.71823	0.36866
10.165	11.2655	0.30497	22.3345	1.19751	7.61084	0.46985
7.6177	10.6191	0.26476	20.4367	0.98503	6.56897	0.3817
5.7081	10.3709	0.27915	20.2217	1.02722	7	0.42405
4.2784	10.2498	0.24824	19.4613	0.98773	7.42956	0.41578
3.2065	10.394	0.26049	19.3263	0.92909	7.9399	0.43684
2.401	10.7171	0.25894	19.5809	0.93411	7.23547	0.39227
1.8005	10.849	0.26617	20.0514	0.97972	8.60099	0.44634
1.3483	10.9211	0.26433	20.4173	0.9928	8.75616	0.44744
1.0104	11.2019	0.27076	20.8922	0.9895	8.50837	0.39931
0.75806	11.4886	0.27293	21.3698	1.01748	8.40739	0.38531
0.56802	11.6184	0.28249	21.7274	1.03445	8.70394	0.35741
0.42589	11.5538	0.27788	22.0061	1.04202	8.6468	0.36749
0.31839	11.6476	0.28257	21.7189	1.05168	9.30443	0.37775
0.23878	11.6388	0.28092	22.1196	1.09736	9.38719	0.3836
0.17926	11.8268	0.28324	21.8339	1.04392	8.98621	0.3988
0.13402	11.8385	0.29036	22.4487	1.08742	9.65369	0.36336
0.10033	11.9043	0.28695	22.6929	1.0932	9.2335	0.41176
0.07539	11.821	0.31517	22.6322	1.09317	9.44483	0.38747
0.05663	11.8748	0.30641	22.2902	1.11094	9.55961	0.36876
0.04216	11.8676	0.29306	22.4021	1.11577	9.57291	0.3576
0.03178	11.819	0.29499	22.1639	1.06491	9.82512	0.38554
0.02384	11.8798	0.28709	23.2296	1.14638	10.3557	0.42257
0.01787	11.8476	0.2852	22.3151	1.11062	9.82217	0.41358
0.01332	11.8582	0.28578	22.7316	1.1307	9.86355	0.39769
0.01005	11.8228	0.28582	22.4915	1.09679	9.75123	0.43025

Table A3.2. NMRD data for **3.1**, **3.3**, and **3.4** at 298 K.

Frequency (MHz)	Dendron **3.1**		Polymersome **3.3**		Polymersome **3.4**	
	r_1 (mM^{-1}s^{-1})	± error (mM^{-1}s^{-1})	r_1 (mM^{-1}s^{-1})	± error (mM^{-1}s^{-1})	r_1 (mM^{-1}s^{-1})	± error (mM^{-1}s^{-1})
42.485	12.12974	0.308419	24.70432	1.202339	7.675889	0.440764
32.226	11.57483	0.297817	24.32695	1.155758	8.508374	0.430055
24.151	11.01165	0.274025	22.76779	1.093878	8.187685	0.326891
18.095	10.7773	0.27112	22.62621	1.143689	8.252217	0.299043
13.56	10.24124	0.256736	20.18495	1.146539	7.230542	0.327636
10.165	9.982981	0.278239	18.49589	0.994324	7.226601	0.373374
7.6177	9.529907	0.25443	17.33842	0.933652	8.051232	0.296329
5.7081	9.277963	0.23684	17.1	0.829593	8.232512	0.332303
4.2784	9.143037	0.238939	16.54358	0.808106	8.333005	0.291729
3.2065	9.123537	0.244629	16.73642	0.863996	8.324138	0.299654
2.401	9.458981	0.230666	17.21684	0.82571	8.579803	0.314226
1.8005	9.874537	0.243801	17.83	0.867142	8.837931	0.308924
1.3483	9.832926	0.240478	18.03611	0.870415	8.933498	0.332639
1.0104	10.1245	0.248905	18.38716	0.890337	9.749754	0.369044
0.75806	10.34187	0.251679	18.62432	0.894888	9.553202	0.355386
0.56802	10.38541	0.25377	18.94705	0.902074	9.370443	0.363834
0.42589	10.43285	0.252389	19.09358	0.900006	9.554187	0.357284
0.31839	10.40139	0.256121	19.66316	0.993456	9.399507	0.317746
0.23878	10.68167	0.260583	19.30158	0.971088	9.200985	0.36774
0.17926	10.60106	0.259376	19.65337	1.000355	10.14089	0.408701
0.13402	10.56869	0.26436	19.45042	0.941913	9.776355	0.334029
0.10033	10.71293	0.271159	19.16611	0.964125	8.791133	0.312885
0.07539	10.44635	0.26105	19.23768	0.986247	9.223645	0.444246
0.05663	10.56539	0.261974	19.69958	0.963367	9.727094	0.362393
0.04216	10.60959	0.263527	19.95242	0.991791	10.94581	0.552264
0.03178	10.62474	0.269735	19.43695	0.970396	9.330049	0.466202
0.02384	10.67987	0.273295	19.96768	0.987754	11.52217	0.519033
0.01787	10.6393	0.26195	19.37705	0.942645	10.90394	0.478739
0.01332	10.67291	0.26032	19.19758	0.93875	11.66059	0.553324
0.01005	10.57759	0.257902	18.79895	0.949368	9.871429	0.493652

Table A3.3. NMRD data for unpurified compound **3.2** at 298 and 310 K.

Frequency (MHz)	298 K		310 K	
	r_1 (mM^{-1}s^{-1})	± error (mM^{-1}s^{-1})	r_1 (mM^{-1}s^{-1})	± error (mM^{-1}s^{-1})
42.485	7.164357	0.239302	5.806553	0.198736
32.226	7.4717	0.26715	5.95605	0.215379
24.151	7.61	0.262536	6.12295	0.210226
18.095	7.84835	0.270608	6.39345	0.238233
13.56	7.81255	0.283246	6.5026	0.224501
10.165	7.442025	0.292533	5.94605	0.282405
7.6177	7.62545	0.265663	6.40275	0.239543
5.7081	7.9683	0.285034	6.863	0.251785
4.2784	8.0546	0.278805	6.9062	0.243733
3.2065	8.51975	0.290723	7.11605	0.247265
2.401	8.4612	0.286282	7.456	0.257229
1.8005	8.84115	0.296912	7.66125	0.268017
1.3483	8.9957	0.302398	7.78315	0.265708
1.0104	9.1258	0.306825	7.8839	0.261812
0.75806	9.1464	0.30944	7.87605	0.289503
0.56802	9.241	0.31658	7.83935	0.275286
0.42589	9.3689	0.317881	8.01545	0.269447
0.31839	9.29925	0.317361	7.88775	0.277594
0.23878	9.37455	0.320122	8.0635	0.278503
0.17926	9.46935	0.319043	7.95385	0.272022
0.13402	9.3859	0.315734	8.1297	0.274145
0.10033	9.3894	0.312762	8.0159	0.268276
0.075388	9.5268	0.314929	8.15365	0.276447
0.056625	9.3446	0.314749	8.15405	0.283728
0.042161	9.4225	0.32211	8.1109	0.272298
0.031778	9.4146	0.323253	7.9203	0.275189
0.023836	9.3698	0.3204	8.03265	0.276627
0.017874	9.43465	0.32513	8.1256	0.273448
0.013316	9.38825	0.319244	8.0661	0.279237
0.010053	9.32145	0.320652	8.10275	0.289865
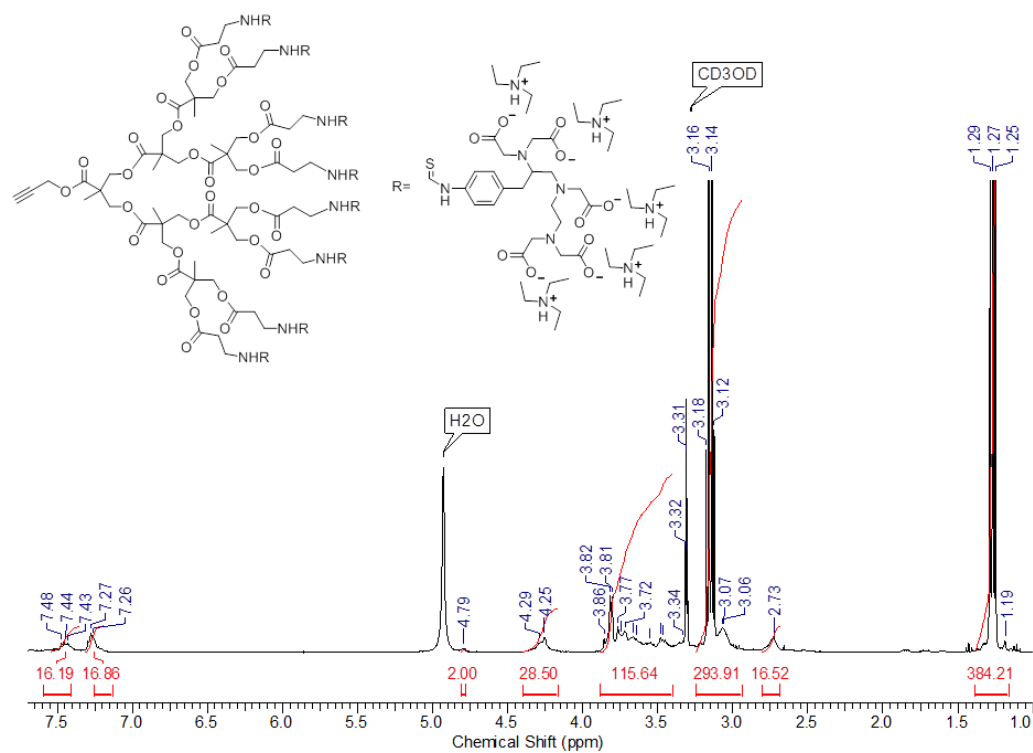
Figure A3.5. ^{1}H NMR of dendron **3.7** (400 MHz , CD$_3$OD).
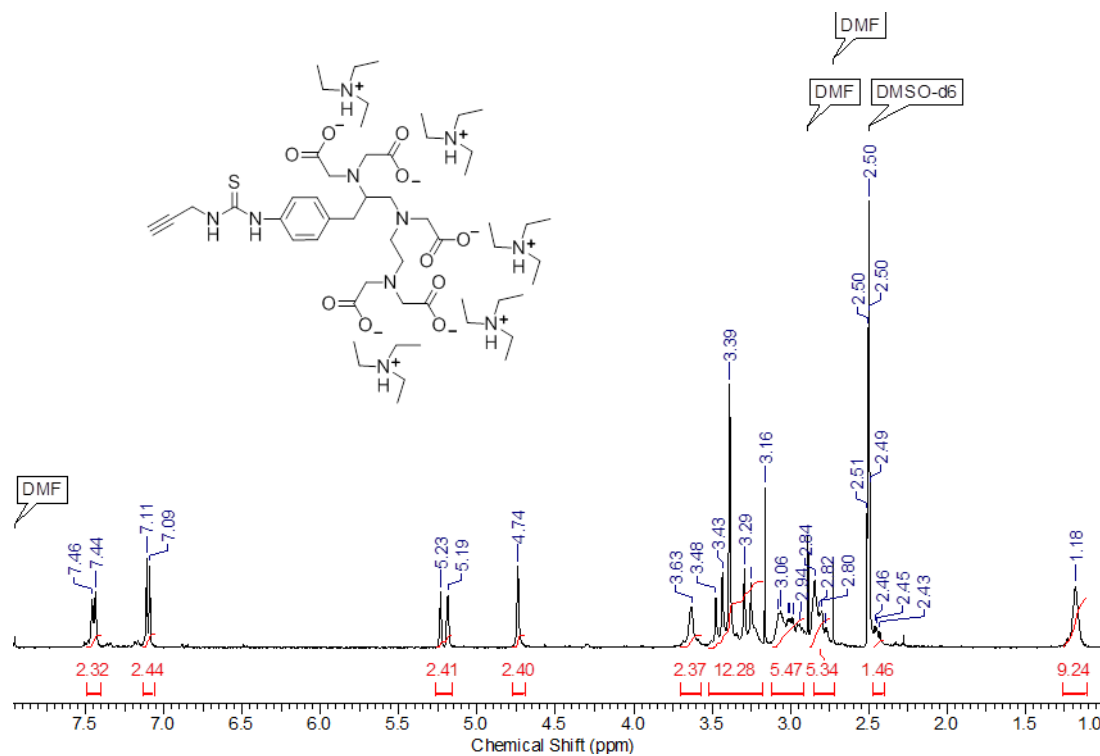
Figure A3.6. ^{1}H NMR of compound **3.8** (400 MHz , (CD$_3$)$_2$SO).

Appendix 4: Supporting Information for Chapter 4
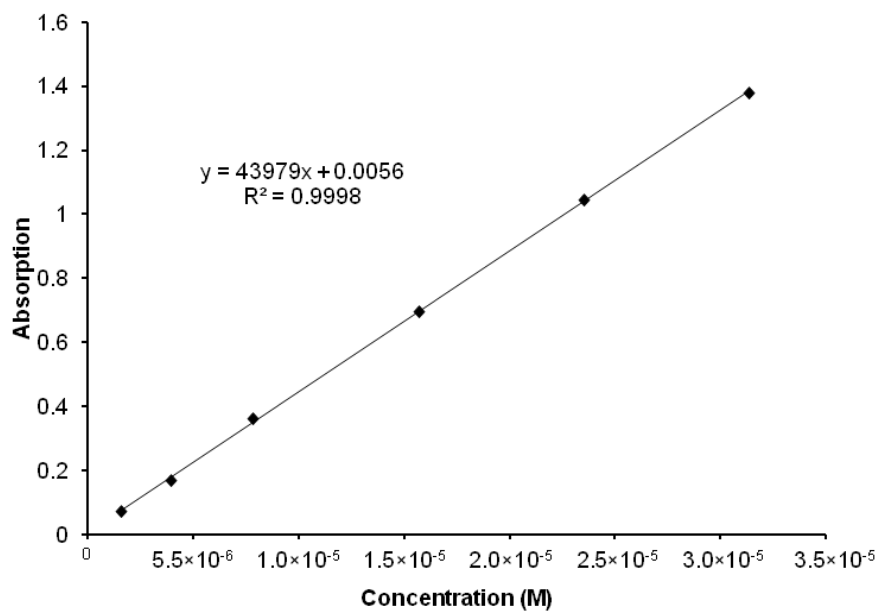
Figure A4.1. Calibration curve for the determination of extinction coefficient of rhodamine-labeled sialodendron **4.4**.
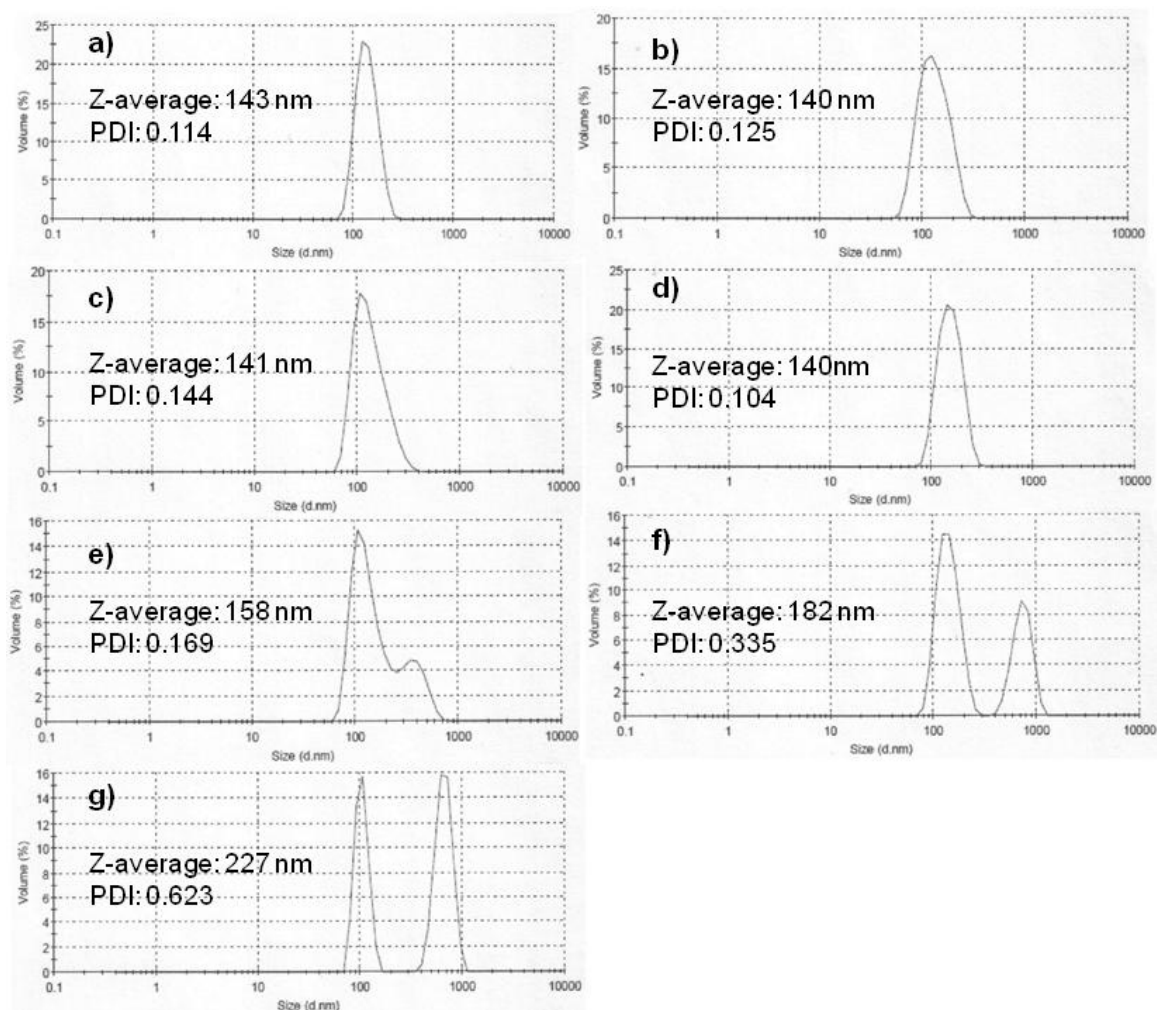
Figure A4.2. Size distribution profiles following functionalization of polymersomes containing (a) 5 wt%; (b) 7 wt%; (c) 10 wt%; (d) 20 wt%; (e) 40 wt%; (f) 70 wt%; and (g) 100 wt% azide copolymer **2.6** with the rhodamine-labeled sialodendron **4.4**.

a)

		Size (d.nm):	% Intensity	Width (d.nm):
Z-Average (d.nm): 138.1	Peak 1:	158.5	100.0	59.14
PdI: 0.130	Peak 2:	0.000	0.0	0.000
Intercept: 0.960	Peak 3:	0.000	0.0	0.000
Result quality : Good				

b)

		Size (d.nm):	% Intensity	Width (d.nm):
Z-Average (d.nm): 141.7	Peak 1:	159.9	100.0	57.33
PdI: 0.109	Peak 2:	0.000	0.0	0.000
Intercept: 0.970	Peak 3:	0.000	0.0	0.000
Result quality : Good				
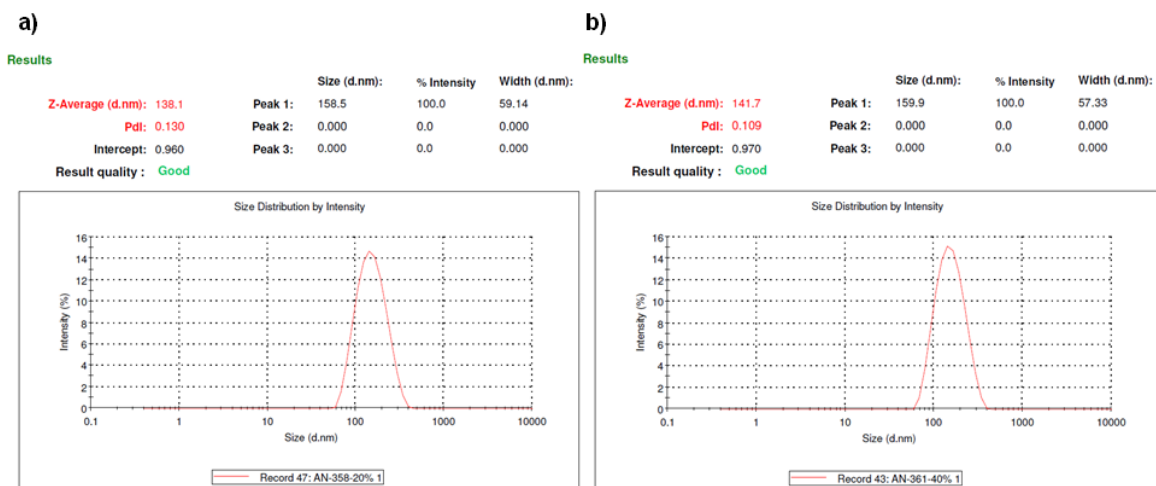
Figure A4.3. Intensity-based size distribution profiles for polymersomes composed of a) 20% w/w azide-functionalized copolymer **2.6** and b) 40% w/w azide-functionalized copolymer **2.6** following "click" conjugation of dendron **4.3**.

a) Z-average: 145 nm

b) Z-average: 154 nm
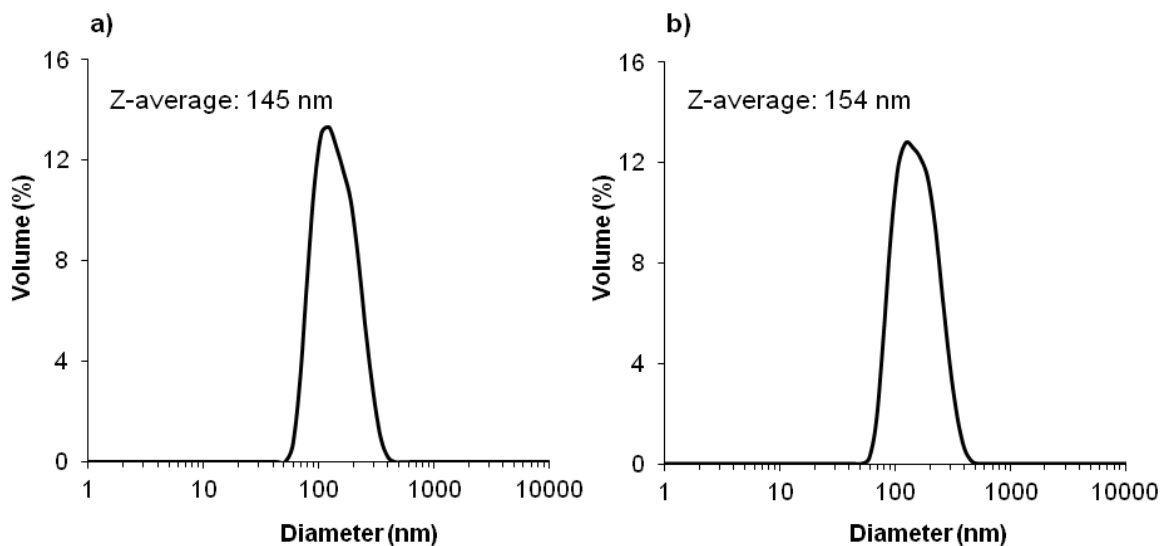
Figure A4.4. Size distribution profiles for (a) zanamivir-loaded naked polymersomes and (b) zanamivir loaded dendritic sialopolymersomes.
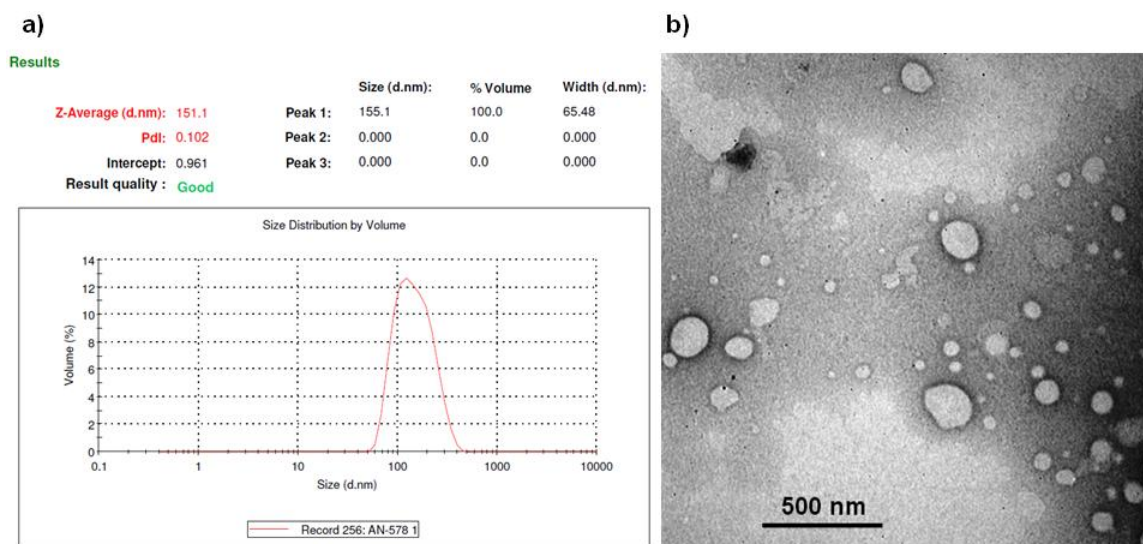
Figure A4.5. a) Size distribution profile and b) TEM image of zanamivir-loaded naked polymersomes after releasing the drug.
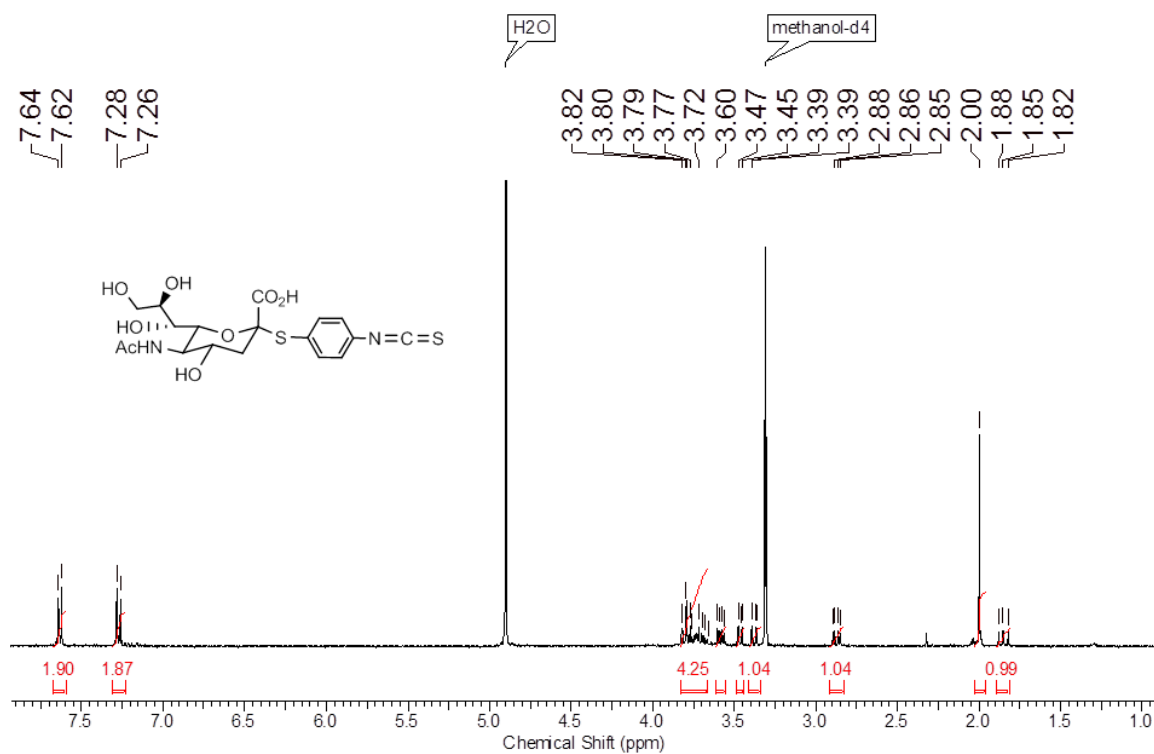
Figure A4.6. ^{1}H NMR spectrum of compound **4.2** (400 MHz, CD$_3$OD).
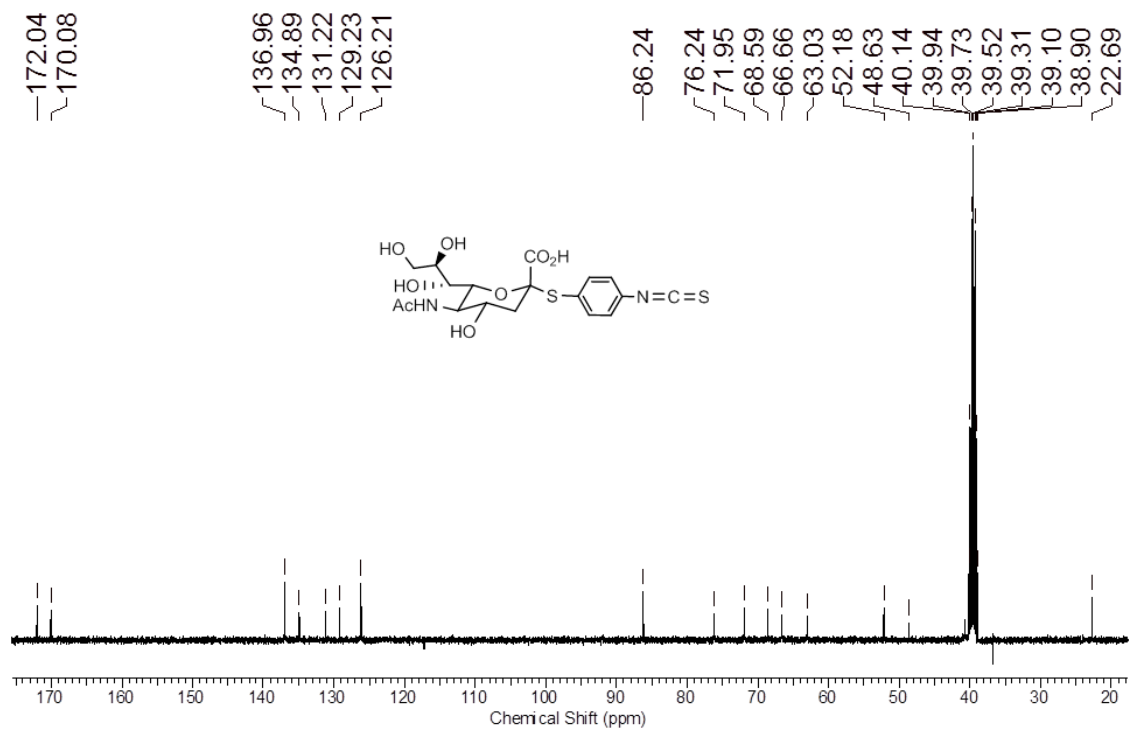
Figure A4.7. ^{13}C NMR spectrum of compound **4.2** (100 MHz, (CD$_3$)$_2$SO).
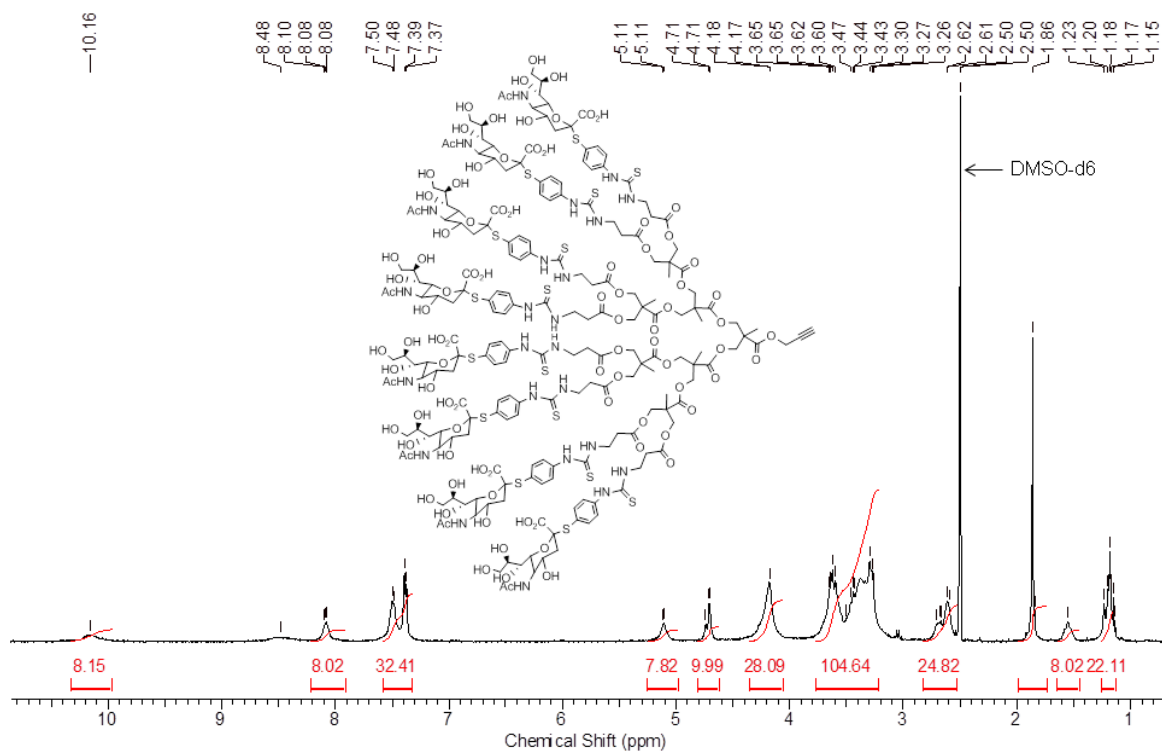
Figure A4.8. ^{1}H NMR spectrum of sialodendron **4.3** (400 MHz, (CD$_3$)$_2$SO).
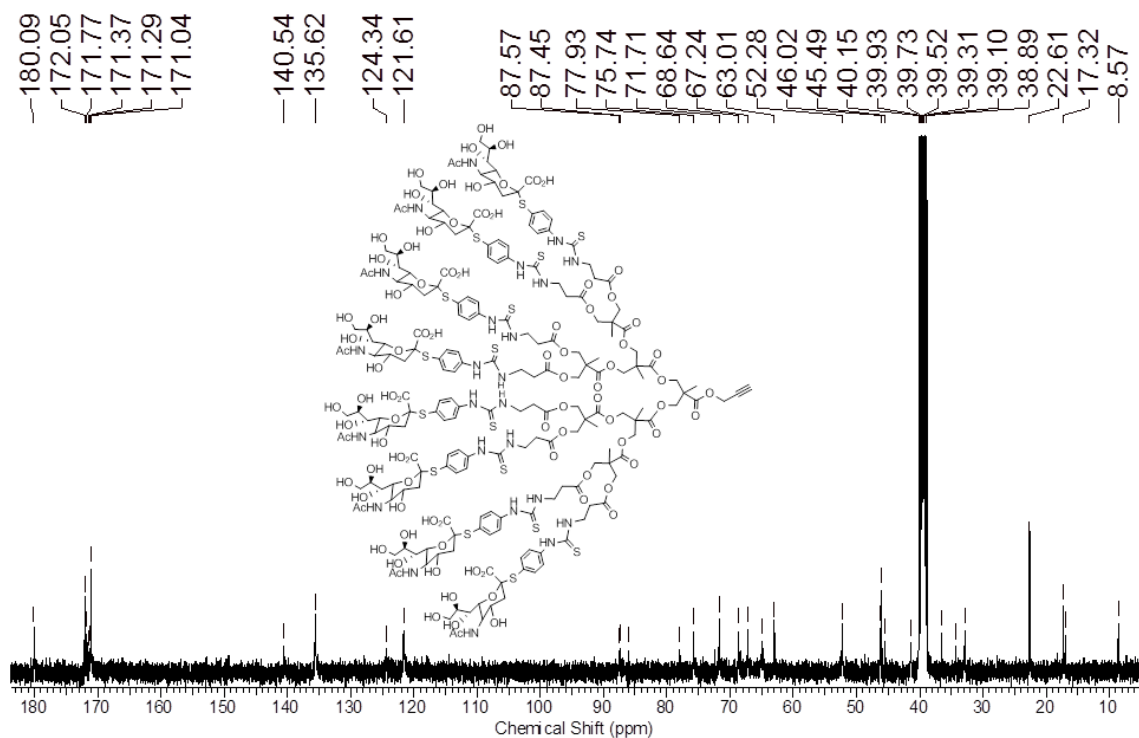
Figure A4.9. ^{13}C NMR spectrum of sialodendron **4.3** (100 MHz, (CD$_3$)$_2$SO).
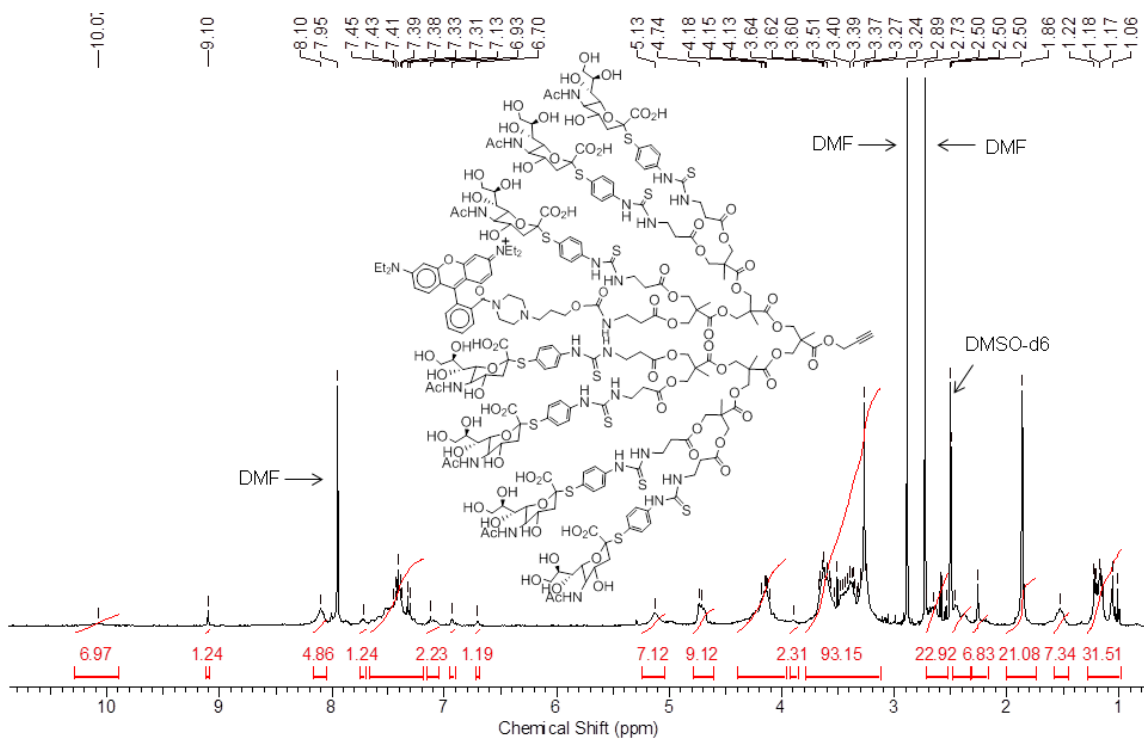
Figure A4.10. ^{1}H NMR spectrum of rhodamine-labeled sialodendron **4.4** (400 MHz, (CD$_3$)$_2$SO).

Appendix 5: Supporting Information for Chapter 5
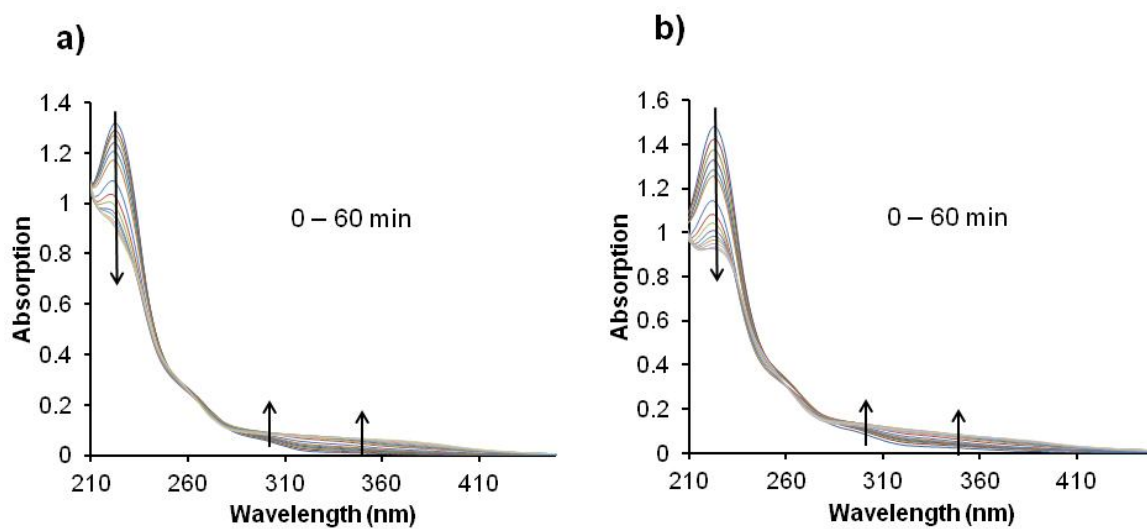
Figure A5.1. Evolution of UV-visible spectra for a) G1 dendrimer (**5.14**) and b) G2 dendrimer (**5.15**) upon irradiation with 350 nm light for 60 minutes.
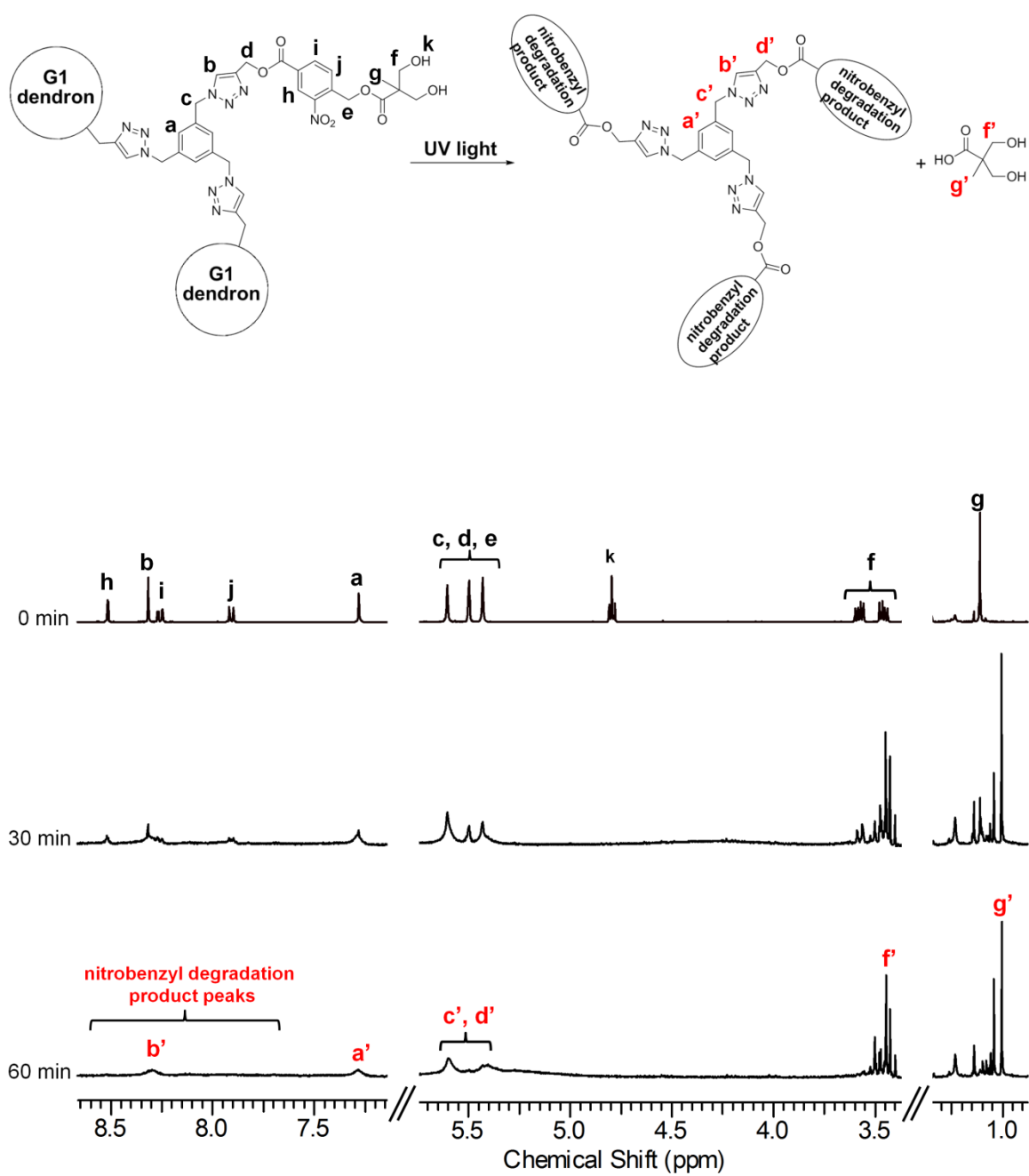
Figure A5.2. Evolution of ^{1}H NMR spectra during the photolysis of G1 dendrimer (**5.14**) in (CD$_3$)$_2$SO at 400 MHz.
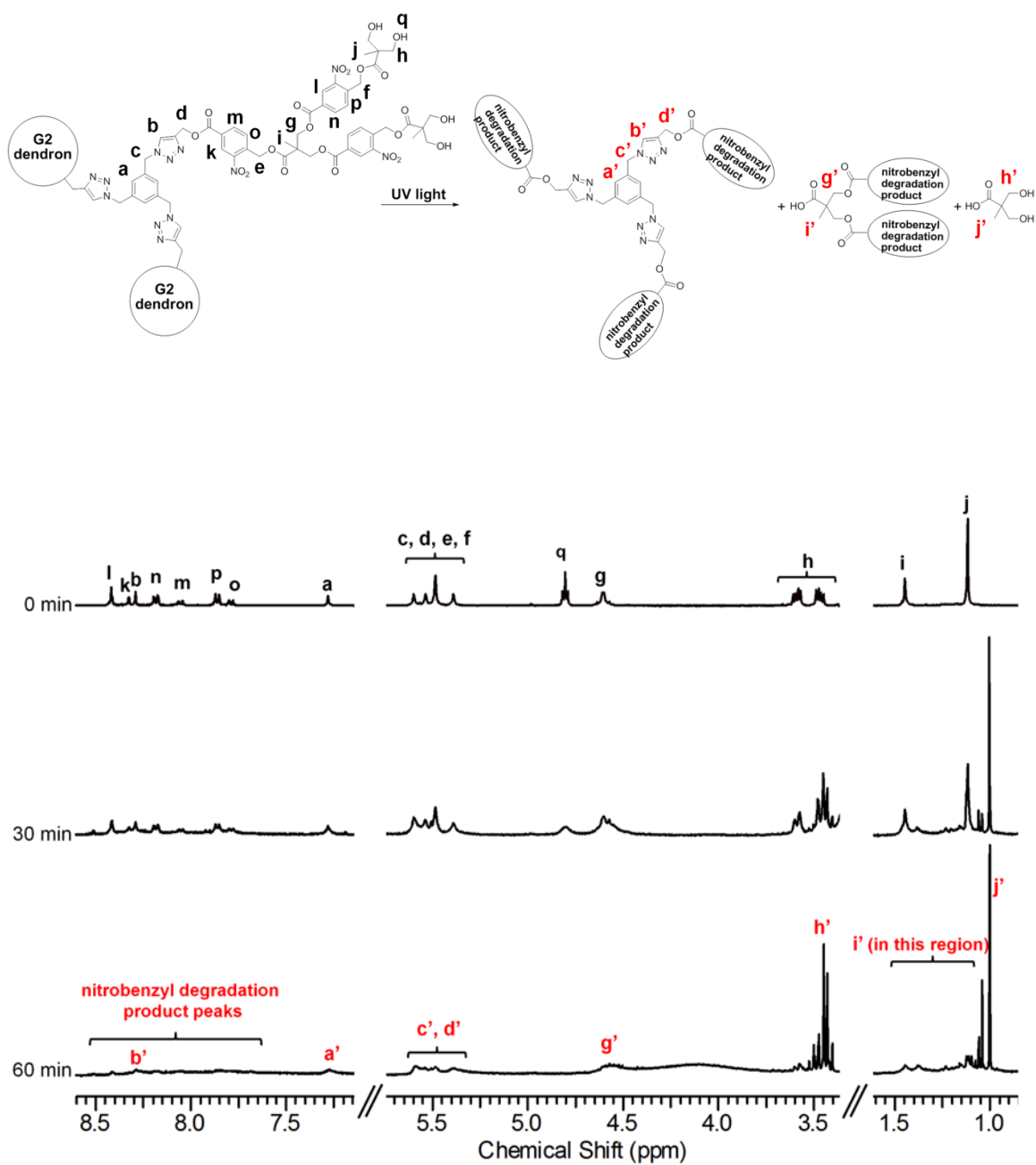
Figure A5.3. Evolution of ^{1}H NMR spectra during the photolysis of G2 dendrimer (**5.15**) in (CD$_3$)$_2$SO at 400 MHz.
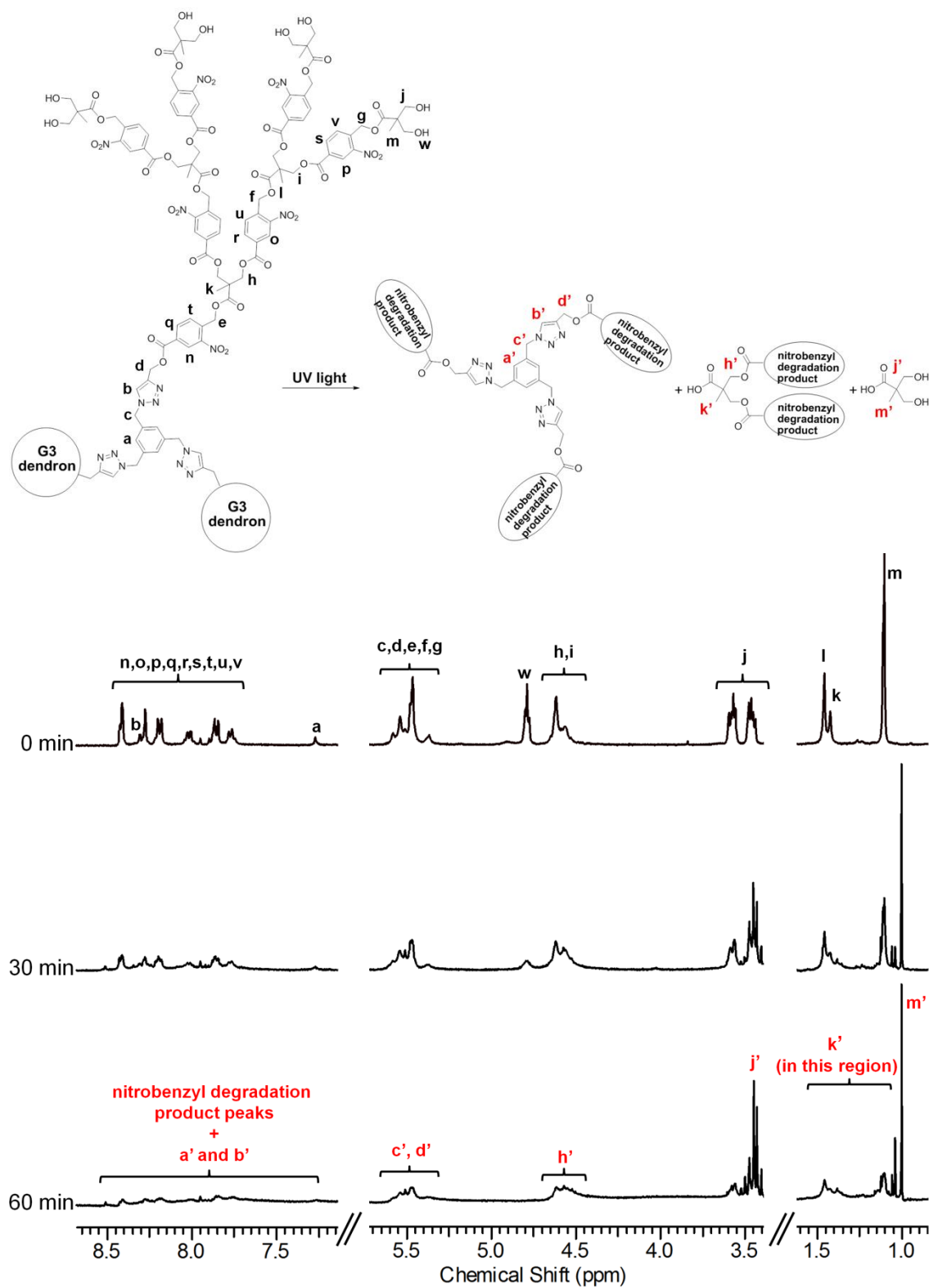
Figure A5.4. Evolution of ^{1}H NMR spectra during the photolysis of G3 dendrimer (**5.16**) in (CD$_3$)$_2$SO at 400 MHz.
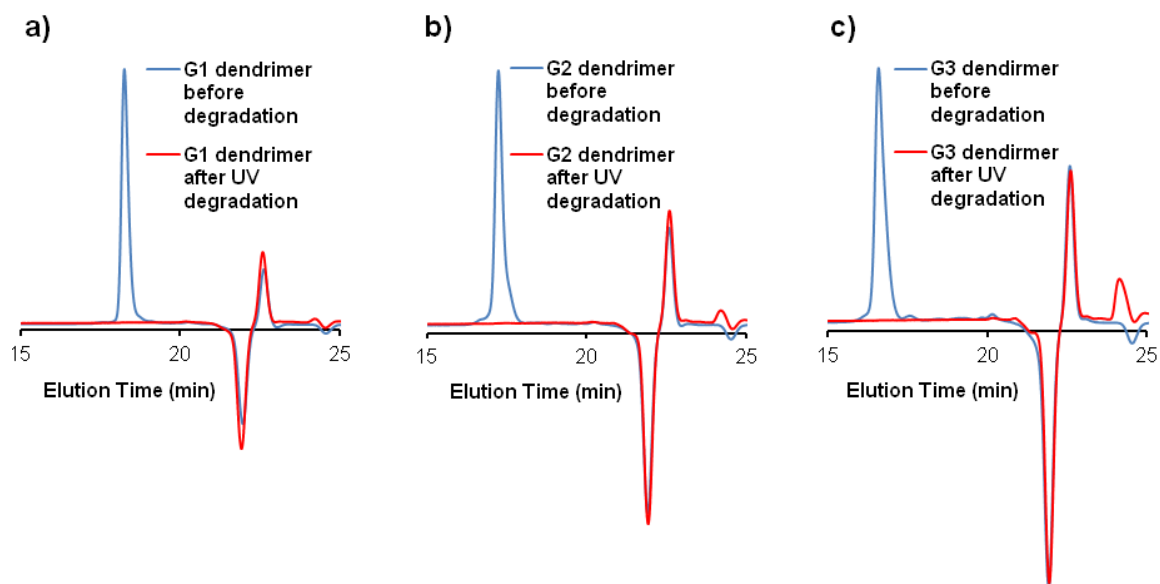
Figure A5.5. SEC traces of a) G1 dendrimer **5.14**, b) G2 dendrimer **5.15**, and c) G3 dendirmer **5.16** before and after UV degradation.
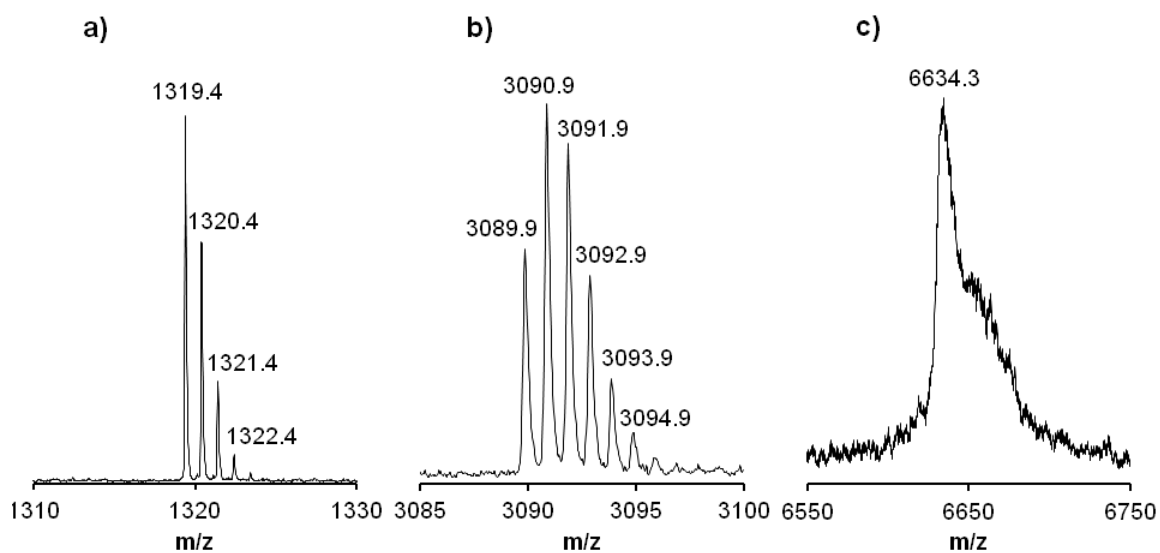
Figure A5.6. MALDI-TOF spectra for a) G1 dendrimer **5.14**, b) G2 dendrimer **5.15**, and c) G3 dendrimer **5.16**. It should be noted that the laser used for MALDI-TOF experiments operates at 360 nm and thus effectively photodegrades the dendrimers. As a result, some photodegradation products were also observed in these spectra, which are not shown.
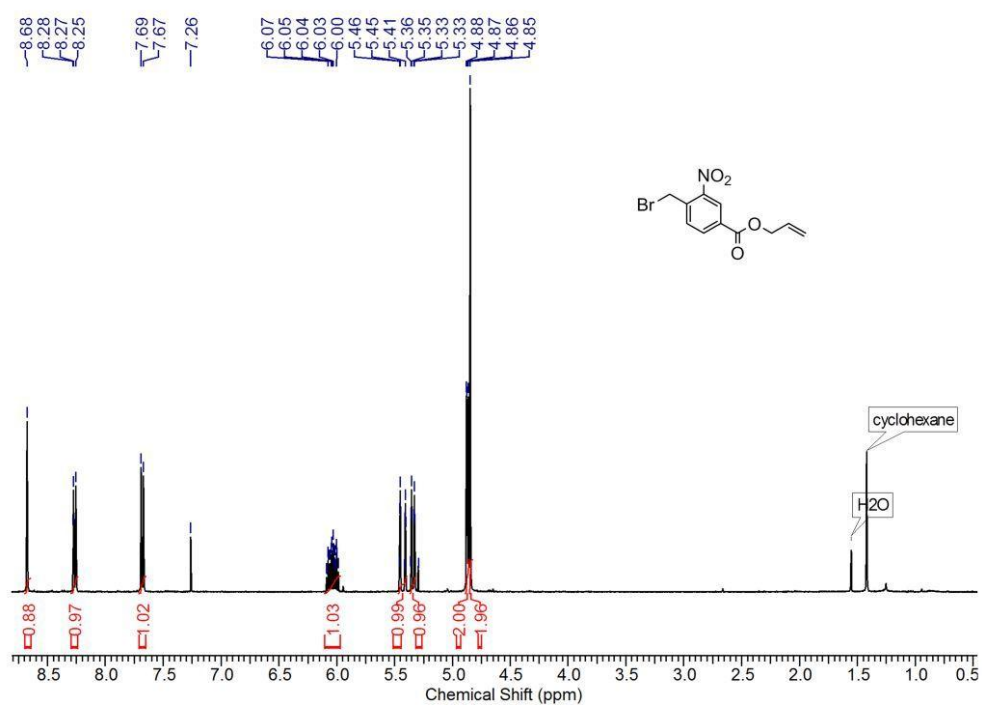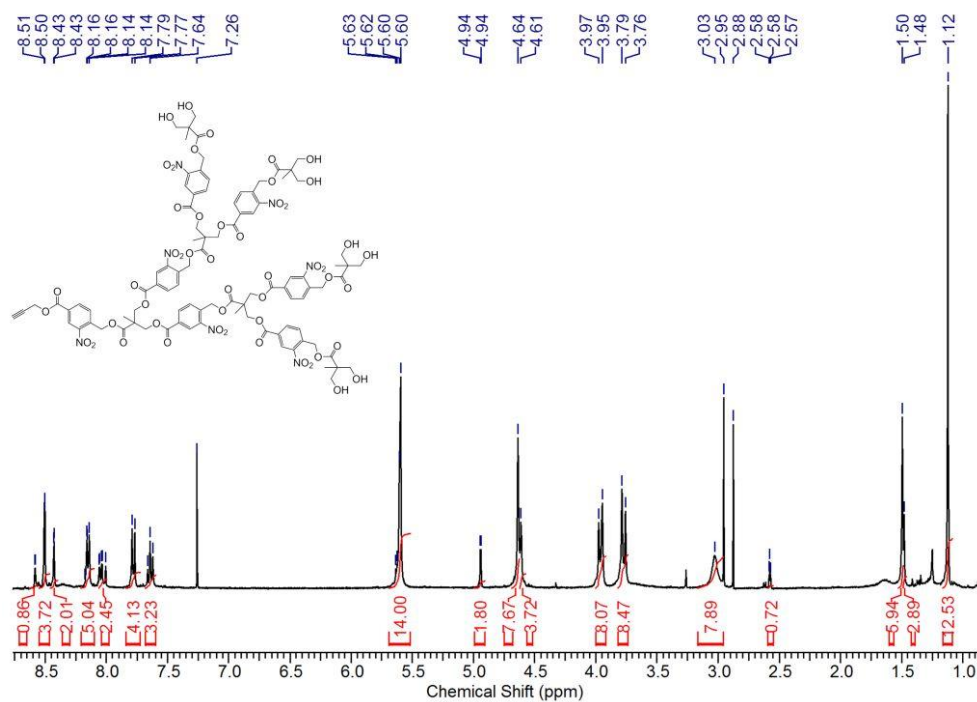
Figure A5.7. ^{1}H NMR spectrum of compound **5.2** (400 MHz, CDCl$_3$).
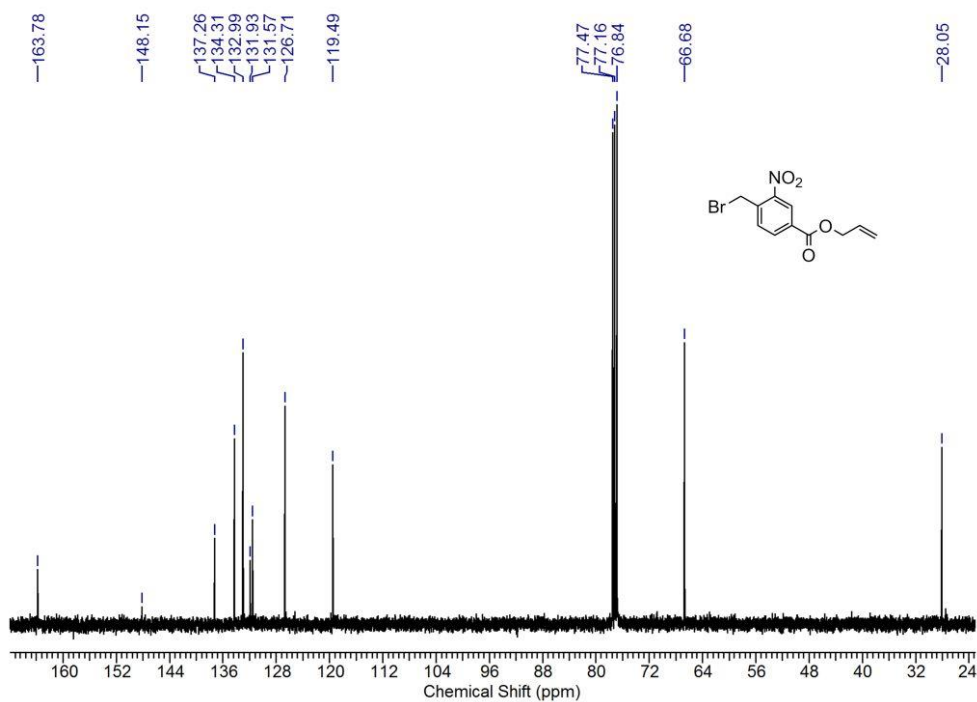
Figure A5.8. ^{13}C NMR spectrum of compound **5.2** (100 MHz, CDCl$_3$).
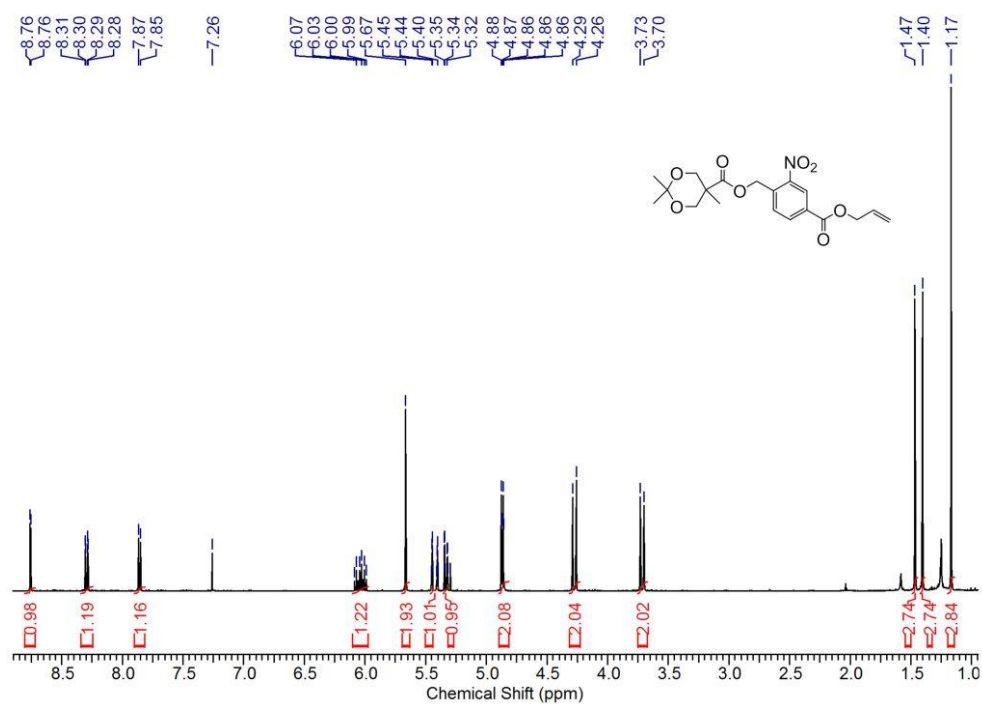
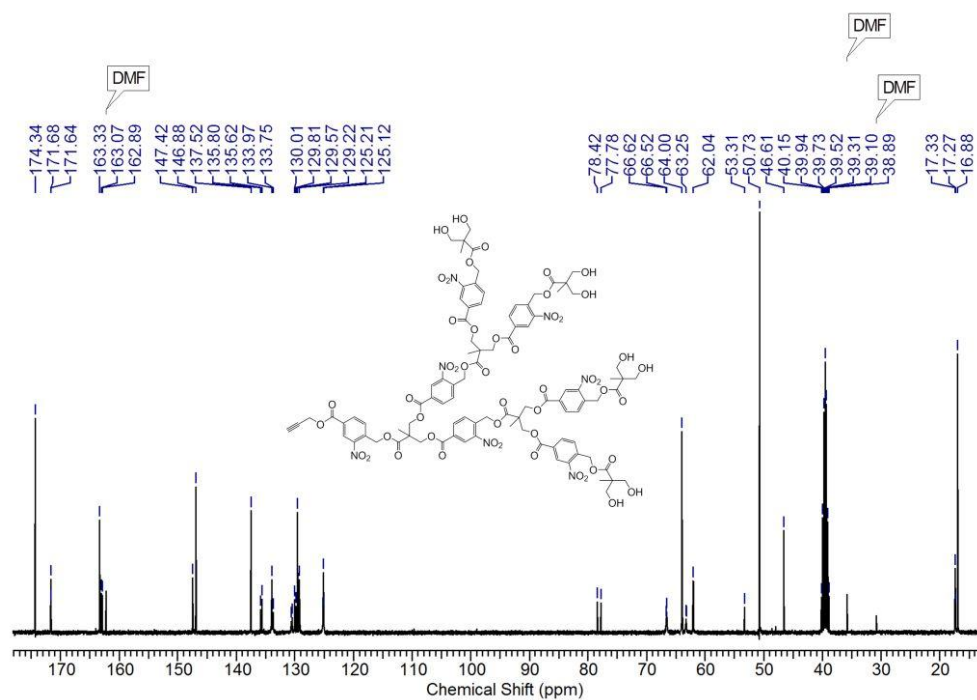**Figure A5.9**. ^{1}H NMR spectrum of compound **5.4** (400 MHz, CDCl$_3$).
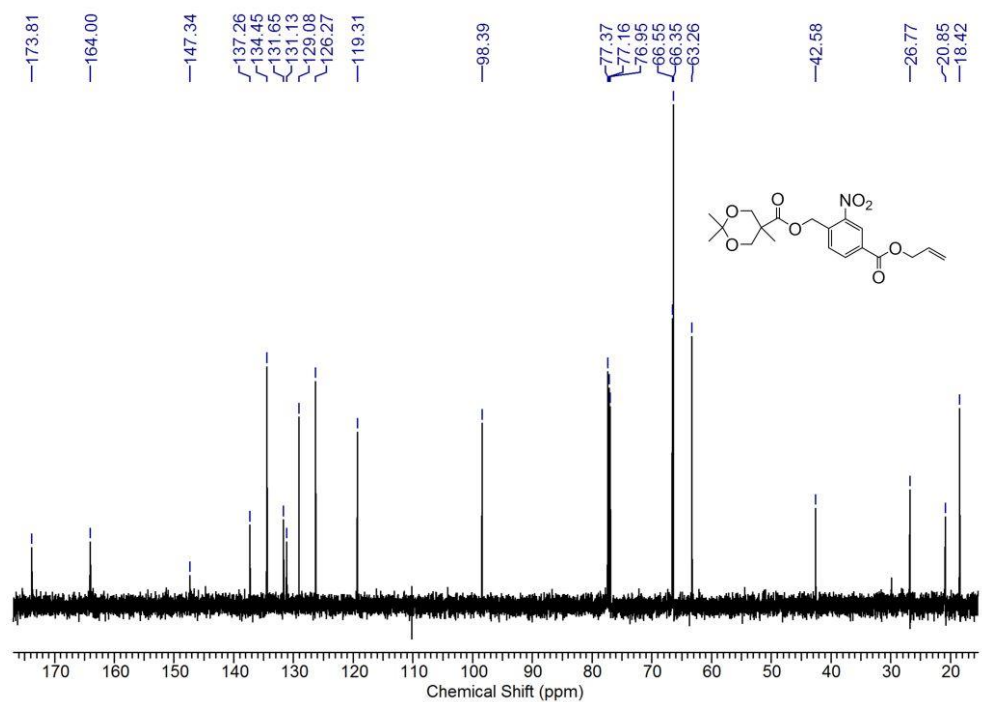
Figure A5.10. ^{13}C NMR spectrum of compound **5.4** (100 MHz, CDCl$_3$).
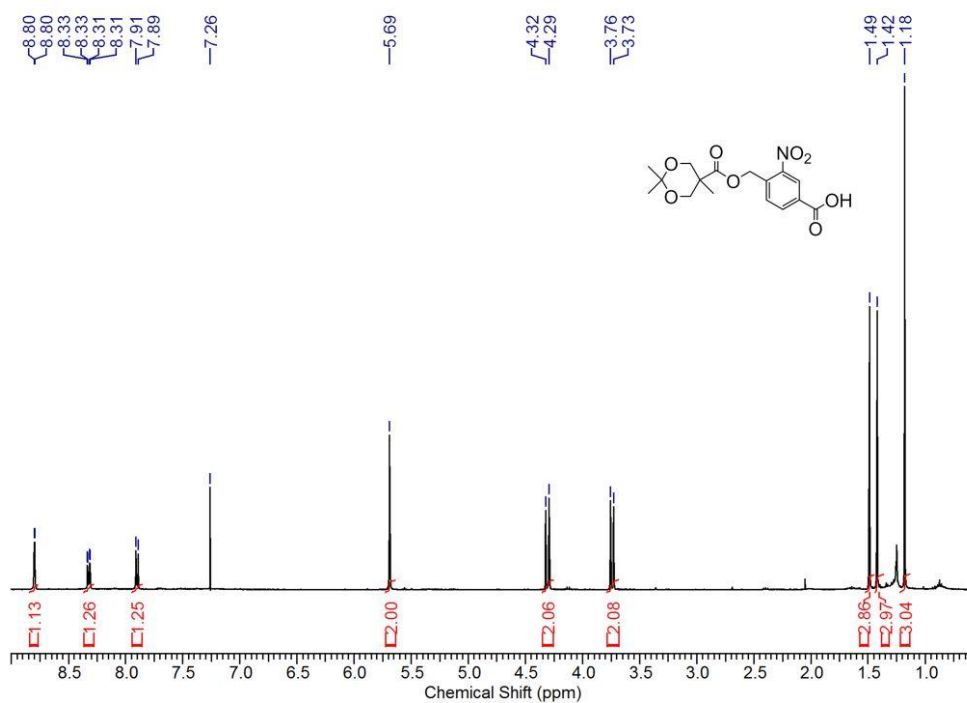
Figure A5.11. ^{1}H NMR spectrum of compound **5.5** (400 MHz, CDCl$_3$).
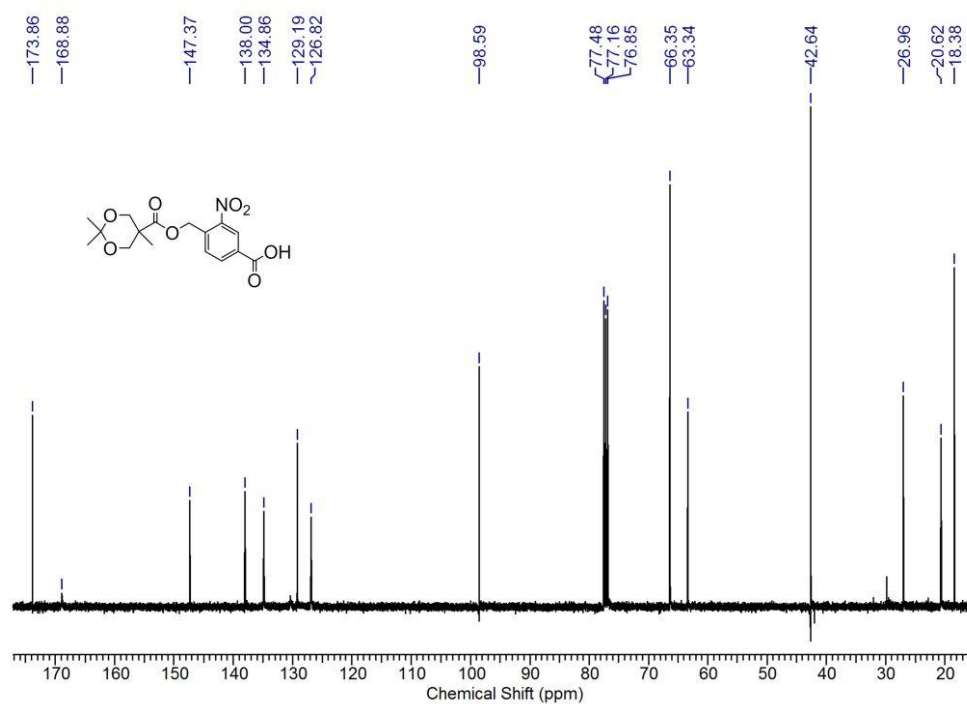
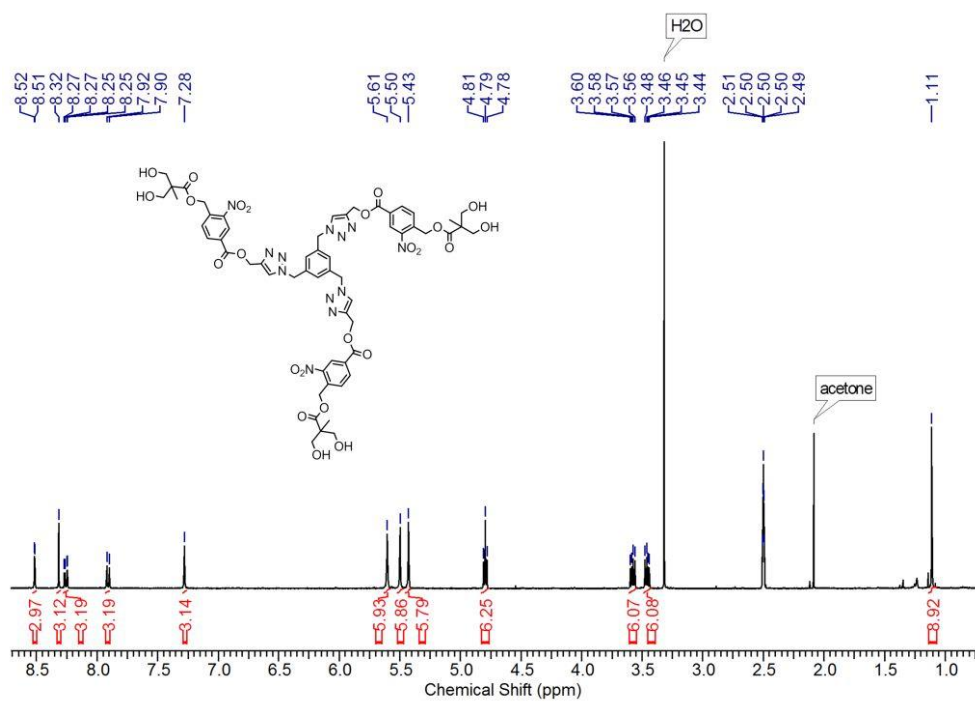**Figure A5.12**. ^{13}C NMR spectrum of compound **5.5** (100 MHz, CDCl$_3$).
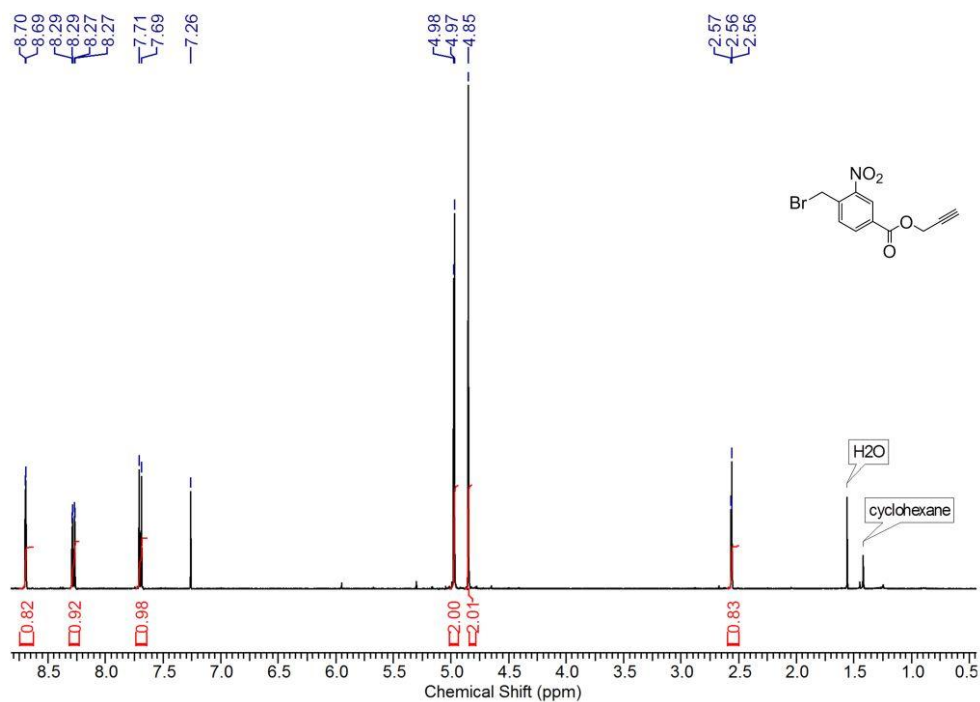
Figure A5.13. ^{1}H NMR spectrum of compound **5.6** (400 MHz, CDCl$_3$).
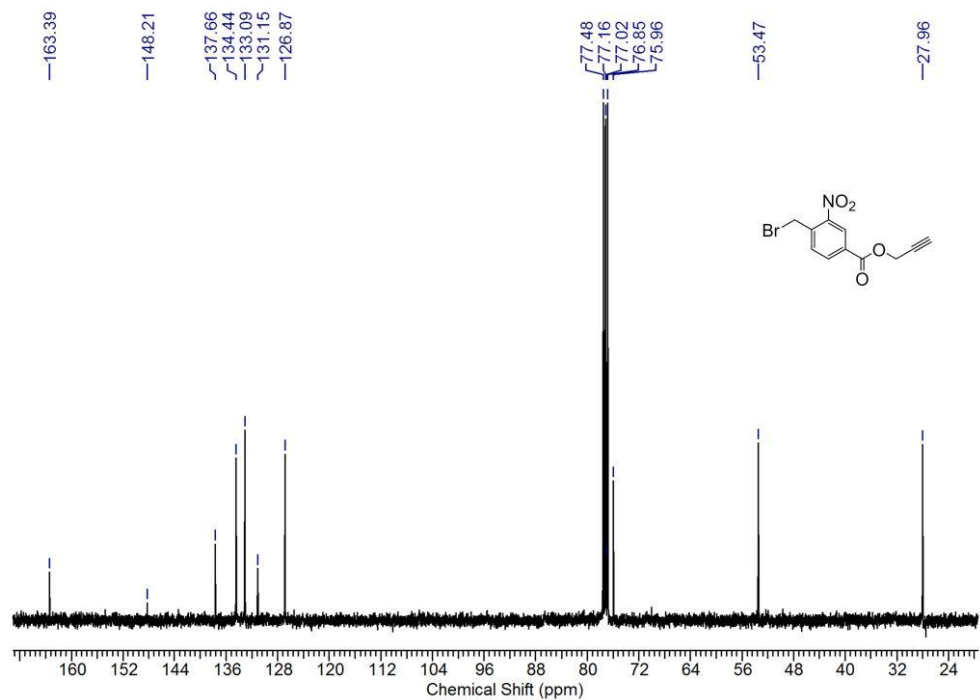
Figure A5.14. ^{13}C NMR spectrum of compound **5.6** (100 MHz, CDCl$_3$).
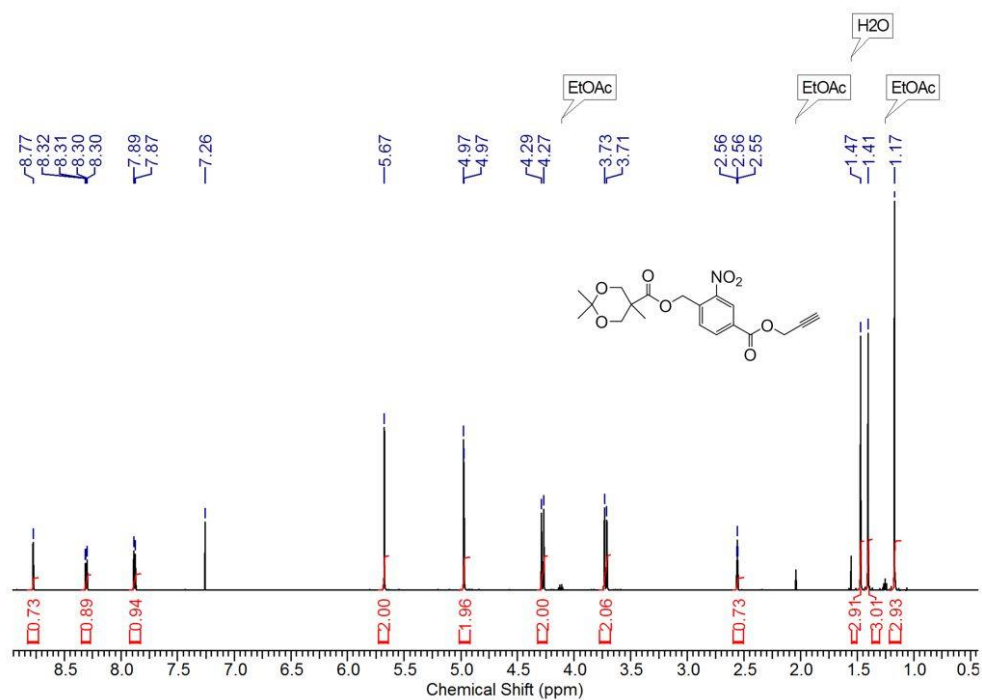
Figure A5.15. ^{1}H NMR spectrum of compound **5.7** (400 MHz, CDCl$_3$).
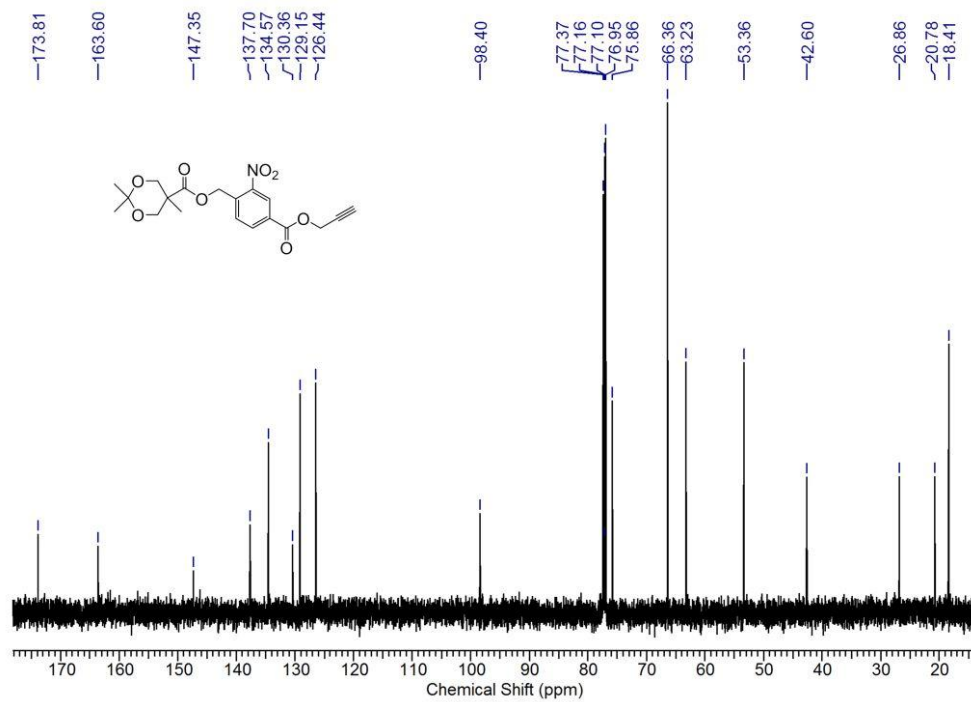
Figure A5.16. ^{13}C NMR spectrum of compound **5.7** (100 MHz, CDCl$_3$).
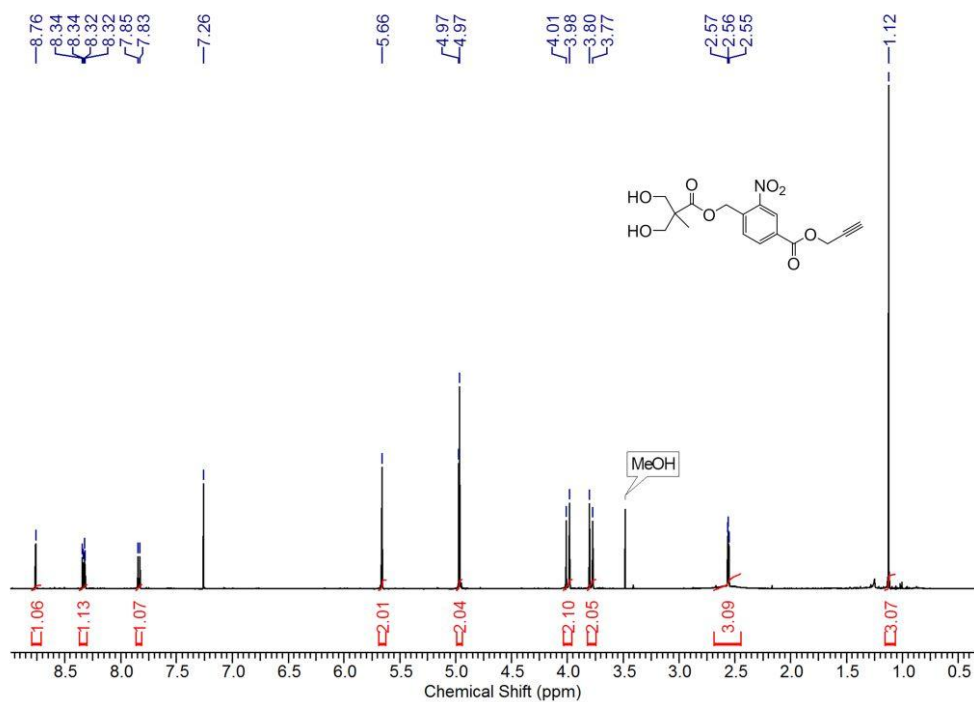
Figure A5.17. ^{1}H NMR spectrum of compound **5.8** (400 MHz, CDCl$_3$).
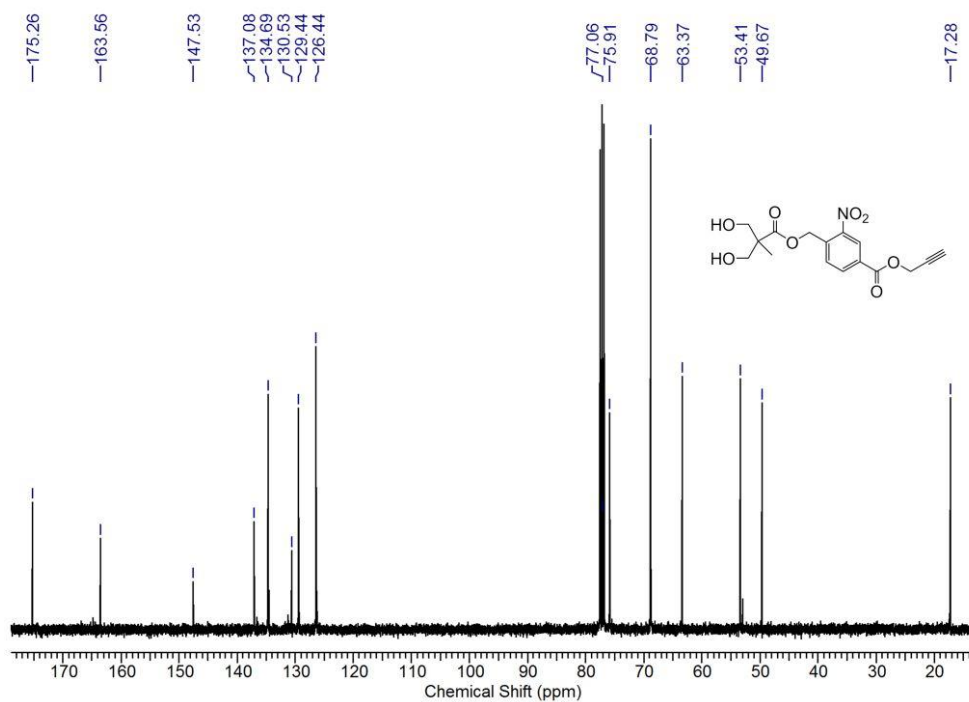
Figure A5.18. ^{13}C NMR spectrum of compound **5.8** (100 MHz, CDCl$_3$).
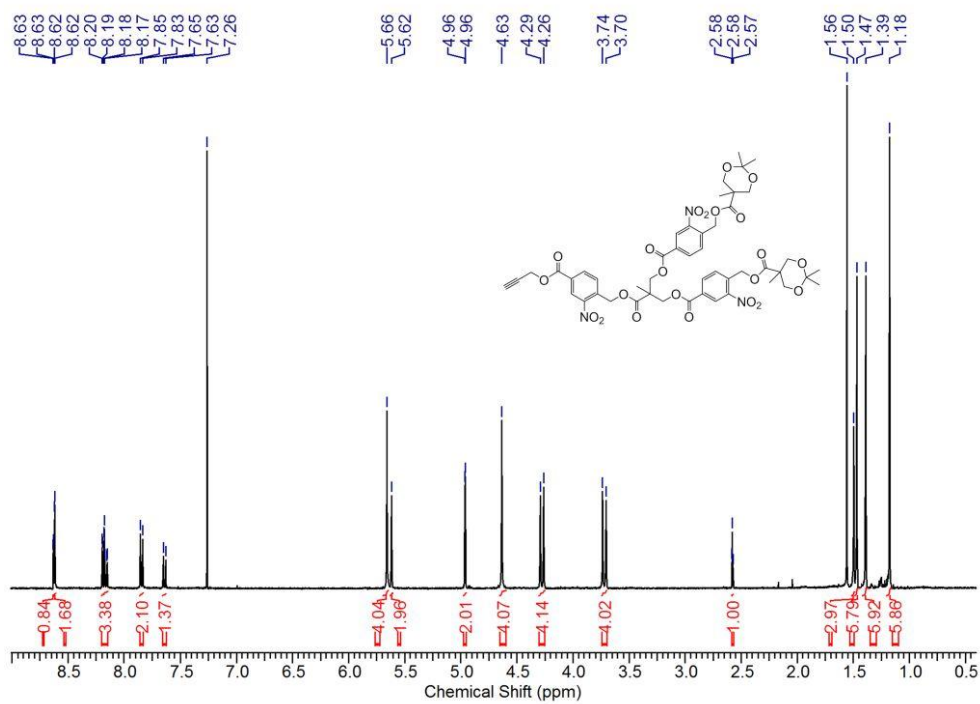
Figure A5.19. ^{1}H NMR spectrum of compound **5.9** (400 MHz, CDCl$_3$).
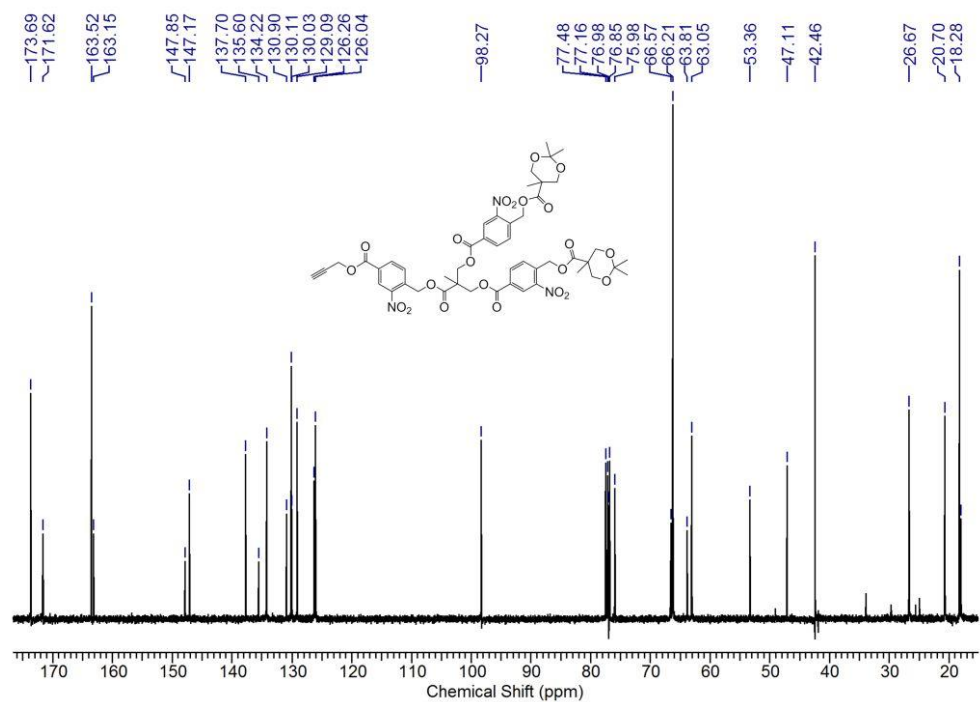
Figure A5.20. ^{13}C NMR spectrum of compound **5.9** (100 MHz, CDCl$_3$).
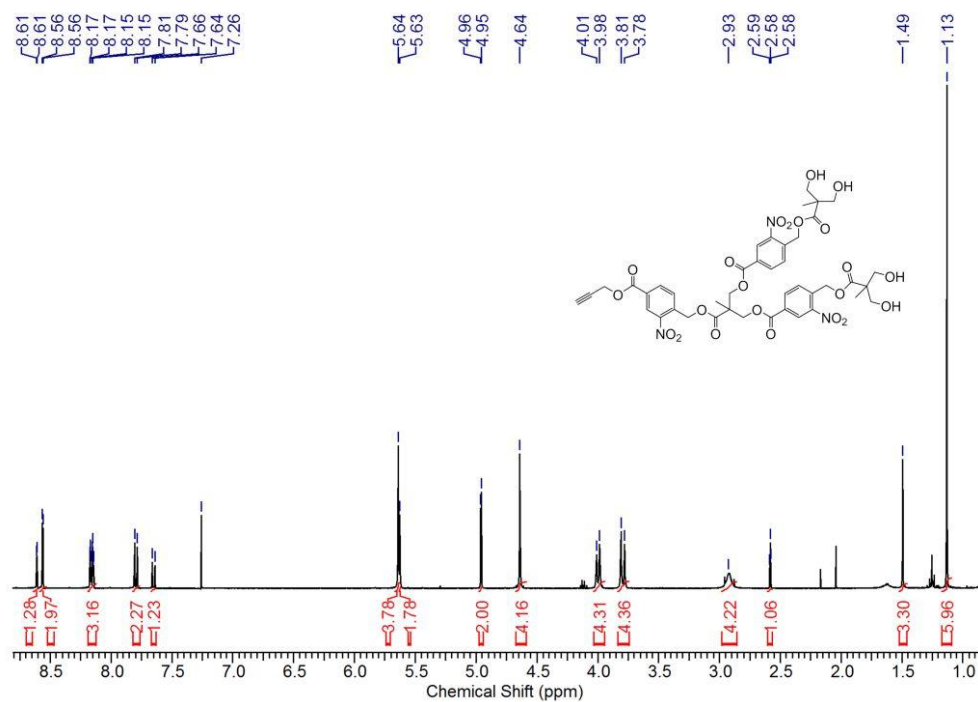
Figure A5.21. ^{1}H NMR spectrum of compound **5.10** (400 MHz, CDCl$_3$).
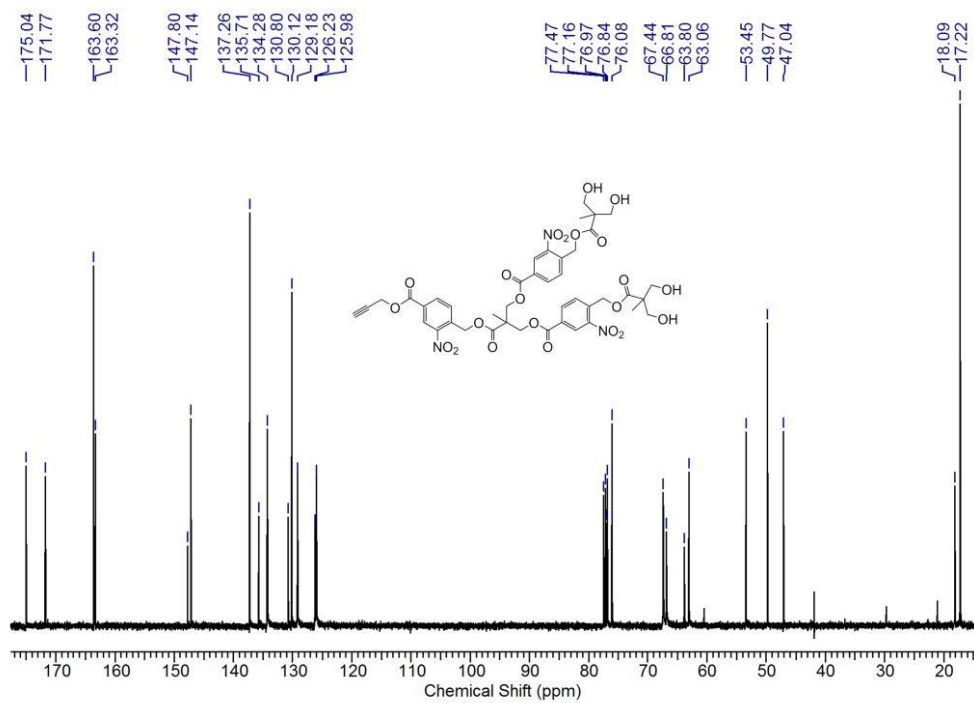
Figure A5.22. ^{13}C NMR spectrum of compound **5.10** (100 MHz, CDCl$_3$).
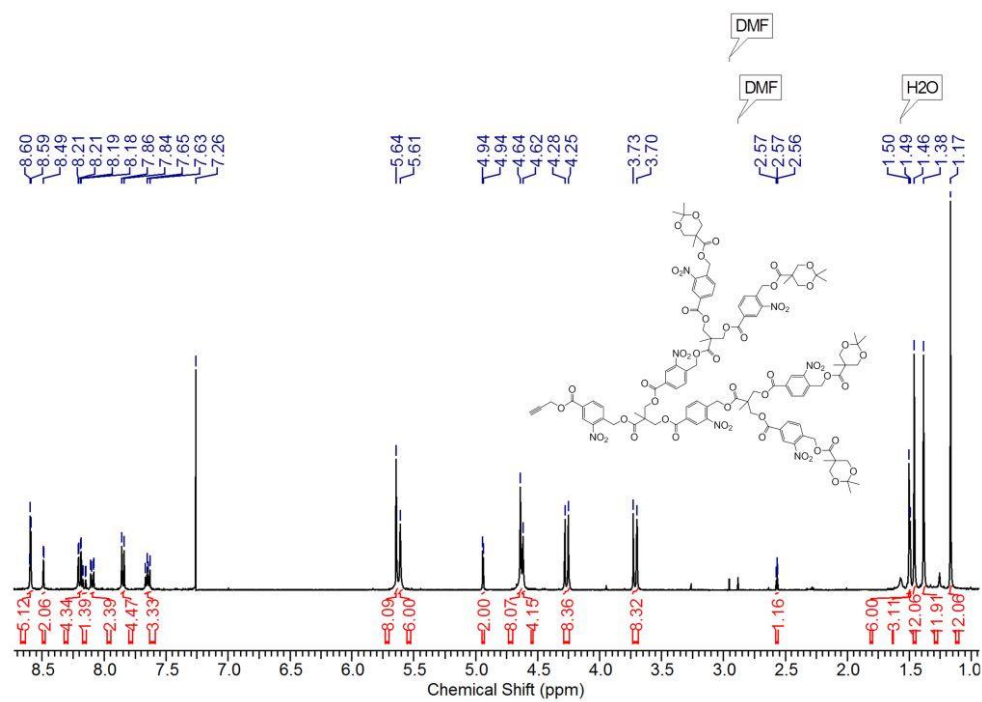
Figure A5.23. ^{1}H NMR spectrum of compound **5.11** (400 MHz, CDCl$_3$).
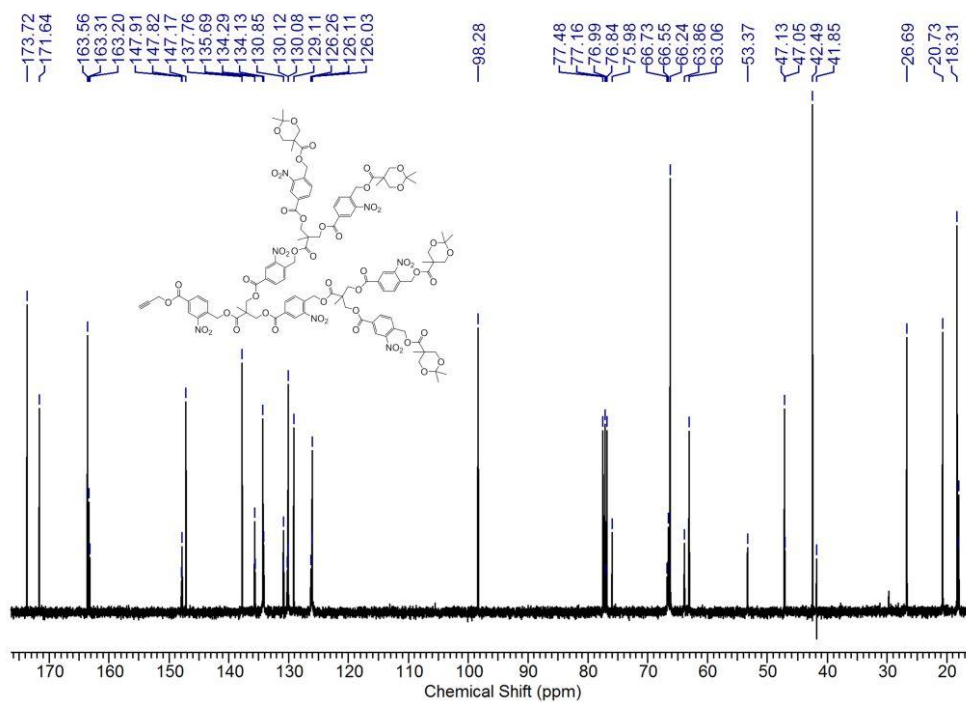
Figure A5.24. ^{13}C NMR spectrum of compound **5.11** (100 MHz, CDCl$_3$).

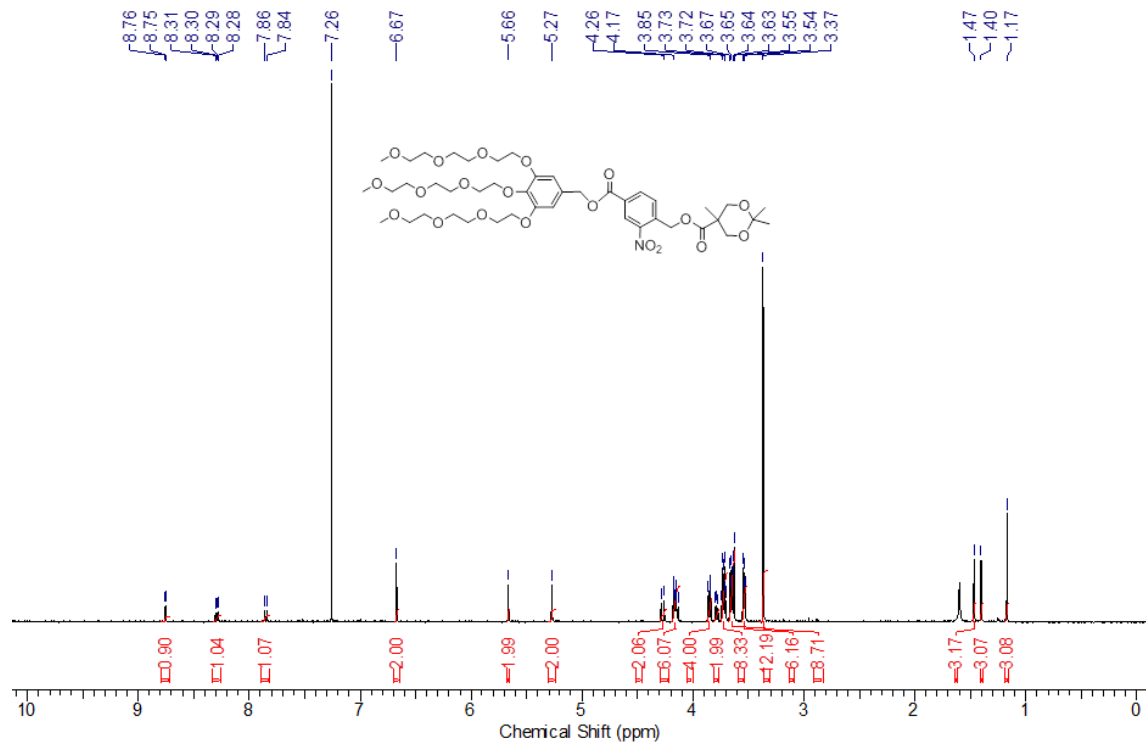**Figure A5.25**. ^{1}H NMR spectrum of compound **5.12** (400 MHz, CDCl$_3$).

Figure A5.26. ^{13}C NMR spectrum of compound **5.12** (100 MHz, (CD$_3$)$_2$SO).

Figure A5.27. ^{1}H NMR spectrum of compound **5.14** (400 MHz, (CD$_3$)$_2$SO).
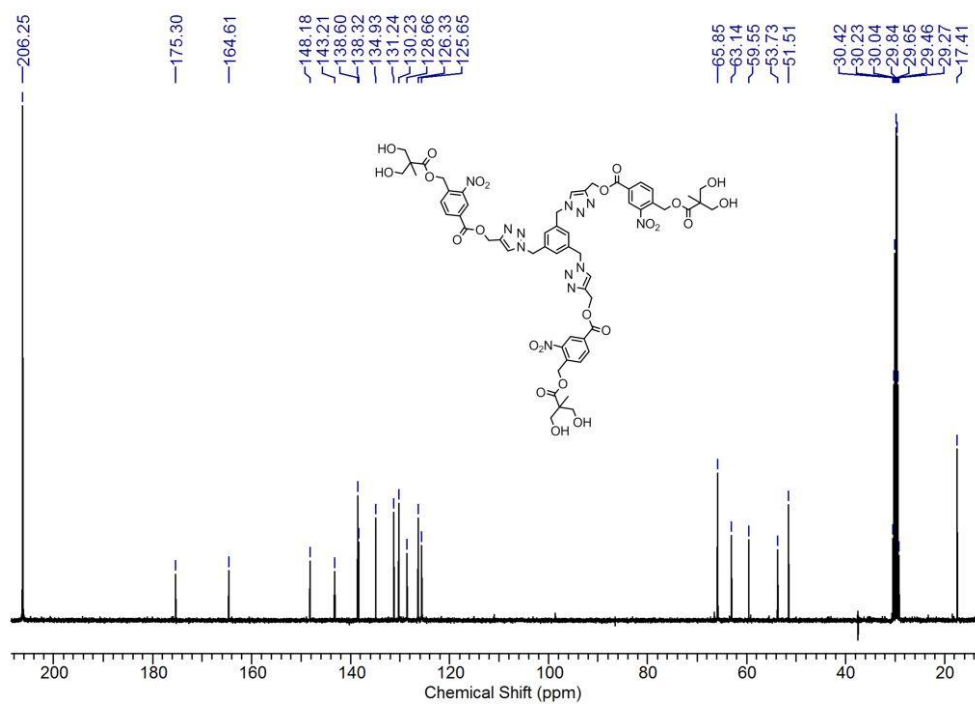
Figure A5.28. ^{13}C NMR spectrum of compound **5.14** (100 MHz, (CD$_3$)$_2$SO).
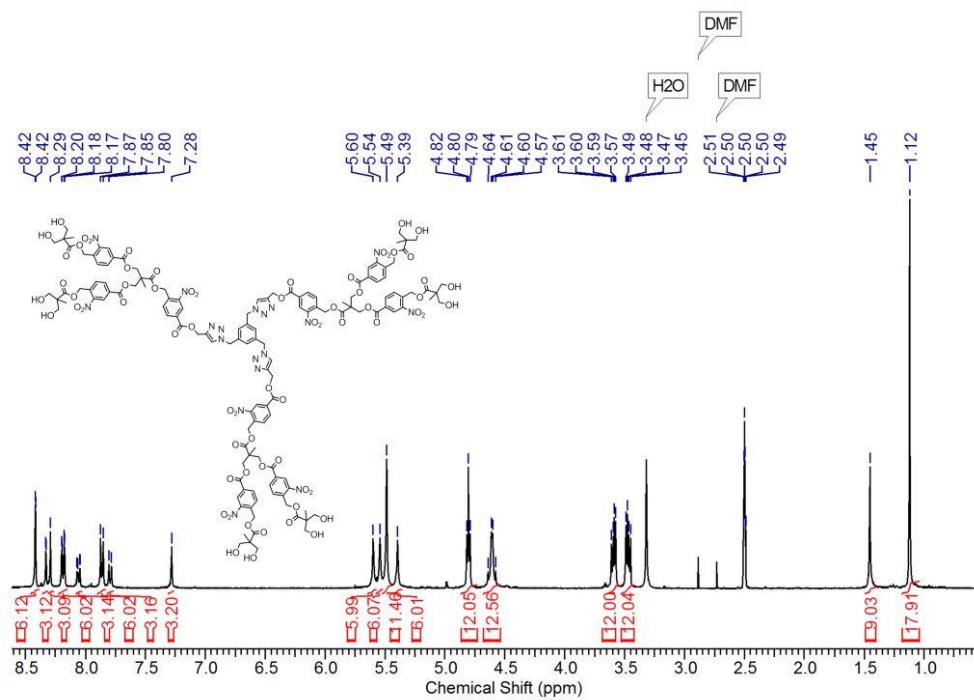
Figure A5.29. ^{1}H NMR spectrum of compound **5.15** (400 MHz, (CD$_3$)$_2$SO).
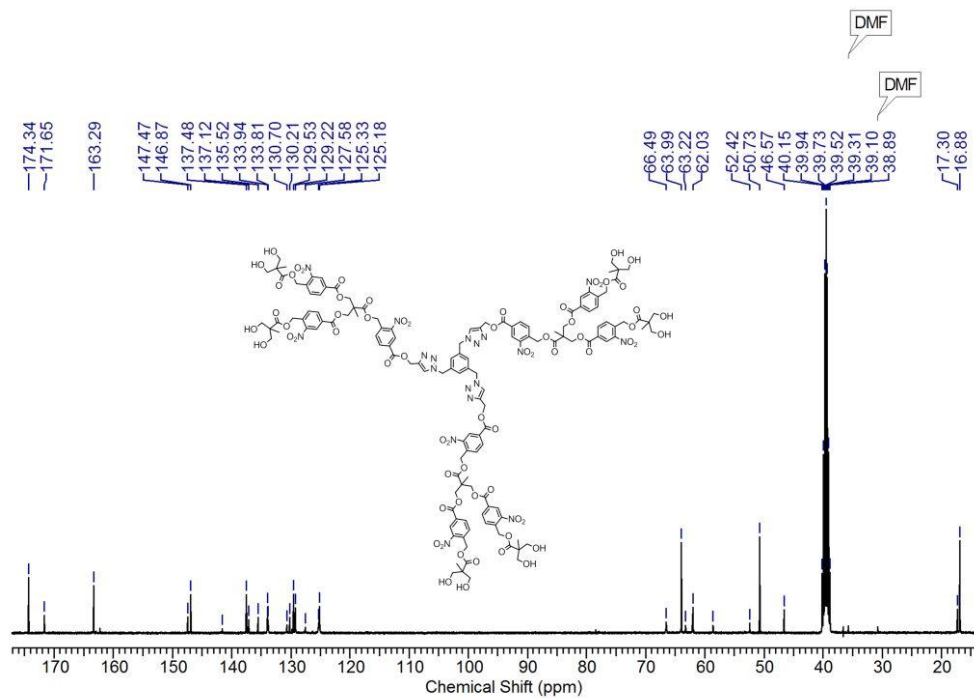
Figure A5.30. ^{13}C NMR spectrum of compound **5.15** (100 MHz, (CD$_3$)$_2$SO).
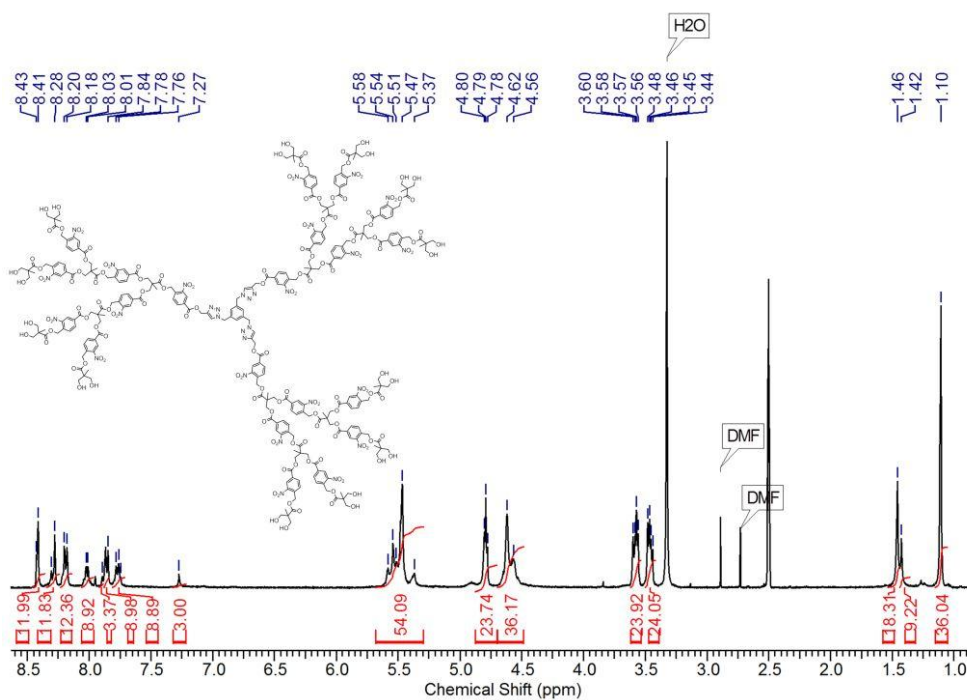
Figure A5.31. ^{1}H NMR spectrum of compound **5.16** (400 MHz, (CD$_3$)$_2$SO).
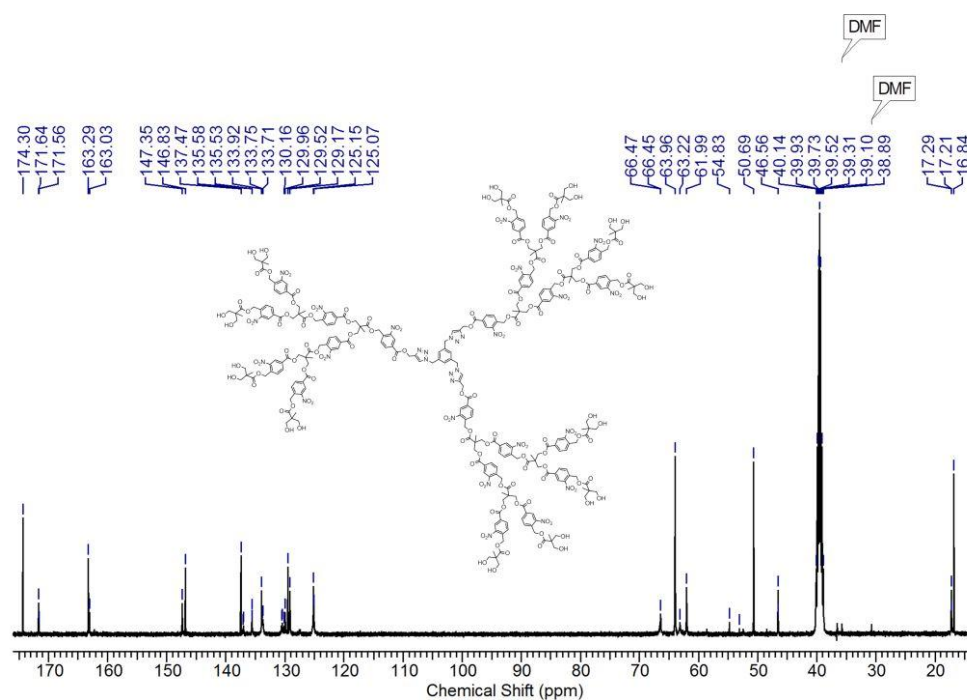
Figure A5.32. ^{13}C NMR spectrum of compound **5.16** (100 MHz, (CD$_3$)$_2$SO).

Appendix 6: Supporting Information for Chapter 6

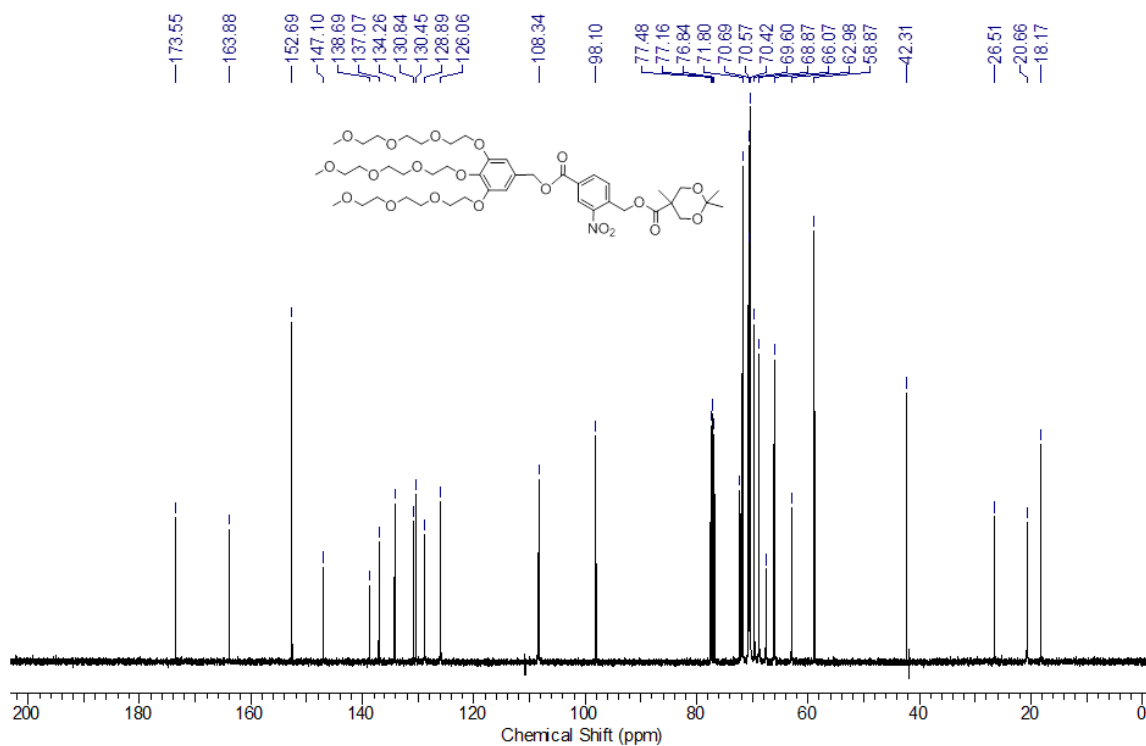**Figure A6.1**. ^{1}H NMR spectrum of compound **6.2** (400 MHz, CDCl$_3$).

Figure A6.2. ^{13}C NMR spectrum of compound **6.2** (100 MHz, CDCl$_3$).
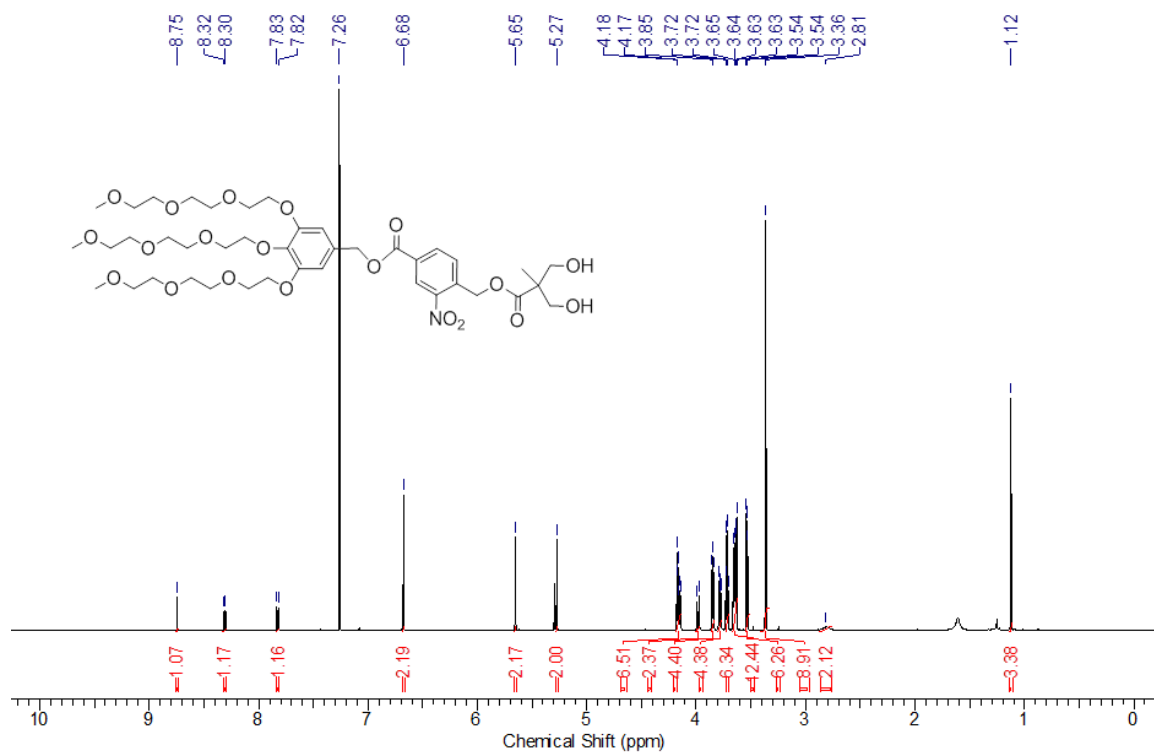
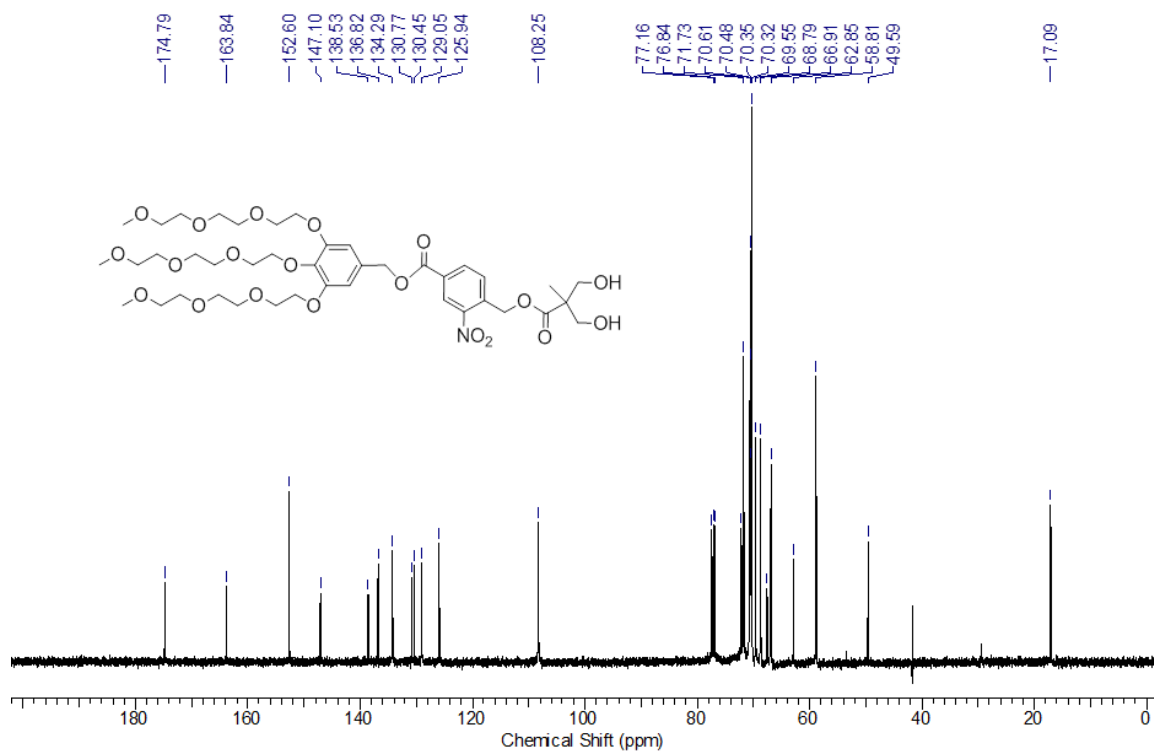**Figure A6.3**. ^{1}H NMR spectrum of compound **6.3** (400 MHz, CDCl$_3$).

Figure A6.4. ^{13}C NMR spectrum of compound **6.3** (100 MHz, CDCl$_3$).
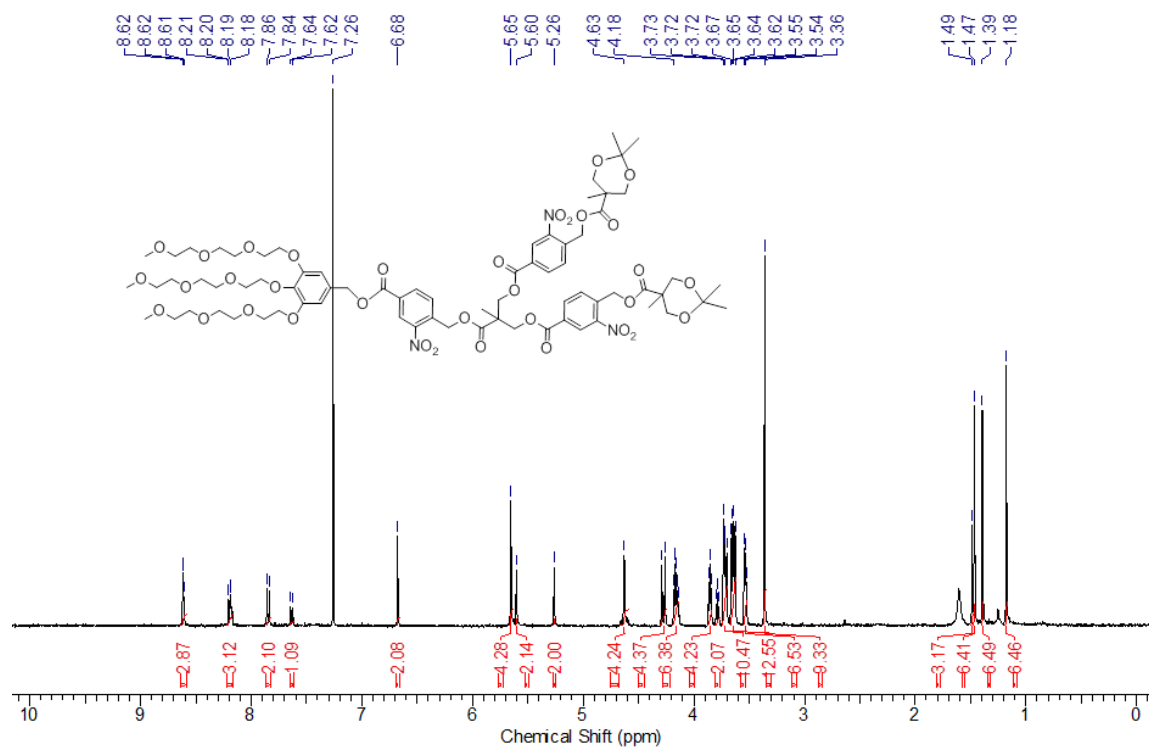
Figure A6.5. ^{1}H NMR spectrum of compound **6.4** (400 MHz, CDCl$_3$).

Figure A6.6. ^{13}C NMR spectrum of compound **6.4** (100 MHz, CDCl$_3$).

Figure A6.7. ^{1}H NMR spectrum of compound **6.5** (400 MHz, CDCl$_3$).

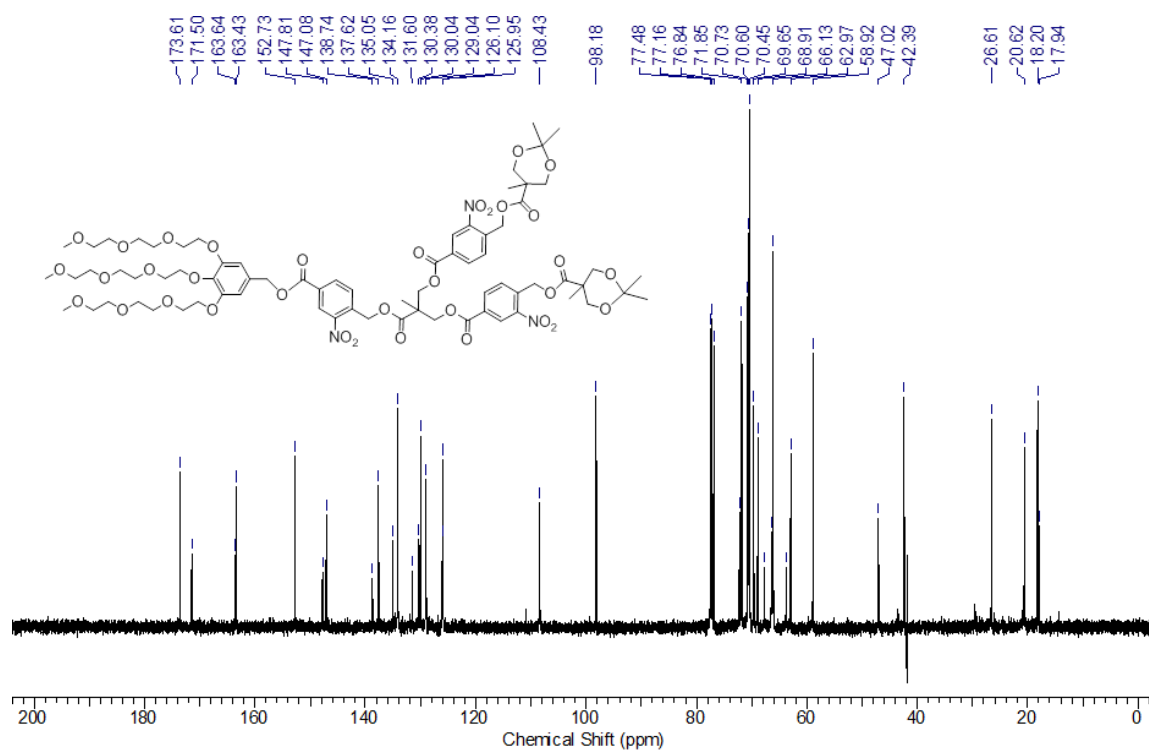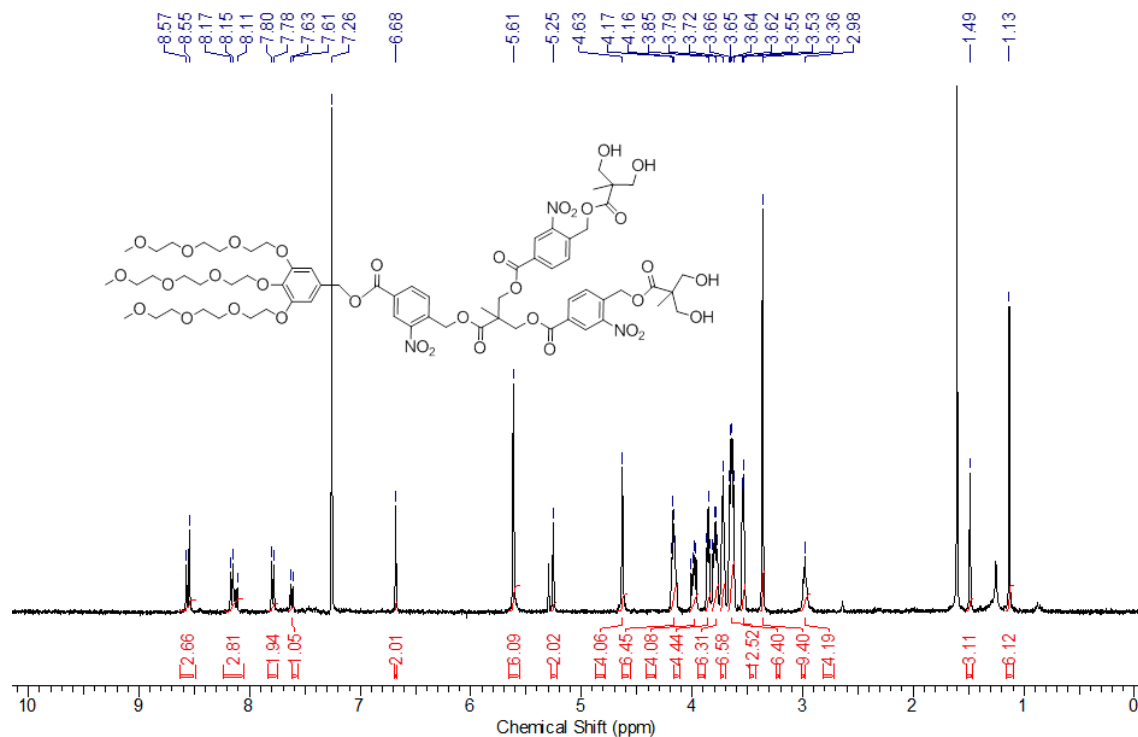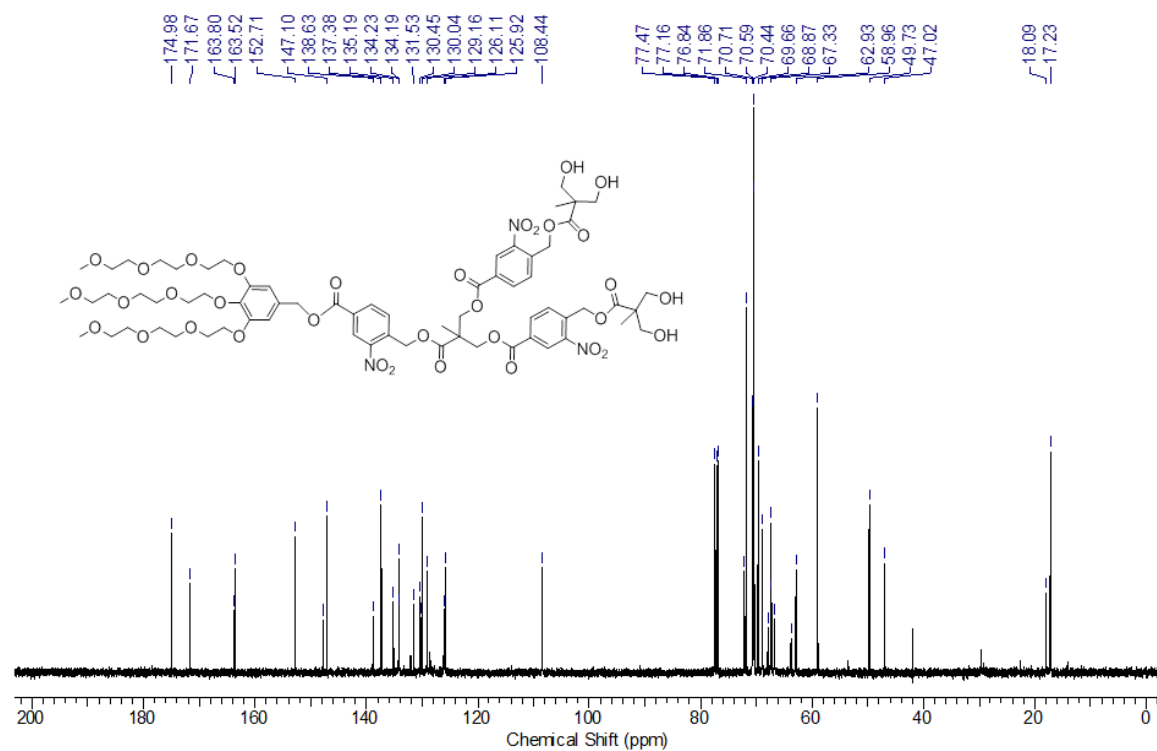**Figure A6.8**. ^{13}C NMR spectrum of compound **6.5** (100 MHz, CDCl$_3$).

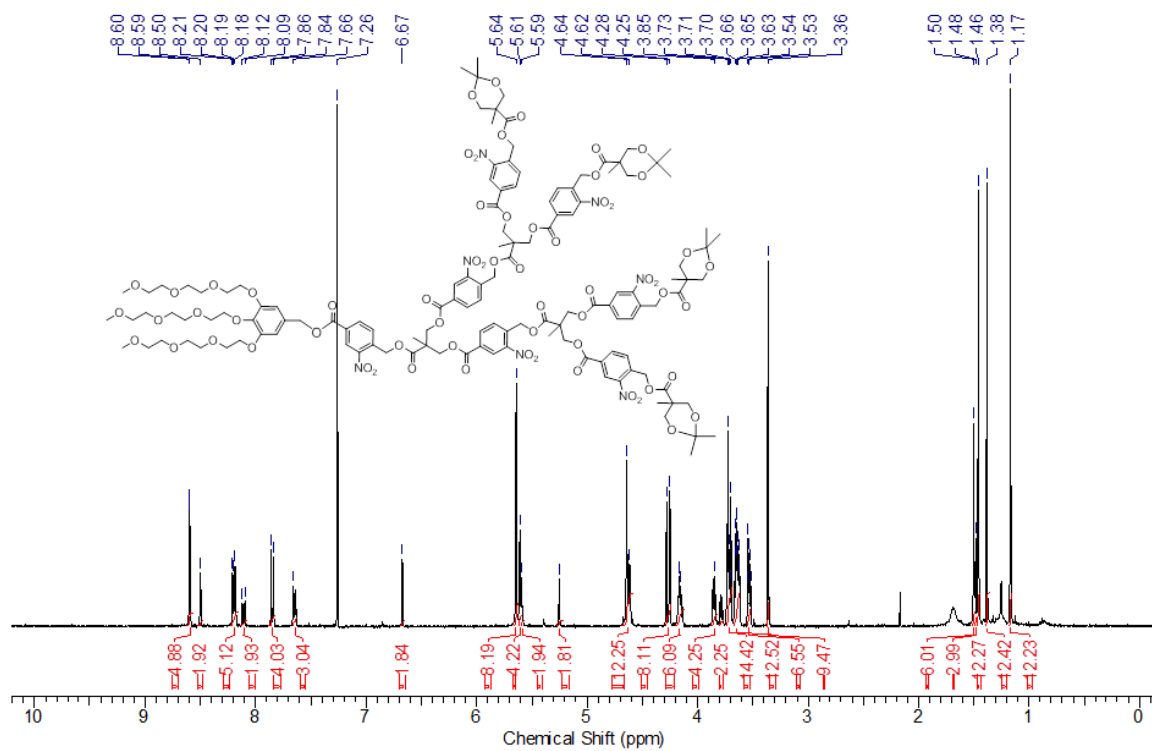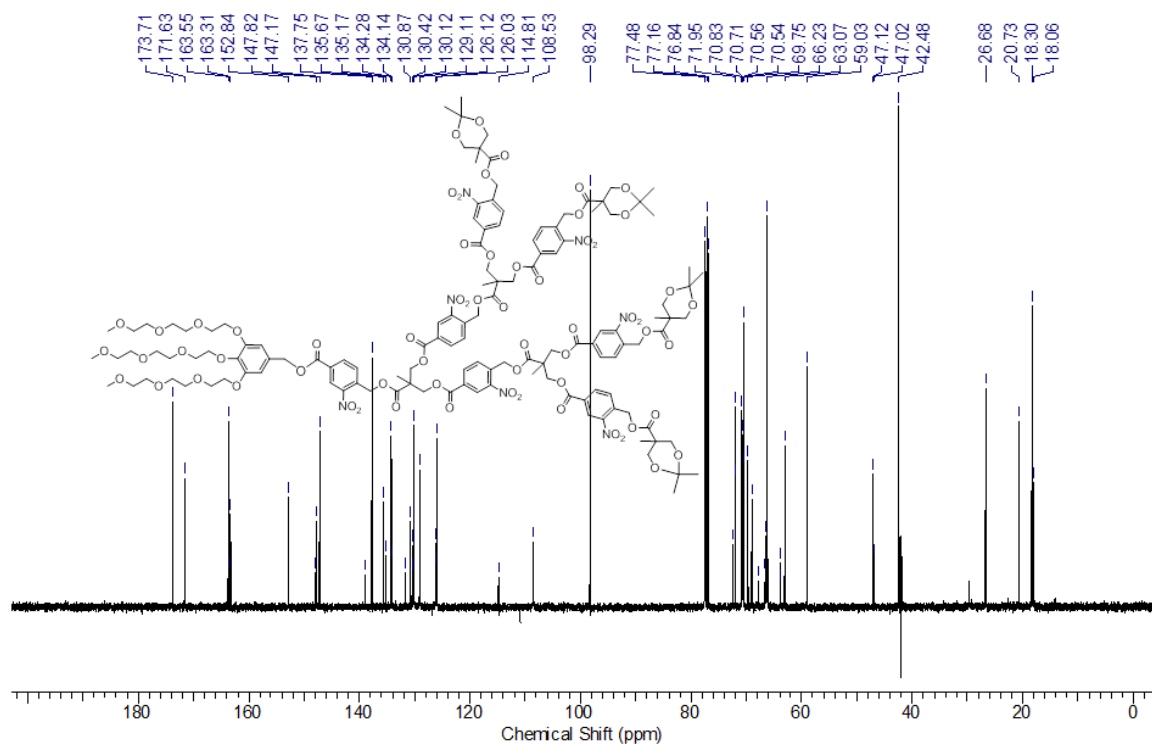**Figure A6.9**. ^{1}H NMR spectrum of compound **6.6** (400 MHz, CDCl$_3$).

Figure A6.10. ^{13}C NMR spectrum of compound **6.6** (100 MHz, CDCl$_3$).

Curriculum Vitae

EDUCATION

Western University, London, Canada   2009-present
    Ph.D., Organic and Polymer Chemistry
    Research Supervisor: Dr. Elizabeth R. Gillies

University of Toronto, Canada   2008-2009
    M.Sc., Inorganic Chemistry
    Thesis title "Investigation of Anion Dependence of Fluorescent Sensors Toward
    Transition Metal Ions"
    Research Supervisor: Dr. Datong Song

K. N. Toosi University of Technology, Tehran, Iran   2001-2005
    B.Sc. Chemistry
    4th year project title "Methodology in the Synthesis of Thiol Esters"
    Project Supervisor: Dr. Barahman Movassagh

RESEARCH EXPERIENCE

Graduate Research Assistant, Gillies Group,   2009-present
Western University, London, Canada

Graduate Research Assistant, Song Group,   2008-2009
University of Toronto, Canada

4th Year Undergraduate Project, Movassagh Group,   2004-2005
K. N. Toosi University of Technology, Tehran, Iran

TEACHING EXPERIENCE

Graduate Teaching Assistant, Western University, London, Canada   2009-present

- Laboratory teaching assistant for Organic Chemistry for Life Sciences
- Laboratory teaching assistant for Organic Chemistry II
- Tutorial teaching assistant for Organic and Inorganic Structural Elucidation
- Laboratory teaching assistant for Discovering Chemistry for first year
  undergraduate students

Graduate Teaching Assistant, University of Toronto, Canada   2008-2009

- Laboratory teaching assistant for Organic Chemistry I
- Laboratory teaching assistant for Organic Chemistry II

AWARDS & SCHOLARSHIPS

- Graduate Thesis Research Award, Western University, London, Ontario (2013)
- Dr. Joseph Soltys Award in Chemistry, Western University, London, Ontario (2012)
- Queen Elizabeth II Graduate Scholarships in Science and Technology (September 2011 – May 2012)
- Third place Poster Award, Ontario Nanoscience and Nanotechnology Workshop, London ON, May 16th- May 18th 2010
- Western Graduate Research Scholarship (WGRS), Western University, London, Ontario (2009 – 2010)
- Recognized as distinguished student from K. N. Toosi University of Technology (2003-2004)

SELECTED PRESENTATIONS

E. R. Gillies, **A. Nazemi**, C. V. Bonduelle, R. C. Amos; "Dendrimer-Functionalized Block Copolymer Assemblies: New Architectural Hybrids for Therapeutic and Delivery Applications" *96th Canadian Society for Chemistry Conference,* Quebec, Quebec, May 26-30, 2013. [oral presentation]

A. Nazemi, R. C. Amos, C. V. Bonduelle, E. R. Gillies; "Biodegradable Polymersome-Dendron Hybrid Materials for Biomedical Applications" Gordon Conference on Self-Assembly & Supramolecular Chemistry, Les Diablerets, Switzerland, May 5-10, 2013 [poster presentation]

A. Nazemi, R. C. Amos, C. V. Bonduelle, E .R. Gillies; "Biodegradable Dendritic Polymersomes as Scaffolds for Biomedical Applications" *244th American Chemical Society National Meeting & Exposition, Philadelphia*, PA, August 19-23, 2012 [poster presentation]

Soleimani, R.; **Nazemi, A.**; Homenick, C. M.; Maris, M.; Martinez, F. M.; Scholl, T. J.; Gillies, E. R. " Development of Optimized Gd(III) Contrast Agents: An Exploration of Macromolecular Architecture" *244th American Chemical Society National Meeting & Exposition, Philadelphia*, PA, August 19-23, 2012 [oral presentation]

A. Nazemi, R. C. Amos, C. V. Bonduelle, E .R. Gillies; "Dendritic Surface Functionalization of Bionanomaterials, Controlling Properties and Functions" CAMBR Distinguished Lecturer and Research Day, London, ON, June 23rd, 2011. [oral presentation]

A. Nazemi, R. C. Amos, C. V. Bonduelle, E .R. Gillies; "Dendritic Surface Functionalization of Bionanomaterials, Controlling Properties and Functions" *94th Canadian Society for Chemistry Conference,* Montreal, Quebec, June 5-9, 2011. [oral presentation]

A. Nazemi, C. V. Bonduelle, R. C. Amos, E .R. Gillies; "Surface Functionalized Biodegradable and Biocompatible Polymer Vesicles" *93nd Canadian Society for Chemistry Conference,* Toronto ON, May 29th – June 2rd 2010. [poster presentation]

Bonduelle, C. V.; **Nazemi A.**; Amos, R. C.; Martin, A.; Li, B.; Gillies, E. R. "Surface Functionalized Polymersomes for Enhanced Cell Uptake and Binding to Biological Targets" *240th American Chemical Society National Meeting & Exposition, Boston*, MA, August 22-26, 2010 [oral presentation]

A. Nazemi, C. V. Bonduelle, R. C. Amos, E .R. Gillies; "Surface Functionalized Biodegradable and Biocompatible Polymer Vesicles" *Ontario Nanoscience and Nanotechnology Workshop,* London ON, May 16th- May 18th 2010. [poster presentation]

PUBLICATIONS

Refereed Articles & Book Chapters:

1. Gobbo, P.; Mossma, Z.; **Nazemi, A.**; Niaux, A.; Gillies, E. R.; Biesinger, M. C.; Workentin, M. S. "Strained-Alkyne Modified Water-Soluble AuNPs: Interfacial Stain-Promoted Cycloaddition for Formation of AuNP- Decorated Polymersomes" (*manuscript submitted to Mater. Horiz.*).

2. **Nazemi, A.**; Haeryfar, S. M. M.; Gillies, E. R. "Multifunctional Dendritic Sialopolymersomes as Potential Antiviral Agents: Their Lectin Binding and Drug Release Properties" *Langmuir,* **2013**, *29*, 6420.

3. **Nazemi, A.**; Schon, T. B.; Gillies, E. R. "Senthesis and Degradation of Backbone Photodegradable Polyester Dendrimers" *Org. Lett.* **2013**, *15*, 1830.

4. **Nazemi, A.**; Gillies, E. R. "Dendrimer Bioconjugates: Synthesis and Applications" in "Bioconjugates for Biomedical Applications" Narain, R. Ed., John Wiley and Sons, Hoboken, New Jersey (*in press*).

5. **Nazemi, A.**; Gillies, E. R. "Dendritic Surface Functionalization of Nanomaterials: Controlling Properties and Functions for Biomedical Applications" *Braz. J. Pharm. Sci*. **2013** (*invited for special issue, in press*).

6. **Nazemi, A.**; Martinez, F. M.; Scholl, T. J.; Gillies, E. R. " Biodegradable Dendritic Polymersomes as Modular, High Relaxivity MRI Contrast Agents" *RSC Advances,* **2012**, *2*, 7971.

7. Amos, R. C.; **Nazemi, A.**; Bondulle, C. V.; Gillies, E. R. "Tuning Polymersome Surfaces: Functionalization with Dendritic Groups" *Soft Matter,* **2012**, *8*, 5947.

8. **Nazemi, A.**; Amos, R. C.; Bondulle, C. V.; Gillies, E. R. "Dendritic Surface Functionalization of Biodegradable Polymer Assemblies" *J. Polym. Sci., Part A: Polym. Chem.* **2011**, *49*, 2546. (***Featured on the front cover of the journal***)

9. DeWit, M. A.; **Nazemi, A.**; Karamdoust, S.; Beaton, A.; Gillies, E. R. "Design, Synthesis and Assembly of Self-Immolative Linear Block Copolymers." *ACS Symp. Series.* **2011**, *1066*, 9.

10. Atkins, K. M.; Martinez, F. M.; **Nazemi, A.**; Scholl, T. J.; Gillies, E. R. "Poly(para-Phenylene Ethynylene)s Functionalized with Chelates as Potential MRI Contrast Agents" *Can. J. Chem.* **2011**, *89*, 47.

Non-Refereed Contributions:

1. **Nazemi, A.**; Amos, R. C.; Bondulle, C. V.; Gillies, E. R. "Biodegradable Dendritic Polymersomes as Scaffolds for Biomedical Applications" *Polymer Preprints,* **2012**, *53*, 392.

2. Soleimani, R.; **Nazemi, A.**; Homenick, C. M.; Maris, M.; Martinez, F. M.; Scholl, T. J.; Gillies, E. R. " Development of Optimized Gd(III) Contrast Agents: An Exploration of Macromolecular Architecture" *Polymer Preprints,* **2012**, *53*, 446.

3. Bonduelle, C. V.; **Nazemi A.**; Amos, R. C.; Martin, A.; Li, B.; Gillies, E. R. "Surface Functionalized Polymersomes for Enhanced Cell Uptake and Binding to Biological Targets" *Polymer Preprints*, **2010**, *51*, 295.